Reports Due
No action
AGS

GEORGIA INSTITUTE OF TECHNOLOGY
OFFICE OF RESEARCH ADMINISTRATION

RESEARCH PROJECT INITIATION

Date: June 11, 1973

Project Title: A Study of Natural Gas Wankel Driven Air Conditioning Systems

Project No: E-25-634

Principal Investigator: Dr. S. V. Shelton

Sponsor: Atlanta Gas Light Company

Agreement Period: From May 15, 1973 Until May 14, 1974

Type Agreement: Standard Industrial Agreement dated May 14, 1973

Amount: $25,900.00

Reports Required: Quarterly Progress Reports; Technical Summary Report

Sponsor Contact Person (s): Mr. W. J. Goldin
Marketing Manager
Atlanta Gas Light Company
P.O. Box 4569
Atlanta, Georgia 30302
Phone: 522-8051, ext. 276

Assigned to: School of Mechanical Engineering

COPIES TO:

- Principal Investigator
- School Director
- Dean of the College
- Director, Research Administration
- Director, Financial Affairs (2)
- Security-Reports-Property Office ✓
- Patent Coordinator
- Library
- Rich Electronic Computer Center
- Photographic Laboratory
- Project File
- Other

RA-3 (6-71)

GEORGIA INSTITUTE OF TECHNOLOGY
OFFICE OF CONTRACT ADMINISTRATION

SPONSORED PROJECT TERMINATION

no action
ADS

Date: August 30, 1976

Project Title: A Study of Natural Gas Wankel Driven Air Conditioning Systems

Project No: E-25-634

Project Director: Dr. S. V. Shelton

Sponsor: Atlanta Gas Light Company

Effective Termination Date: May 14,1976

Clearance of Accounting Charges: All charges have cleared.

Grant/Contract Closeout Actions Remaining:

- X Final Invoice and Closing Documents
- _ Final Fiscal Report
- _ Final Report of Inventions
- _ Govt. Property Inventory & Related Certificate
- _ Classified Material Certificate
- _ Other _____

Assigned to: School of Mechanical Engineering (School/Laboratory)

COPIES TO:

- Project Director
- Division Chief (EES)
- School/Laboratory Director
- Dean/Director–EES
- Accounting Office
- Procurement Office
- Security Coordinator (OCA)
- Reports Coordinator (OCA)
- Library, Technical Reports Section
- Office of Computing Services
- Director, Physical Plant
- EES Information Office
- Project File (OCA)
- Project Code (GTRI)
- Other _____

CA–4 (3/76)

A Study of Natural Gas Wankel Driven Air Conditioning Systems

Quarterly Report #1

Submitted to

Atlanta Gas Light Company
235 Peachtree Street, NE
Atlanta, Georgia

by

Dr. Sam Shelton, Principle Investigator
School of Mechanical Engineering
Georgia Institute of Technology
Atlanta, Georgia 30332

September 1, 1973

A Study of Natural Gas Wankel Driven Air Conditioning Systems

Quarterly Report #1

Introduction

The research and development program as detailed in the "Proposal for A Study of Natural Gas Wankel Driven Air Conditioning Systems" has been initiated and the two parallel first year efforts, engine testing and system analysis, are well under way. There have been no major delays in procuring equipment and the program is currently on schedule. The start up phase requiring a much higher rate of expenditure of manpower and resources is now over and engine test data and system analysis results will be produced during the second quarter.

Engine Tests

Three engines, (130 hp Toyo Kogyo, 35 hp OMC, and 18 hp Sachs) and one dynomometer have been ordered and all but the OMC engine received. Three dynomometer test beds with proper instrumentation have been prepared and the Toyo Kogyo and Sachs engines will be operating by September 15, 1973.

Due to a liscensing problem with the OMC engine, which currently does not allow OMC to sell the engine for industrial use, procurement of this engine was delayed so that OMC's three week plant close down for vacation delayed shipment. Curtis Wright can, of course, sell these engines and it was procured through them. This engine is expected, however, to have been received and operating by October 1, 1973.

Power and efficiency data will first be taken on these three engines

with gasoline to provide a base line and then operation on natural gas will begin. They will be run continuously with power and efficiency data being obtained early in the tests.

Related 6 hp Sachs Engine Tests

Prior to the initiation of this contract, tests were begun on a 6 hp Sachs engine which was procured by the School in 1965 and since used for undergraduate laboratory experiments. This engine was torn down and inspected early this year and, due to the original ones being badly worn, new seals installed. The engine was then run on propane for approximately 1000 hours at 3000 rpm under heavy load (3 hp). With tear down intervals of approximately 300 hours, seal wear was determined and found to be extremely low. In fact, extrapolation of this preliminary data to the point where apex seal replacement is recommended yields an engine life of over 30,000 hours. This is about three times longer than expected for any of the engines at the start of this program. The engine thermal efficiency was 22 percent.

This data must be considered highly preliminary and public release of it should be restricted. However, under any circumstances it is very encouraging. There is no reason to believe that natural gas fuel will provide substantially different data than the propane fuel.

This 6 hp Sachs engine is essentially identical to the 18 hp Sachs which is one of the three engines originally scheduled to be tested. In fact, the 18 hp engine is a newer design than the earlier 6 hp engine and would be expected to perform better.

System Analysis

In order to proceed with a system design and analysis which will

produce accurate system performance estimates, performance data is being collected on necessary off-the-shelf components, i.e., evaporators, condensers, and compressors. Along with engine performance data being taken, this will allow a complete system design and performance calculation with various configurations and components being used to determine the best system.

Operating costs of this system in a residence will then be compared to existing air conditioning systems by using actual daily degree days data for Atlanta. This will yield economic information on both the proposed air conditioning and heating systems.

Conclusions

At this time the program is on schedule and no negative results have been obtained. Preliminary engine reliability tests look much better than originally hoped for which will probably make the heat pump system a viable system. Due to the large additional running time required during heating, it was uncertain that the original 10,000 hour goal between major overhauls would be high enough. However, 20,000 hours now seems to be a realistic and possibly conservative goal.

Due to the preliminary nature of this information, it is felt that any release of this data should be restricted until more results are obtained.

GEORGIA INSTITUTE OF TECHNOLOGY
School of Mechanical Engineering
Atlanta, Georgia

A Study of Natural Gas Rotary Engine Driven Heat Pumps

First Annual Report

S. V. Shelton
Principal Investigator

Sponsored by

Atlanta Gas Light Company
Atlanta, Georgia

July 1974

GEORGIA INSTITUTE OF TECHNOLOGY
School of Mechanical Engineering
Atlanta, Georgia

First Annual Report

A Study of Natural Gas Rotary Engine Driven Heat Pumps

by

M. Boyd
T. Durham
R. Johnston
W. Johnson
S. Shelton

Sponsored by

Atlanta Gas Light Company
Atlanta, Georgia

July 1974

Stothe P. Kezios, Director
School of Mechanical Engineering

S. V. Shelton
Principal Investigator

TABLE OF CONTENTS

TABLE OF CONTENTS
(continued)

Summary

With rising energy costs in recent years more efficient space heating and cooling systems than presently available are becoming more economically feasible, and even necessary. This is true for natural gas systems as well as electric systems. More than thirty percent of our most desirable fossil fuel's demand, natural gas, is consumed for space conditioning. Basic thermodynamics show that even the efficient natural gas furnace can not ever approach the theoretical maximum heating efficiency. The natural gas heat pump can in theory approach this theoretical limit. This study investigates analytically the efficiency of a Wankel rotary engine driven natural gas heat pump using presently available components and experimentally determines the performance and durability of three available rotary engines.

Using experimentally determined engine data and manufacturer's specifications for other components, the annual heating and cooling coefficient of performance (COP) for a rotary engine powered natural gas heat pump in Atlanta, Georgia was calculated to be 1.3 and 1.0 respectively. This compares with gas furnace and gas absorption COP's of .7 to .8 and .5 respectively.

Three rotary engines were comprehensively tested; 1) Toyo Kogyo 130 hp, 2) Outboard Marine 45 hp, and 3) Sachs and Fichel 16 hp. The optimum speed on all these engines for power and efficiency was about 3600 rpm. The optimum air-fuel ratio was found to be near stoichiometric for both power and efficiency. At this optimum speed and mixture ratio the Toyo Kogyo produced 55 hp with a 25 percent thermal efficiency, the

OMC produced 22 hp with a 22 percent efficiency, and the Sachs engine produced 8 hp at a 21 percent efficiency. Over 60 percent of the waste heat in the Sachs engine was contained in the exhaust which is very easily recoverable.

Wear tests show the most critical Wankel engine wear component, the rotor seals, have suprisingly low wear rates. These wear rates were consistently shown to be 5 to 10 times lower than wear rates on gasoline. Seal life before performance deterioration conservatively extrapolates to between 8,000 and 30,000 hours at 3600 rpm in all engines tested.

The annual natural gas demand load factor of this heat pump in Atlanta, Georgia would be .63 compared to .38 for a gas furnace. Both heating and cooling in an Atlanta residence would be accomplished with less gas than consumed for heating alone by a gas furnace. The air pollution impact of this unit would be four times less severe than even an electric heat pump receiving its power from a coal burning, emission controlled, power plant.

The national impact of a marketable residential and commercial gas driven heat pump would be dramatic. American Gas Association calculations show it would save as much gas annually in 1990 as produced by coal gasification facilities costing $16 billion in present dollars.

On the basis of this study, two systems are recommended for experimental testing. One being a 5 ton residential system driven by the Sachs engine and the other being a 25 ton commercial system driven by the Toyo Kogyo engine.

LIST OF FIGURES

LIST OF FIGURES (continued)

LIST OF FIGURES (continued)

CHAPTER I

INTRODUCTION

Background

With the energy crisis a present day reality, the U. S. must look to more utilization of its coal reserves and more efficient systems for using our more desirable petroleum and natural gas supplies. Natural gas is a particularly desirable fuel because it is the cleanest burning of all fossil fuels, requires no refining, and is easily recovered and shipped with no detrimental environmental impact. All of this gives impetus to the efficient utilization of our natural gas resources. Rising natural gas cost adds economics to this impetus. More natural gas is used for space heating than any other single use and represents approximately 1/3 of our natural gas demand in the U. S.

This study is therefore investigating experimentally and analytically a system for drastically increasing the already high efficiency of space heating and cooling by natural gas. This system is the natural gas heat pump.

Analysis by the American Gas Institute[9] has shown that if natural gas heat pumps were installed in place of natural gas furnaces beginning in 1976, the accumulative savings in natural gas would be about 12×10^{12} cubic feet by 1990, (or 3×10^{12} cubic feet annually). This is equivalent to that quantity of gas projected to be produced from coal gasification at a capital expenditure of about $16 billion. This AGA analysis assumes that the natural gas heat pump will make up only 40% of the raw heating unit market by 1990.

Heat Pump System

The basic heat pump system which uses work to pump heat from a low temperature to a higher temperature is shown below in Figure 1.

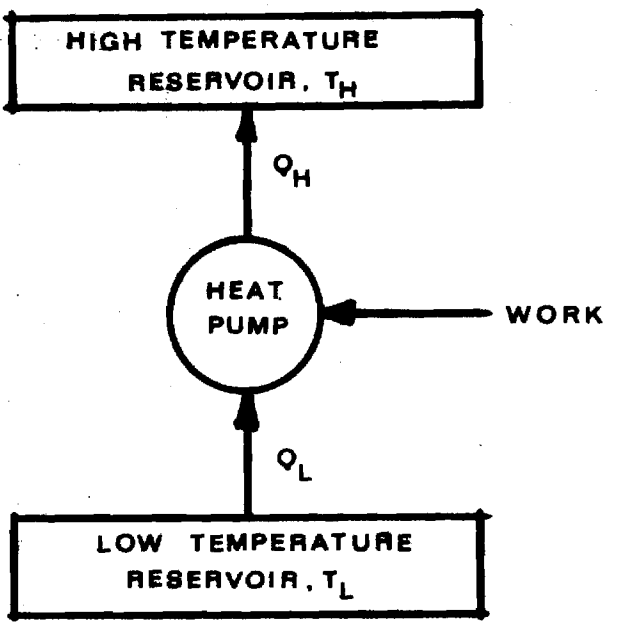

Figure 1. Thermodynamic Heat Pump

Heat is absorbed from a low temperature (T_L) reservoir and rejected at a higher temperature (T_H) reservoir.

For air conditioning in the summer the low temperature reservoir which is giving up heat (being cooled) is the room air and the high temperature reservoir to which heat is being released is the outside atmosphere. The schematic of the common vapor-compression cycle for accomplishing this pumping of heat is shown in Figure 2.

In this air conditioning mode, the high temperature condenser is placed outside and heats the atmosphere (typically $90^{o}F$), while the evaporator is inside the house cooling the room air (typically $75^{o}F$).

Rather than driving the compressor with an electric motor, a natural

gas fueled engine may be used for the prime mover. This produces a natural gas driven air conditioning system.

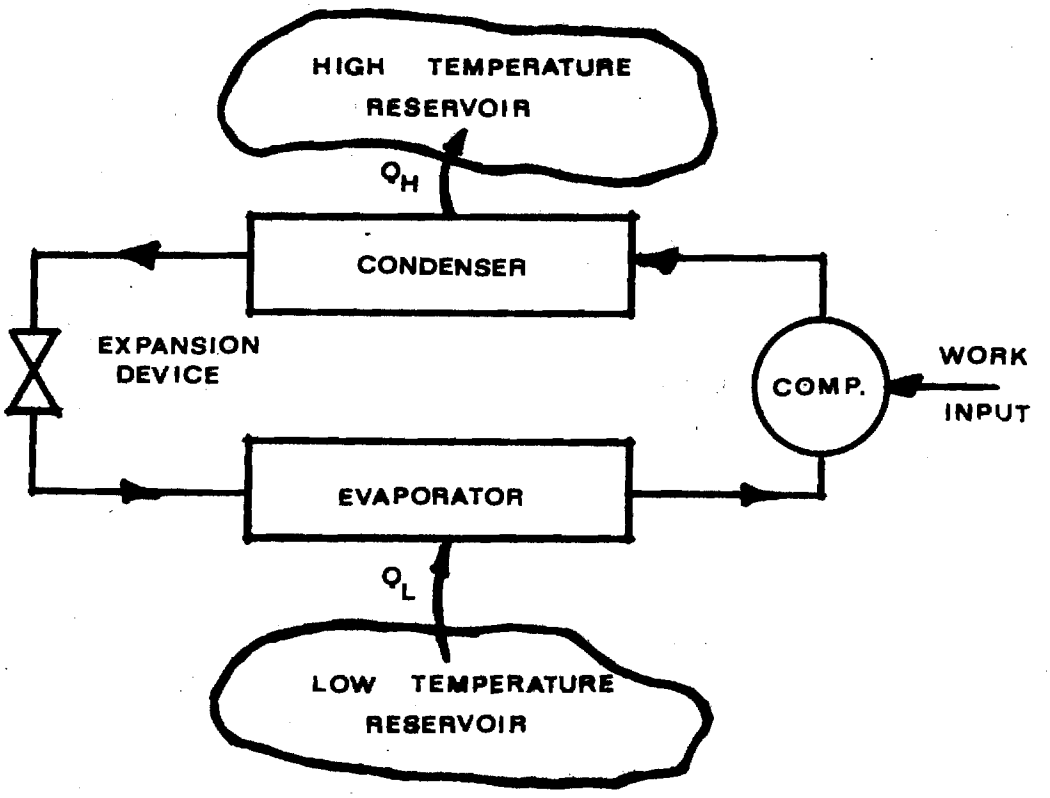

Figure 2. Vapor Compression Heat Pump Operation.

In the winter the position of the condenser and evaporator may be reversed causing the condenser to heat the inside room air the evaporator to absorb heat from the atmosphere. An electric motor may be used to drive the compressor and an electric heat pump is the result.

By driving the compressor with a natural gas fueled engine, a natural gas heating system is produced. In addition to the heat input to the room air by the condenser, the hot exhaust coming from the engine may also be recovered to heat the room air as shown in Figure 3.

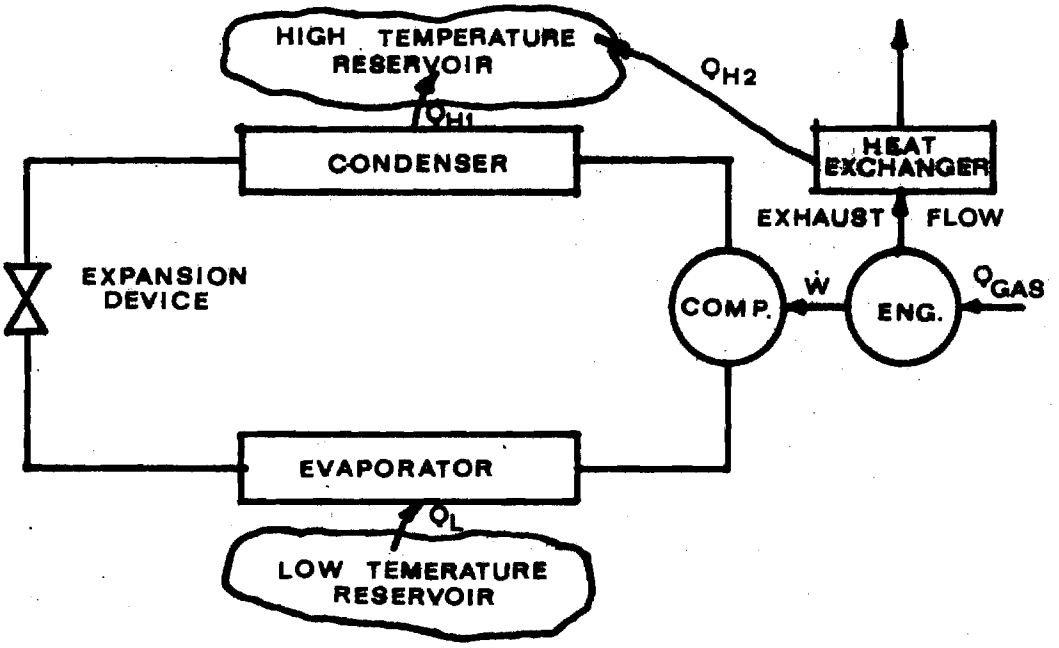

Figure 3. Natural Gas Heating by a Heat Pump.

Rather than having two systems, one for room heating and one for room cooling, a single system may be used and the condenser and evaporator switched from outdoors to indoors and visa versa by reversing the Freon flow direction with a four way reversing valve. Also, rather than having an extra coil for transmitting the exhaust heat to the room air, the condenser may serve this function by using the Freon as the exhaust heat recovery medium. These changes result in a natural gas heat pump as shown in Figure 4.

The electric heat pump made its break into the commercial market in the 50's and has made steady progress in obtaining more of the electric heating appliance market, especially in the South. By its basic nature, it uses electricity in a more efficient manner for space heating than resistance heating does.

However, any electrical heating system, whether resistance or heat pump, has the disadvantage that about two-thirds of the fossil fuel's combustion energy is thrown away into the rivers, or atmosphere, in the form of heat at the electric power plant. Due to the power plants remote location it is too costly to utilize this waste heat. Therefore, natural

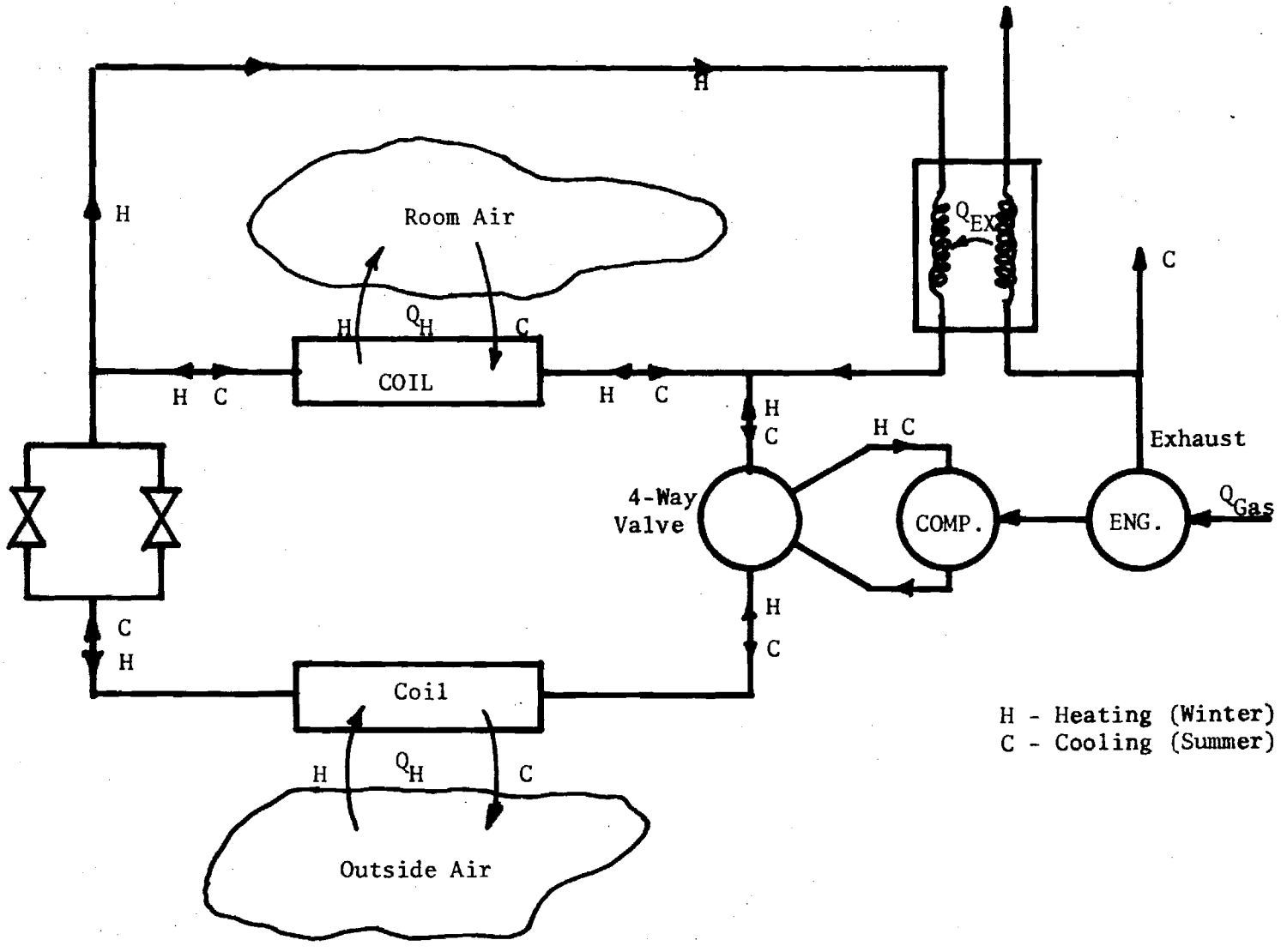

Figure 4. Natural Gas Heat Pump System.

gas space heating is less costly and has been more widely used. Exactly analogous to the comparison of the electric resistance furnace to the electric heat pump is the comparison of the natural gas furance to the natural gas heat pump. The natural gas heat pump offers far more efficient utilization of our natural gas than a natural gas furance.

The feasibility of such a natural gas heat pump is the subject of this study.

CHAPTER II

HEAT PUMP PERFORMANCE ANALYSIS

Introduction

In order to determine the desirability of the natural gas fueled engine driven heat pump as an air conditioner and heating system, a system as shown in Figure 4 consisting of off-the-shelf components was analyzed. The system heating capacity, cooling capacity, heating COP and cooling COP was determined. Since these results are weather dependent, annual typical (1964) weather conditions in Atlanta, Georgia were chosen. The compressor was taken to be a York automotive type compressor. This compressor is not the most desirable from the efficiency standpoint but detailed performance data for it was available. Freon-22 was used as the working fluid.

Cycle Analysis

The T-s diagram showing the thermodynamic path of the working fluid in the subject system is shown in Figure 5. States 1, 2, 3, and 4 are the evaporator, compressor, condenser, and expansion valve exit conditions. States 1 and 3 were taken to be $5^{o}F$ superheated and $5^{o}F$ subcooled respectively.

The ideal compressor work is given by

$$\dot{W}_{ideal} = \dot{m} \, (h_{2s} - h_1) \qquad (1)$$

where:

$\dot{m}$ = freon mass flow rate

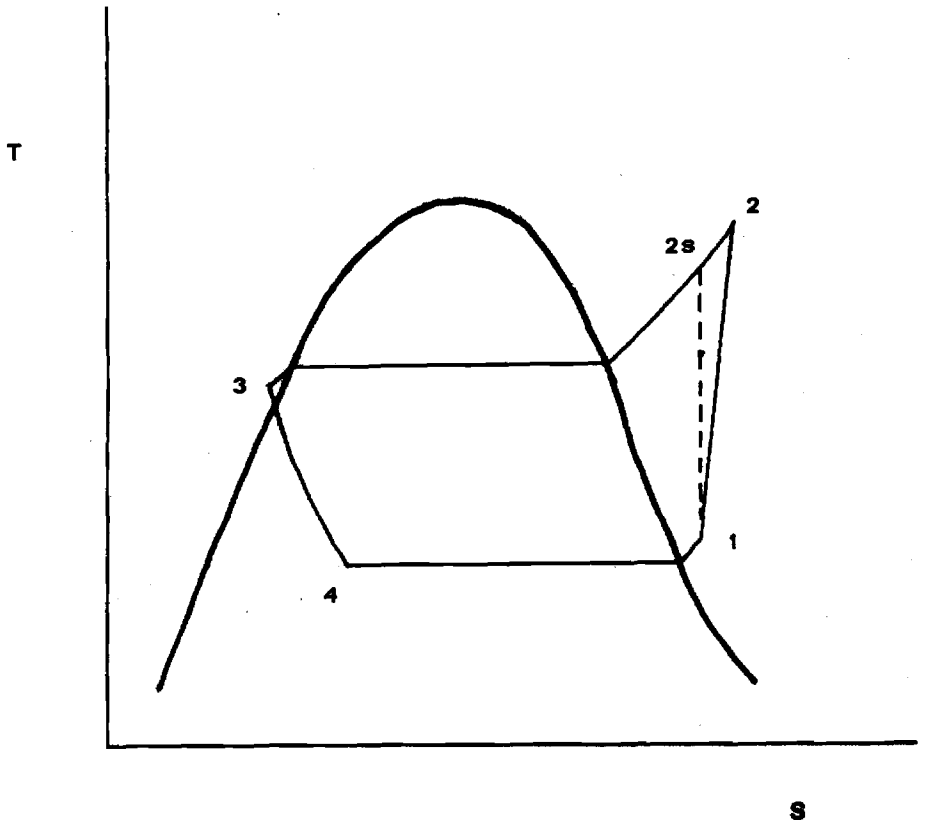

Figure 5. Working Fluid T-S Diagram

h_{2s} = enthalpy at state 2s

h_1 = enthalpy at state 1

However, the compressor does not run ideally, but has inefficiencies associated with it. The isentropic efficiency of the compressor is defined as

$$\eta_s = \frac{h_{2s} - h_1}{h_2 - h_1} \tag{2}$$

The actual work is:

$$\dot{W}_{act} = \dot{m} (h_2 - h_1) \tag{3}$$

or substituting Equation 2 into Equation 3,

$$\dot{W}_{act} = \dot{m} \left(\frac{h_{2s} - h_1}{\eta_s}\right) \tag{4}$$

The heat rejected by the condenser is given by the equation:

$$\dot{Q}_{cond} = \dot{m} (h_2 - h_3) \tag{5}$$

For the cooling mode, $\dot{Q}_{cond}$ is the amount of heat rejected to the atmosphere.

The heat received by the evaporator is given by:

$$\dot{Q}_{evap} = \dot{m} (h_1 - h_4) \tag{6}$$

For the cooling mode, $\dot{Q}_{evap}$ is the amount of heat taken from the house. In the heating mode, $\dot{Q}_{evap}$ is the heat gained from the outdoor air.

The mass flow rate is given by:

$$\dot{m} = \rho \eta_v \dot{V} \tag{7}$$

where ρ is the vapor density at the compressor inlet, η_v is the compressor

volumetric efficiency, and $\dot{V}$ is the compressor piston displacement per unit time (given by piston displacement per revolution times the compressor speed).

The heating mode rejects not only $\dot{Q}_{cond}$ to the house but also the recovered exhaust heat. The exhaust gases from the heat pump are drawn through a heat exchanger to evaporate additional fluid before it enters the condenser as shown in Figure 4. The exhaust heat recovered is

$$\dot{Q}_{rec} = F_{rec}\ \dot{Q}_{waste} = F_{rec}\ (1-\eta_{th})(\dot{W}_{comp}/\eta_{th}) \tag{8}$$

where:

F_{rec} = fraction of engine waste heat recovered

η_{th} = thermal efficiency of the heat pump

Therefore, the total heat available in the heating mode is:

$$\dot{Q}_{heating} = \dot{Q}_{cond} + \dot{Q}_{rec} \tag{9}$$

The coefficient of performance (COP) is the efficiency parameter desired in this analysis. The COP is the ratio of the desired cooling or heating output to the input energy of the gas. For the cooling mode, the COP is

$$COP_c = \frac{Q_{evap}}{Q_{gas}} \tag{10}$$

Using:

$$Q_{gas} = W_{comp}/\eta_{th} \tag{11}$$

one obtains:

$$COP_c = \frac{Q_{evap}\ \eta_{th}}{W_{comp}} \tag{12}$$

The COP_H is

$$COP_H = \frac{Q_{heating}}{Q_{gas}} \tag{13}$$

where

$$Q_{heating} = Q_{cond} + Q_{rec} \tag{14}$$

Substituting Equation 8 into Equation 14,

$$Q_{heating} = Q_{cond} + F_{rec}\ (1-\eta_{th})(W_{comp}/\eta_{th}) \tag{15}$$

Substituting Equation 15 and Equation 11 into Equation 13,

$$COP_H = \frac{Q_{cond} + F_{rec}\ (1-\eta_{th})(W_{comp}/\eta_{th})}{\dot{W}_{comp}/\eta_{th}}$$

or simplifying,

$$COP_H = \frac{\eta_{th}\ \dot{Q}_{cond}}{\dot{W}_{comp}} + F_{rec}\ (1-\eta_{th}) \tag{16}$$

Annual Average COP

The annual average COP_H and COP_c are given by

$$\overline{COP_H} = \bar{Q}_H/\bar{Q}_{gas} \tag{17}$$

$$\overline{COP_C} = \bar{Q}_c/\bar{Q}_{gas} \tag{18}$$

where $\overline{(\ )}$ denotes annual quantities and Q_{gas} is the heating value of natural gas used. The cooling and heating rate required by a residence is proportional to the temperature difference between 65^oF and the outside air temperature. Therefore one may write:

$$\dot{Q}_H = K\ (65 - T_A);\ T_a < 65^oF \tag{19}$$

$$\dot{Q}_c = K\ (T_A - 65);\ T_a > 65^oF \tag{20}$$

where T_a is the outside air temperature in ^oF and K is a constant. At an outside temperature of 65^oF the indoor appliances supply enough heat to keep the indoor temperature in the comfort range.

The values $\overline{Q}_H$, and $\overline{Q}_c$ are then given by:

$$\overline{Q}_c = \frac{1}{t_c}\int_o^{t_c} K\,(T - 65)\,dt; \quad T>65 \tag{21}$$

$$\overline{Q}_H = \frac{1}{t_h}\int_o^{t_h} K\,(65 - T)\,dt; \quad T<65 \tag{22}$$

The annual gas demand for cooling is:

$$\overline{Q}_{gas} = \frac{1}{t_c}\int_o^{t_c} \frac{K(T - 65)}{COP_c}\,dt; \quad T>65 \tag{23}$$

and for heating:

$$\overline{Q_{gas}} = \frac{1}{t_h}\int_o^{t_h} \frac{K(65 - T)}{COP_H}\,dt; \quad T<65 \tag{24}$$

where t is time and t_h and t_c are the heating and cooling periods for the year. Note the COP_H and COP_c in Equations 22 and 23 vary with temperature and are not constant. Substituting Equations 21 and 23 into Equation 17 and 22 and 24 into 18 one finds:

$$\overline{COP_H} = \frac{\int_o^{t_h} (65^oF - T)\,dt}{\int_o^{t} \frac{(65^oF - T)}{COP_H}\,dt} \tag{25}$$

$$\overline{COP_c} = \frac{\int_o^{t_c} (T - 65^oF)\,dt}{\int_o^{t_c} \frac{(T - 65^oF)}{COP_c}\,dt} \tag{26}$$

These intergrals were evaluated by using the typical year (1964) hourly temperature data for Atlanta, Georgia. The number of hours annually at $10^{o}F$ temperature intervals were found for this year to be:

^{o}F	Hours/Year
0 - 9	0
10 - 19	25
20 - 29	240
30 - 39	851
40 - 49	1417
50 - 59	1433
60 - 69	1792
70 - 79	2177
80 - 89	848
90 - 99	.77

This information along with COP_H and COP_c expressed as a function of outside temperature allows evaluation of the $\overline{COP_H}$ and $\overline{COP_c}$ in Equations 25 and 26.

Numerical Evaluation

All calculations for the refrigeration cycle were based upon Freon 22. The properties were taken from a Pressure-Enthalpy diagram by the E. I. DuPont deNemours & Company.

First, limits were put on the speed that the compressor would be allowed to run. The compressor speeds would be between 1000 and 3000 rpm. The capacity of the evaporator was held constant at 3 tons or 600 Btu/min as long as the speed of the compressor was between 1000 and 3000 rpm. If the necessary speed of the compressor was greater than 3000 rpm for obtaining 600 Btu/min, then the compressor would be held at a maximum of 3000 rpm, with the result of having less capacity. In all calculations, the volumetric and isentropic efficiencies of the compressor were taken from actual compressor data of the York 210 compressor (Figures 6 and 7). Its displacement is 10.3 cubic inches per revolution. The recovery factor was taken to be 0.7 and the engine thermal efficiency 0.2. These values were determined from laboratory tests of the Wankel engine discussed in this report.

Figure 8 is a plot of $\dot{Q}_{evap}$ ($\dot{Q}_{cooling}$) versus evaporator temperature. From the graph, it is seen that at lower evaporator temperatures and higher condenser temperatures, the full cooling load of 600 Btu/min could not be reached within the 1000 - 3000 rpm compressor speed.

Figure 9 is a plot of the compressor work versus evaporator temperature. When the $\dot{Q}_{evap}$ is constant, as it is for $T_{evap} = 40^{o}F$ and $60^{o}F$, the work of the compressor decreased with decreasing condenser temperature. This is expected from Equation 4. At an evaporator temperature of $0^{o}F$, reverse trend is true because as the condenser temperature drops, the pressure ratio across the compressor decreases increasing the volumetric efficiency

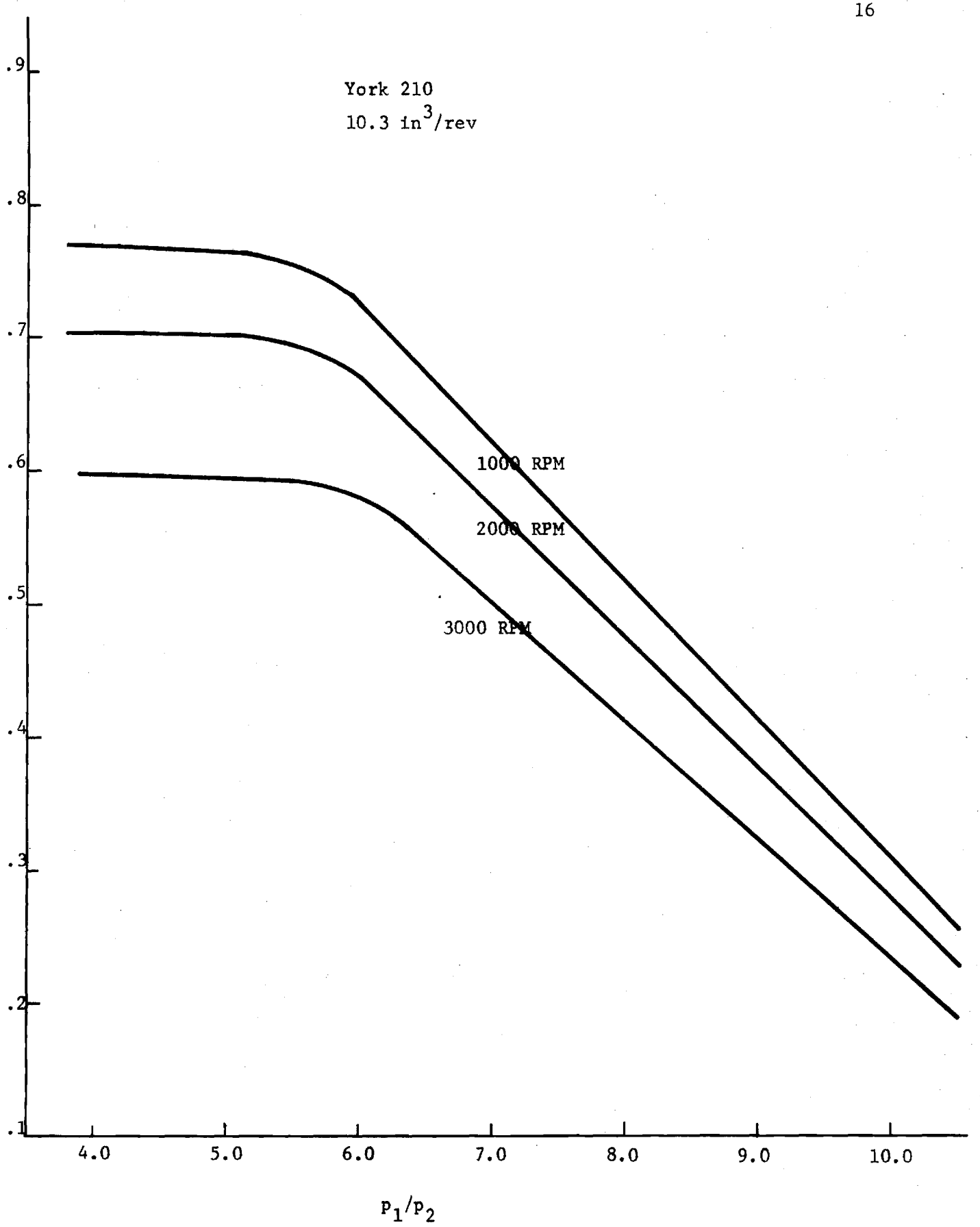

Figure 6. Compressor Volumetric Efficiency vs. Pressure Ratio.

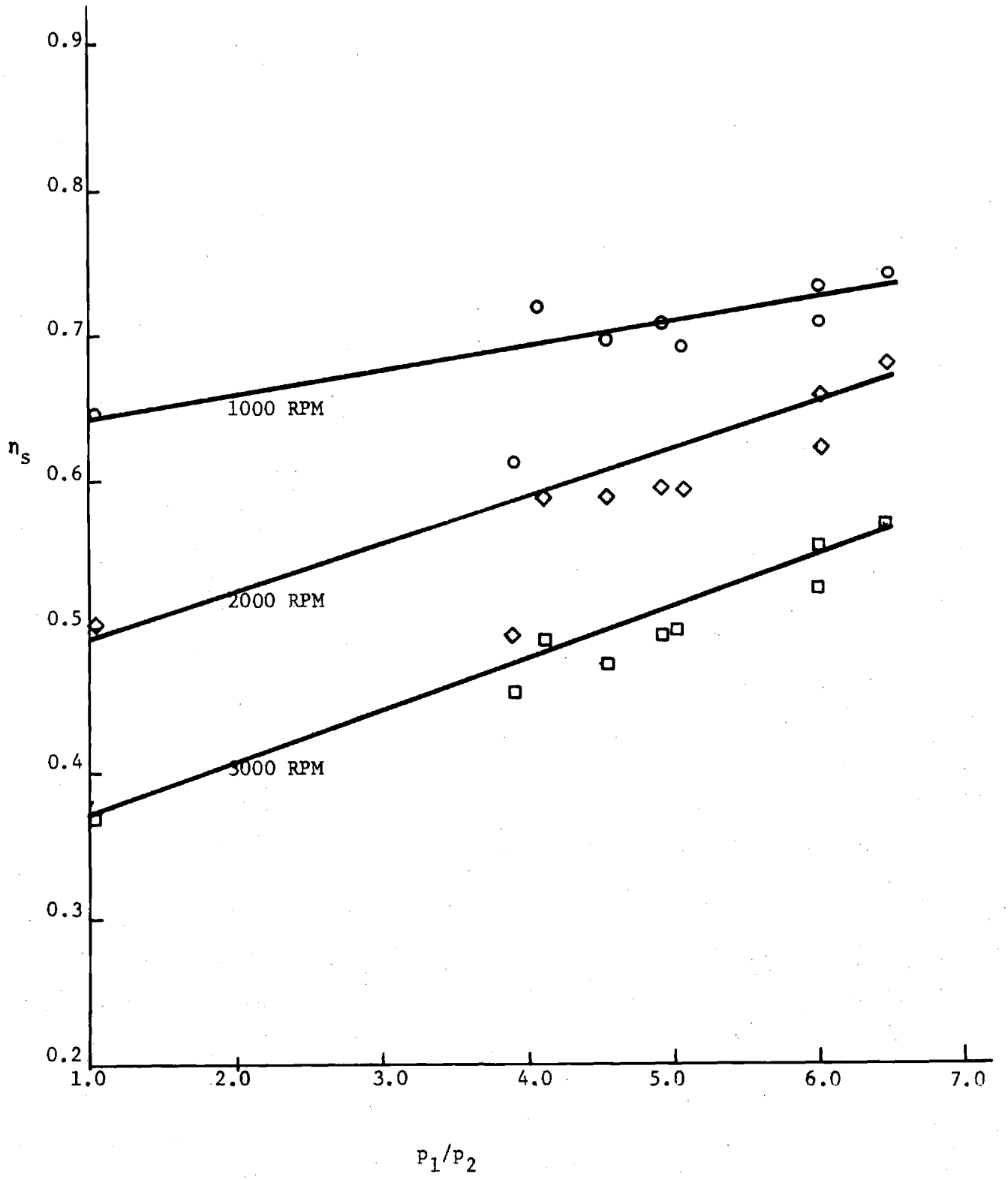

Figure 7. Compressor Isentropic Efficiency vs. Pressure Ratio.

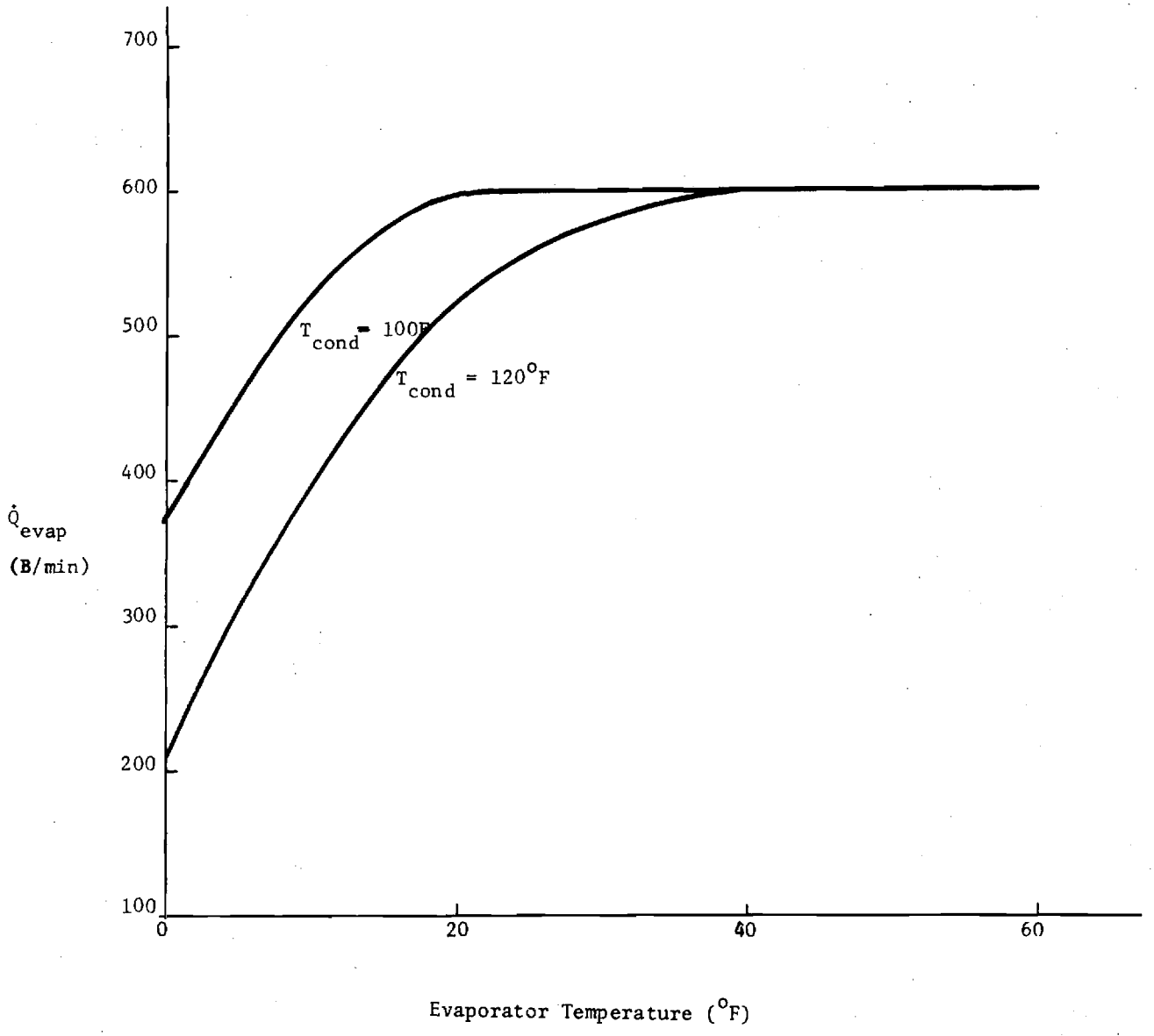

Figure 8. Evaporation Heat Absorption Rate vs. Evaporator Temperature.

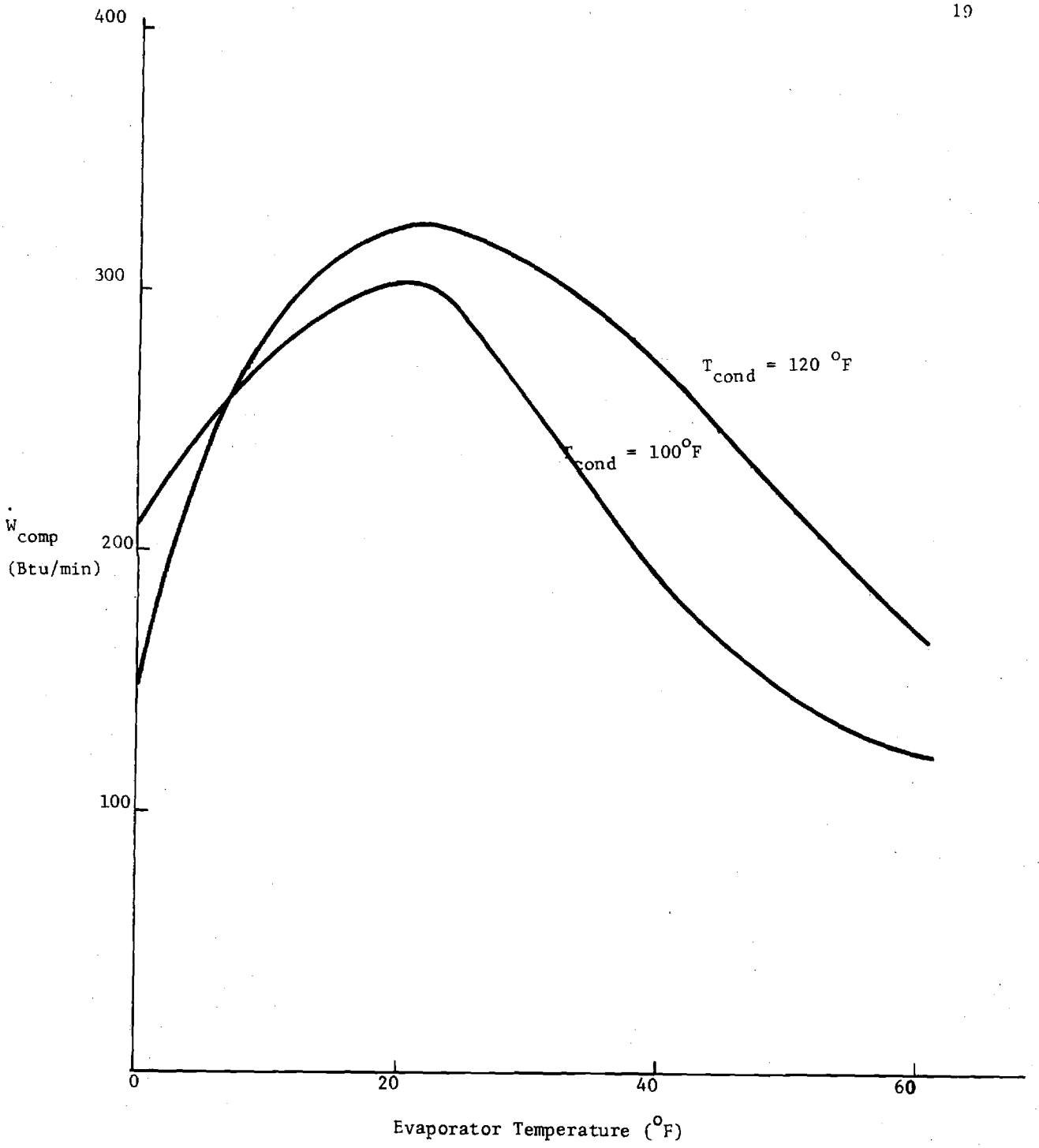

Figure 9. Compressor Power vs. Evaporator Temperature.

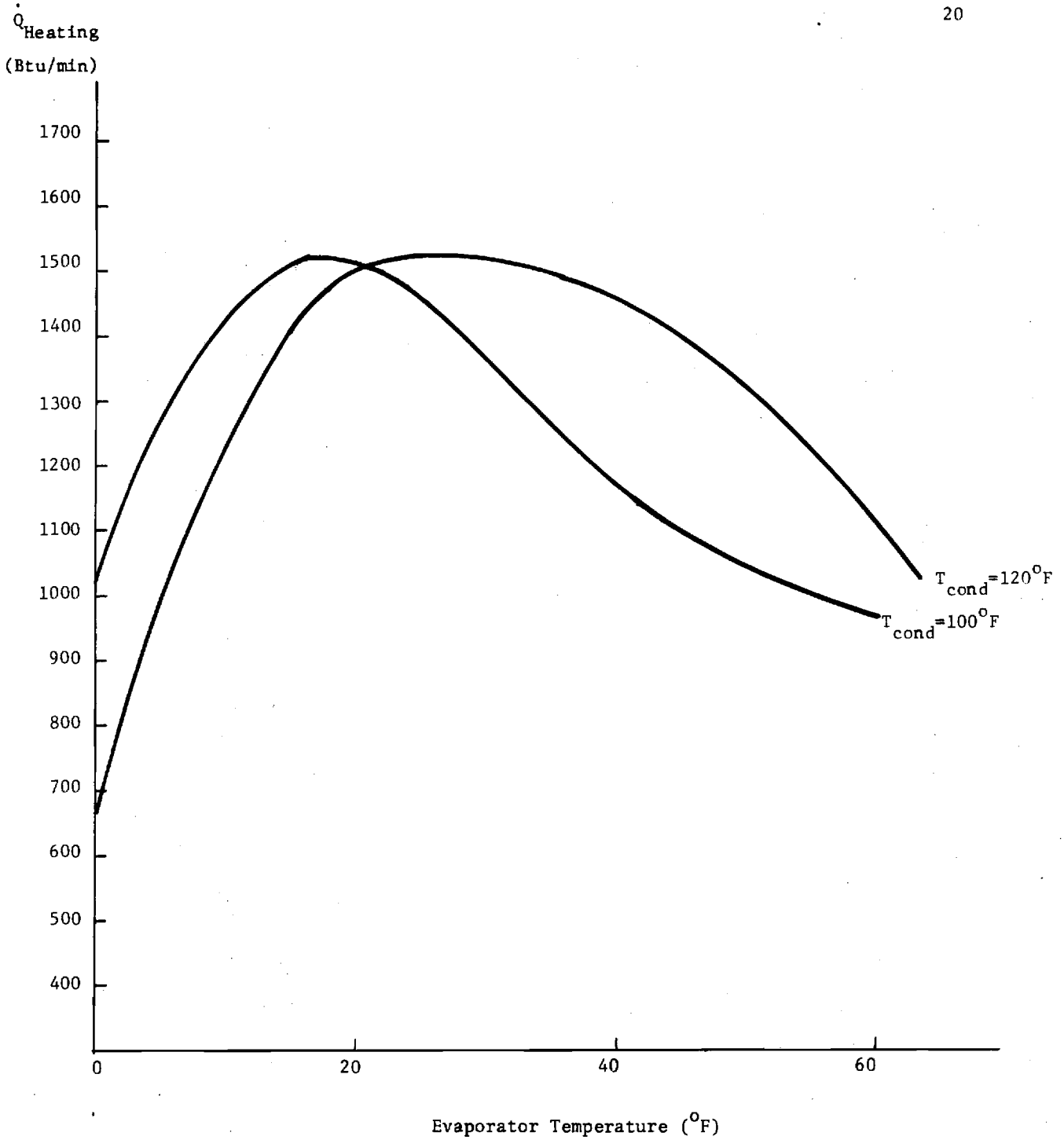

Figure 10. Combined Heat Rejection Rate From the Condenser and Exhaust Heat Exchanger.

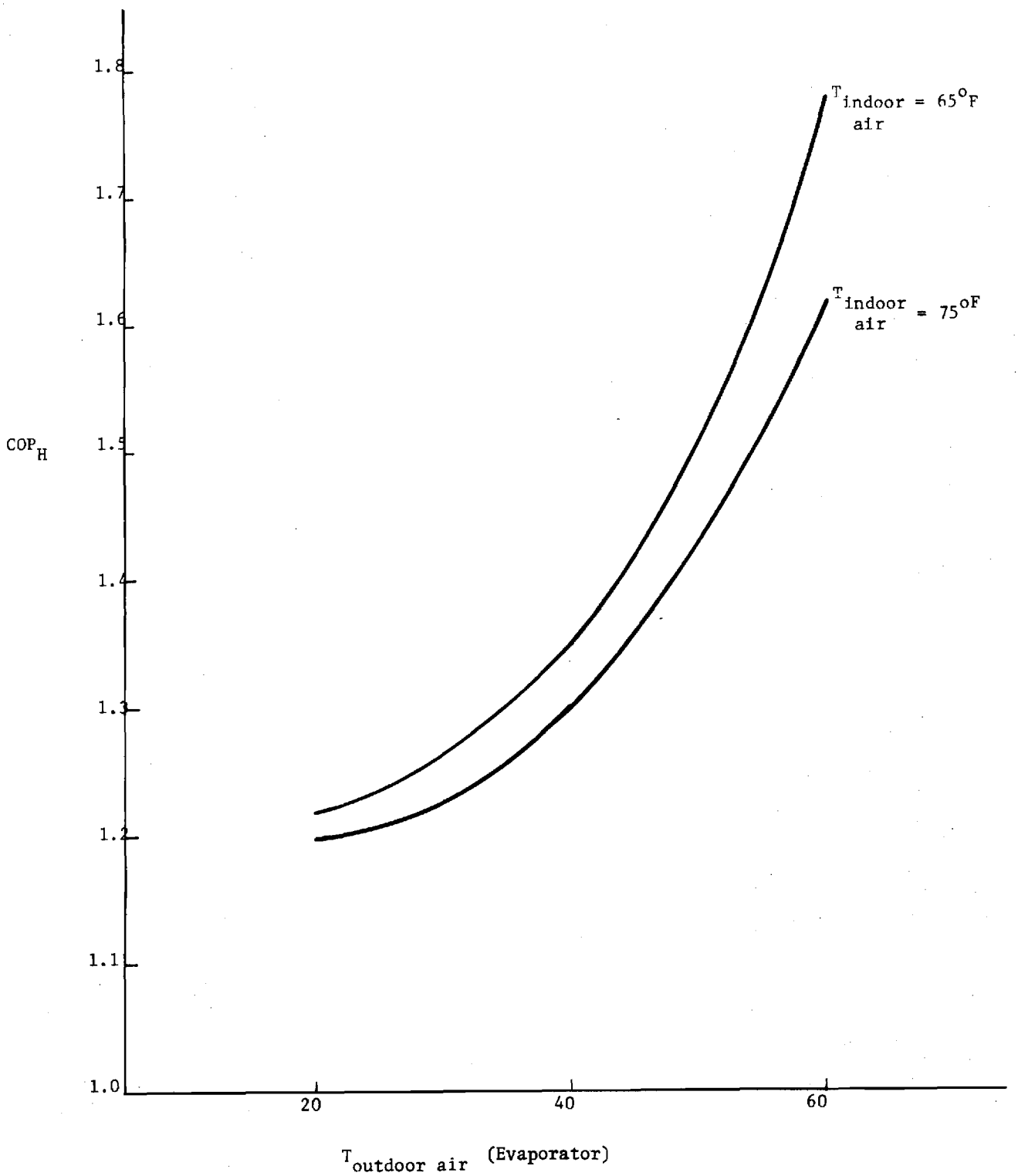

Figure 11. Heating COP vs. Outdoor Air Temperature.

of the compressor as shown in Figure 6. This increases mass flow more than the work per unit mass flow is decreased.

The relationship between the evaporator temperature (^{o}F) and its incoming air temperature (^{o}F) was taken as:

$$T_A = T_{evap} + 0.020\ \dot{Q}_{evap}\ \text{Btu/min} \tag{27}$$

and for the condenser temperature in relationship to its incoming air temperature

$$T_A = T_{cond} - 0.020\ \dot{Q}_{cond}\ \text{Btu/min} \tag{28}$$

These relationships were arrived at after study of several air coil performance curves. The qualitative relationship is correct and the quantitative accuracy appears very reasonable for well designed evaporators and condensers.

Using Equations 27 and 28 in conjunction with Figure 8, 9, and 10, the results shown in Figures 11 and 12 are obtained which yield the heating and cooling COP's as a function of outdoor temperature. The characteristic decreasing COP with increasing ΔT between outside and inside temperatures are apparent. Over conditions taken, ($20 \leq T_a \leq 90$), the COP_H ranges from 1.1 to 1.7 and COP_c ranges from 1.25 to .75. Curves for indoor temperatures of $65^{o}F$ and $75^{o}F$ are shown.

The annual average $\overline{COP_H}$ and $\overline{COP_c}$ may now be calculated from Figures 10 and 11 and Equations 25 and 26 along with the weather data previously shown. These calculations show:

$$\overline{COP_H} = 1.3$$

$$\overline{COP_c} = 0.9$$

These values are very encouraging when compared with other systems.

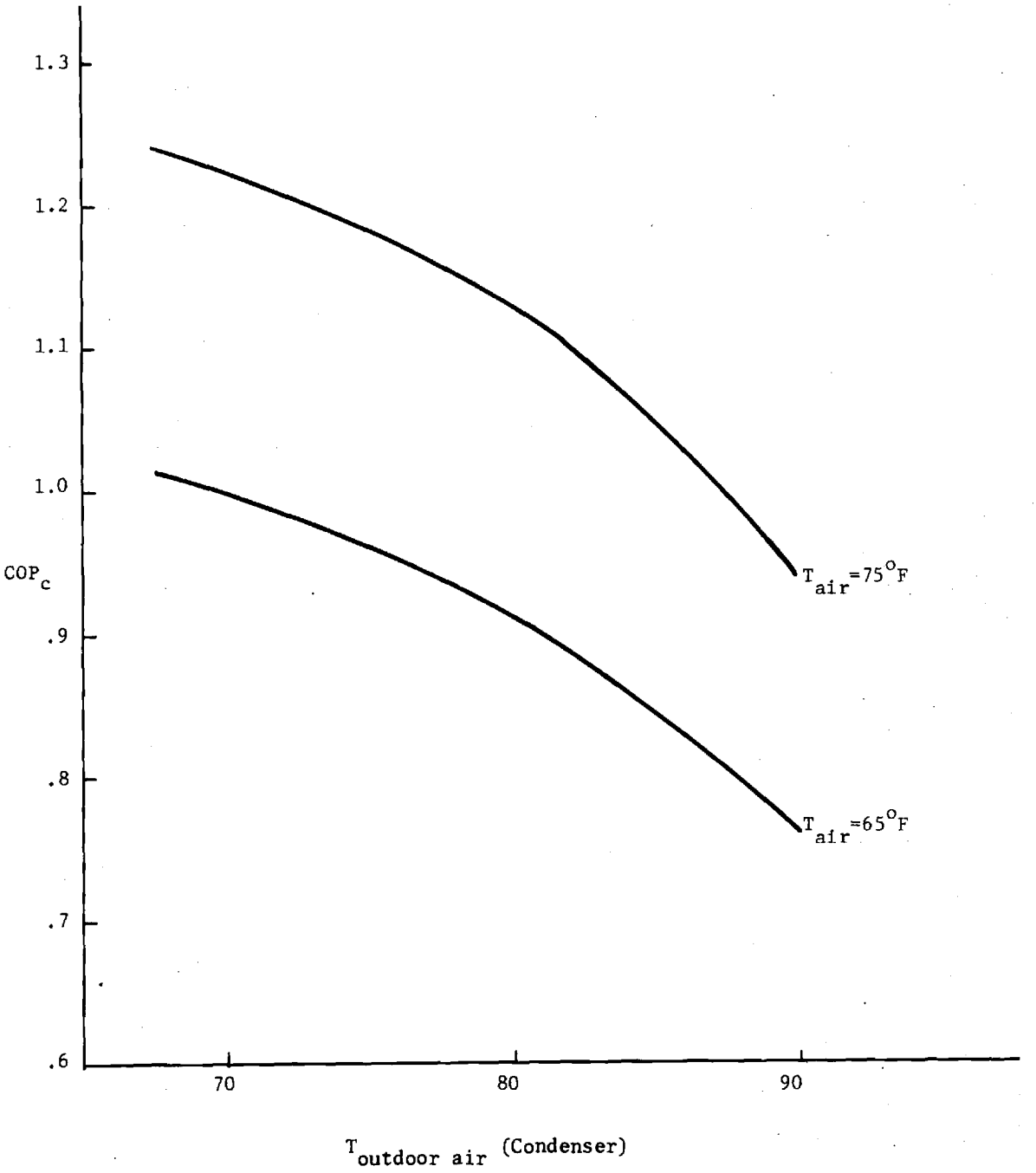

Figure 12. Cooling COP vs. Outdoor Air Temperature.

From their literature search, Calvert and Harden[13] found the COP for a gas furnace can be taken to be 0.7. For an absorption system, the COP is approximately 0.5. An electrical air conditioner has a cooling input about twice its electrical input. The COP_c, as defined in this paper, is the ratio of the cooling or heating output to the heating value of the fuel at the power plant. For an electrical system, the electrical output to the house is generally taken as 0.3 of the fuel energy input at the power plant. The COP_c for the electrical system is then .3 x 2 = .6.

From this analysis, the COP for the natural gas heat pump is significantly higher than that found in other systems. The COP_H is about 86% greater than the COP_H for a gas furnace. For the cooling mode, COP_c is about 80% greater than that for the absorption system and 50% greater than the electrical system when the power plant efficiency is included. These comparisons are shown in Figure 13.

Conclusion

From the calculations performed in this analysis, it is apparent that the refrigeration cycle powered by an engine is worth investigating. The COP obtained from both the heating and cooling modes is significantly higher than existing systems. In conclusion, it appears that this system could offer a dramatic reduction in energy consumption for residential heating and cooling, the two largest residential energy usages.

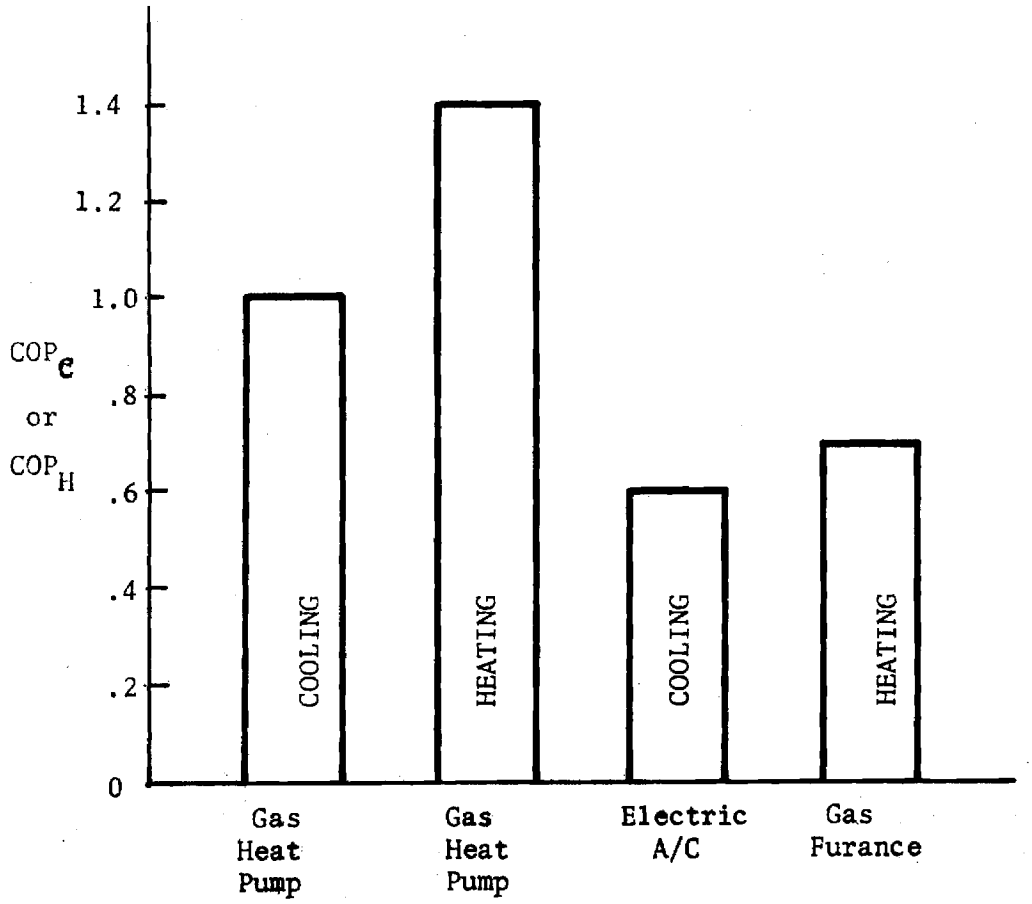

Figure 13. Comparison of Cooling and Heating COP's for Alternate Systems.

CHAPTER III

WANKEL ROTARY ENGINES AS PRIME MOVERS

Introduction

The primary problem in reducing the previously described heat pump to commercial practice is the prime mover. Previous projects by Washington Gas Light Company[1] and Janitrol using natural gas fueled reciprocating I. C. engines have shown that a more reliable natural gas prime mover must be found. These engines were significantly derated making them very large, heavy, costly, and less efficient. The decrease in efficiency is due to the fact that engines have maximum efficiency at full load. Derating requires a larger engine to produce the same horsepower which means higher mechanical losses and lower efficiency.

However, regardless of size, weight, or efficiency, the engine must be highly reliable in order to reach the commercial market.

The Wankel Rotary Engine

One type of engine that shows promise for high reliability as a stationary natural gas fueled prime mover is the Wankel rotary engine. The Wankel possesses certain characteristics that render it superior to a conventional piston engine operating under similar conditions.

The Wankel engine operates on the Otto cycle and has the same processes as a conventional reciprocating internal combustion engine. The Wankel however is extremely simple in design. Fundamentally there are only two moving parts, the rotor and the eccentric shaft. The rotor revolves directly on the eccentric shaft which negates the need for

connecting rods. Intake and exhaust gases pass through parts so valves and valve operating mechanisms are not required. Figure 14 shows an exploded view of the principle engine parts. One important fact is that the output torque is transmitted to the shaft through the eccentric. The internal and external gears shown are timing gears designed to maintain the phase relationship between the rotor and eccentric shaft rotation. The smaller external gear (coaxial with the eccentric shaft) is fixed to one side of the housing.

Since the rotor is three sided there are three separate cycles operating simultaneously. Figure 14 shows the processes which occur in sequence in each rotor of a Wankel engine. There are three power impulses for each rotor revolution, however since the eccentric shaft rotates at three times the speed of the rotor, there is only one power pulse per rotor for each revolution of the output shaft.

The simplicity of the design of the Wankel as compared to conventional engines makes the use of rotary engines in stationary applications very attractive. The smaller number of moving parts makes maintenance easier and the lower specific weight (lb/hp) and size is also an advantage. Another advantage of the Wankel engine is the lower vibration level. It has been shown that the amplitude of vibration of a piston engine is over five times that of a Wankel[2]. This reduction of vibration is important in stationary long life applications since it reduces metal fatigue of brackets and accessories.

The parts of the Wankel engine which have been shown to wear out first are the rotor seals. Tests conducted on gasoline on various Wankel engines have indicated a rather disappointingly short rotor seal life[2,3]. The rotor seals are located at the apex of each rotor and act as a gas seal. Preliminary tests conducted at Georgia Tech prior to

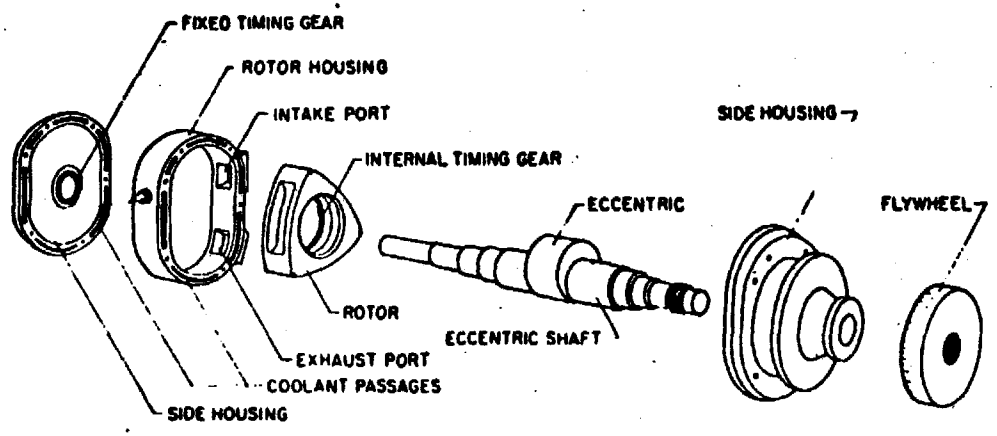

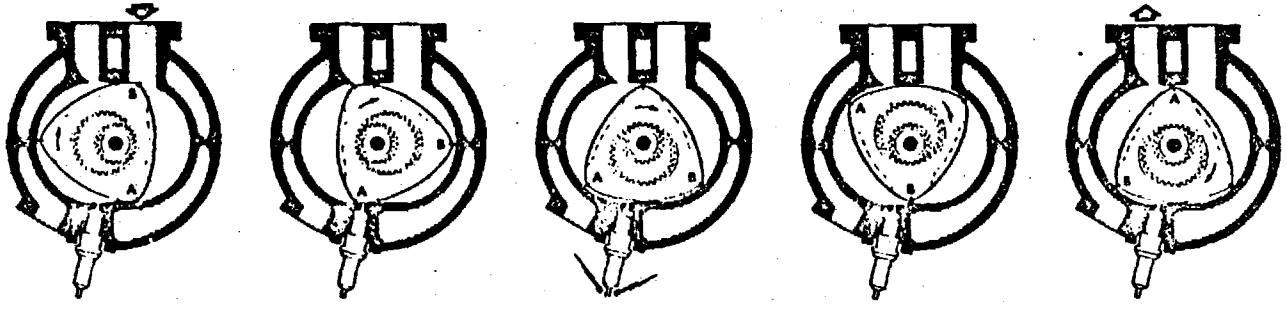

Figure 14. Basics of a Single Rotor Wankel Engine.

this project indicated a much longer seal life when the engine is operated on natural gas. This increased seal life would appear to give the Wankel the long life characteristics needed in a natural gas heat pump.

Another problem in natural gas heat pumps, related to the prime mover, is the waste heat recovery. The size and equipment necessary to recover this low temperature heat is large and adds to the capital cost of the system. This waste heat is generally in the form of 150°F to 250°F cooling air or water and 1000°F exhaust gases.

In reciprocating I. C. engines the waste heat is usually split about 40/60 between the cooling medium and the exhaust gases; i.e. 60% (or more) of the waste is contained in the cooling medium and 40% (or less) in the exhaust gases.

The waste heat in a Wankel rotary is in somewhat of a different form. Due to the short exhaust passages from the combustion chamber to the exhaust manifold, little cooling of the exhaust is accomplished. This results in Wankel exhaust temperatures in the 1500 to 2000°F range. The waste heat is then split about 40/60 between the cooling media and the exhaust gases.

This higher exhaust temperature, and consequent different split in waste heat containment, has significant implications in the natural gas heat pump in that a majority of the waste heat from the Wankel is at a high temperature making it easy to recover. Smaller, more compact and less expensive heat recovery equipment may therefore result. In fact, in many cases only the high temperature exhaust heat may possibly be recovered resulting in very small, and inexpensive heat recovery.

Wankel Test Engines

Four Wankel rotary engines were selected for testing to determine the characteristics of the natural gas fuel Wankel. The specifications of each are shown in Table 1. The Toyo Kogyo was chosen as appropriate for the larger commercial applications, while the OMC, and two smaller Sachs engines were selected to cover the size spectrum in which engines are presently available. These engines were tested on natural gas to determine power, efficiency, exhaust emissions, and seal wear on todays Wankel rotary engines.

Table 1

Test Engine Specifications

	Toyo Kogyo TK0839	OMC	Sachs KM914A	Sachs KM37
Rotors	2	1	1	1
Displacement	573cc (35 in^3)x2	528cc (32 in^3)	300cc (18.3 in^3)	108cc (6.59 in^3)
Cooling	Water	Air	Air	Air
Max. Hp	130 hp/7000 rpm	45 hp	16 hp/4500 rpm	5.5 hp/4900 rpm
Max. Torque	115 ft-lb/4000 rpm		18.8 ft-lb/3500 rpm	
Weight	215 lbs.		70 lbs.	34 lbs.

CHAPTER IV

TOYO KOGYO ENGINE TESTS

Introduction

A Toyo Kogyo TK039 engine was obtained from Curtis Wright Corp. for testing. This engine is sold by Toyo Kogyo in their European version of the Mazda RX2. It does not contain the thermal reactor and associated emission control systems found on the American Mazdas. The engine was mounted on a water dyno with elaborate safety cut-off switches for automatic shut down in case of any failure which would be harmful to the engine.

The engine was tested as delivered on gasoline to establish base line performance data. It was then converted to natural gas and performance and emission data obtained. Long term tests were then undertaken to determine seal wear at constant load and speed (3600 rpm). The equipment and data will be described in subsequent sections. The exhaust emissions instrumentation used on all engines is described in Appendix A.

Equipment

Dynamometer

The dynamometer used was a Taylor hydraulic dynamometer with a 6500 RPM maximum operating speed and a dynamometer constant of 6000. A Fairbanks-Morse 200 pound capacity beam scale was fitted to the dynamometer for accurate torque and horsepower readings. The dynamometer was coupled to the engine directly; no clutch or transmission was used. Water supply to the dynamometer was directly from the building supply through flexible

rubber hose so that torque readings would not be affected. Exhaust water was dumped outside through a low restriction 2-1/2 inch pipe.

Electrical System

Since the primary purpose of the test was the accumulation of long-time wear data, it was necessary to implement a fail-safe control system capable of long periods of unattended operation and sensitive to any out of tolerance condition which might damage equipment or facilities. The electrical system was independent of external power and automatically shut-down when any one of seven safety circuits activated. These safety circuits consisted of the following malfunction inputs: (Figure 15)

1) Low oil pressure
2) Low oil temperature
3) High water temperature
4) Low dynomometer water pressure
5) Low cooling water pressure (this input doubled as an overspeed protector at high RPM, the engine water pump inlet pressure dropped low enough to trip the water pressure switch. The activation point of the switch could be adjusted by the cooling water pressure regulator. (Figure 18).
6) Manual kill button-located on the control panel
7) Emergency kill button-located on the top of the carburetor

When operating on methane, an engine vacuum switch was placed in series with the power relay and the normally closed 12 volt d.c. solenoid operated gas valve. This provided a safety back-up to assure fuel cut-off in the event of a malfunction. With the exception of this vacuum switch, all safety circuits could be defeated by an overide switch located

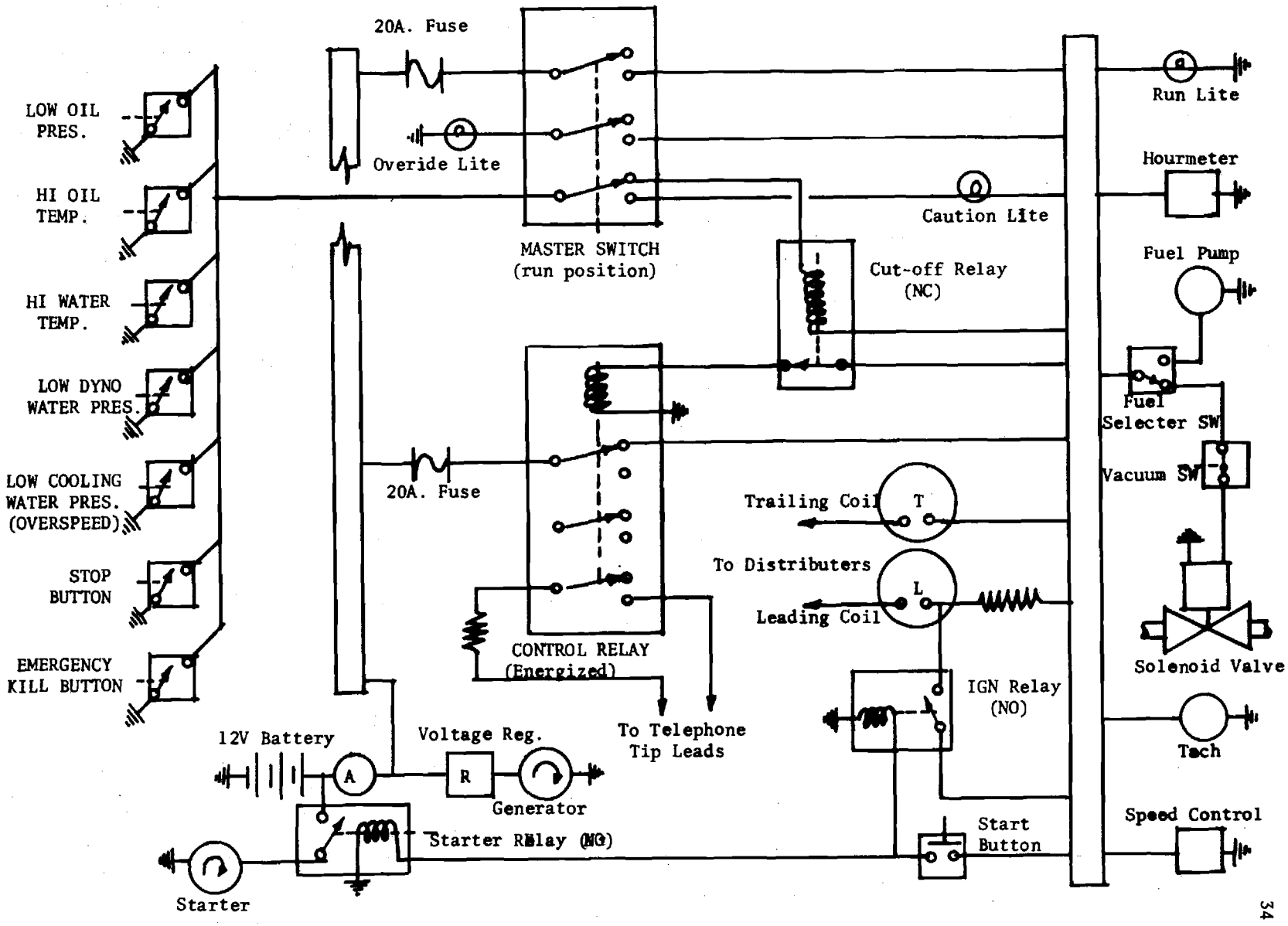

Figure 15. Mazda Electrical Control Schematic.

on the control panel. RPM control was achieved by using a conventional automobile cruise control unit. The unit was a "Speedostat" manufactured by the Dana Corp. This unit is commonly used on General Motors automobiles. It was electrically operated from the control panel and converted a mechanical RPM input into a vacuum output which operated the carburetor. The RPM input was taken from the rear dynomometer shaft and was transmitted by a standard automotive speedometer cable. It was necessary to reduce the speed of the cable by a factor of 4 in order to drive the speed control within its design RPM range. This was achieved by cascading two Stewart Warner speedometer speed reducers.

Since it was required to operate the engine for long periods without a technician being present, a telephone monitoring circuit was devised which enabled a technician to remotely determine whether the engine was still operating. To achieve this, a six hundred ohm resistor was automatically shunted across the telephone tip leads when the control relay deactivated due to any engine or accessory malfunction. This seized the telephone circuit which gave a busy signal when dialed from a remote location.

At the times when more than one engine was being tested, this system did not enable the caller to determine which engine was shut down so another monitoring system was devised and built (Figure 16). The second system automatically answered the phone and allowed an operator to auraly monitor the laboratory from a remote location. By dialing the laboratory telephone one could then listen to the engines and determine their condition.

Operational instrumentation was housed in a control panel. Instruments used were all of Stewart-Warner manufacture and included 0-8000 rpm Model 970 tachometer, oil pressure 0-100 psi, oil temperature 270^{o}F, water

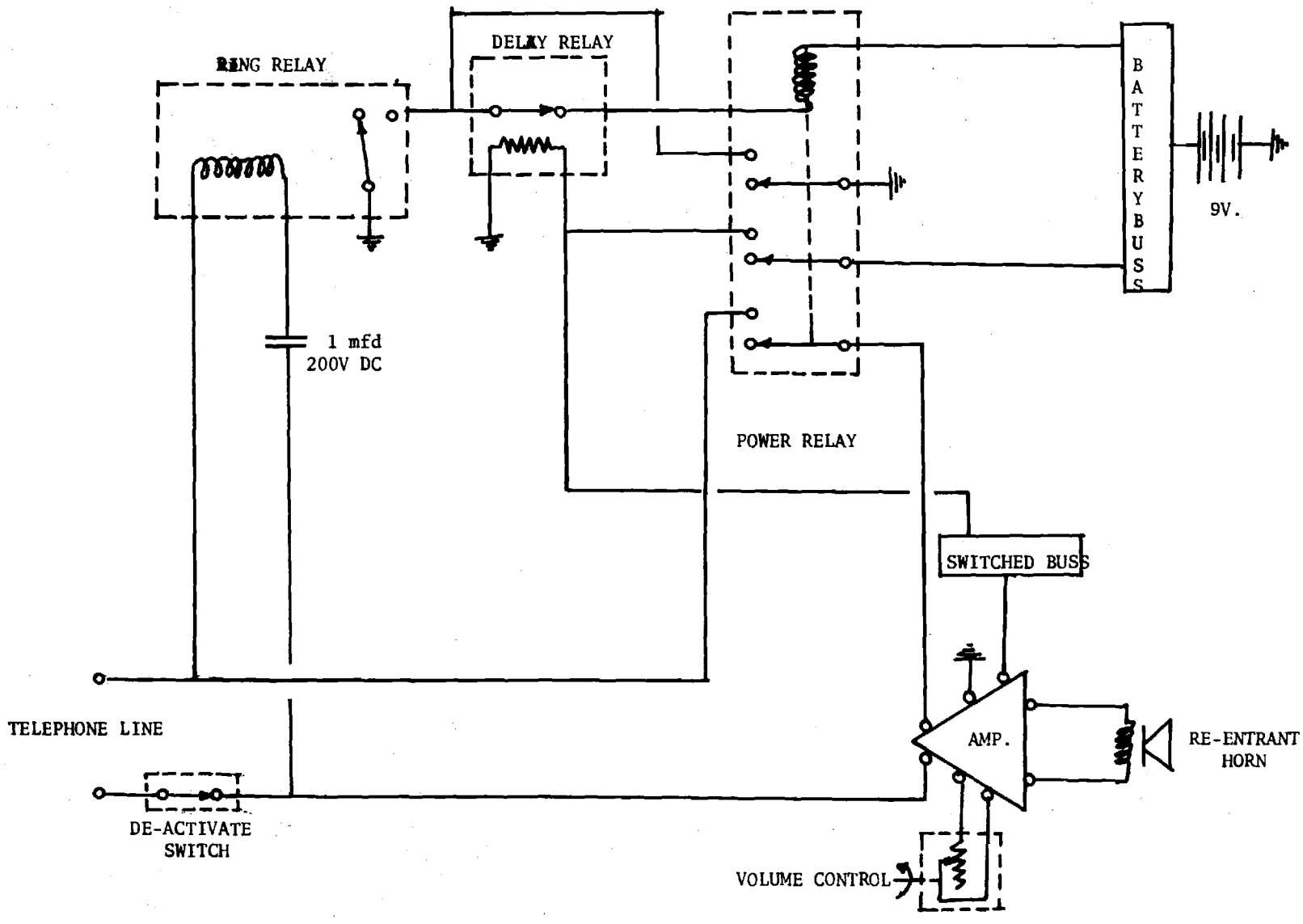

Figure 16. Telephone Monitor Schematic

temperature 250°F, amperes, vacuum gauge 0-30 inches Hg, and a 10,000 hour hourmeter.

Ignition System

The TK0839 engine is equipped with two distributors, and the fuel is ignited by two spark plugs firing sequentially in each rotor chamber. At factory specifications, the leading spark plugs fire when each rotor face is at top dead center of its cycle, and the trailing spark plugs fire 10° after top dead center (at idle with no vacuum advance).

All the testing of the engine using gasoline was accomplished using factory ignition timing specifications. Due to the lower flame speed of natural gas and a higher octane rating, it was necessary to determine optimum spark timing on natural gas which would not result in cylinder pressures above that obtained on gasoline. This was necessary in order to obtain optimum performance and avoid the possibility of engine seal failure with the carbon apex seals. A special spark plug with a pieziolectric pressure transducer was installed. The pressure was monitored with an oscilliscope and scope camera. Scope pictures were made (operating the engine on gasoline at factory timing specs) at all conditions where maximum combustion pressures were expected. These pressures were recorded. It was determined later using the same procedures that this pressure could not be reached much less exceeded on methane at any timing setting. However, an optimum timing setting for methane was determined by achieving the maximum area under the pressure curve, and consequently maximum torque. These traces are shown in Figure 17 .

Cooling System

The TK0839 engine is water cooled and the stock water pump was used. Engine oil is also circulated through the two rotors for cooling purposes.

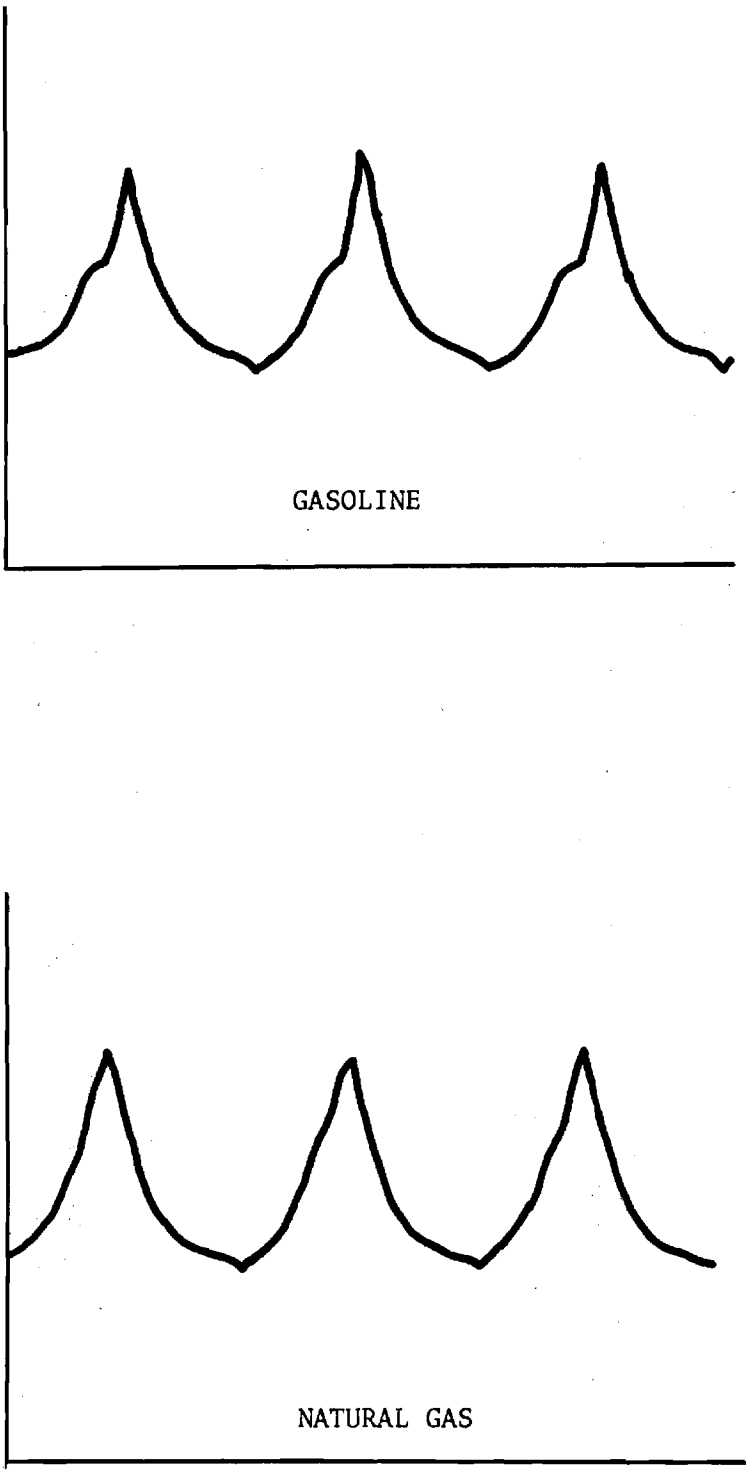

Figure 17 . Chamber Pressure Traces in Gasoline and Natural Gas.

In the automobile this requires a relatively large oil to air heat exchanger to cool the oil. This sytem was discarded in favor of a oil to water marine oil cooler manufactured by Chris Craft Inc. The oil cooler had a secondary function of preheating the cooling water prior to entering the engine block. The controlling component of the cooling system was the stock thermostat supplied with the engine. (See Figure 18) In order to achieve stability of operating temperatures, it was necessary to limit the pressure differential across the thermostat. This was accomplished by installing a pressure regulator on the inlet side of the water pump and a 20 foot standpipe on the drainage side of the engine to a constant back pressure. A 5 psi pressure differential between inlet and outlet resulted in temperature oscillations of less than 4 degrees at all operating conditions encountered.

Fuel System

Gasoline was supplied to the engine from a small two-gallon can (which could be easily weighed) through an electric fuel pump to the stock four-barrel carburetor. This provided enough gasoline for several tests before refilling was necessary.

Natural gas was supplied through an alternate arrangement. Gas entered the building from the gas main and was passed through a dry gas meter, an electric solenoid valve and a regulator. From the regulator, it was routed through a one inch flexible hose to an Impco mixing valve mounted on the carburetor. An adapter plate was made for the carburetor, and operation was similar to standard automotive natural gas dual fuel systems. Manual throttle control was accomplished with a marine type throttle similar to those used in outboard motor application. Engine exhaust was routed out of the building through a specially designed thick

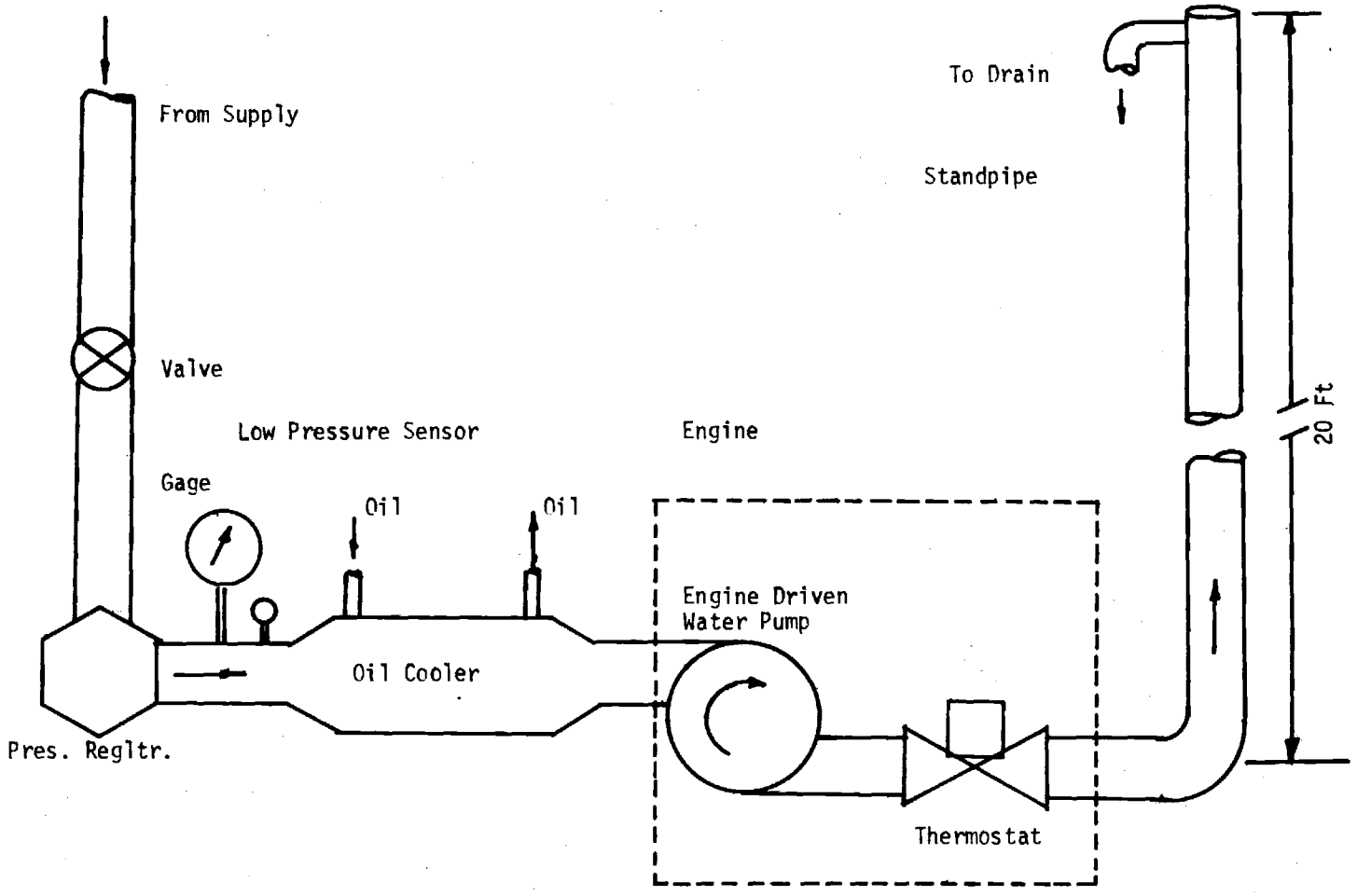

Figure 18. Mazda Cooling System Schematic

walled header system and two standard automobile mufflers located outside the building. The system was well sealed and the laboratory was well ventilated with a large exhaust fan.

Exhaust Temperature

A chromel-alumel thermocouple was installed in the exhaust manifold directly opposite the exhaust ports. The thermocouple was referenced to an ice bath. A Hewlett Packard null volt meter was used to measure voltage.

Tests Procedure and Results

Engine Preparation

The engine was received directly from the factory and the first thing that was accomplished was a complete disassembly of the engine to measure all seals. The rotor apex seals, the side seals and the corner seals were measured using a Starret 0-1 inch # TY36RL micrometer. The engine was then reassembled and placed on the dynamometer test stand.

Gasoline Power and Efficiency Tests

Once the engine was in an operational configuration, the first tests to be conducted were power and efficiency on gasoline. As previously described a two gallon gasoline can mounted on a scale and a stop watch were used to measure fuel consumption. Tests were made at three different torque settings and at six different RPM's giving a total of 18 different readings. At each RPM the engine was run at wide open throttle (WOT) and the WOT torque was determined. Then the engine was run at 2/3 and 1/3 of this torque.

Figure 19 shows the horsepower vs. RPM curves produced by the gasoline powered engine at three different load settings. As can be seen, horsepower

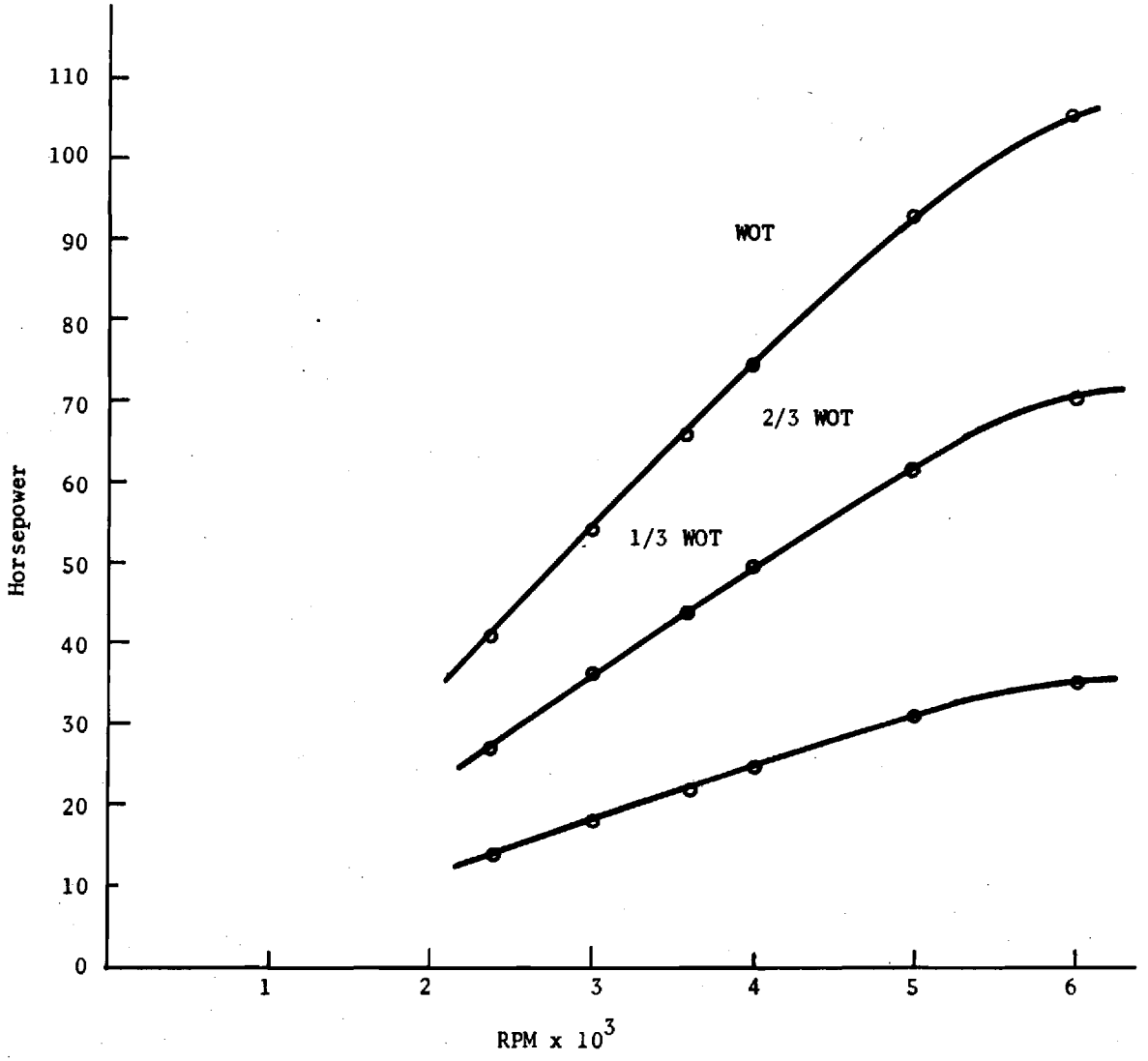

Figure 19 . Mazda RX-2 Horsepower vs.RPM (Gasoline).

increases nearly linearly with RPM at each load setting. This is indicative of a very nearly constant engine torque throughout the entire RPM range. In these tests no attempt was made to change the air fuel ratios from those supplied by the factory carburetor.

Figure 20 shows the thermal efficiency vs. RPM curves for the gasoline powered engine at three different load settings. Maximum efficiency is obtained at about 4200 RPM at 2/3 of wide open throttle. A comparison of Figure 19 with Figure 20 shows that the engine would be developing about 50 horsepower at this RPM and load setting.

Figure 20A shows fuel consumption plotted against horsepower at three different power settings. These curves increase nearly linearly as might be expected. Note that at 2/3 of the wide open throttle torque, the curve has a large discontinuity at the point where the secondaries of the carburetor open. Spot checks for repeatability were run and results indicate a repeatability of $\pm$ 5%.

Natural Gas Power, Efficiency, and Emission Tests

Natural gas tests were run on the engine after it had about 1200 hours on it. The reason for the delay was problems in the operation of the emission testing equipment. Natural gas data was taken at five different engine speeds. For each engine speed the equivalance ratio was varied from .9 to 1.0 to 1.1. The air-fuel ratio was accurately determined using FID analysis of the intake mixture and relations[6] given in Appendix B. For each equivalence ratio at each RPM the load was varied from a WOT load, 2/3 WOT torque, and 1/3 WOT torque.

At each particular setting of RPM equivalence ratio and load, the following data were taken; manifold vacuum, fuel flow rate, exhaust temperature, volume concentration of hydrocarbons, volume concentrations

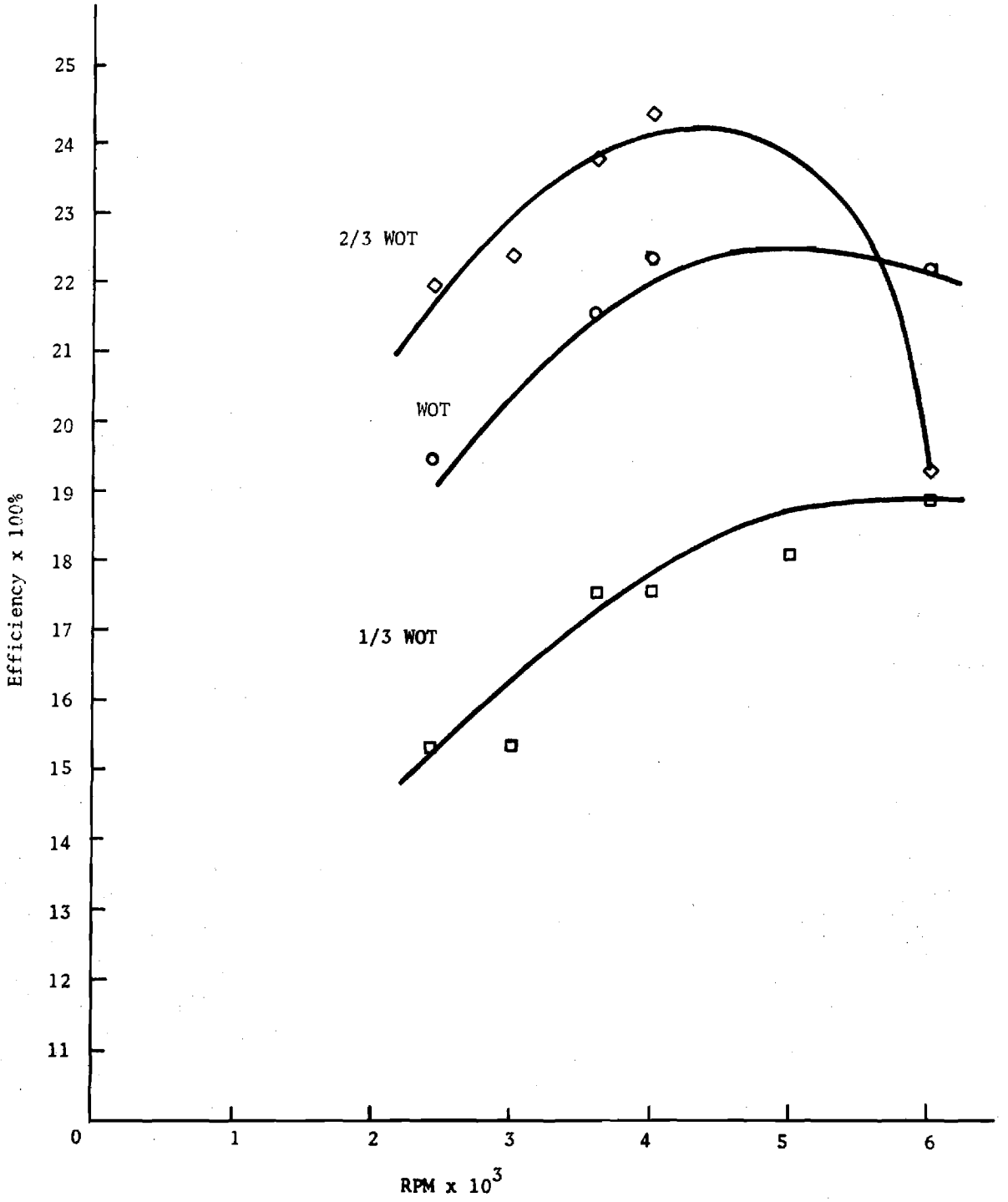

Figure 20. Mazda RX-2 Thermal Efficiency vs. RPM (Gasoline).

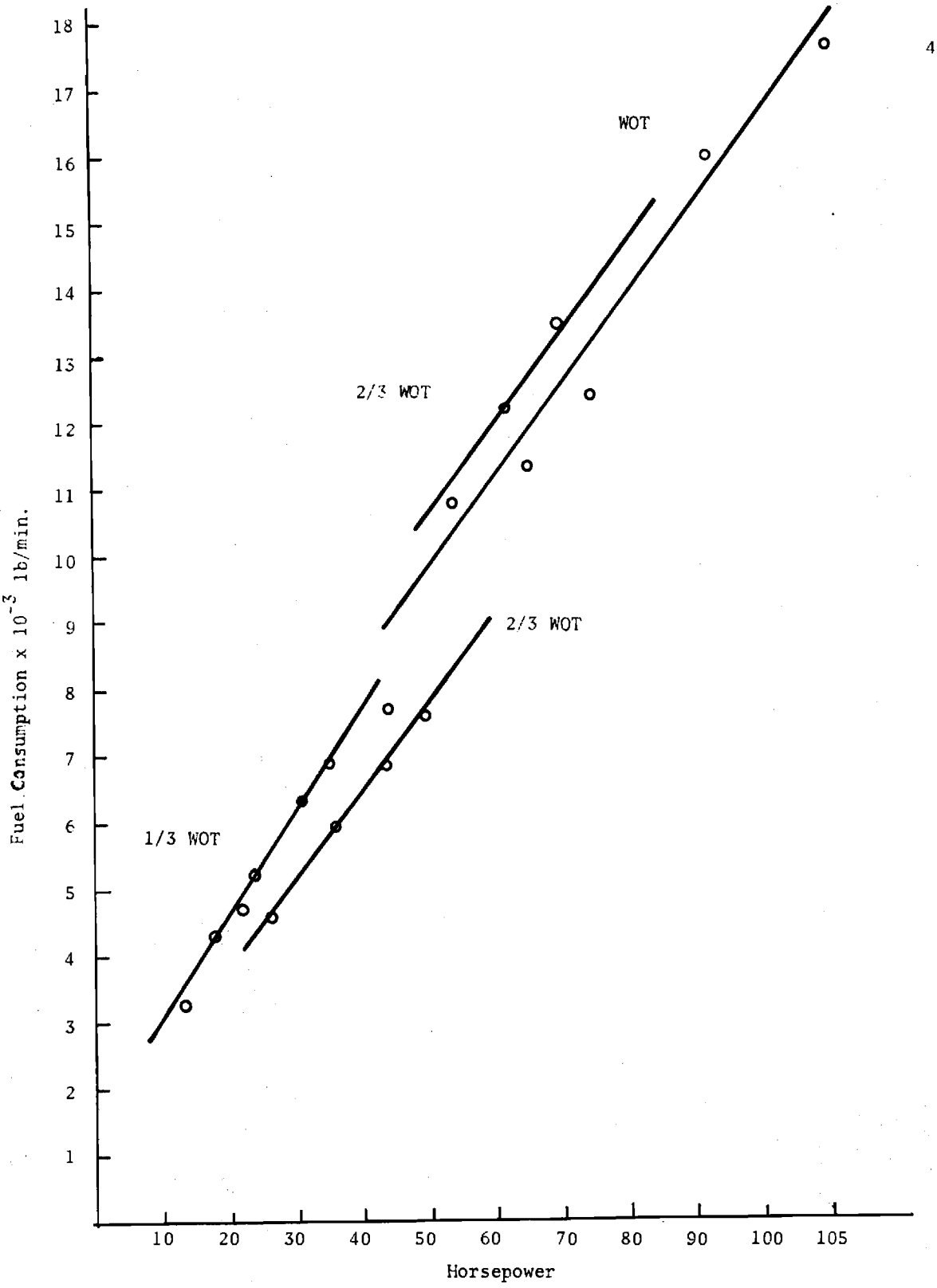

Figure 20A. Mazda RX-2 Fuel Consumption vs. Horsepower (Gasoline).

of NO, volume concentration of CO_2 and volume concentration of CO. In all, 500 data points were taken.

The procedure used was as follows. The engine was first run at wide open throttle at the designated RPM and equivalence ratio. The WOT torque was determined. After the engine stabilized the data readings were taken from the instruments previously described. The engine was run at WOT for all three equivalence ratios and then the 2/3 WOT torque or 1/3 WOT torque values were set and the speed control was used to stabilize the engine. In this way all five engine speeds were tested.

Figures 21 , 22 , and 23 show curves of horsepower vs. RPM for three torque settings. Figure 21 shows data run at an equivalence ratio of 0.9. Figure 22 shows data for a stoichiometric air fuel ratio. Figure 23 shows data for a 1.1 ER. These curves show that the engine tends to loose power at the higher RPM's when operated at leaner mixtures. At the stoichiometric and rich fuel settings the curves rise nearly linearly closely paralleling the earlier gasoline curves. The engine on natural gas produced about 15% less power than on gasoline. This has been noted by earlier researchers and is attributable to the lower flame speed of methane combined with the high volume occupied by the gaseous fuel.

Figures 24 , 25 and 26 show curves of thermal efficiency vs. RPM at ER of .9, 1.0, 1.1 respectively. The best thermal efficiencies were obtained at the stoichiometric air fuel mixture. At a .9 ER (fuel lean) lean misfire tended to lower efficiency considerably. At a 1.1 ER (fuel rich) the engine ran well, but had a lower efficiency. Also as the thermal efficiency decreased the exhaust temperature increased. These are given in Appendix D.

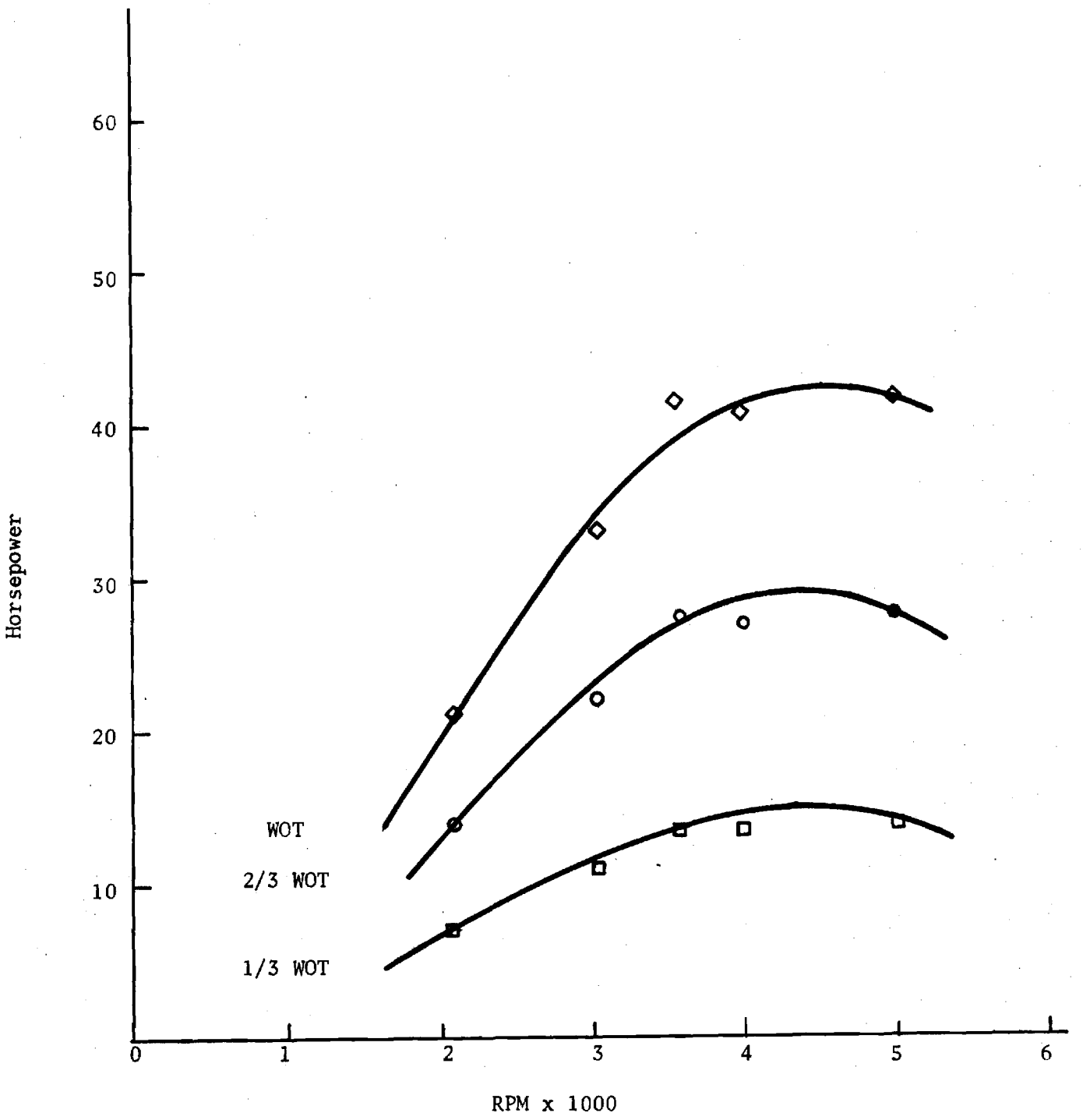

Figure 21 . Mazda RX-2 Horsepower vs. RPM at ER = 0.9 (Methane).

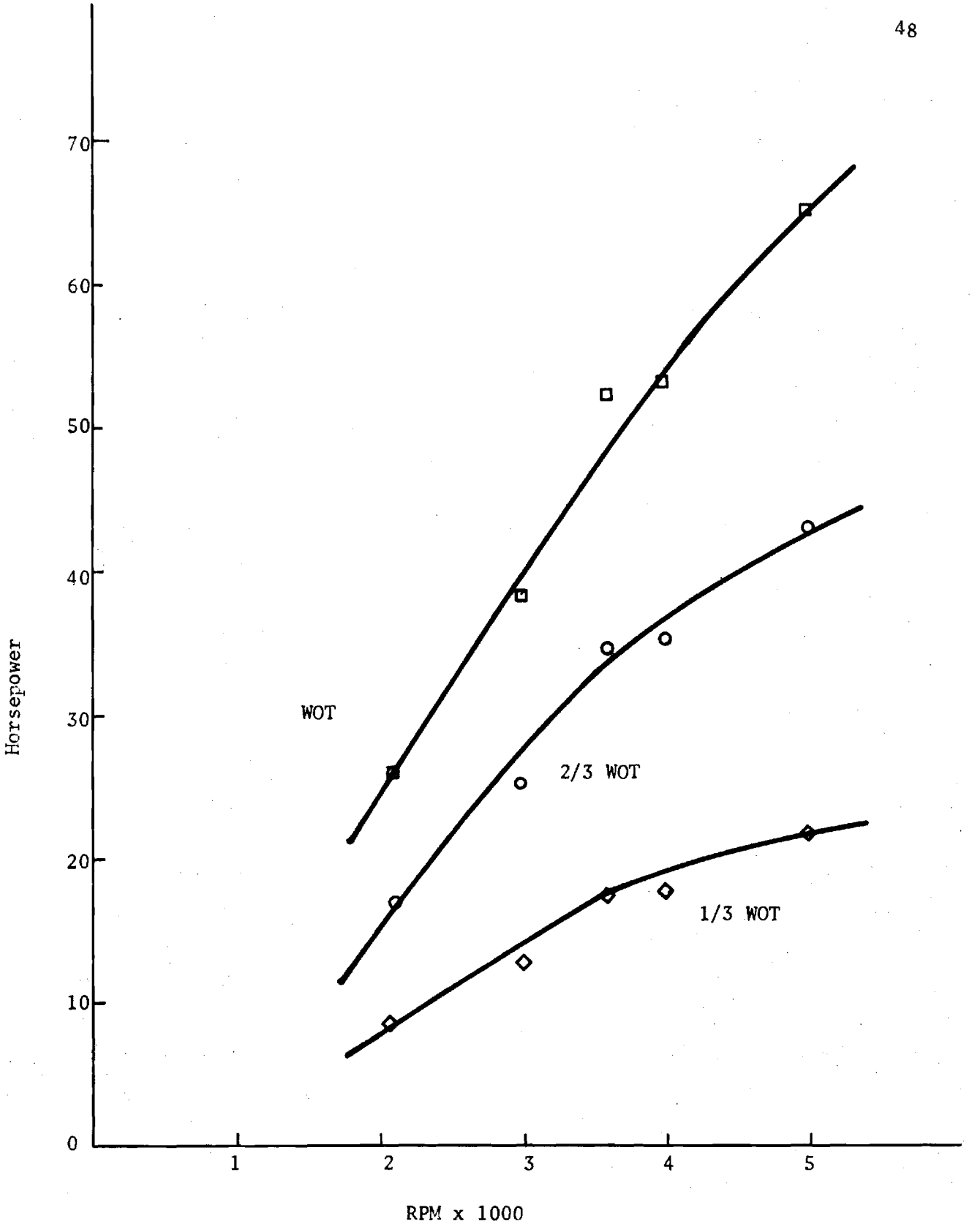

Figure 22 . Mazda RX-2 Horsepower vs. RPM at ER = 1.0 (Methane).

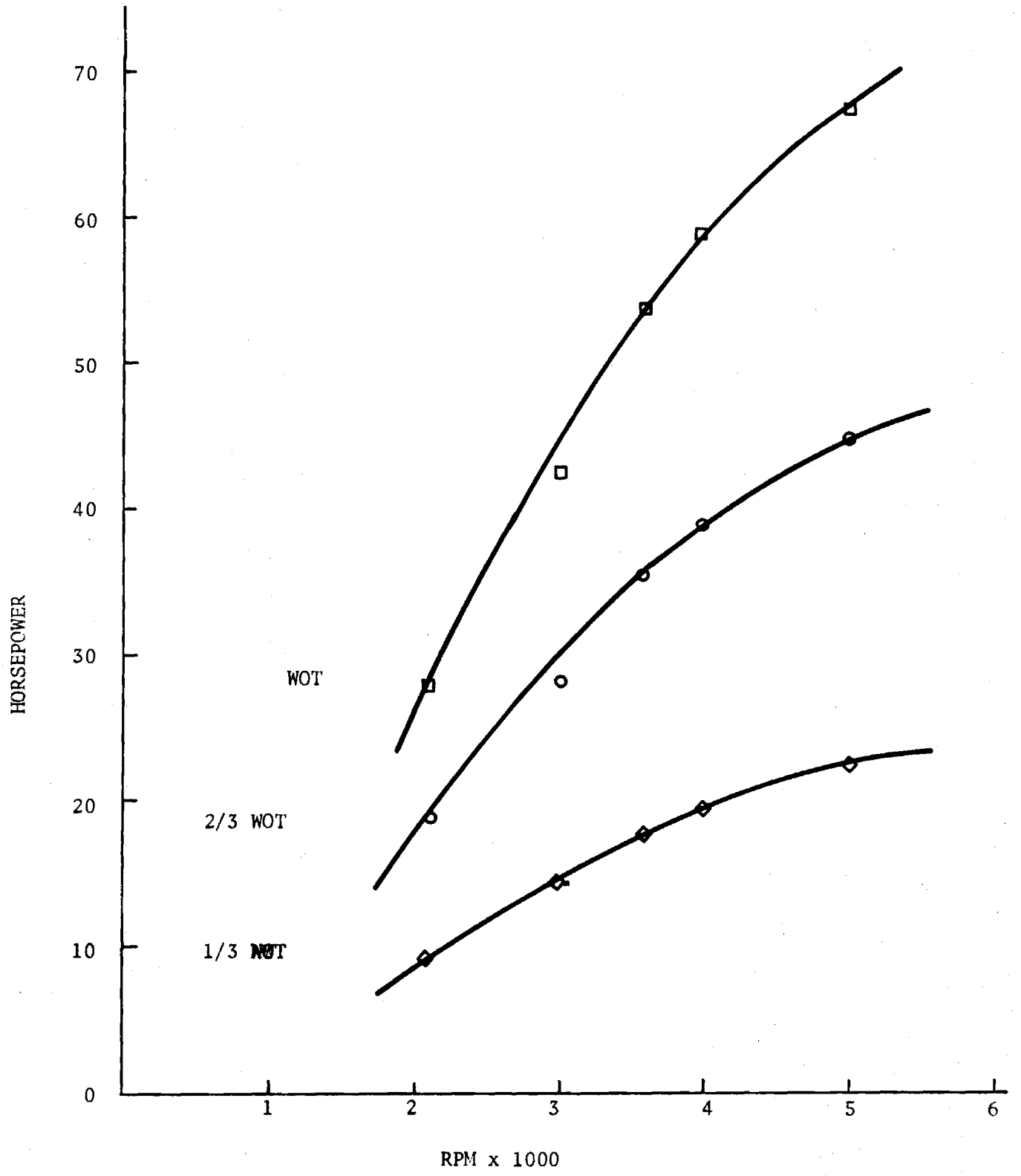

Figure 23 . Mazda RX-2 Horsepower vs.RPM at ER = 1.1 (Methane).

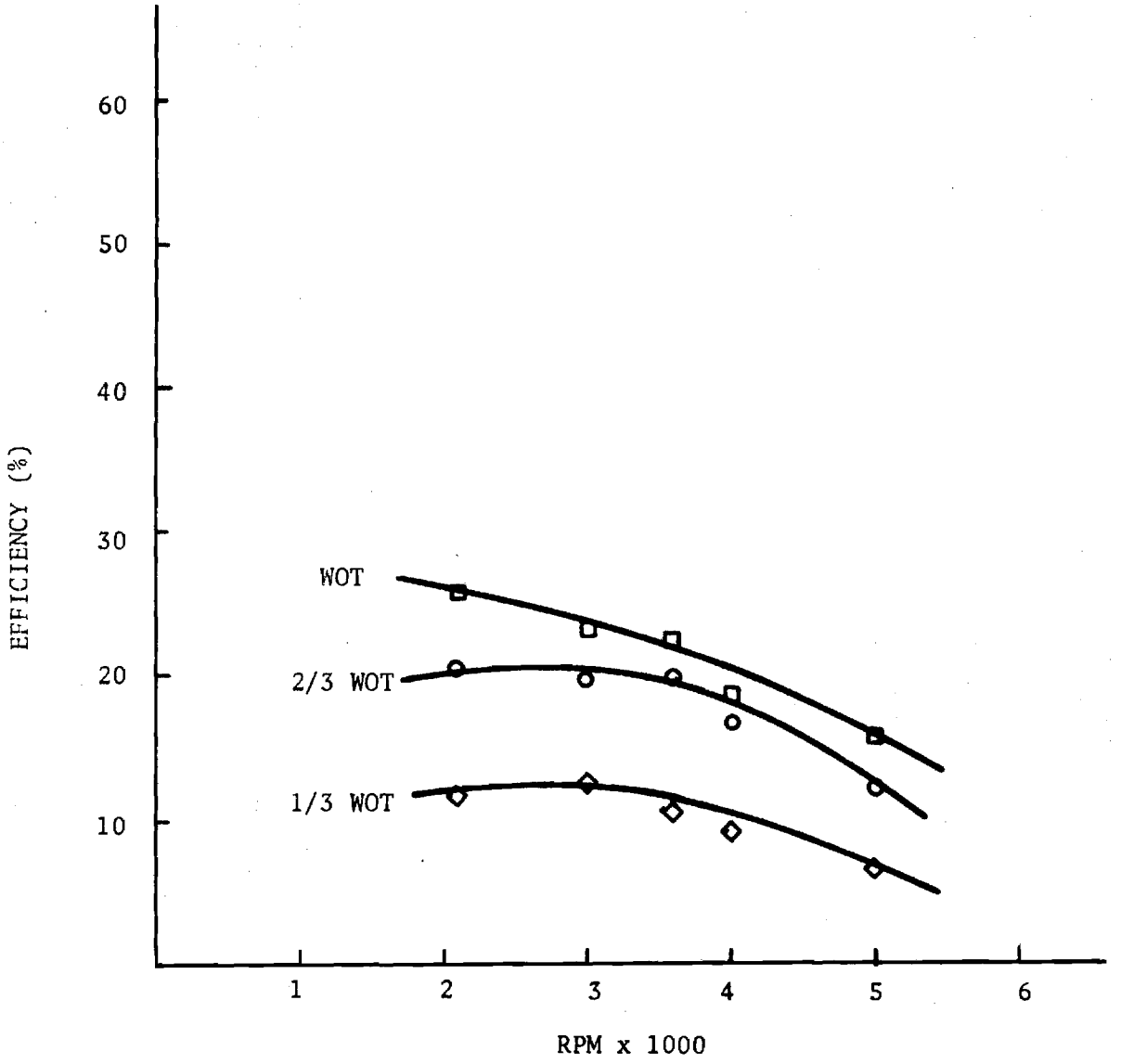

Figure 24 . Mazda RX-2 Thermal Efficiency vs.RPM at ER = 0.9 (Methane).

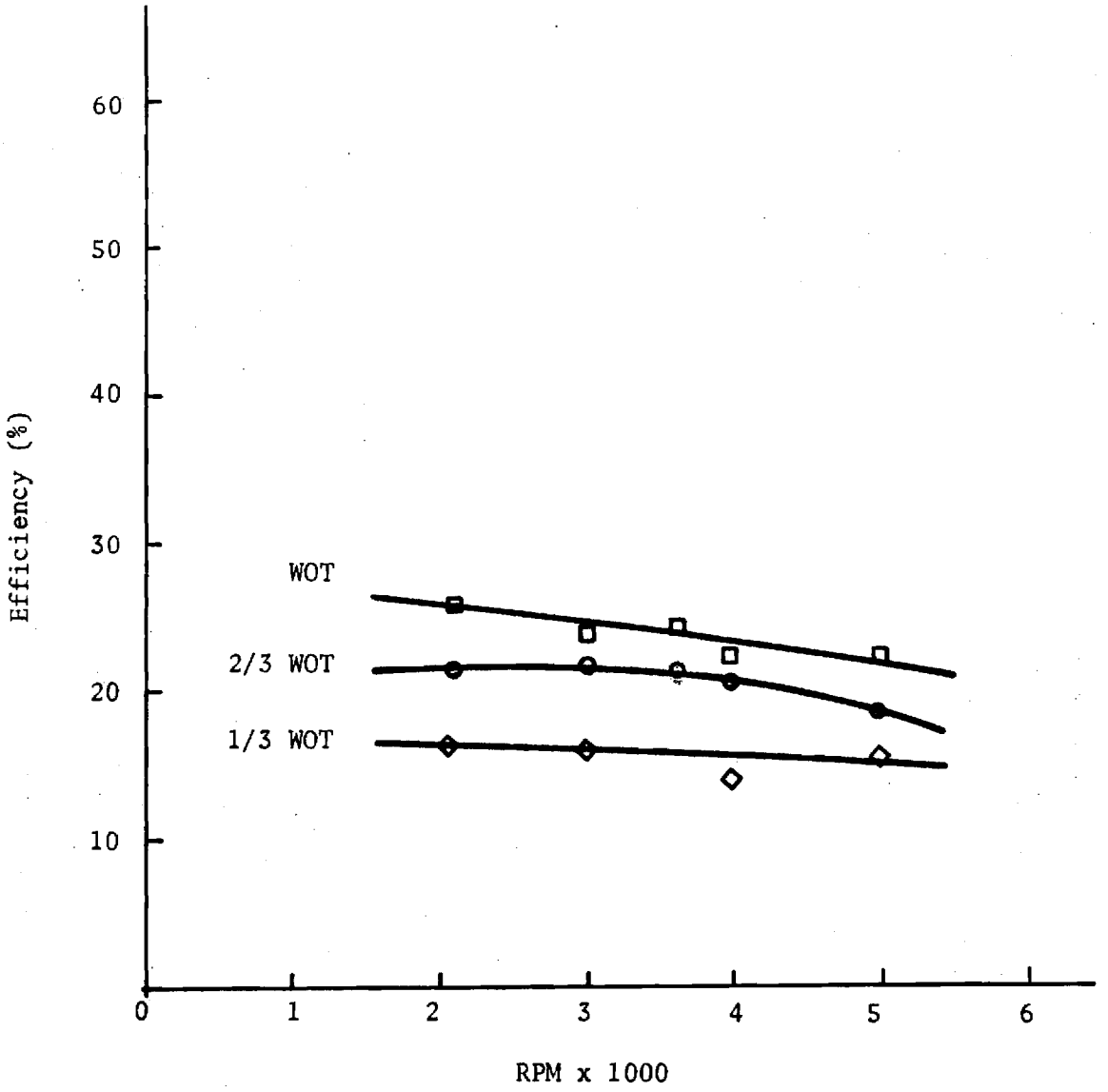

Figure 25 . Mazda RX-2 Thermal Efficiency vs.RPM at ER = 1.0 (Methane).

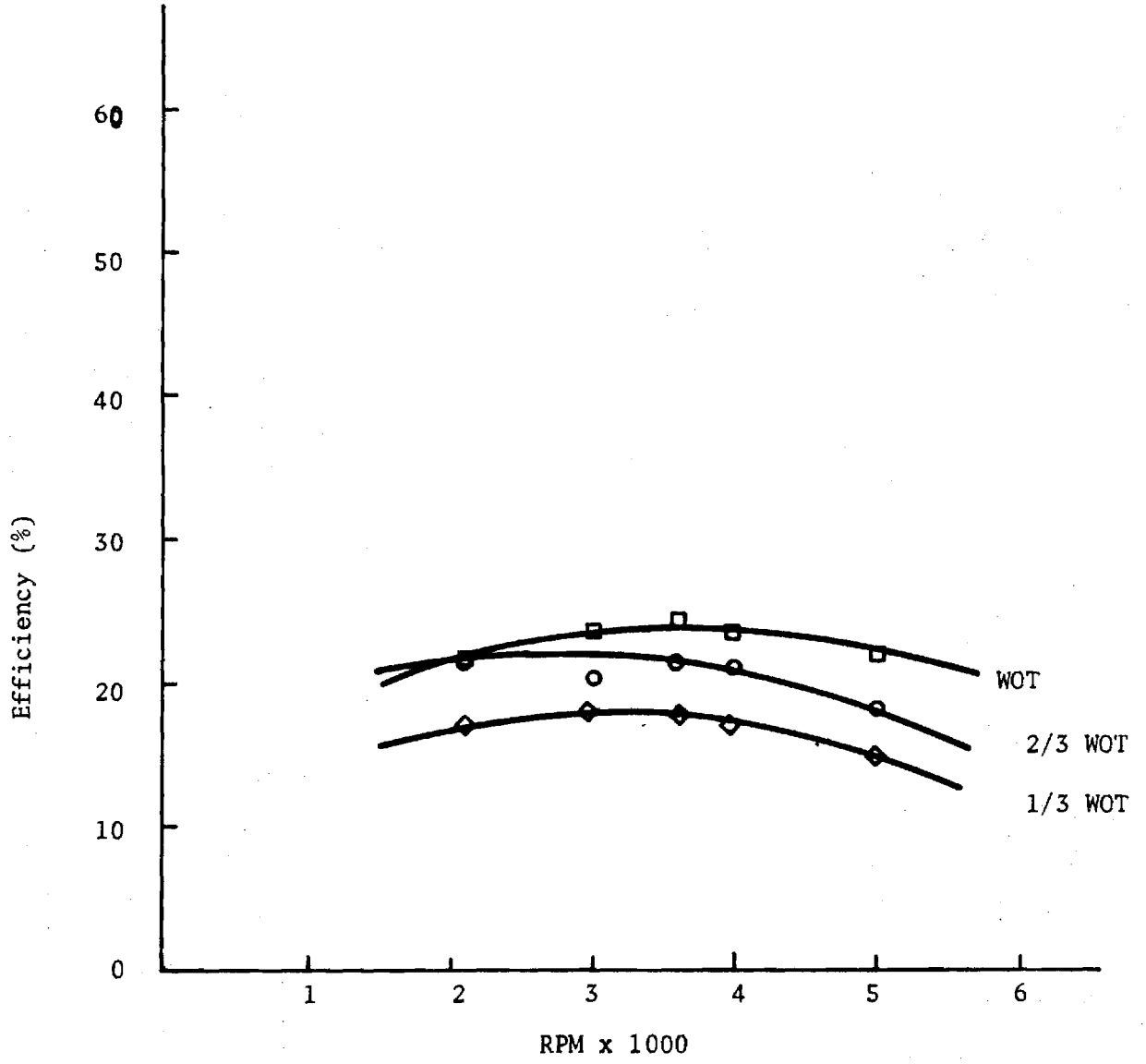

Figure 26 . Mazda RX-2 Thermal Efficiency vs.RPM at ER = 1.1 (Methane).

Natural Gas Exhaust Emission

Exhaust emissions tests were conducted only on methane. Hydrocarbon, NO_x, CO, and CO_2 concentrations were monitored at three different loads, five different engine speeds and three different air fuel ratios and a complete matrix of data points was assembled. The data is shown in Figures 27 through 35 . All pollution concentrations are expressed on a gm/hp-hr basis and the method showing the conversion from dry volume concentration to mass per hp-hr is shown in Appendix C . Spot checks for repeatability revealed an approximate repeatability of ±5% in the following curves.

Figures 27 , 28 , and 29 are fairly typical of hydrocarbon emission with air fuel ratio. At the 1/3 WOT torque setting lean misfire causes the hydrocarbon emissions to increase drastically as a .9 ER is approached. At a stoichiometric air fuel ratio hydrocarbon emissions are at a minimum. Figures 27 , 28 , and 29 also show the basic tendency of the engine toward lower hydrocarbon emissions with increased engine speed and RPM.

Figures 30 , 31 , and 32 show grams of carbon monoxide per horsepower hour vs. A/F ratio for three different loads. The amount of carbon monoxide increases as the mixture becomes rich as expected. CO curves at all three load conditions are very similar because CO depends almost solely on air fuel mixture.

Figures 33 , 34 , and 35 show grams of NO_x per horsepower hour vs. A/F ratio for three different loads. Since the maximum amount of NO is formed at the highest combustion temperature, the amount of NO tends to be maximum at stoichiometric air fuel mixtures. Lean misfire can also cause and increase in combustion temperature.

Figures 33 , 34 and 35 do not yield typical NO curves. This data was obtained with an NO_xNDIR instrument and its accuracy can be questioned. However, it should yield good results as to the magnitude of NO emissions expected from natural gas fueled Wankels.

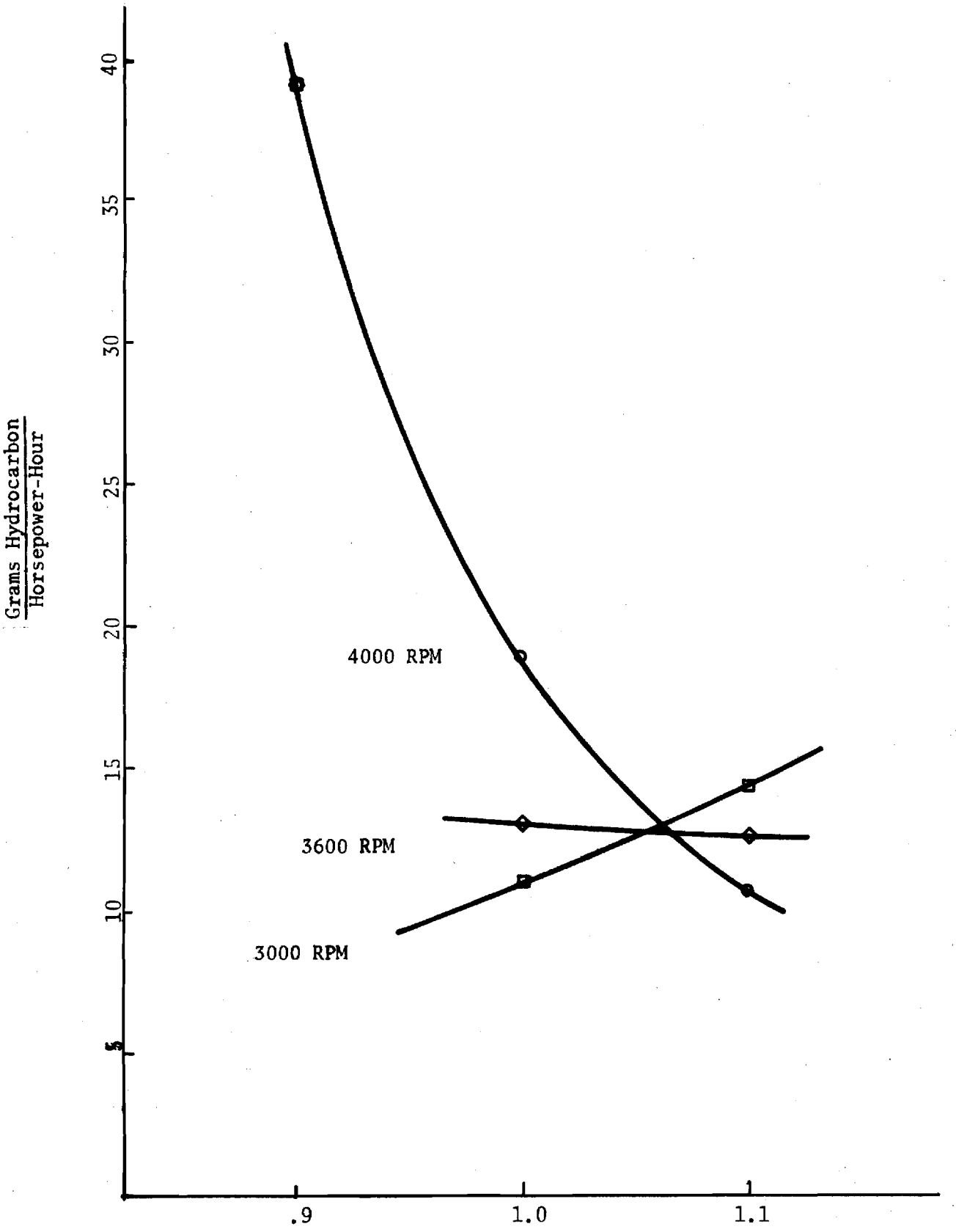

Figure 27. Mazda RX-2 Hydrocarbon Emissions vs. ER at 1/3 WOT Torque (Methane)

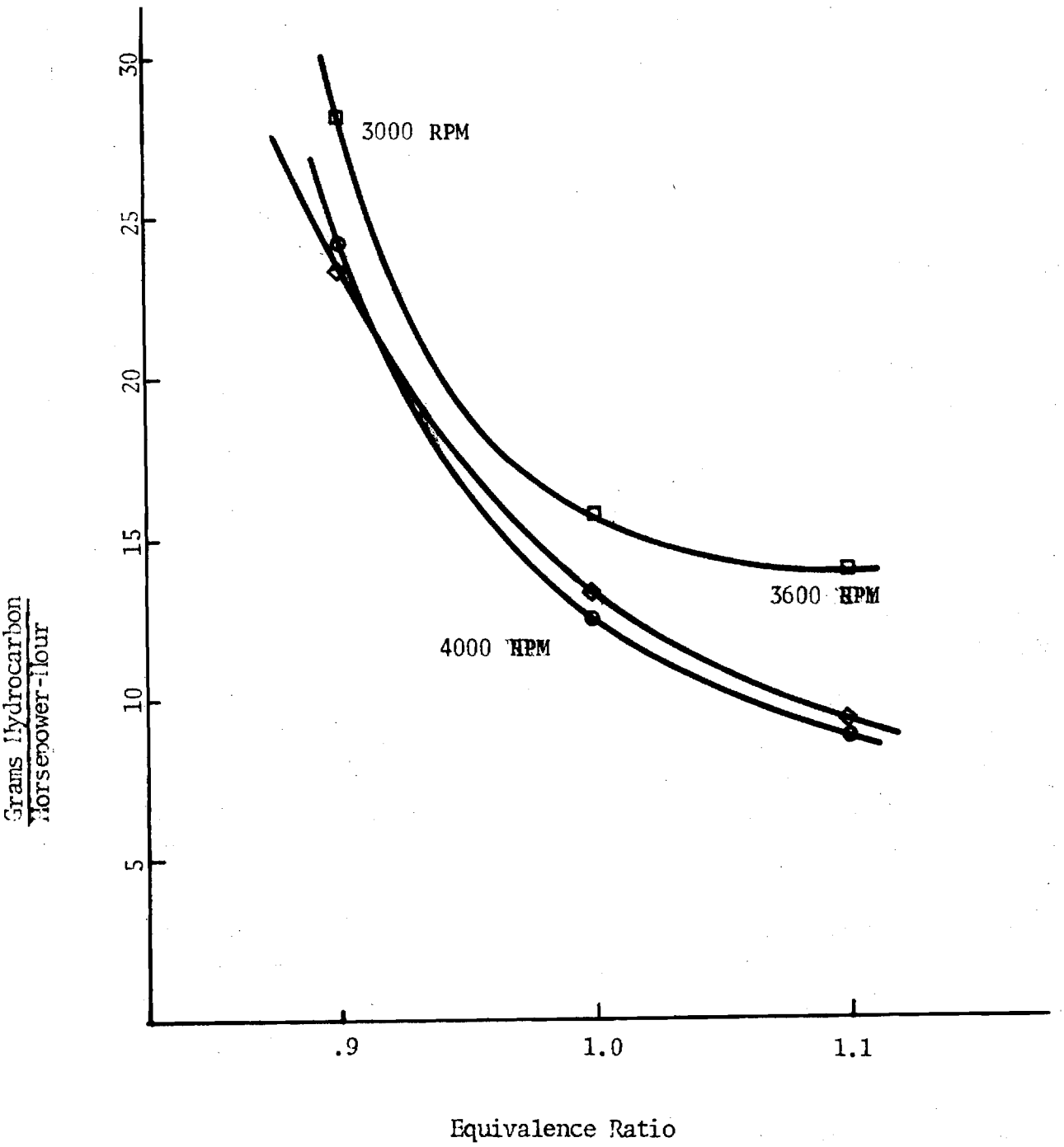

Figure 28. Mazda RX-2 Hydrocarbon Emissions Vs. ER at 2/3 WOT Torque (Methane)

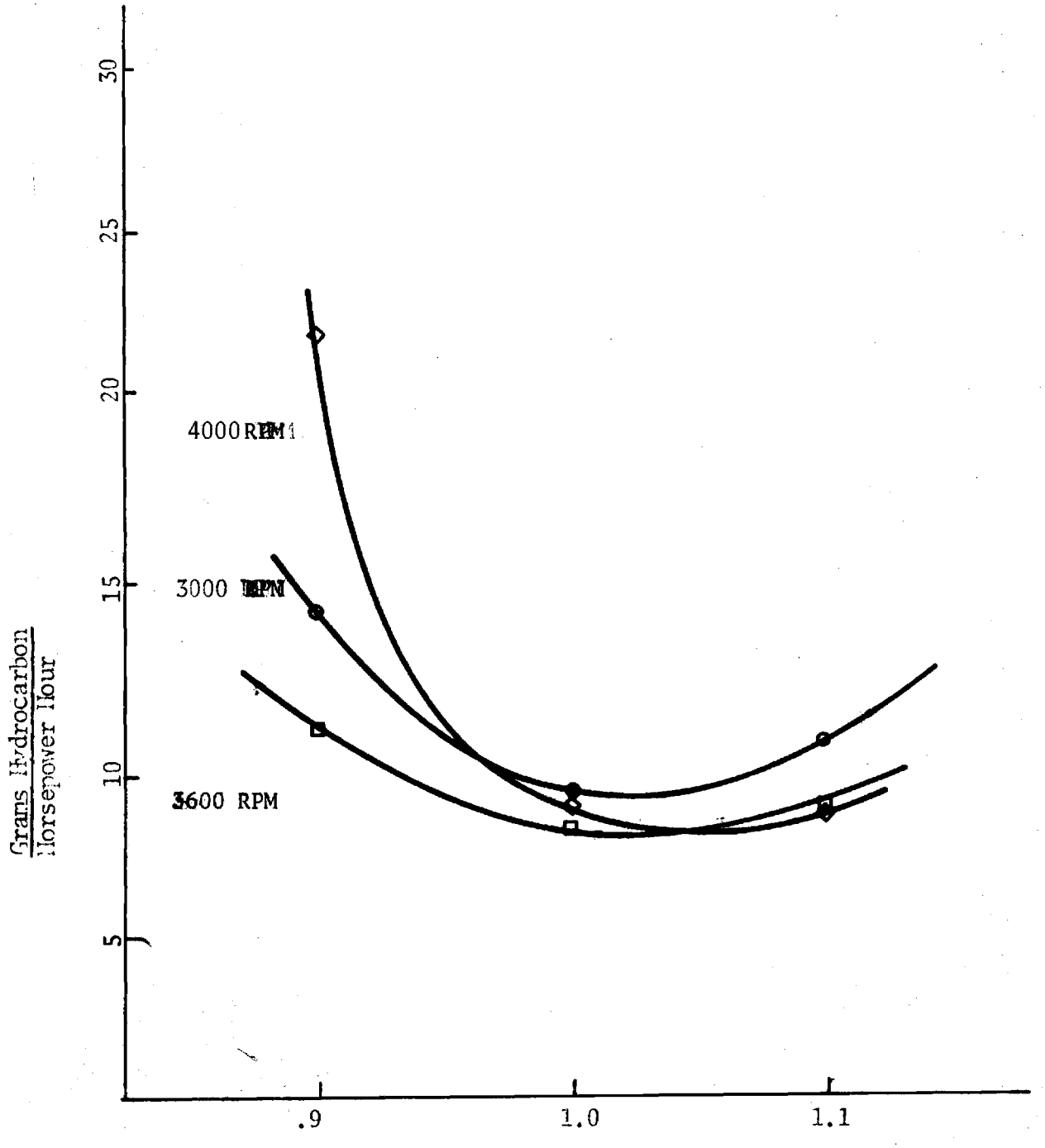

Figure 29. Mazda RX-2 Hydrocarbon Emissions Vs. ER at WOT (Methane)

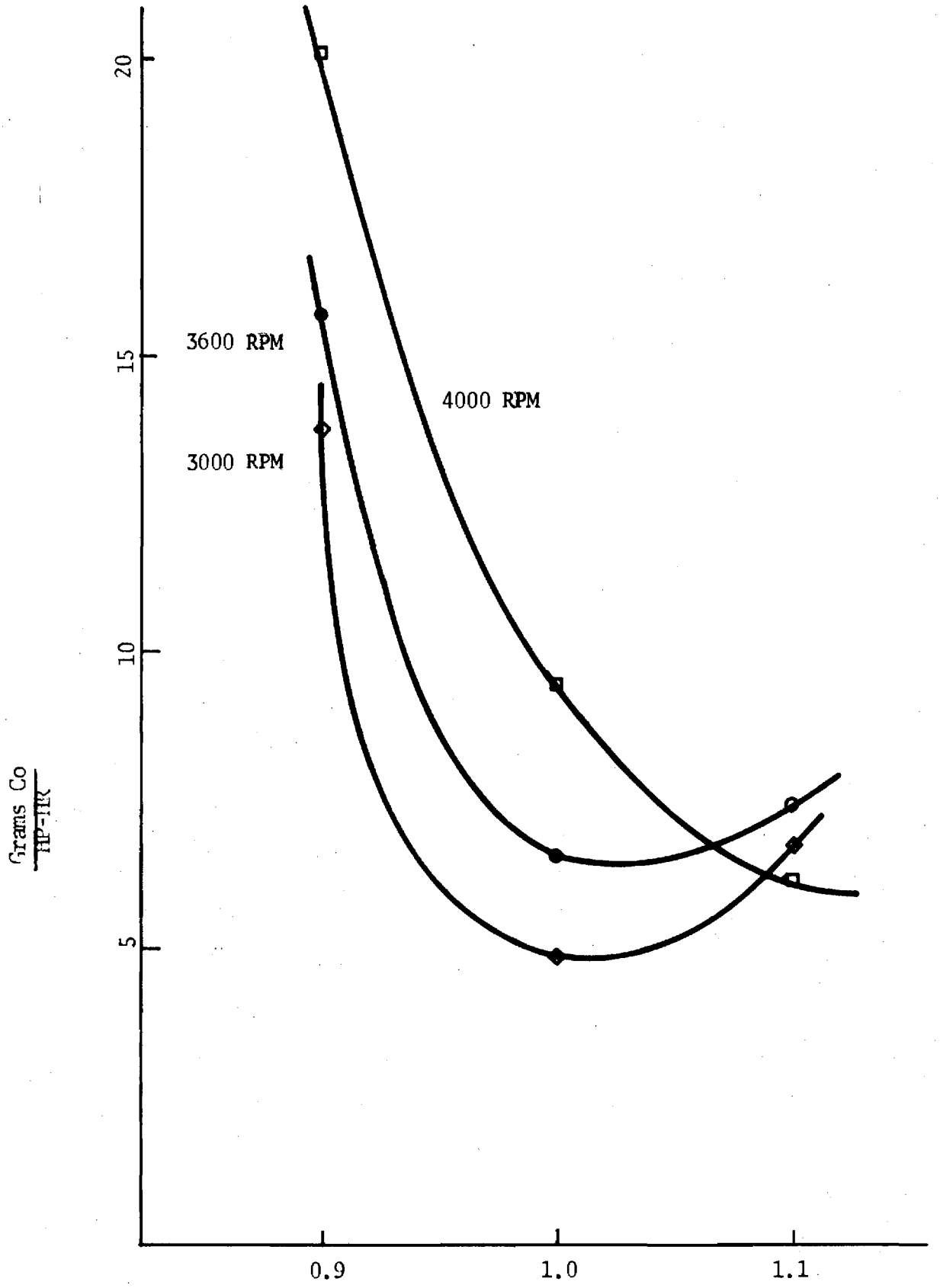

Figure 30. Mazda RX-2 Co Emissions Vs. ER At 1/3 WOT Torque (Methane)

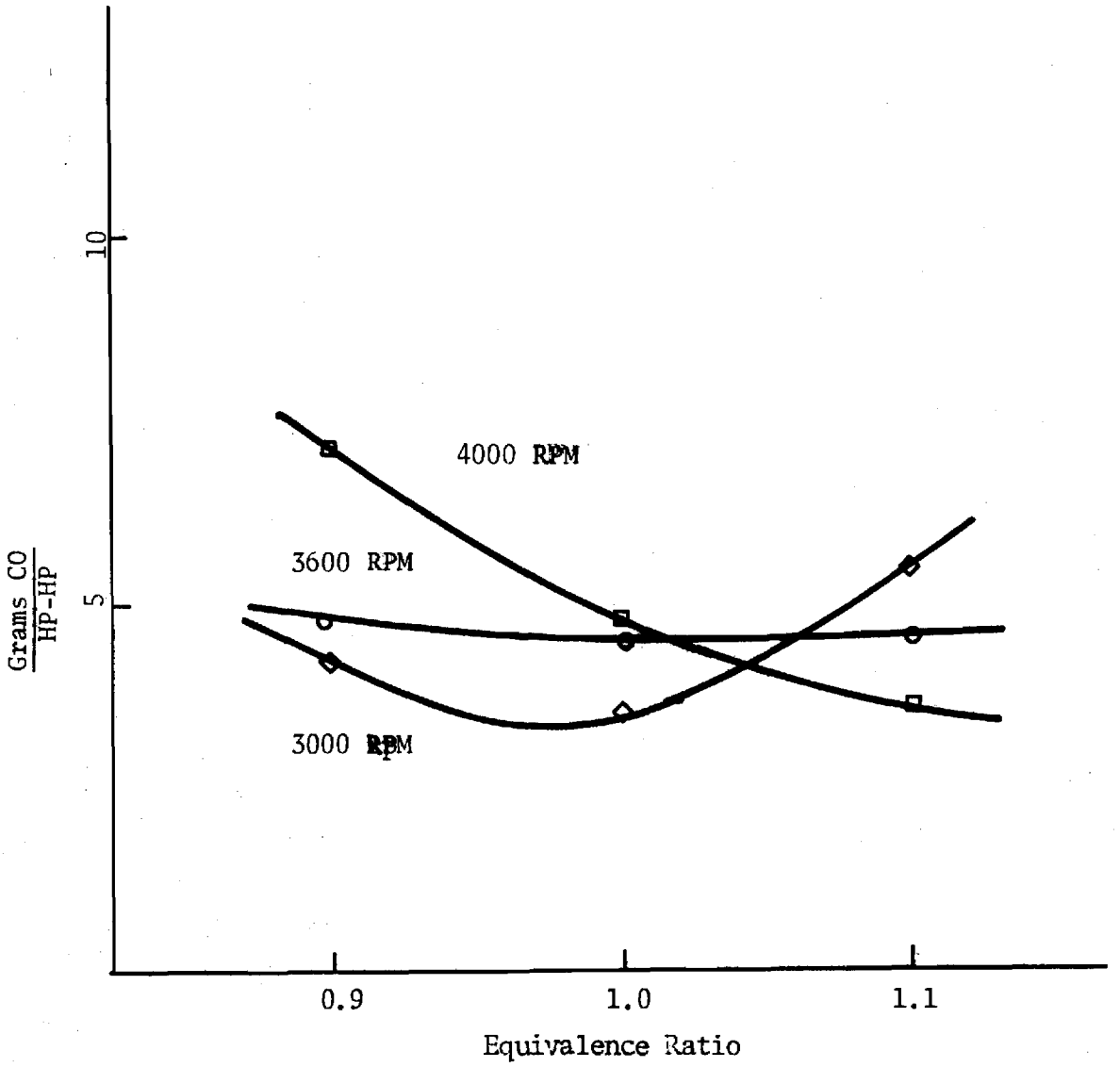

Figure 31. Mazda RX-2 Co Emissions Vs. ER At 2/3 WOT Torque (Methane)

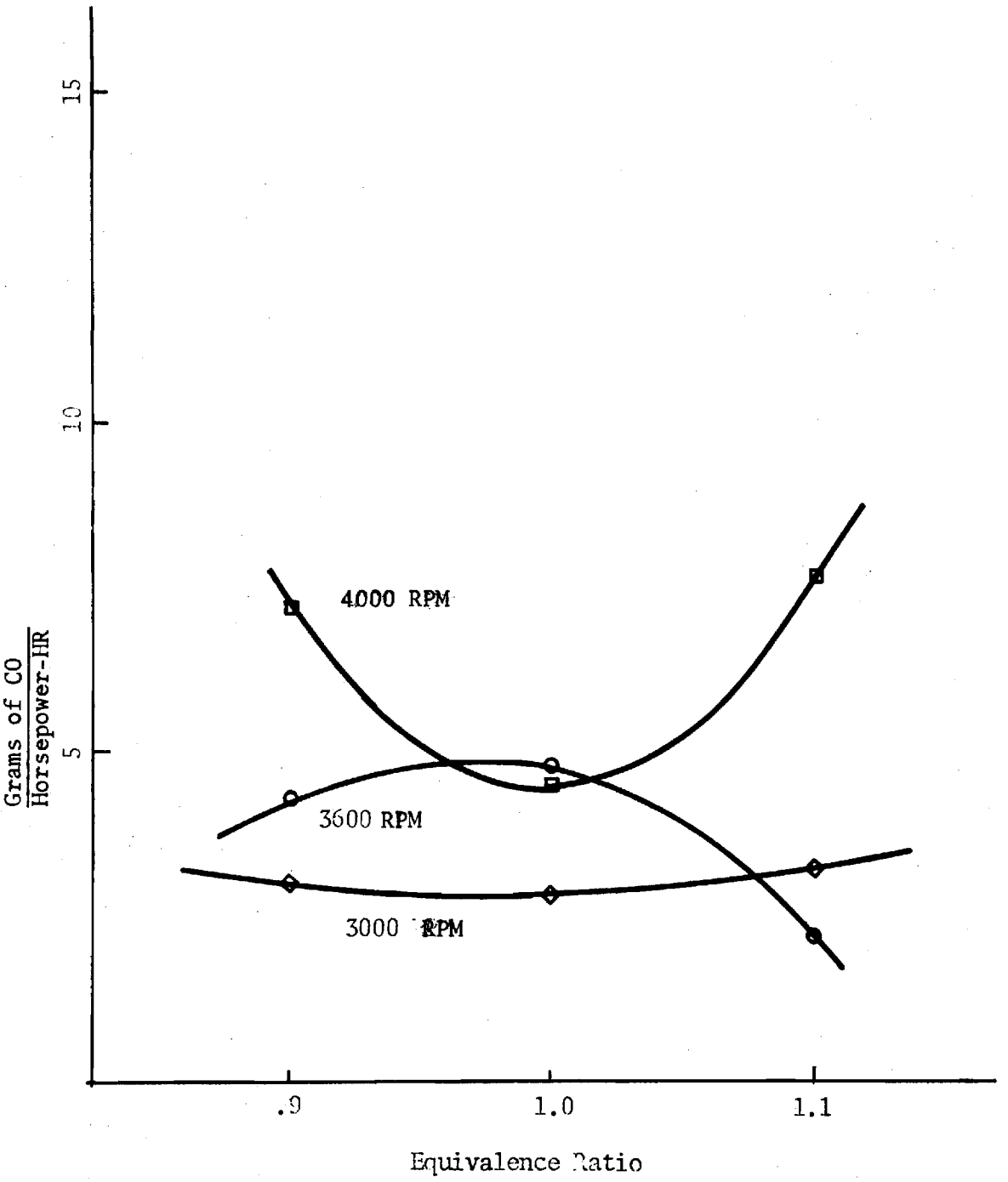

Figure 32. Mazda RX-2 Co Emissions Vs. ER At WOT (Methane)

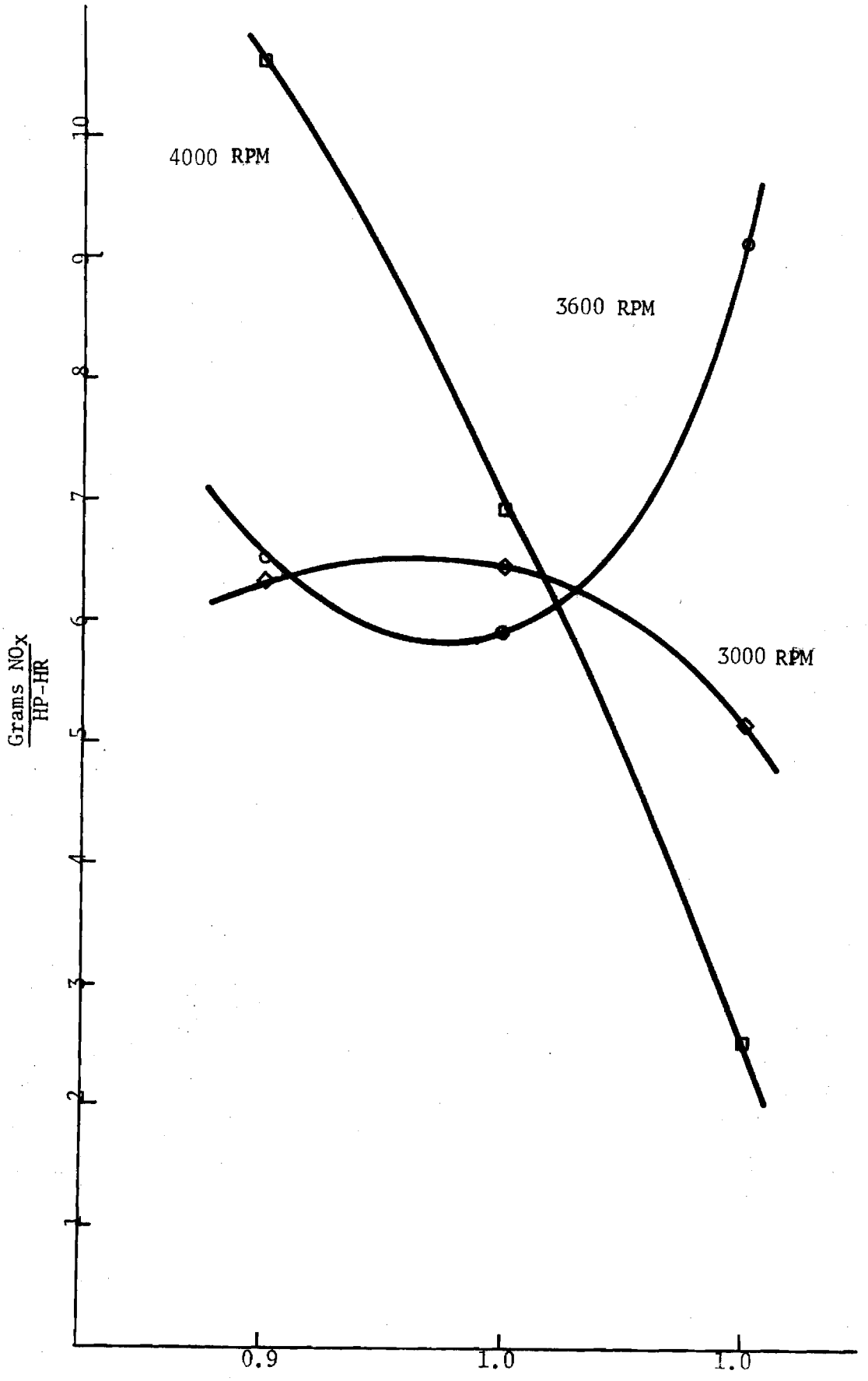

Figure 33. Mazda RX-2 NO_x Emissions vs. ER at 1/3 WOT Torque (Methane)

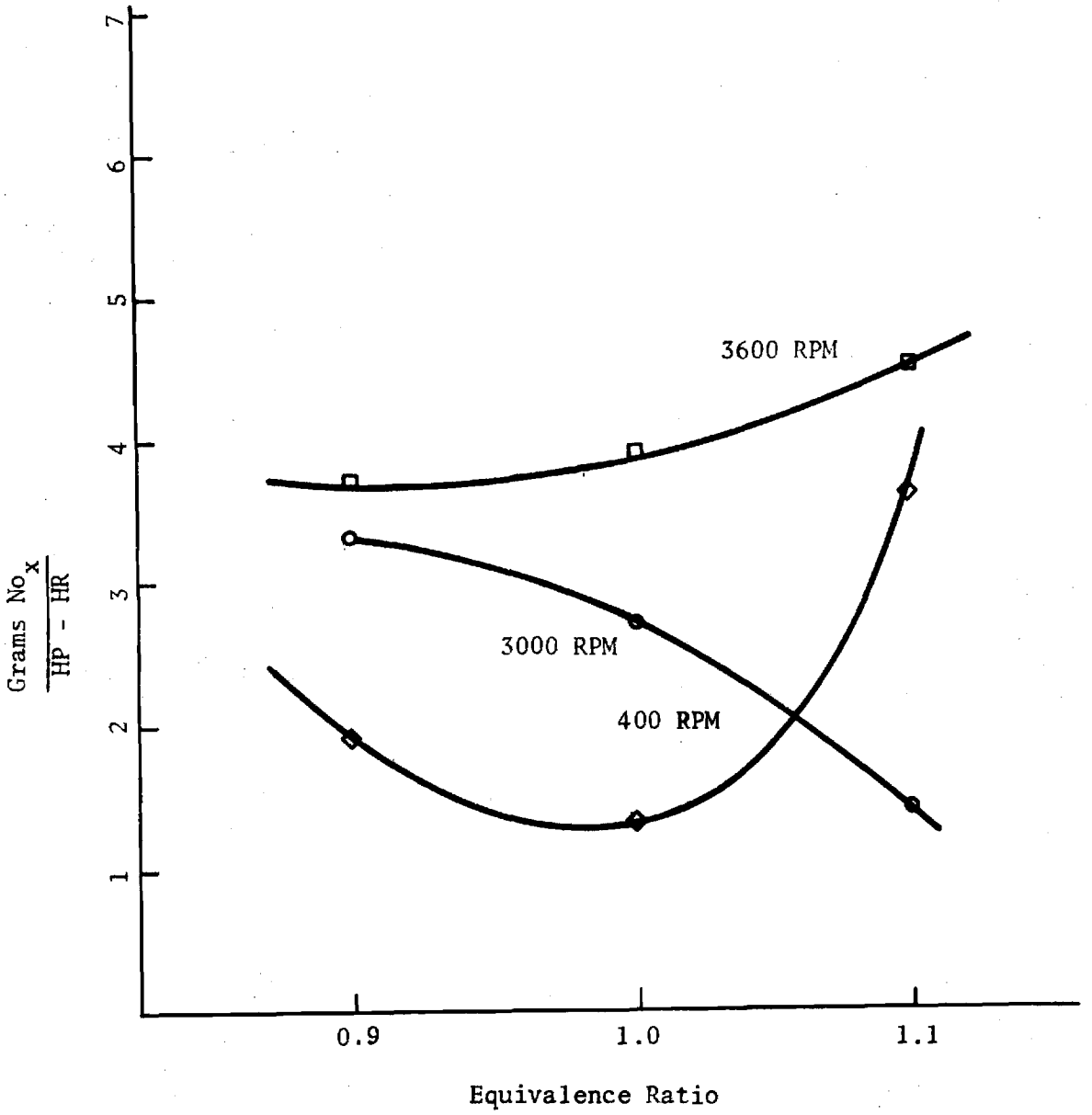

Figure 34 . Mazda RX-2 NO_x Emissions *vs.* ER at 2/3 WOT Torque (Methane).

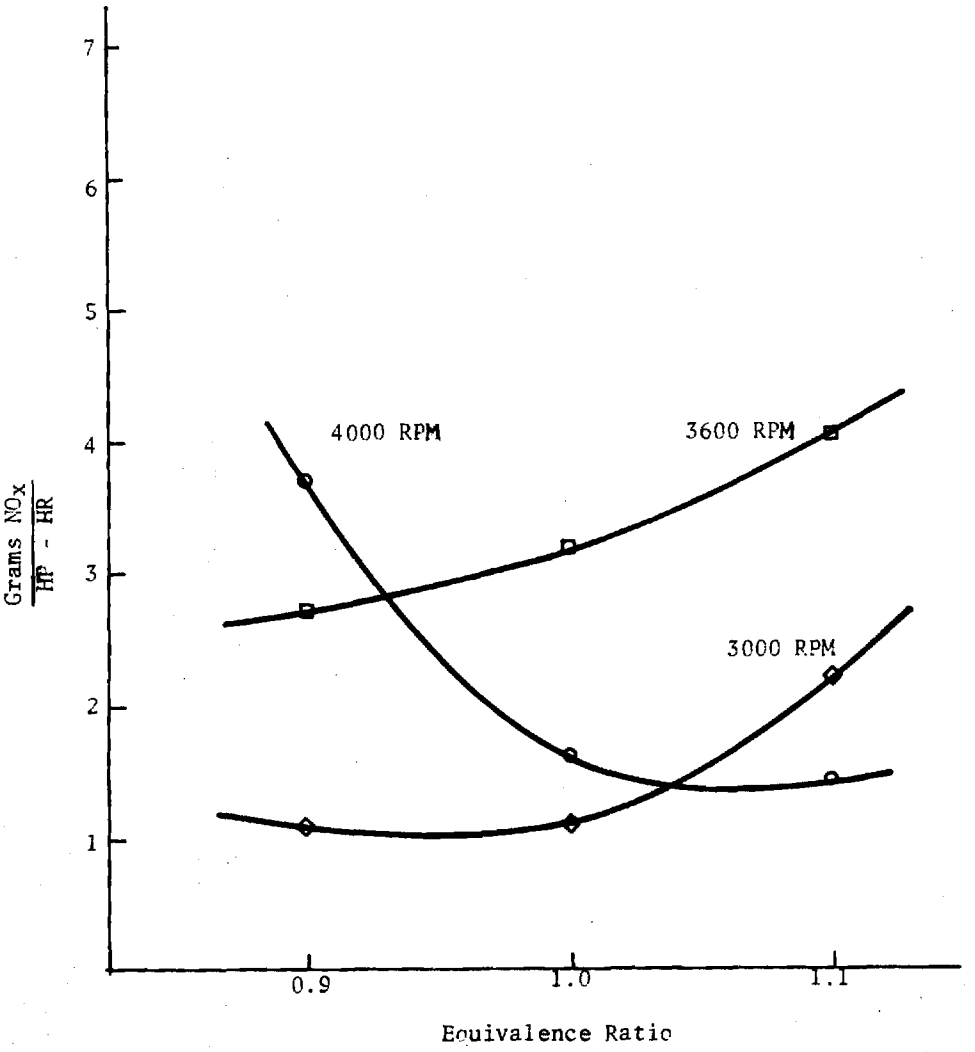

Figure 35 . Mazda RX-2 No_x Emissions vs. ER at WOT (Methane).

In order to determine the operating condition for minimum exhaust emissions, an exhaust emissions correlation study was carried out. This regressions analysis was carried out to determine the relationship between exhaust emissions and: 1) speed, 2) air-fuel ratio, 3) power output, 4) efficiency, and 5) lean misfire.

For purposes of this regression analysis a weighted emissions factor was used which weights each pollutant as to its toxicity and sums them.[11,12]

The results showed that the minimum weighted exhaust emissions results at the maximum engine efficiency without lean misfire. Air-fuel ratio in itself was not important nor was speed or power. This is an important result as it shows that engine efficiency does not need to be traded off for low exhaust emissions nor does low exhaust emissions need to be traded off for engine efficiency. The details of the analysis is shown in Appendix E.

Endurance and Wear Test

After the gasoline data were obtained, the engine was switched to operation on natural gas and the wear tests were begun. An accurate permanent record of the engine operation was kept showing the time the engine was stopped, started, the hours accumulated, fuel consumption, oil added and any maintenance performed. The oil injection rate was fixed at the factory specs for gasoline and resulted in it using one quart of oil every 20.5 hours of operation.

The engine was operated at 3600 RPM at a torque of 48 ft-lb. At this RPM and load, the engine develops 30 HP. For a frame of reference, this RPM would propel the Mazda automobile 65 mph. The engine was checked daily during the wear tests. From 21 September 1973 to 16 November 1973 the engine was run for 1183.6 hours. It used 58 quarts of oil and 407,000 cubic feet of natural gas. The load and RPM varied occasionally, but an overall efficiency for this time can be calculated from the above data assuming the horsepower and speed constant. This gives a 21.6% thermal efficiency.

Very little maintenance was performed on the engine during the wear test. This is quite remarkable considering that from an automotive standpoint the engine would have had in excess of 60,000 miles on it at the completion of the test. After about 100 hours of operation the engine began to throw oil through the rear shaft seal. It was determined that faulty reassembly was the problem and a new seal was installed. After about 500 hours the ignition coil wire had to be replaced. Periodically the air fuel mixture had to be adjusted to insure smooth operation. The original spark plugs remained in the engine during the entire tests.

After 1211.2 hours, the engine was disassembled. The seals were thoroughly cleaned and measured. There are 6 apex seals and three height measurements were made on each. There are 12 corner (one measurement each) and 24 side seals which were each measured in three different places for height. Only the apex seals showed measurable wear. The maximum recommended wear before replacement is .0787 of an inch.[14] At 1211.2 hours the maximum seal wear was .0123 inch. with a standard deviation of .002. Projecting this linearly gives a maximum life of 7687 hours. It has been shown[3,4] that seal wear rate decreases with engine hours and the actual life can be expected to be greater than this figure.

Conclusions

From these test results on the Toyo Kogyo TK039 engine the following conclusions can be drawn.

The maximum power on gasoline at 3600 rpm and 5000 rpm is 65 and 90 hp respectively. On natural gas the maximum power at the same 3600 rpm and 5000 rpm is about 55 and 70 hp respectively. This represents a drop in maximum power of about 20 percent in changing from gasoline to natural gas. As the natural gas air-fuel ratio is leaned, the power drops significantly to a maximum at 3600 rpm of 40 hp.

The maximum thermal efficiency of the engine on gasoline as provided from the factory is about 24% at 2/3 WOT and 4000 rpm. On natural gas the maximum efficiency was the same. Little or no advantage in efficiency was gained by leaning the mixture beyond stoichiometric. At the stoichiometric condition, thermal efficiency was almost constant with engine speed. As expected, thermal efficiency on natural gas decreased with decreasing power setting. The optimum thermal efficiency occurs at stoichiometric

CHAPTER V

OMC ENGINE TESTS

Introduction

The Outboard Marine Corp. (OMC) was the first U. S. firm to start commercial production of a Wankel engine in 1972. This engine is currently marketed in a snowmobile. The initial engine produced had a maximum power output of 35 hp. After one year of production it was modified to produce 45 hp.

After significant delay due to OMC's licensing arrangement with Curtis Wright Corp., a 45 hp version of OMC's engine was received for testing. Due to several engine problems, seal wear data tests were not ~~able to~~ be run. Only engine performance data was obtained.

These engine problems started when the engine was received and disassembled for reference measurements. At this time it was found that the rotor housing was deformed due to improper assembly. After receiving a new housing the engine was assembled and tests begun. Starting quickly became a problem due to low compression and disassembly was necessary to "unstick" the rotor seals. The next problem which arose during performance testing was a broken crank shaft.

The engine test setup and performance data will be presented and discussed.

Equipment

The engine was set up in a similar nature to the Toyo Kogyo engine. A water brake dynamometer was used with safety cut-off devices installed for continuous unattended running.

The speed was measured with a Heath Kit tachometer. This selection was made due to the design feature which enabled adaption to the unique ignition design of the single rotor Wankel which requires one ignition sequence per revolution. Though the Heathkit tachometer has a slow response time, the accuracy of the device was found to equal that of the mechanical, flyball tachometer on the Go Power dynamometer apparatus which was used as a laboratory standard.

Two 0-100 microammeter relays were specified and installed on the control panel to monitor the rotor housing temperatures at the exhaust port and at the spark plug as specified by the literature furnished by OMC. At the temperature of 470^{o}F and 500^{o}F for the thermocouple readings at the spark plug and at the exhaust housing respectively, the meters would disconnect the power to the electrical power circuit of the control panel, thus stopping the engine. The thermocouples were of the chromel-alumel type.

Other safety features included a normally open vacuum switch to disconnect the power source and gas supply when the engine is off, in order to prevent a gas leak and to prevent the possibility of overspeed when the engine goes to WOT (zero vacuum condition). A normally open dynamometer water pressure switch was incorporated to stop the engine when the water pressure to the dynamometer dropped below 4 psig. These and all other circuits are shown in Figures 36 and 37. An overspeed sensor was integrated into the powerpack by the manufacturer which stopped the engine upon sensing a speed in excess of 5500 rpm.

To maintain a constant speed for continuous operation, the test cell was equipped with a Speed-o-Stat automatic speed control which varied the throttle with load to maintain a constant rpm. A vacuum pump was used as a vacuum source for the throttle control diaphragm which controlled the throttle. The vacuum pump operates from a 120 VAC line from the wall junction

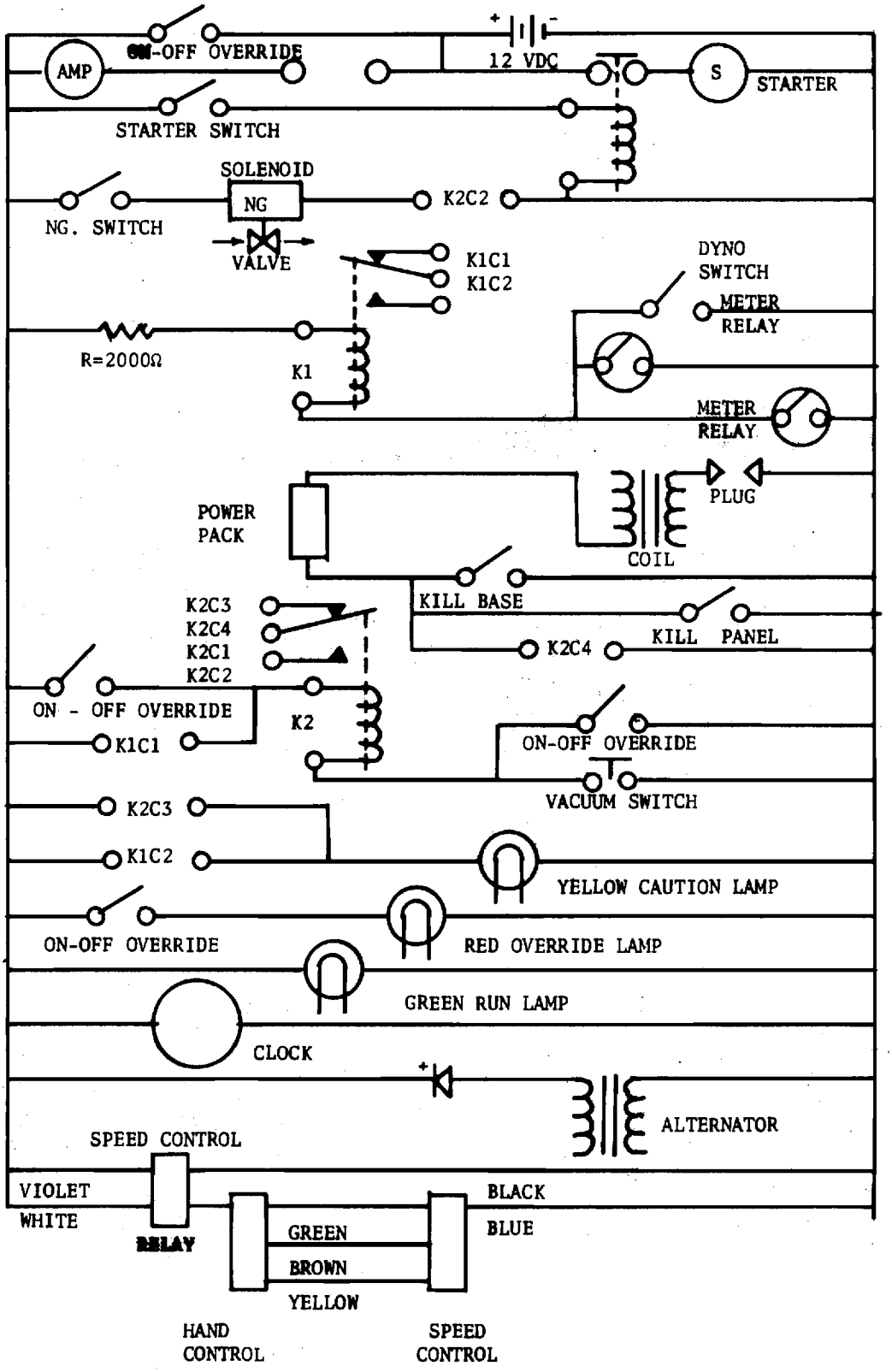

Figure 36 . OMC 45 HP RC. Engine.

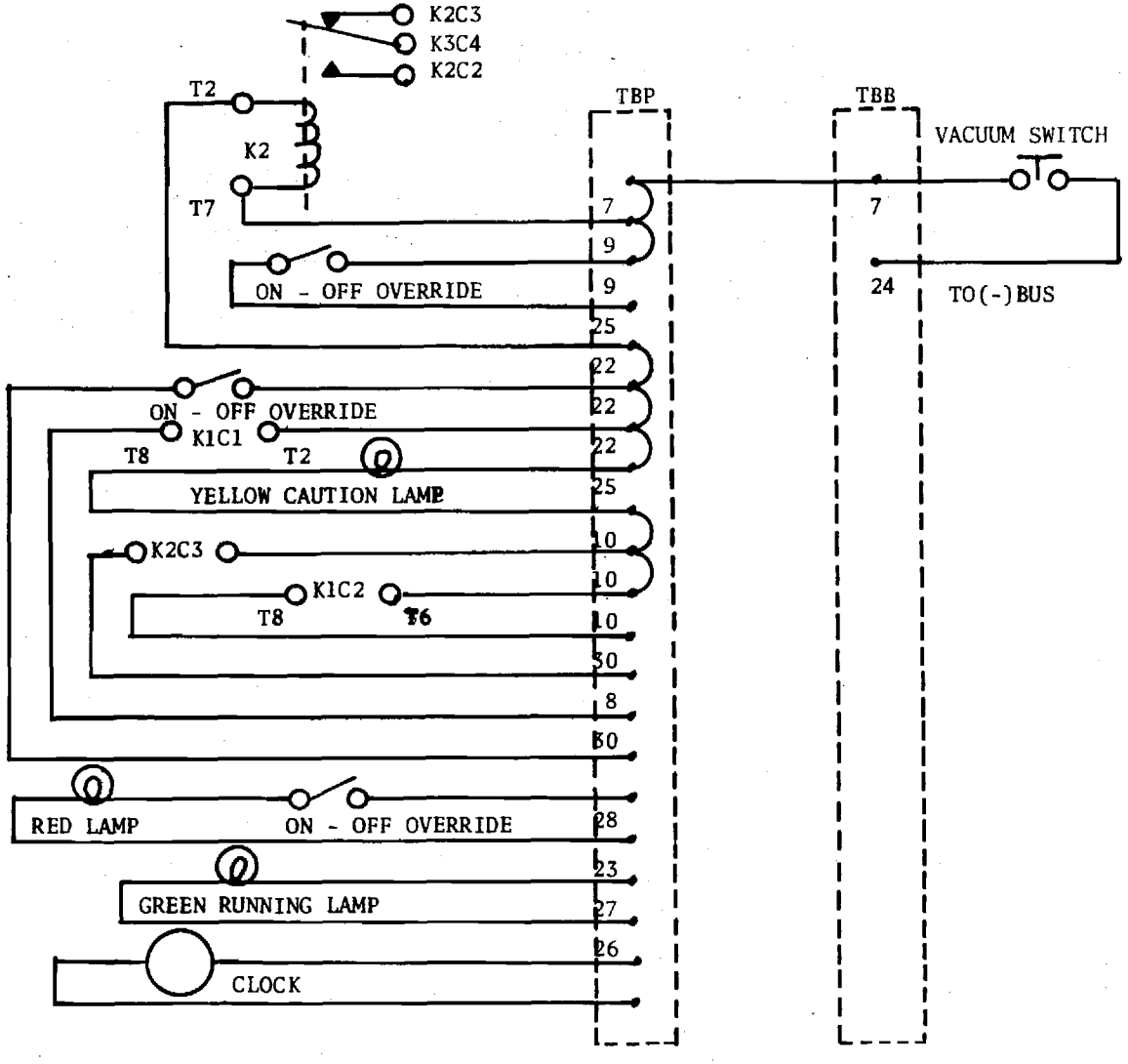

Figure 37 OMC Monitoring and Automatic Shutdown Wiring Diagram.

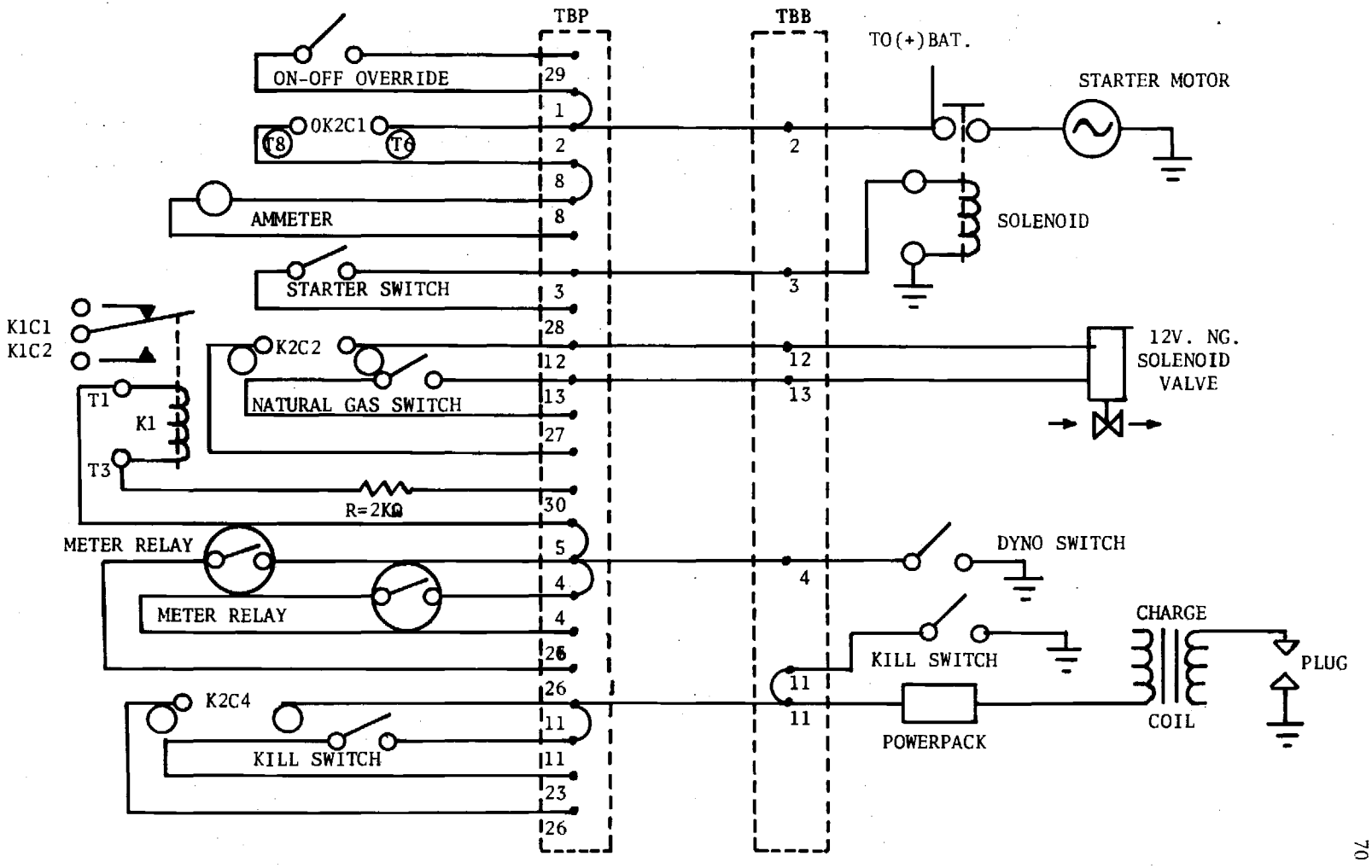

Figure 37 (continued). OMC Monitoring and Automatic Shutdown Wiring Diagram.

near the test cell. The speed control electrical schematic is shown in Figure 38.

The engine mount was constructed from one-half inch thick hot rolled steel plate and two hot rolled, unequal leg structural steel angles. Hot rolled steel was used because of its availability and, thus due to its increased strength, the mount is overdesigned. Once positioned the base was made permanent and should not be moved. When the engine is removed the engine mounting bolts should be the only bolts removed.

The dynamometer coupler, upon the suggestion of the OMC literature, was of a solid type construction consisting of a splined eccentric shaft coupler slipfit and bolted to a solid dynamometer shaft coupler with a 3/8 inch keyway to prevent slippage. The splined coupler was furnished courtesy of OMC.

Seal wear was measured, throughout the experiment, with the same Sears 0.0001 inch accuracy micrometer, number ME-15.

A Taylor waterbrake dynamometer model D-22 was used to load the engine for performance tests and wear studies.

The natural gas carburetor for the 45 hp OMC RC engine was a Impco model 100. The model 100 carburetor is designed for a more steady flow rate than the model 110-A and was thus chosen for the 45 hp OMC engine due to its greater displacement.

The natural gas was metered by flow meters of the standard residential type supplied by the Atlanta Gas Light Co.

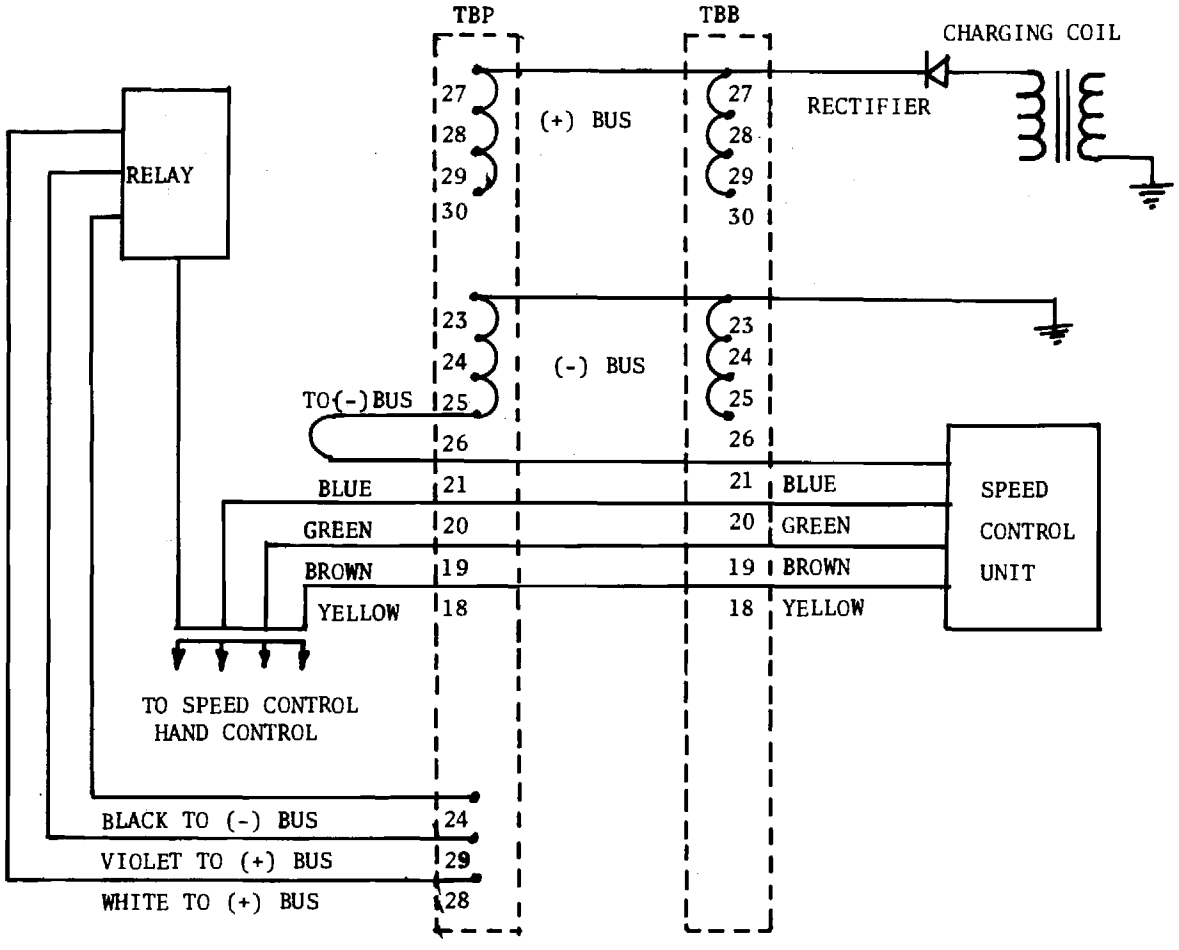

Figure 38. OMC Speed Control and Charging Wiring Diagram.

A Meriam laminar flow element, serial no. B-00322 was used to measure air flow rates for the heat balance and volumetric efficiency tests. A Meriam manometer, serial no. T18571, was used in conjunction with the flow element to measure the air flow rates.

Engine Tests and Results

Procedure

The engine was tested on gasoline and subsequently natural gas. During these tests gasoline flow was measured by a scale and stopwatch to determine the mass of gas flowing in a given time. Natural gas volume flow in a given time was determined by a standard natural gas meter. This meters most sensitive scale showed five cubic feet of flow for one revolution of the hand. Torque and rpm was measured with the previously discussed dynamometer and tachometer.

Gasoline Performance Tests

The horsepower vs. speed results are shown in Figure 39. The peak power of 36 hp occurred at 5500 rpm. At 3600 rpm the maximum power was 25 hp. A dip in the data is noted at 5000 rpm which is evidently a result of the "charge tuning" of the combination side and peripherial intake ports. These points were repeatedly checked and it was determined that the effect was real and not measurement or repeatability error.

The fuel consumption data is displayed in Figures 40 and 41. As expected, the brake specific fuel consumption (BSFC) decreases with increasing power output except for the anamaly at the 5000 rpm point noted in the power curves. It is seen from the BSFC vs. Speed curves that the BSFC decreases with increasing speed until about 4500 rpm at which point it starts to increase.

Figure 42 shows the fuel consumption data expressed in terms of thermal

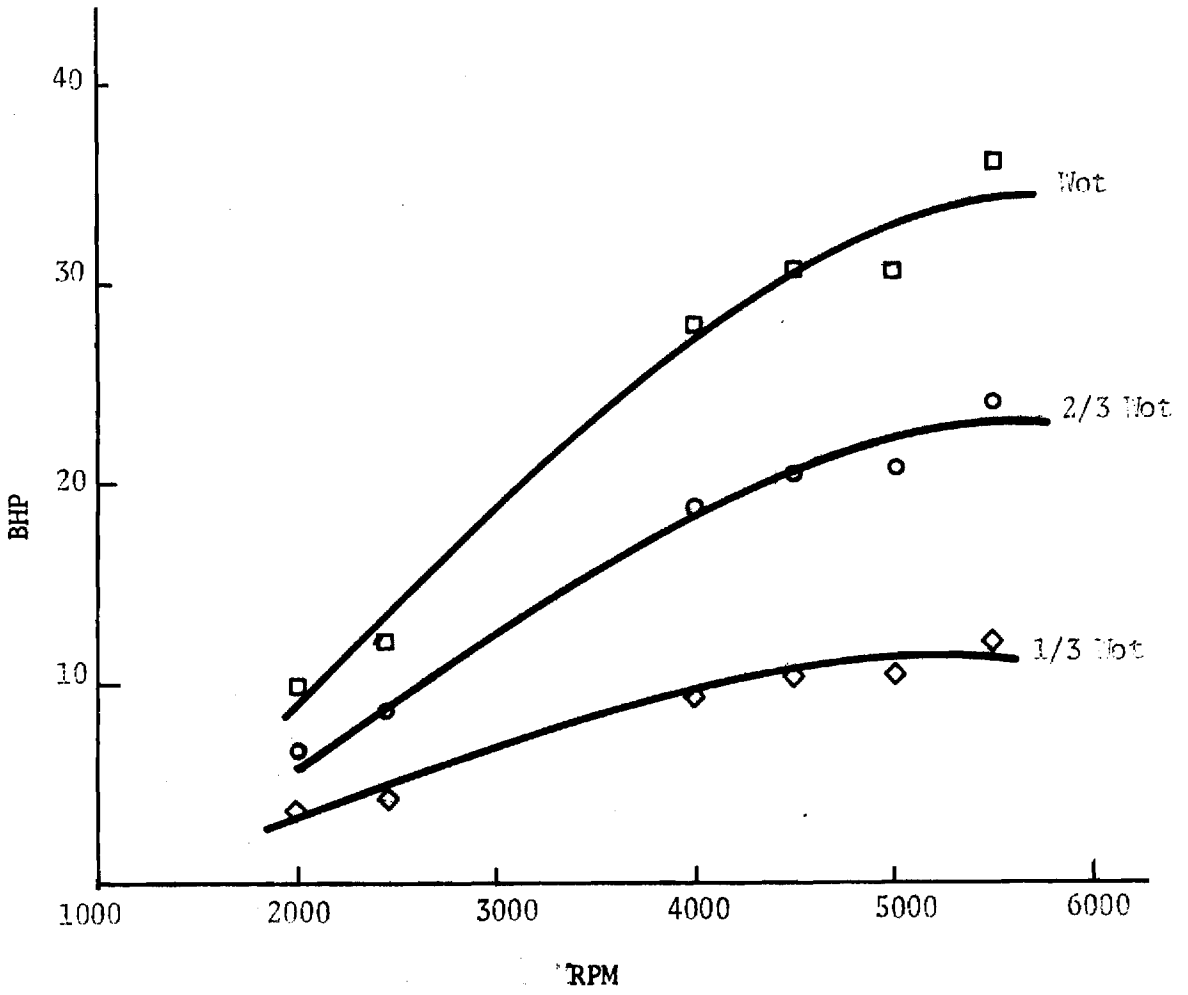

Figure 39. OMC Wankel Rotary Engine Horse-Power vs. RPM (Gasoline)

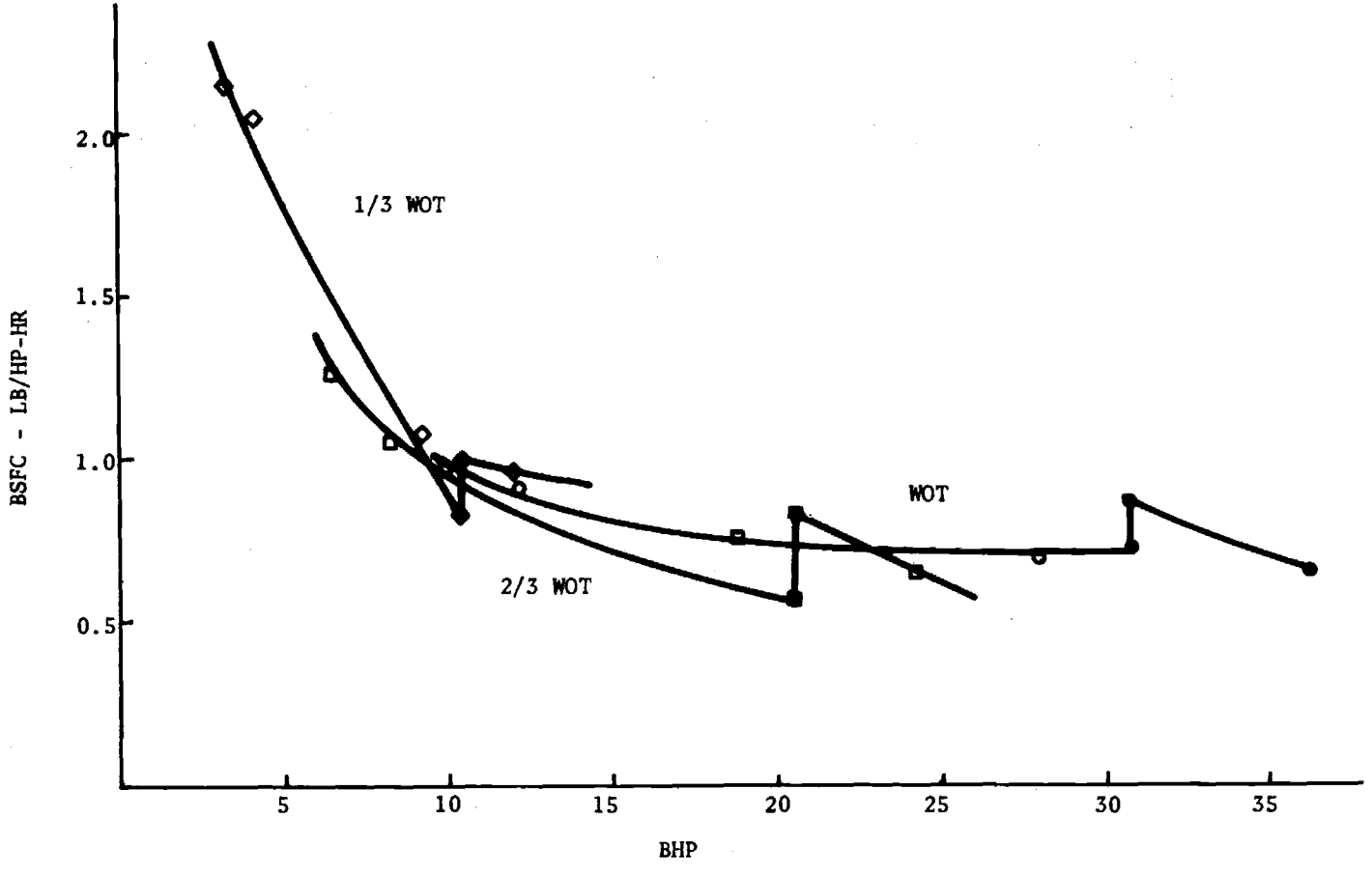

Figure 40 . OMC Wankel Rotary Engine Brake Specific Fuel Consumption vs. Brake Horsepower (Gasoline).

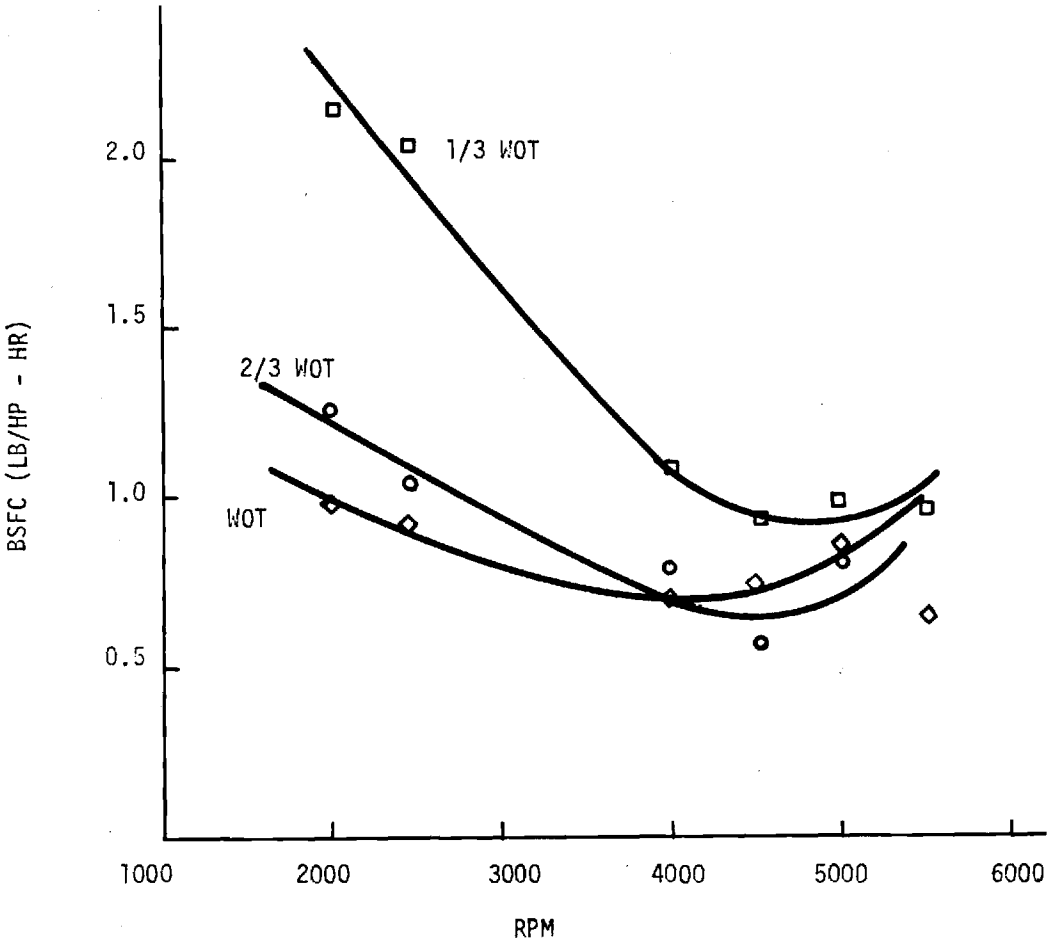

Figure 41. OMC Wankel Rotary Engine
Brake Specific Fuel Consumption vs RPM
(Gasoline)

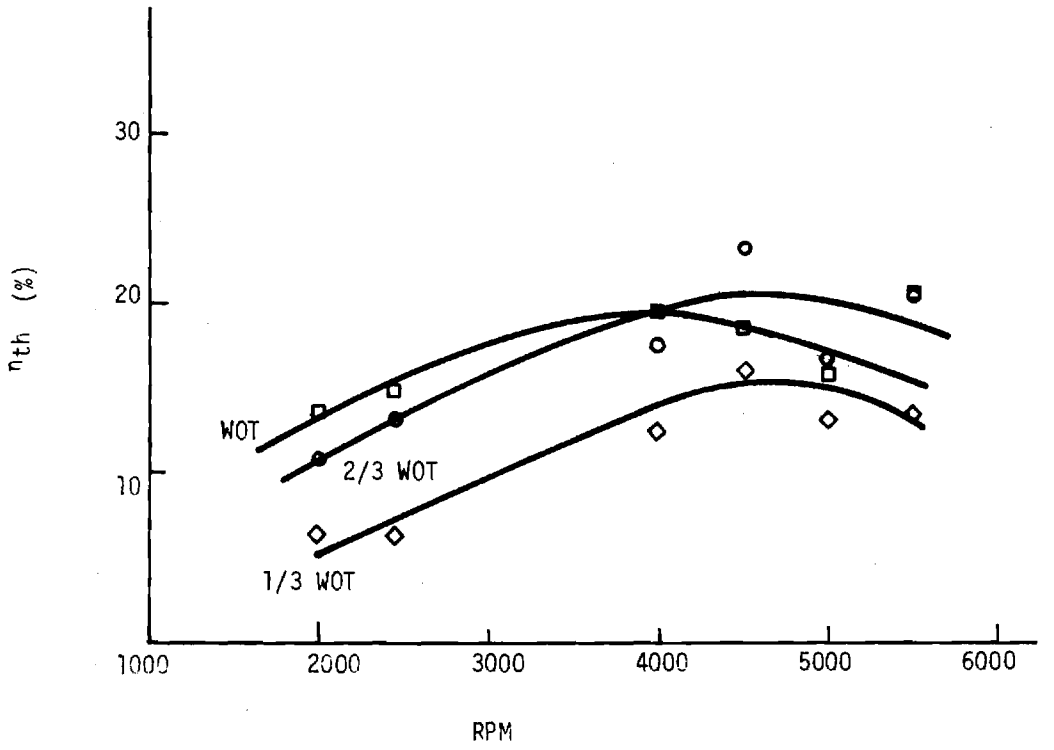

Figure 42. OMC Wankel Rotary Engine
Thermal Efficiency vs RPM
(Gasoline)

efficiency. The maximum thermal efficiency is to be about 23% at the optimum speed of 4500 rpm.

It should be noted this data was taken with factory supplied carburetor calibration and that no attempt was made to maintain a constant air-fuel setting.

Natural Gas Performance Tests

The natural gas performance tests were obtained at WOT, 2/3 WOT, and 1/3 WOT at speeds from about 3500 rpm to 5500 rpm. All tests were at a stochiometric air-fuel ratio. No further data was obtained at lower speeds and other air-fuel ratios due to crankshaft failure. Due to the induction triggered capacitance ignition system being integral with the flywheel, spark timing on this engine was not variable and therefore all natural gas tests were run at the factory (gasoline) setting.

The power curves in Figure 43 at WOT, 2/3 WOT, and 1/3 WOT show the peak power of 27 hp occuring at 5500 rpm with the same dip in the curve at 5000 rpm as shown in the gasoline power curve. At 3600 rpm, the maximum power is 23 hp.

The BSFC (cubic feet of natural gas per horsepower per hour) is shown in Figure 44 with thermal efficiency shown in Figure 45. The curves show the optimum efficiency is obtained at about 3600 rpm where BSFC is 13 ft^3/hp-hr and a thermal efficiency of 22 percent. Although no data was taken below this speed the curves appear to be flattening out and would be expected to follow the normal trend of returning to lesser efficiencies at the lower rpm's.

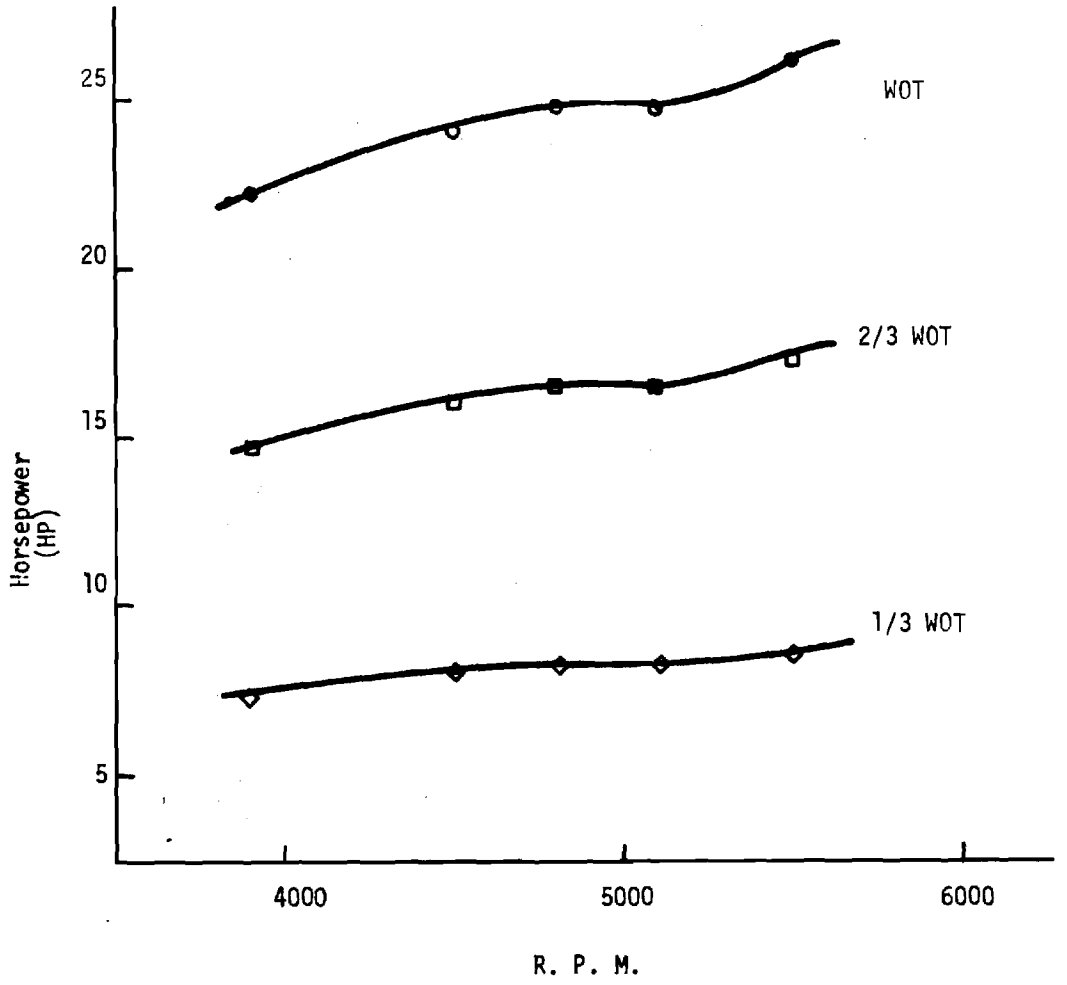

Figure 43. OMC Wankel Rotary Engine
Horsepower vs R. P. M.
(Natural Gas)

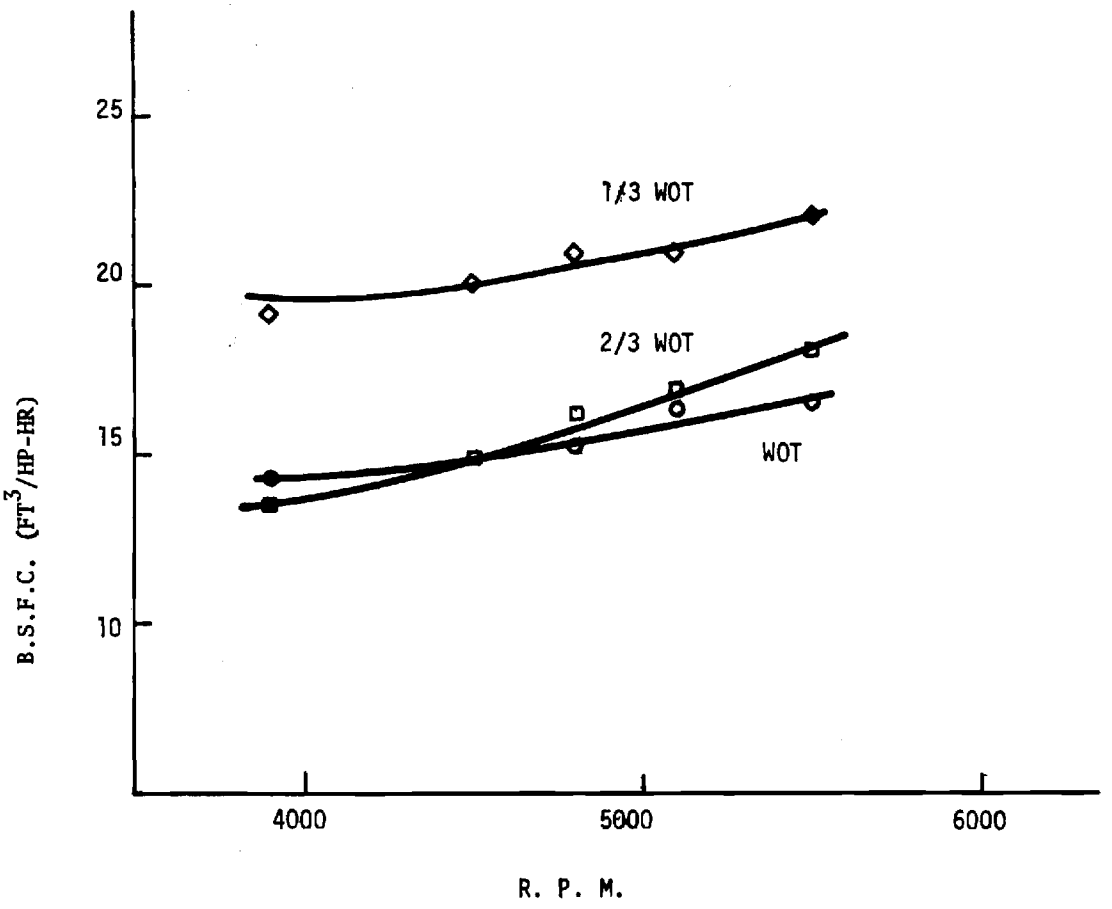

Figure 44. OMC Wankle Rotary Engine
Brake Specific Fuel Consumption vs R. P. M.
(Natural Gas)

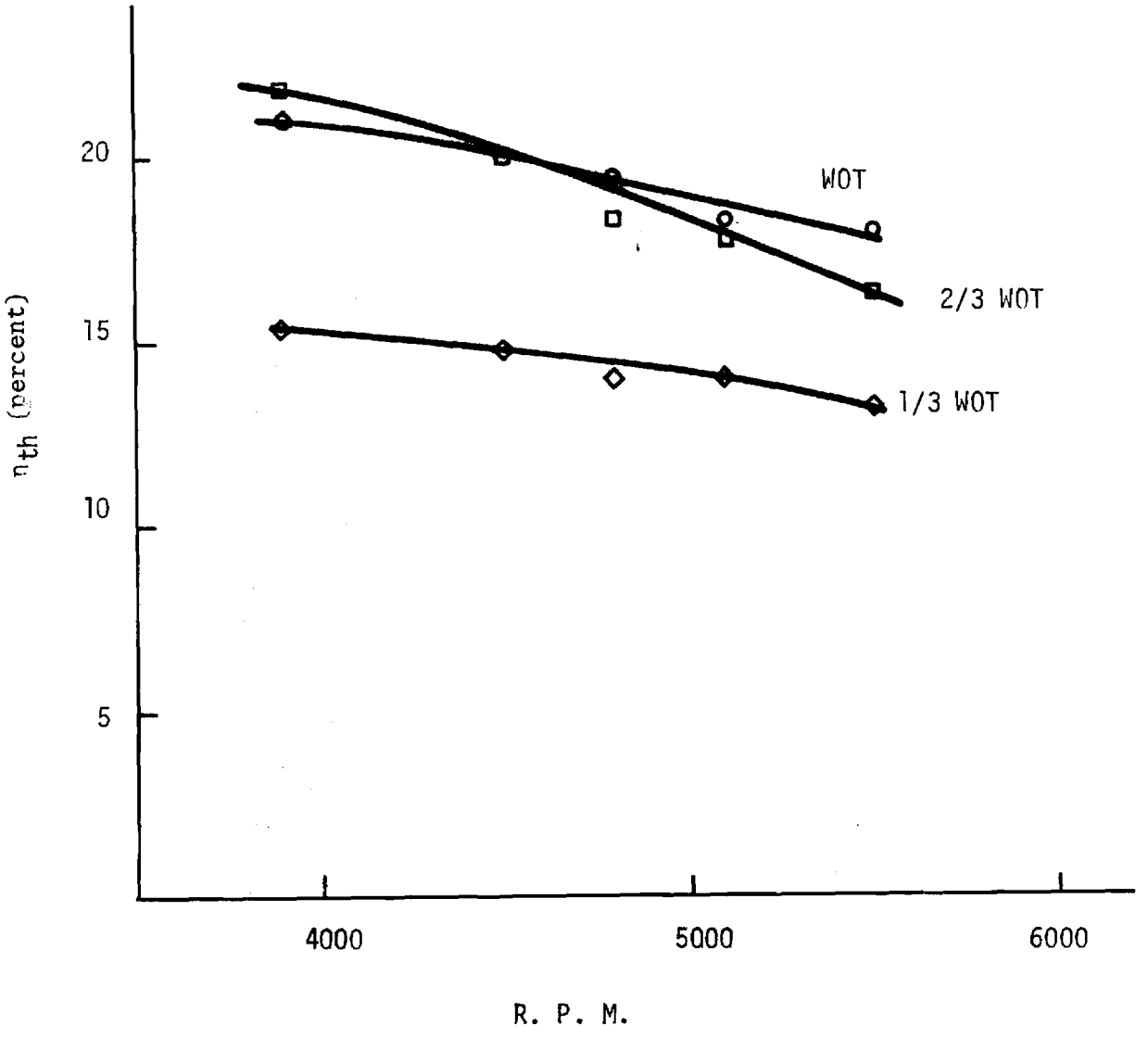

Figure 45. OMC Wankel Rotary Engine
Thermal Efficiency vs R. P. M.
(Natural Gas)

Conclusions

The OMC performance tests show the maximum power available at 5500 rpm dropped from 36 hp on gasoline to 25 hp on natural gas. At 3600 rpm the maximum power drop is less significant being from 25 hp to 23 hp.

The maximum thermal efficiency on both gasoline and natural gas was about the same (22%) for both gasoline and natural gas. However, on gasoline this optimum occurred at 4500 rpm whereas on natural gas it occurred at about 3600 rpm. At the 3600 rpm point, the thermal efficiency improved in going from gasoline to natural gas (20% to 22%).

In spite of the engines excellent performance test results, several mechanical problems arose with the engine which makes it questionable as to its reliability in a stationary application. Whether these problems were unique to this particular engine only or whether similar problems would arise with others of the same model is not known.

It should also be noted that the engine had a very high noise level when operating. This was particularly noticeable when compared to the other engines tested. Most of this noise was emitted from the mixed flow (radial and axial) cooling fan.

Chapter VI

SACHS ENGINE TESTS

Introduction

The engine used for this study was a Sachs Wankel Engine Model KM914A, single rotor, air-cooled engine. The engine is factory rated at 4500 rpm at 16 hp (DIN) and at 3000 rpm at 11 hp (DIN). Sachs also manufactures and markets a KM48 Wankel engine similar in every respect except smaller. This KM48 engine is rated at 8 hp (DIN) at 4500 rpm and 5.5 hp (DIN) at 3000 rpm. Since the engines are similar, it was felt that a test on either engine would give representative data for determining the operating characteristics of the other. Therefore, only the larger KM914A was tested but efficiency, natural gas derating, and wear results should be similar to the smaller KM48.

Equipment

The engine setup was similar in nature and function as the previous two engines discussed. Therefore, the experimental test equipment will not be belabored.

The dynomometer used to load the engine for both performance testing and long term wear studies was a Go-Power DY-9D. The load and speed limitation of this dyno is 60 hp and 16,000 rpm. It has a turbulent action waterbrake power absorption unit. Load is controlled by a valve which regulates flow into the absorption unit. The torque is measured by a load cell which activates a pressure type gauge which is calibrated in pounds force. Overall system accuracy is stated to be $\pm$ 2%.

Speed was measured by the mechanical drive tachometer driven off the absorption unit. Its range is 500 to 6000 rpm with a stated accuracy of $\pm$ 1.5%.

In gasoline operation, fuel was fed by gravity from either a burnett or two gallon gasoline tank. A two way valve selected the desired source. During fuel flow measurements, the gasoline volume flow was measured over a time interval measured by a stop watch. The gasoline volume was measured to the nearest 1 cc for a total volume of 100 cc.

In natural gas operation, natural gas was fed from a standard commercial gas meter with the most sensitive scale registering two cubic feet of gas per revolution. Gas flow rate was determined by measuring the time required for at least two cubic feet of natural gas to be consumed by the engine.

The natural gas was fed to an Impco carburetor model 110A attached in series to the factory supplied gasoline carburetor. This allowed easy conversion from one fuel to the other during testing.

The ignition system was modified for the long term wear tests to eliminate the original magneto points. Although the original points did not give any problems during the 2000 hours of testing, it is felt that for longer term reliability, they would be one of the first components requiring maintenance. This is true for the other engines tested as well.

A 1973 Chrysler automotive solid state induction triggered (pointless) ignition system was thereby adapted to the engine for testing. It performed well and no problems were encountered with it. The original ignition system was also left in-tac and was operating well at the end of the tests. In spite of the original spark plug not being replaced during the 2000 hours, both ignition systems fired the plug with no misfire.

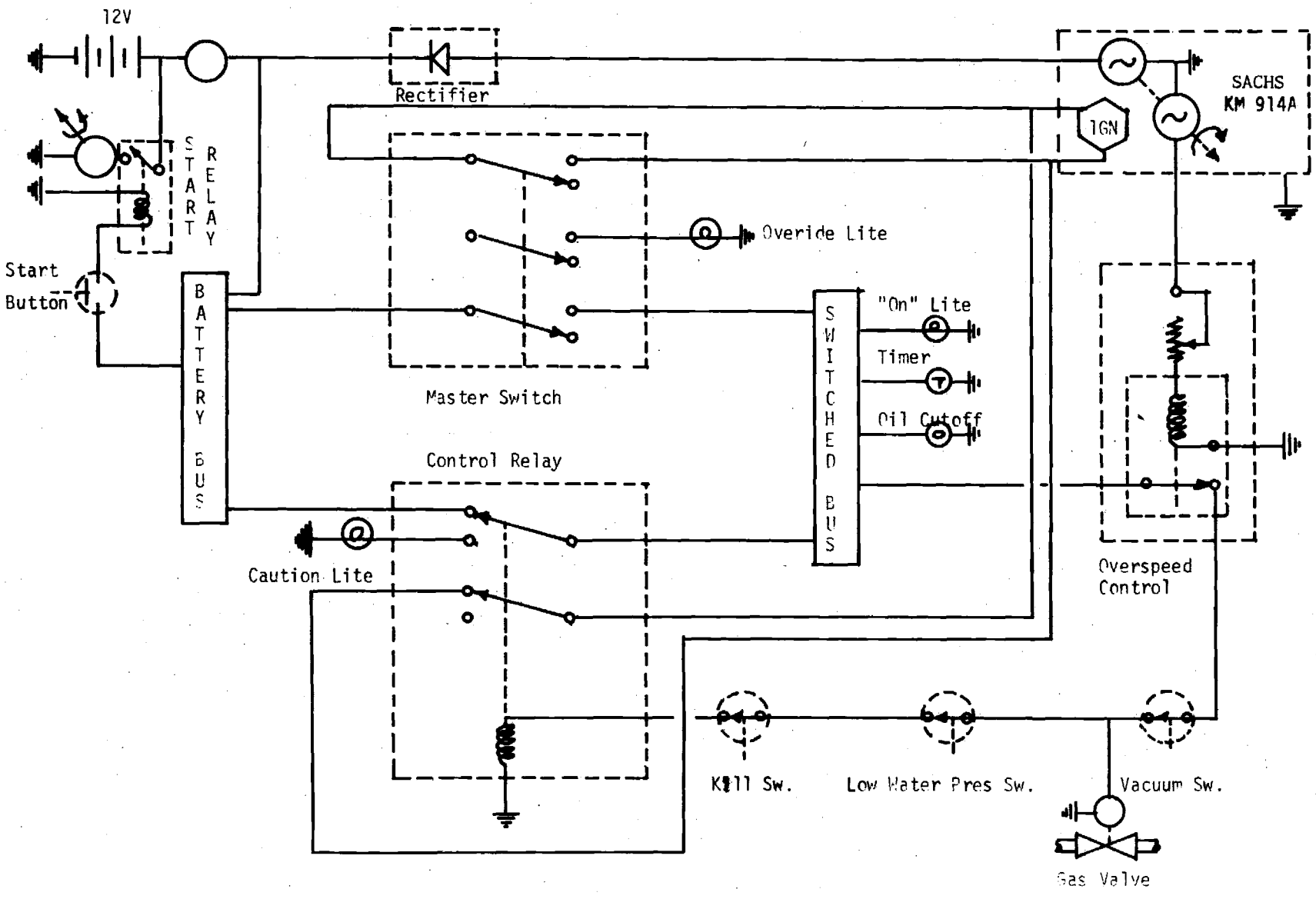

Figure 46. Control Circuit - Sachs KM914A.

As with the other test engines, it was equipped with monitoring and automatic shutdown circuits. These are shown in Figure 46. They consist of an overspeed control, dyno water supply pressure monitor, and vacuum switch for insuring natural gas shut-off upon engine shutdown.

Test Results

Gasoline

Horsepower and efficiency tests at various speeds (1500 rpm to 5500 rpm) were run on gasoline with the engine fuel and ignition system set up according to factory specifications. The resulting power curves at WOT, 2/3 WOT, and 1/3 WOT are shown in Figure 47. The maximum power of 15.5 hp was very close to the factory stated 16 hp with 14.5 hp being produced at 3600 rpm.

The resulting thermal efficiency of this engine was also surprisingly good for an engine of its size as shown in Figure 48. Maximum efficiency of 18 percent was found at 3600 rpm WOT. This decreased to 7 percent at 5500 rpm and 1/3 WOT. The decrease in efficiency at 3600 rpm in going from WOT to 2/3 WOT was only from 18 percent to 17 percent.

Natural Gas

The horsepower curve on natural gas is shown in Figure 49 for the near optimum equivalence ratio of one; i.e. stoichiometric. Factory spark advance (12^{o} BTDC) is also held constant. Peak power is about 8 hp at 3600 to 4000 rpm.

Thermal efficiency at various loads, and speeds between 3000 and 5000 rpm, with 12^{o} BTDC spark setting is shown in Figure 50. The peak of 21 percent occurs at 3000 rpm, WOT. It drops only slightly at 2/3 WOT to 18 percent at both 3000 and 4000 rpm.

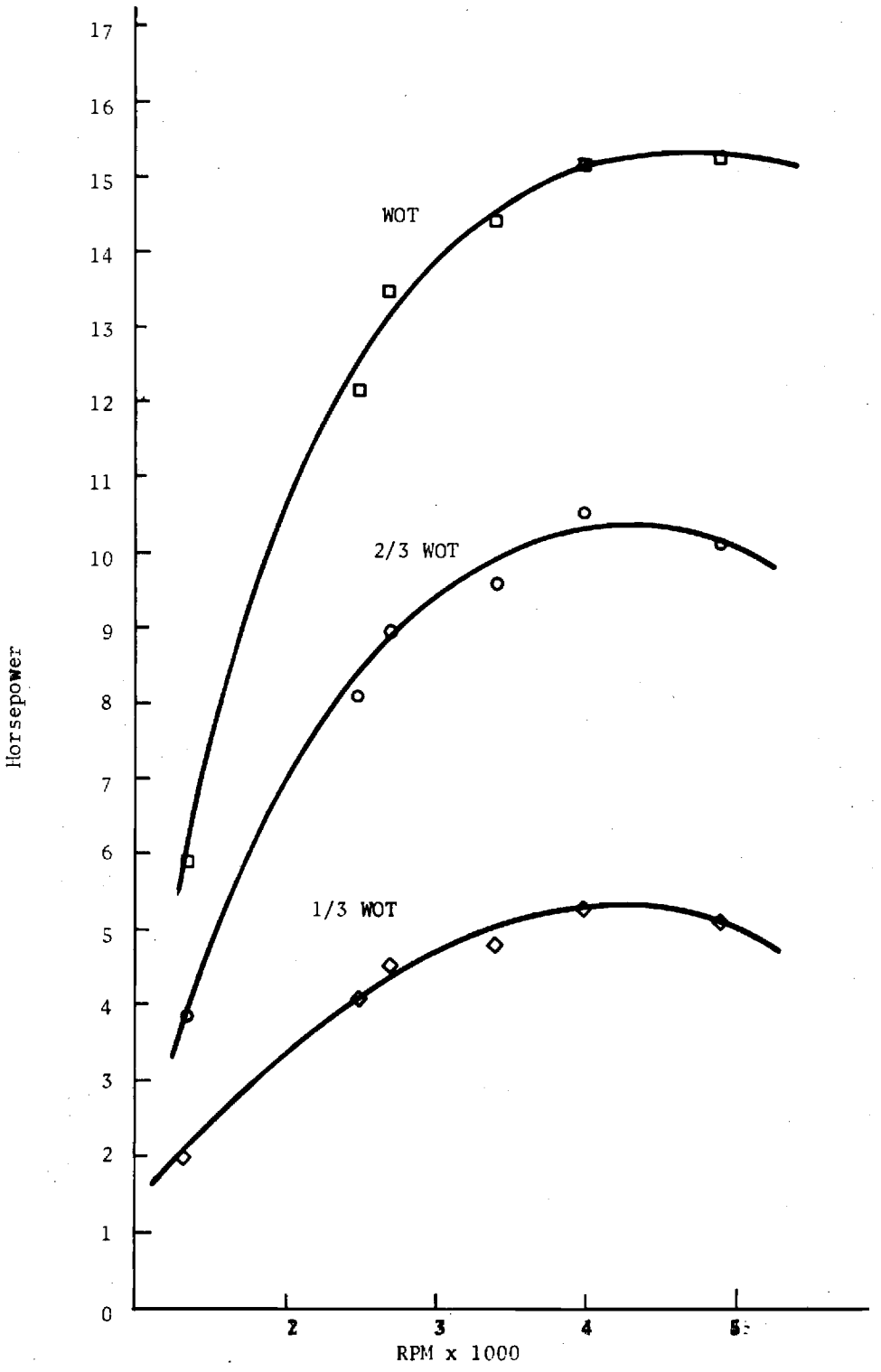

Figure 47 . Sachs KM-914A Horsepower vs.RPM (Gasoline).

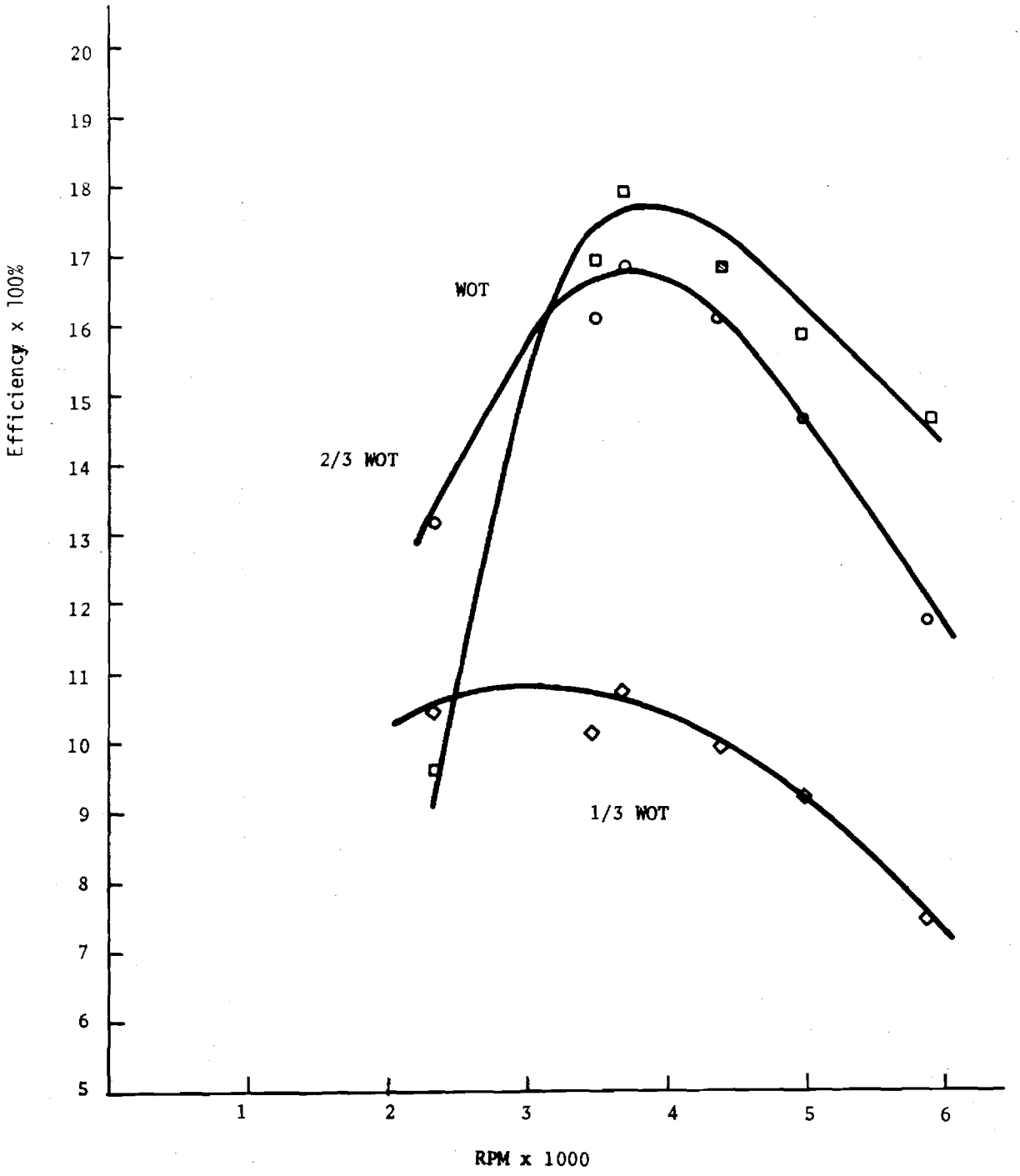

Figure 48. Sachs KM-914A Thermal Efficiency vs.RPM (Gasoline).

Stoichiometric
Air-Fuel Ratio

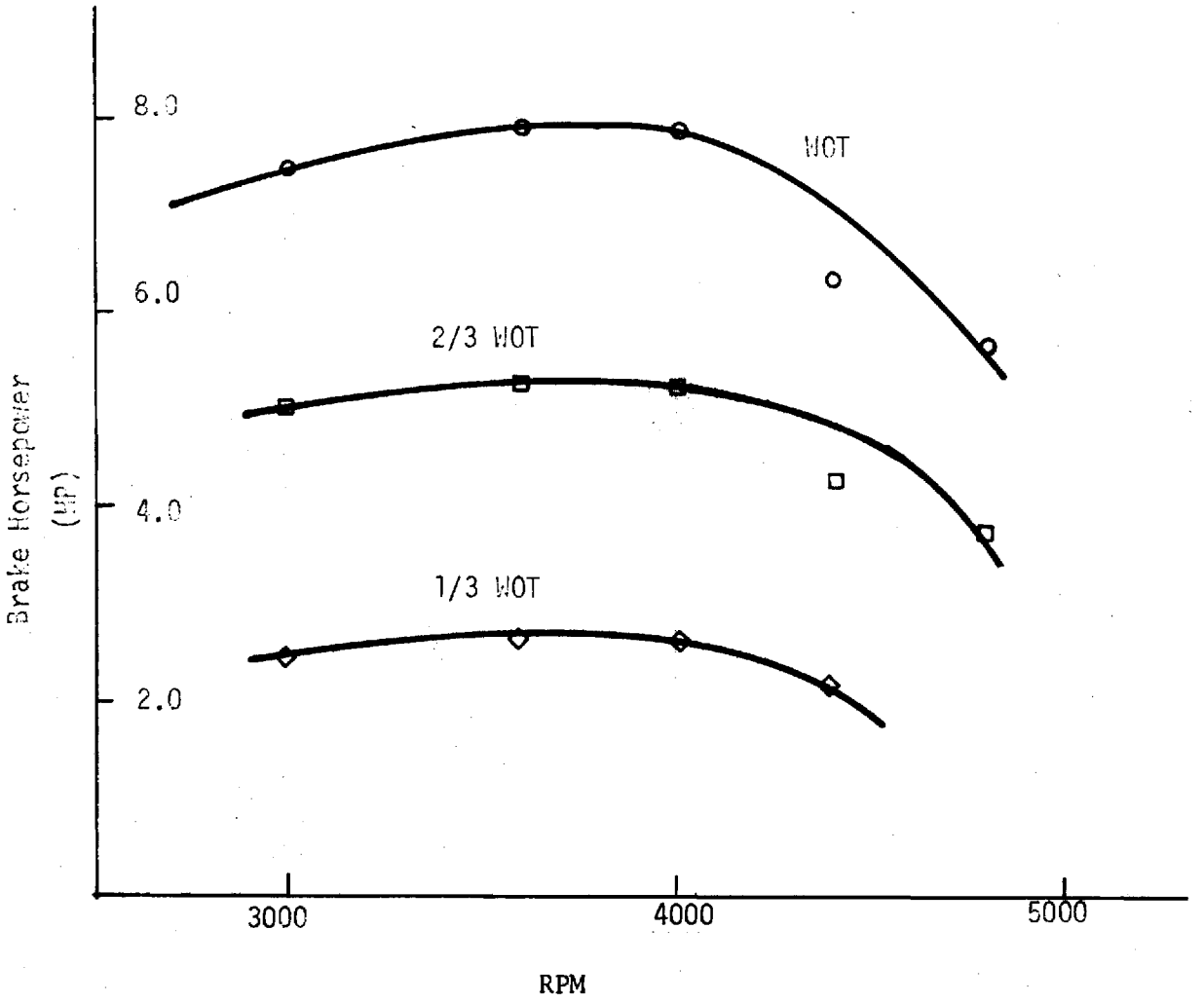

Figure 49. Sachs Rotary Engine - 16 HP
Horsepower vs RPM
(Natural Gas)

Stoichiometric Air-Fuel Ratio
Factory Spark Setting 12° BTDC

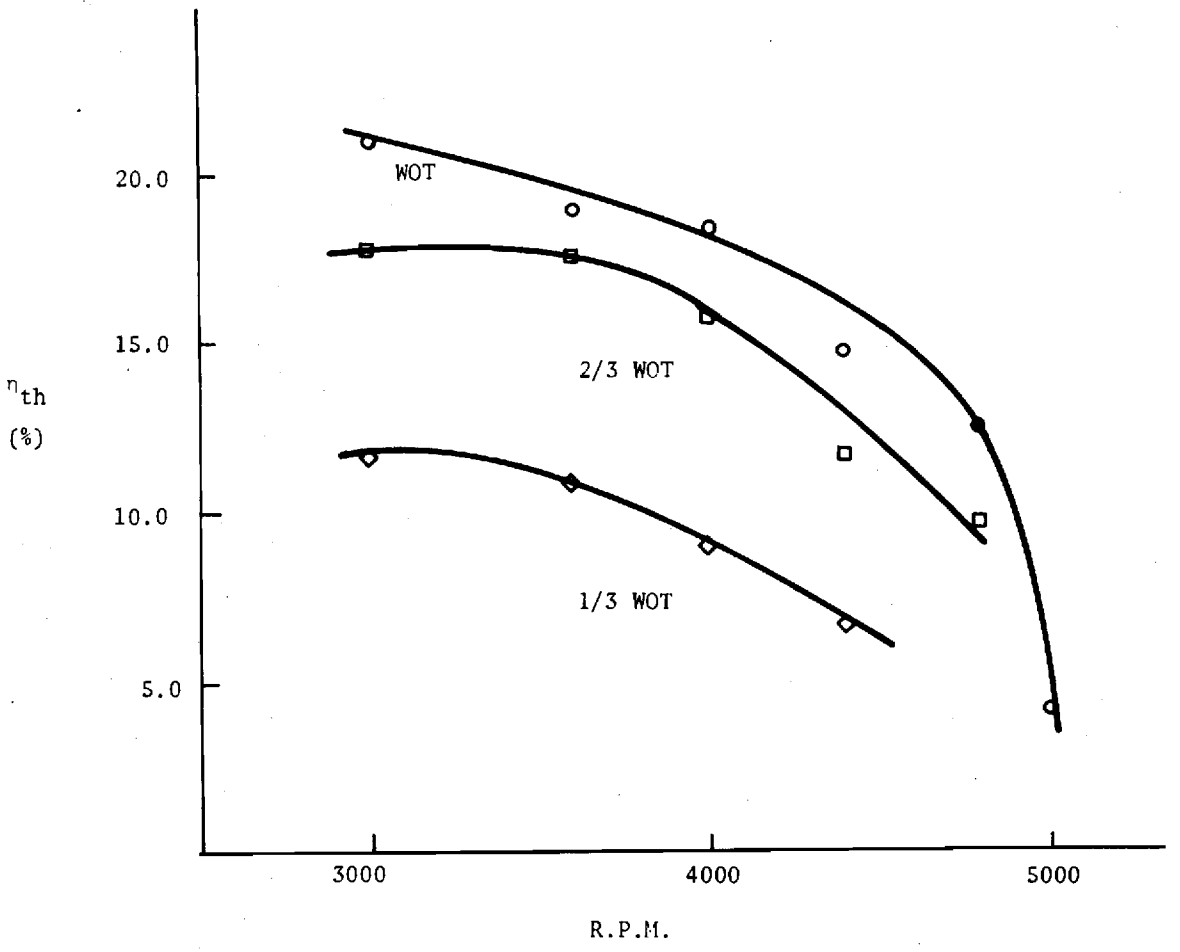

Figure 50 . Sachs Rotary Engine - 16 hp Thermal Efficiency vs. R.P.M. (Natural Gas).

Thermal efficiency at the desirable 3600 rpm is shown versus air-fuel ratio in Figure 51 with the spark advanced to 18° BTDC. The peak is shown at the previously discussed stoichiometric point. This value is about 21 percent. slightly higher than the 18 percent at the same condition but with 12° BTDC spark timing.

Volumetric efficiency (based on air mass flow only) was also determined for this engine on natural gas as displaced in Figure 52 versus air-fuel ratio. It shows the expected decline in air mass flow at rich mixture due to the natural gas displacing some of the air. The low value of around 50 percent is due to the engine being of a charged-cooled rotor design meaning that the rotor is cooled by the intake mixture being passed through the rotor before entering the combustion chamber. This heats the air significantly above room temperature reducing its density.

From exhaust temperature measurements and the air mass flow rates made at 3600 rpm, WOT, and varying air-fuel ratio an exhaust energy flow was calculated with the results shown in Figure 53.

This figure demonstrates a unique characteristic of rotary engines, i.e., that a high percentage of the waste heat energy is contained in the exhaust. Note that at very lean mixture the exhaust contains 65 percent of the total input natural gas energy. At the more optimum (from the thermal efficiency standpoint) stoichiometric air-fuel ratio, the exhaust contains 60 percent of the total energy input to the engine. This results from a high exhaust temperature around 2000°F.

At the rich condition, the energy in the unburned fuel shows up in the miscellaneous category increasing energy flow in that category which also includes cooling losses and cooling fan power consumption. Here again, the thermal efficiency is seen to be about 20 percent.

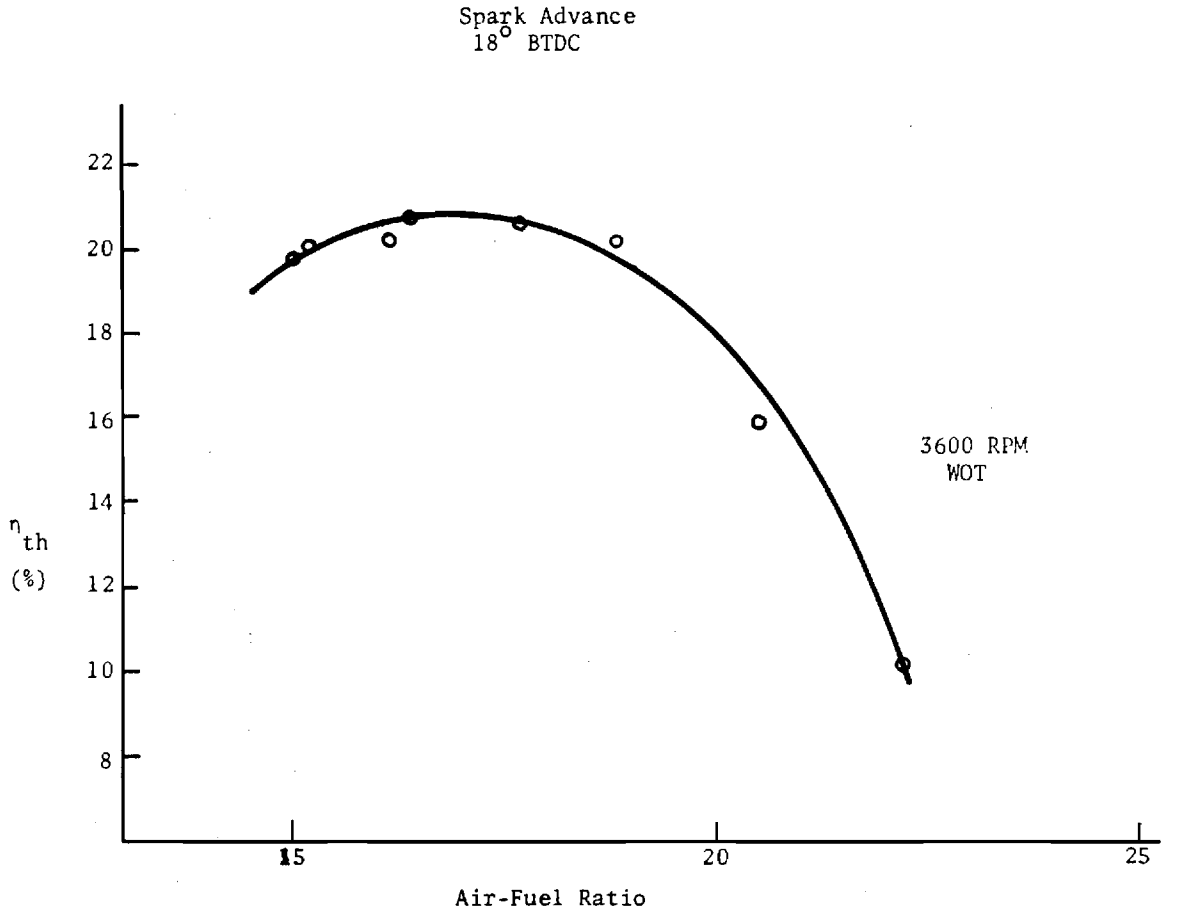

Figure 51 . Sachs Rotary Engine - 16 hp Thermal Efficiency vs. Air-Fuel Ratio (Natural Gas).

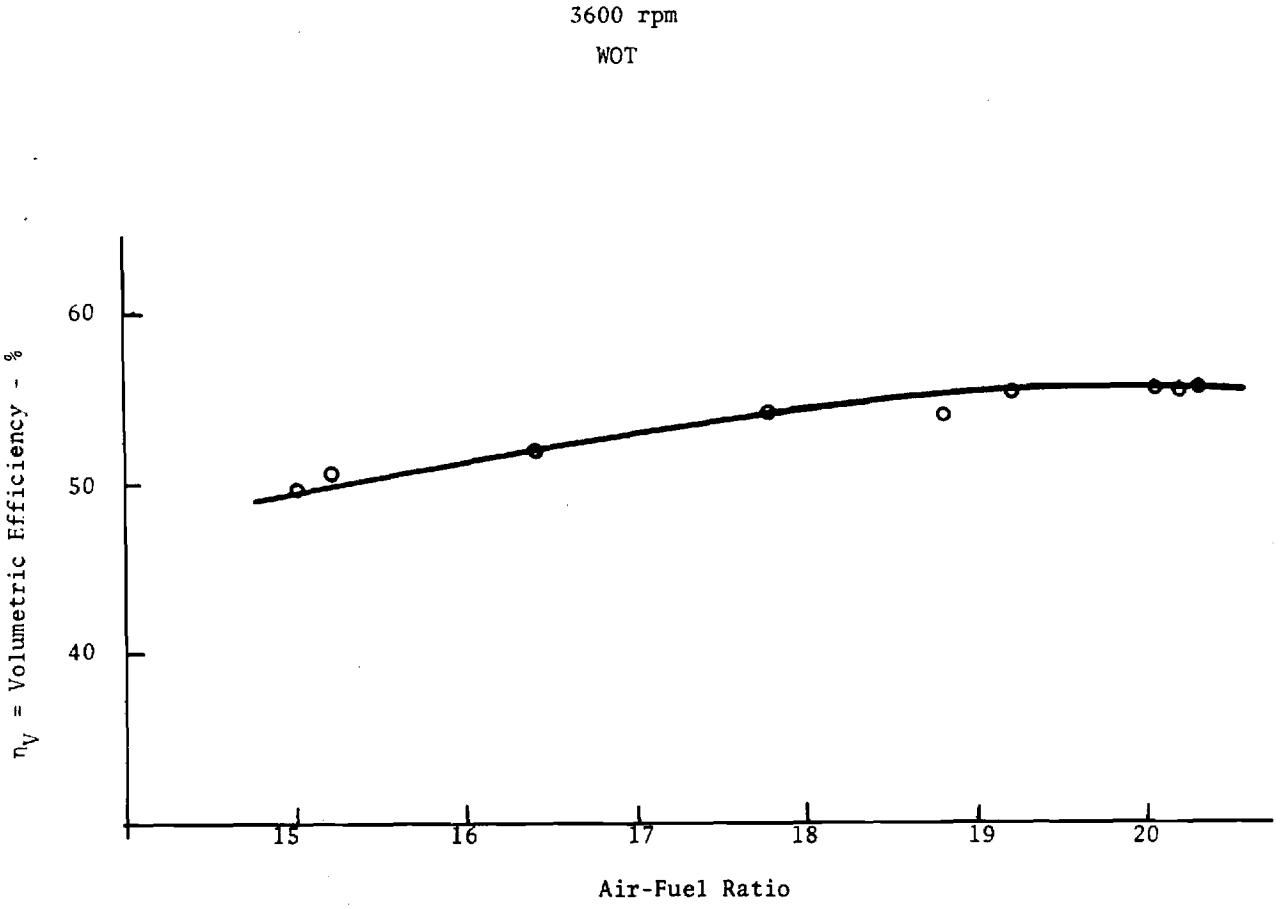

Figure 52 . Sachs Rotary Engine. Volumetric Efficiency vs. Air Fuel Ratio (Natural Gas).

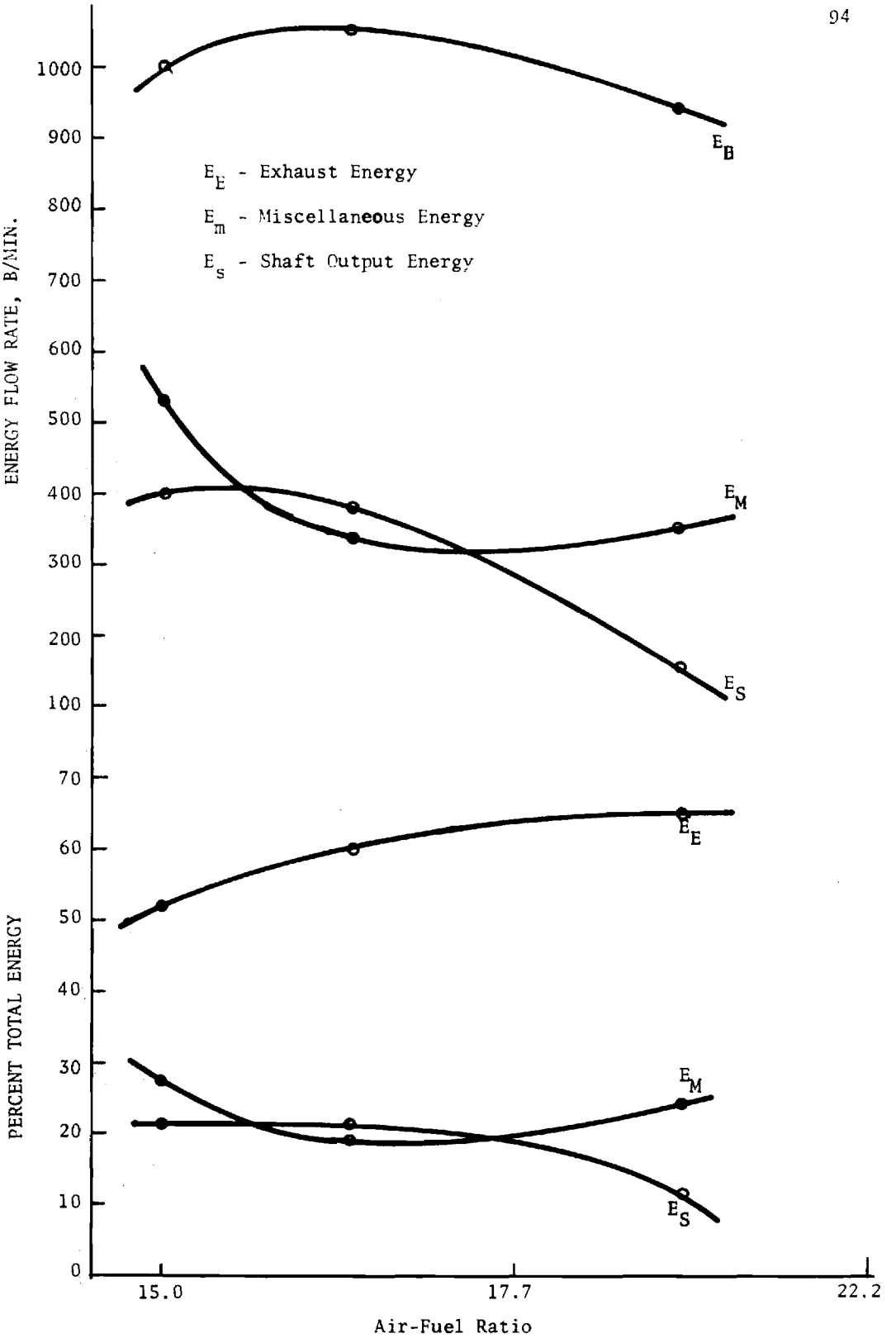

Figure 53 . Sach KM914A Exhaust, Shaft, and Miscellaneous Energy Flow Rates vs. Air-Fuel Ratio.

Seal Wear

The Sachs engine seal dimensions were measured as received from the factory, after 1012, 1584, and 1870 hours of operating at 3600 rpm, 8 hp. The results for the apex, corner, and side seals are shown in Figure 54 . The worst case is the apex seal which shows an average wear rate of 2.1 x 10^{-6} inches per hour. This compares with factory supplied apex wear rates of 13 x 10^{-6} inches per hour on gasoline.[15]

In Figure 55 the seal wear curve for a Sachs KM37 is shown. This 6 hp rated engine was run at 3 hp, 3600 rpm on propane between 0 and 750 hours and on natural gas from 750 to 1250 hours. Its wear rate is seen to be .9 x 10^{-6}in./hr.

Using the manufacturer's recommended allowable wear before replacement[16,17] of .016 inch for the KM914A and 0.020 inch for the KM37, the apex seal life for these engines extrapolate to 8,000 hours and 33,000 hours respectively. The side and corner seals on the KM914A extrapolate to 21,000 and 31,000 hours respectively while the same seals on the KM37 extrapolate to 53,000 and 19,000 hours respectively.

Conclusions

Power production from the Sachs KM914A engine at 3600 rpm changed from 14.5 hp with gasoline to 8 hp with natural gas. This is the peak horsepower on natural gas with it declining at the lower or higher speeds.

Efficiency on gasoline peaks at 18 percent at 3600 rpm while on natural gas the peak was about 20 percent, again at close to 3600 rpm.

The ignition system appears to require no service up to 2000 hours.

At the desirable operating conditions of 3600 rpm and near stoichiometric air-fuel ratios, the recoverable exhaust heat is about 50 percent of the total gas input energy. Since 20 percent of this gas energy is put out as shaft work, 50/80 or about 65 percent of the waste heat is contained in the

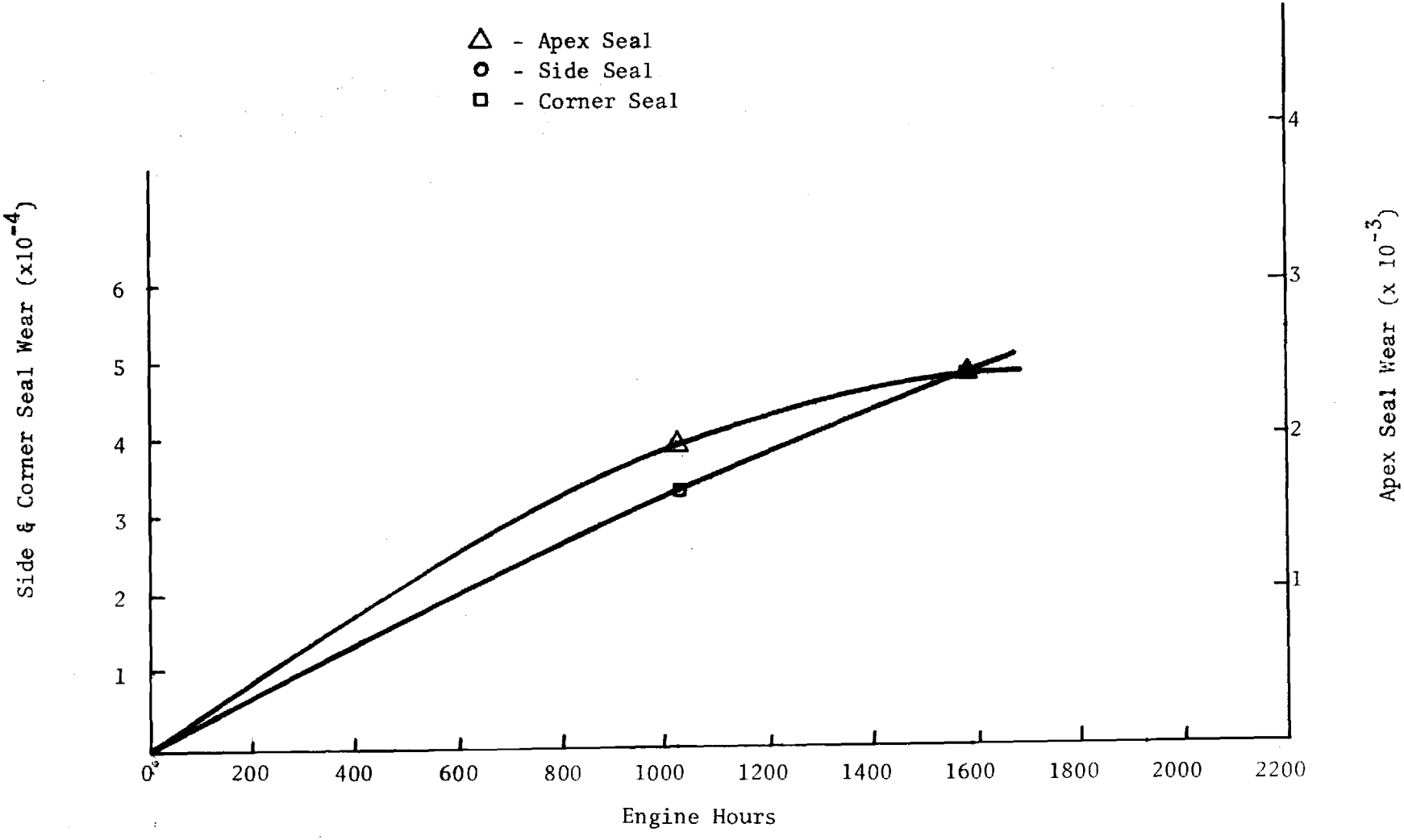

Figure 54. Seal Wear vs. Time - Sachs KM914A

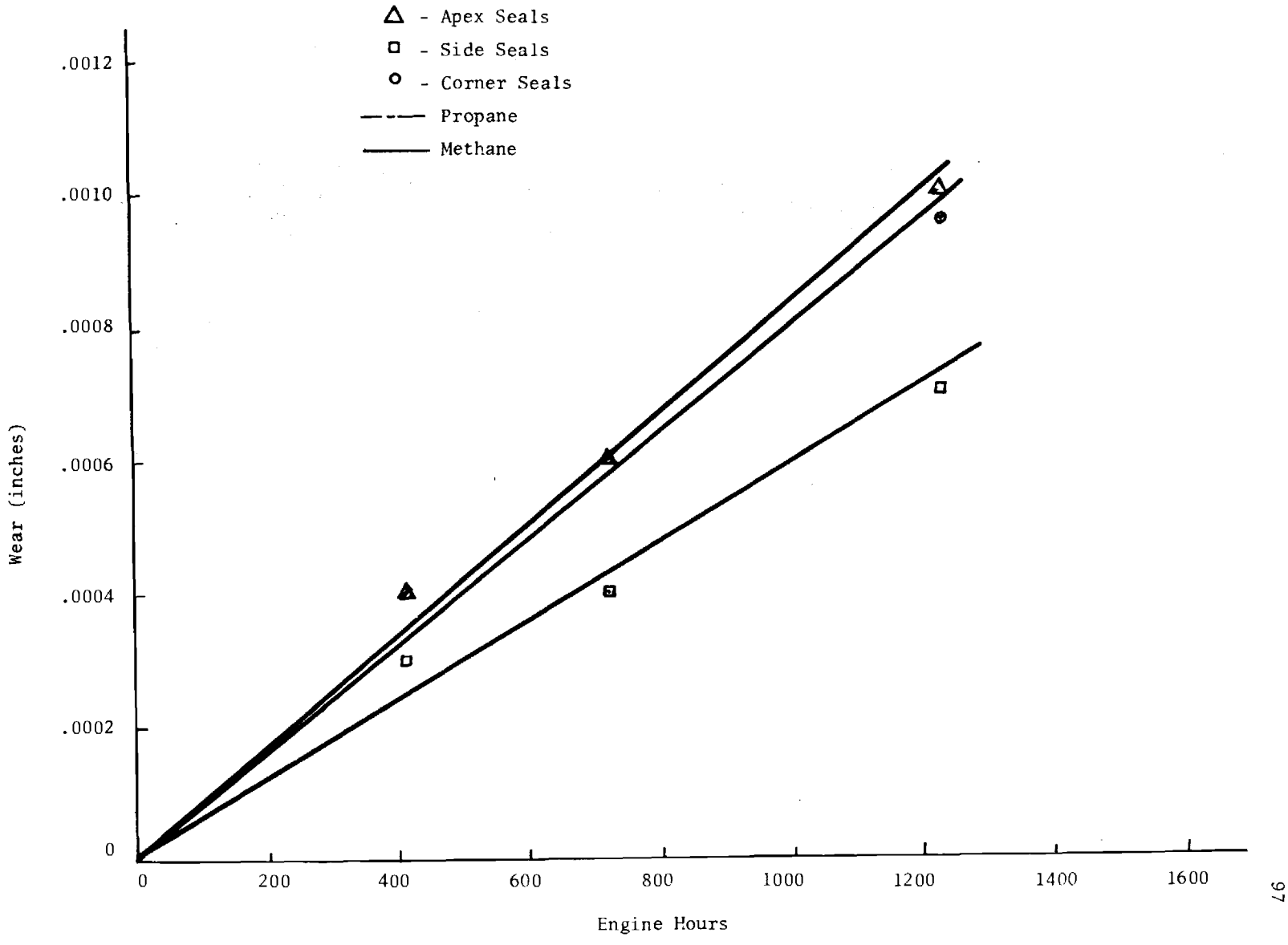

Figure 55. Seal Wear vs. Time - Sachs KM37.

exhaust.

The rotor apex seal wear for two Sachs engines were between 1 and 2 microinches per hour. This results in extrapolated seal life times before performance deterioration between 8,000 and 30,000 hours.

These natural gas rates compare with gasoline wear rates of 9 to 13 microinches per hour for the same engines.

The extrapolated seal lifes should be conservative as all seal wear studies published, as well as this study, show a decreasing wear rate with time. Also, the specified replacement points are recommended if the engine is already torn down. Performance will not be affected at this wear condition.

CHAPTER VII

CONCLUSIONS

Heat Pump Hardware

In light of the system analysis presented in Chapter II and the engine test results presented and discussed in Chapters III through VI, two conclusions can be drawn. First, that natural gas with commercially available hardware will provide space heating and cooling with as little as one-half the natural gas required by an absorption air-conditioner and gas furnace. Secondly, that using a Wankel rotary engine as the prime mover running at 3600 rpm, the rotor seals will last at least 10,000 hours without replacement.

The obvious remaining two areas in question are the reliability and capital cost of the entire system, including the necessary accessories. The system accessories must be evaluated by building a system and placing it in operation.

Two systems are recommended, one being a residential sized 5 ton system and the other being a commercial sized twenty five ton system. The major hardware components have been tentatively selected and are given below.

	Residential	Commercial
Engine:	Sachs KM914A	Toyo Kogyo TK0839
Compressor:	Copeland 4A1	Trane F-230
Generator:	Sears 3KW	None
Waste Heat Exchanger:	Amana HTM	Young type F.
Evaporator:	Amana EG5	Carrier 25 ton
Condensor:	Air Cooled Amana EG5	Air Cooled Kramer C31A22

The engines will be equipped with magnetically triggered solid state ignition systems and modified for natural gas the same as those discussed in this study.

The residential unit will be equipped with an emergency 3 KW generator driven through a Warner magnetic clutch model 1406. The commercial sized unit with the water cooled engines will also be equipped with a cooling water waste heat recovery system.

An electronic control system has been designed for both units consisting of as many solid state components as possible. Several high amperage relays and pressure switches are the only non-solid-state components used. A conventional heat pump thermostat provides the off-on, heat-cool input signal to the system. Both a stand-alone 12 volt battery system and a 120 volt AC system has been designed. Figures 56 and 57 show these circuit designs.

For this all solid state circuit, a high reliability can be expected. The total cost for the components is $67.00.

Natural Gas Conservation

One of the prime advantages of the natural gas heat pump is its obvious fuel conservation characteristics. Basic thermodynamics shows that a natural gas heat pump can theoretically approach the ideal maximum heating efficiency which nature will allow. The national impact of this natural gas conservation is dramatic. This national impact has been studied in reference 8 using pragmatic marketing assumptions. The resulting savings by 1990 would be 2.8 trillion cf annually. It is assumed in these calculations that the share of the heating appliance market captured by the gas industry would continue to decline. The number of heat pump units was assumed to grow as shown in Table 2.

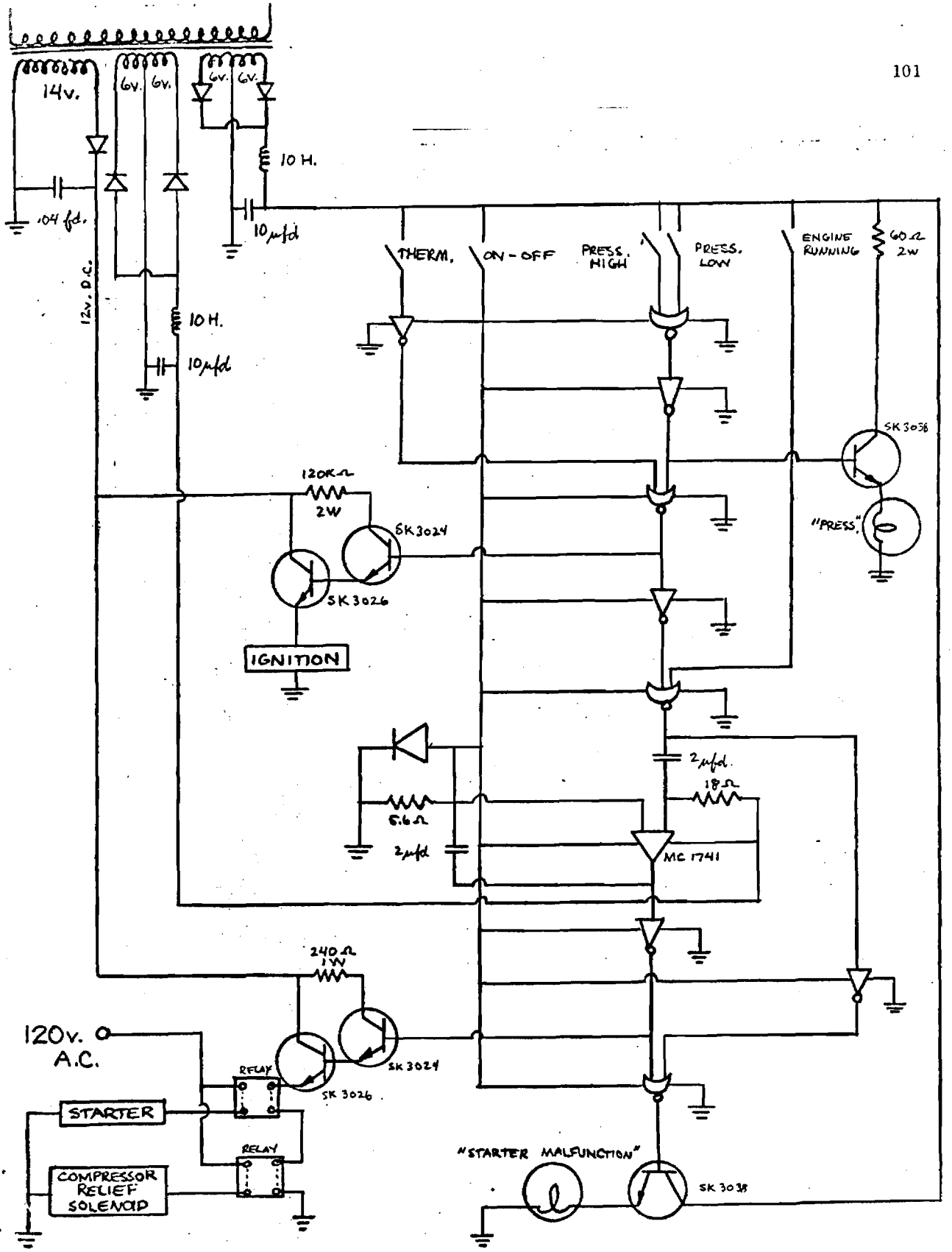

Figure 56. 120 Volt AC Heat Pump Control System.

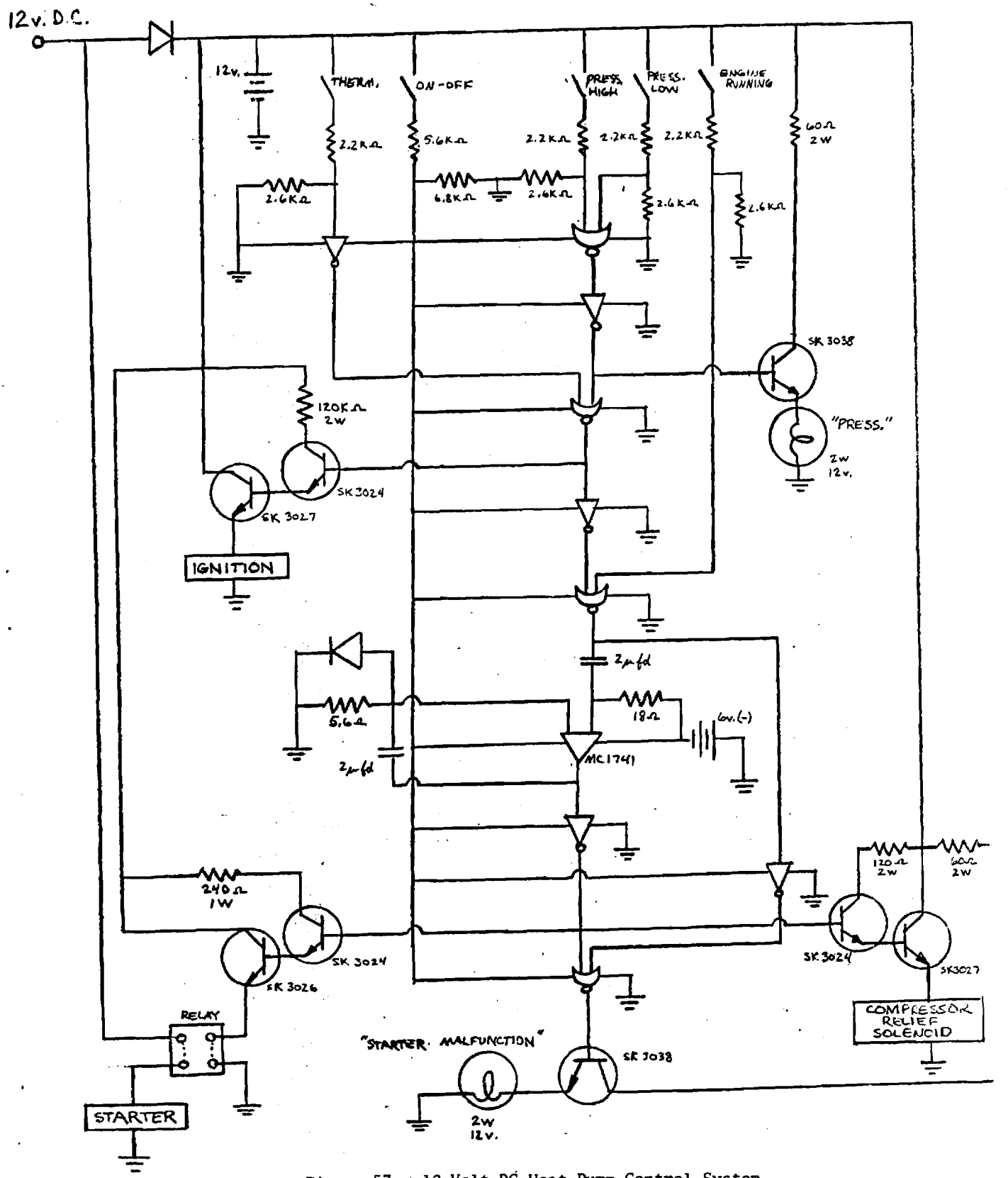

Figure 57. 12 Volt DC Heat Pump Control System.

Since coal gasification facilities by 1990 are expected to be producing 3 trillion cf of synthetic gas annually (slightly more than the 2.8 trillion cf which could be conserved annually by the heat pump, the two alternatives of: 1) coal gasification facilities versus 2) gas heat pumps, should be compared.

Table 2

Heating Market Shore
(of Total Units Sold)

Year	All Gas Systems	Heat Pump Units
1970	60.8%	
1976	52.3%	3.1% (140,000)
1980	51.2%	7.7% (762,000)
1985	50.2%	21% (1,853,000)
1990	50.0%	40% (3,416,000)

Looking at the capital cost alone, present coal gasification plant costs are $5.70 for 1000 cf of synthetic gas production capacity per year[9]. In 1990, the capital investment required to produce 2.8 trillion cf annually would be $16 billion in present dollars. If instead of relying on coal gasification plants at a cost of $16 billion, the heat pump was developed and marketed according to the projections in Table 2, this capital would not be needed due to the 2.8 trillion cf reduction in natural gas demand. This $16 billion coal gasification plant would be replaced by 6,171,000 heat pump units. The capital available for these units would be $2600 per unit. The annual fossil fuel required by the gasification plant would be saved on top of this.

Heat Pump Gas Demand

Another prime advantage of the gas heat pump in addition to its more efficient use of gas, is that it uses it at a rather level demand rate. The monthly demand for a gas furnace (COP_H = .7) is compared to that for the gas heat pump (COP_H = 1.3, COP_C = 1) in Figure 58. The comparison is rather dramatic when it is realized that the gas heat pump heats and cools year around with less total gas than a gas furnace requires for heating only. The furnace annual load factor (average monthly demand over peak demand) is 0.38 compared to the heat pump annual load factor of 0.63. These results were derived for Atlanta, Georgia 10 year weather conditions.

Air Pollution Impact

With present environmental concerns, any new system being considered for wide spread use must be investigated for its environmental impact. With the exhaust emissions data in Chapter III, taken at 3600 rpm and 2/3 WOT, the air pollutant emissions can be compared to existing heating systems.

The systems to be compared with a gaseous heat pump having a COP of 1.3 are electric resistance heating with a COP of .3, electric heat pump heating with a COP of .6, and gas furnace heating with a COP of 0.7. It is assumed that electricity for the electric systems is supplied by a coal fired power plant burning 3 percent sulphur, bituminous coal, the type typically used in Georgia.

Table 3 shows the exhaust emissions from the different systems mentioned. The comparison is based on the mass of pollutant emitted per 10^5 BTU of useful heat produced. Hydrocarbon, NO_x, CO, and SO_x data for the electric and gas furnace systems were obtained from Reference 11 and were given in (lbm pollutant)/(ton coal input) and (lbm pollutant)/(ft^3 gas input)

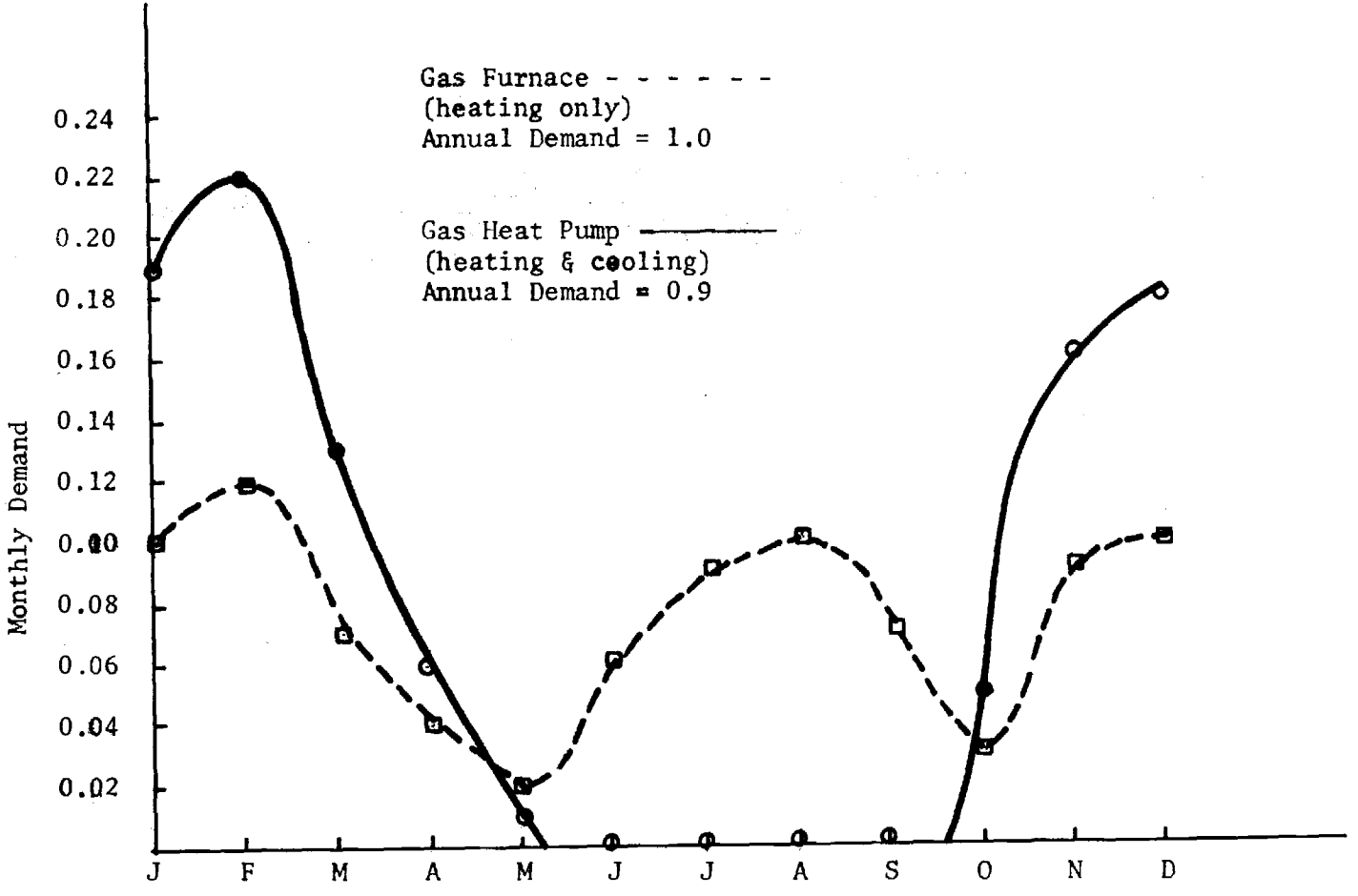

Figure 58. Monthly Gas Demand for Gas Furnace vs. Gas Heat Pump.

Table 3. Emissions of Various Heating Systems (1bm pollutant)/(10^5 BTU useful)

Method of Heating	Particulates	NO_x	HC	CO	SO_x	Total
Resistance	.06	.16	.0023	.0088	1.0	1.231
Electric Heat Pump	.03	.08	.0012	.0044	.5	.615
Gas Furnace	0	.011	.0011	.0024	0	.0246
Gaseous Heat Pump	0	.056	.32	.097	0	.44

Table 4. Toxicity Weighted Emissions of Various Heating Systems (1bm pollutant)/(10^5 BTU useful)

Method of Heating	Particulates	NO_x	HC	CO	SO_x	Total
Toxicity Weighting Factor	1.06	.8	.5	.008	1.0	
Resistance	.064	.128	.0012	.000071	1.0	1.193
Electric Heat Pump	.032	.064	.0006	.000035	.5	.597
Gas Furnace	0	.0087	.00055	.000019	0	.0093
Gaseous Heat Pump	0	.045	.16	.00078	0	.21

respectively. Particulate data were based on the maximum controlled emission rate in Georgia of (.18 lbm particulates)/(10^6 BTU input). Knowing the heating values of natural gas and coal, the emissions were converted to (lbm pollutant)/(10^5 BTU useful heat produced). Hydrocarbon data was given on a methane basis, but was converted to a hexane basis for proper comparison.

The emissions data for the gaseous heat pump system were obtained from the engine emissions data determined in this work and were also converted to (lbm pollutant)/(10^5 BTU usable heat produced).

As can be seen, the HC and CO emissions of the gaseous powered heat pump system are much higher than with any of the other systems. These emissions, however, could possibly be substantially reduced with the use of a catalytic muffler on the engine.

Emissions of NO_x and SO_x, however, are considerably less than those of the two electric systems. Since the toxicity of SO_x is 125 times that of CO, two times that of HC, and 1.25 times that of NO_x, it appears that the electric systems create much more of a health problem than the gaseous heat pump system, due to the high SO_x levels of the electric systems[12].

Table 4 shows the total toxicity weighted emissions from each system. The gaseous fueled heat pump emits three to five times less toxic material into the atmosphere than electric systems. These toxicity weighted emissions are over estimated for the heat pump due to the fact that the non-methane toxicity factor has been used for the hydrocarbons whereas most of the heat pump emissions are methane hydrocarbons. Methane is non-toxic (in fact methane is not included as a pollutant in the ambient air standards) and therefore this toxicity factor of two should be much lower. However, since it was unknown as to what percent of the heat pump hydrocarbon emissions

are methane, the non-methane factor was used. Obviously, no detrimental impact should therefore be realized by widespread use of the system.

REFERENCES

1. Moran, E. C., and Balinger, R. K., "Building Heating and Cooling with a Gas Engine", American Gas Association, Research and Utilization Conference, Cleveland, Ohio, April 16-18, 1963, Catalog No. 154/DR-10.

2. Keller, Helmut, "Small Wankel Engines", Society of Automotive Engineers, Paper No. 680572, 1968.

3. Jones, Charles, "The Curtiss-Wright Rotating Combustion Engines Today", Society of Automotive Engineers Transactions, Vol. 73,1965.

4. Figart, W. T., Leisenring, R. L., Silvestri, W. B., "The RC Engine - A New Approach to Reduce Costs", Society of Automotive Engineers Paper No. 700273, 1970.

5. Chambers, Bill (ed), Mazda Rotary Engine Manual, Auto Book Press, San Marcos, California 1972.

6. Shelton, S., Blackshaw, A., "Combustion Mass Emissions Measurements Using FID Determined Fuel-Air Ratios", Paper 73-40, 1973 Fall Meeting, Fuel Technology/Combustion Instrumentation, El Segundo, California, 29-30 October 1973.

7. Stivender, D. L., "Development of a Fuel-Based Mass Emission Measurement Procedure, Society of Automotive Engineers Paper 710608, 1971.

8. Kennedy, D., "The Potential of the Heat Activated Heat Pump", American Gas Association Monthly, April 1973.

9. The Wall Street Journal, August 7, 1974, page 8.

10. Cuccinelli, K., "The Heat Activated Heat Pump -- A conservation Dividend", American Gas Association Monthly, July-August, 1973.

11. "Compilation of Air Pollution Emission Factors", U.S. Environmental Protection Agency, AP-42, April 1973.

12. Scheel, Jerald W., "A Method for Estimating and Graphically Comparing the Amounts of Air Pollution Emissions Attributable to Automobiles, Buses, Commuter Trains, and Rail Transit", SAE Paper No. 720166, 1972.

13. Calvert, F. O., Harden, D. G., "A Comparative Study of Residential Energy Usage", Proceedings of the Intersociety Energy Conversion Engineering Conference, Paper 739103 (1973) p. 410-415.

14. Chambers, Bill (ed)., Mazda Rotary Engine Manual, Auto Book Press, San Marcos, California, 1972.

15. Palley, L., Personal Letter, Sachs Motors Corporation-Ltd., Dorval, Quebec, January 14, 1974.

16. Repair Manual No. 4013.8 E/2, Sachs-Wankel Engine KM914, Fichtel and Sachs, Schveinfurt, Germany, October 1971.

17. Repair Manual No. 4010.8 E/2 Sachs-Wankel Engine KM37, KM48, Fichtel and Sachs AG, Schweinfurt, Germany, September 1972.

APPENDIX A

EMISSIONS SAMPLING AND MEASUREMENT APPARATUS

The laboratory was fully equipped with proper instrumentation to measure the exhaust emissions from the engines. All equipment was installed in a cabinet called a sample train which was built earlier to facilitate tests of this type. A flame ionization detector (FID) instrument for measuring total hydrocarbons and non-dispersive infrared (NDIR) analyzers for measuring carbon monoxide, carbon dioxide and nitric oxide concentrations on a dry volumetric basis were integrated into this train. Figure A-1 shows the sample train.

Samples tested were pulled through an ice bath before being pumped to the analyzers. The pump was a MB 110-10 welded bellows vacuum pump/compressor manufactured by the Metal Bellows Corporation and was capable of supplying 66 SCFH of gas. The ice bath condensed out 99+% of the water which was collected in a trap. The sample then passed through a Whitey five way valve and to each sampler. The fraction of sample pumped through the NO instrument passed through two Wilkerson model 4001-2 dryers containing indicating silicon gel. All valves were made of either stainless steel or brass. All tubing was stainless steel, tygon or nylon and swagelock tube fittings were used exclusively.

Hydrocarbon Analyzer

A Beckman model 400 hydrocarbon analyzer was used to monitor volume concentration of hydrocarbons in both exhaust gases and intake gases. The theory of operation of the FID is simple. A small amount of

sample gas at a carefully regulated pressure passes directly into a hydrogen flame and is ionized. An ionization current is produced and is carefully monitored. The current carries linearly with hydrocarbon concentration in the sample, and with proper instrument calibration accuracies of $\pm$ 2% are possible.

Calibration of the analyzer was relatively simple. First a zero gas (dry compressed air) was passed through the analyzer and the meter was zeroed. Then a sample of known hydrocarbon concentration (SPAN gas) was passed through the analyzer and an upscale point was set. The span gas used was 9500 ppm propane or 28,500 ppm carbon. The emissions data show ppm in a carbon basis.

The hydrocarbon analyzer was used to set the proper air fuel ratio during the natural gas tests. The procedure for calculation of proper volume concentration corresponding to a given air fuel ratio is described in Appendix B. This particular analyzer had been previously modified in order to measure air-fuel ratio from the intake manifold. A selective solenoid valve was used to select either exhaust sample or intake manifold sample.

NDIR Analysers

Nitric oxide (NO), carbon dioxide (CO_2), and carbon monoxide (CO) concentrations in the exhaust gases were monitored by Olson-Horiba Model AIA-2 NDIR analyzers. The principle of operation in all these analyzers is the same. Infrared light from two identical sources passes through a rotating, slotted disc where it is chopped, and then passes through two cells. The sample being analyzed passes through one cell and a reference gas remains in the other. The amount of radiation absorbed in each cell is directly proportional to the volume concentration of the gas under

consideration. The radiation is detected as it passes out of the cell and causes an upscale reading on a meter. This reading is compared to a special calibration of the particular gas.

Calibration of the NDIR instruments is very similar. First a zero gas (dry compressed air) is passed through the instrument and a zero point is set. Then a span gas of known concentration is passed through each instrument and an appropriate upscale reading is set into the meter corresponding to the concentration of the span gas. Scale readings are then converted to ppm concentrations by use of a calibration curve provided with each instrument.

APPENDIX B

DERIVATION OF AIR-FUEL RATIO FROM INTAKE MIXTURE FID ANALYSIS[6]

C_{HC} = Volume fraction of HC on per carbon basis as measured by flame ionization detector

P = Pressure of intake mixture

M_{air} = Molecular weight of air = 29 lbm/lb mole

M_m = Molecular weight of methane = 16 lbm/lb mole

V = Total volume of air-fuel mixture

A/F = Air-fuel ratio = $\frac{\text{lbm air}}{\text{lbm methane}}$

ρ_{air} = Density of air

ρ_m = Density of methane

R = Ideal gas constant

Using ideal gas equation, the densities of air and propane are expressed as:

$$\rho_{air} = \frac{(P)(M_{air})}{(R)(T)} \qquad \rho_m = \frac{(P)(M_m)}{(R)(T)}$$

The masses of methane and air are calculated by:

$$\text{lbm air} = (V)(1-C_{HC})\ (\rho_{air})$$

$$\text{lbm methane} = (V)\ (C_{HC})\ (\rho_m)$$

An expression for the air-fuel ratio as a fraction of volume HC on a per carbon basis measured by the FID hydrocarbon analyzer is obtained by combining expressions:

$$A/F = \frac{V(1-C_{CH})\ P\ M_{air}/\ RT}{V\ C_{HC}\ \ P\ M_m\ /\ RT}$$

$$= (1-C_{HC})\ M_{air}/C_{HC}\ M_m$$

$= (1.825/C_{HC}) - 1.825$

APPENDIX C

SAMPLE CALCULATIONS OF MASS EMISSIONS FROM MEASURED DRY VOLUME CONCENTRATIONS AT 3600 RPM WOT ON NATURAL GAS

These relationships for converting exhaust dry volume concentrations data to more meaningful mass emissions is fully developed in Reference 7.

HP = 52.02

$\dot{m}_f$ = fuel flow rate gm/hr = 11.540 gm/hr

C_{CO_2} = Dry volume concentration of CO_2 = 11%

C_{HC} = Dry volume concentration of HC = .44%

C_{NO_2} = Dry volume concentration of NO_x = .058%

C_{CO} = Dry volume concentration of CO = .143%

M_f = molecular weight of fuel = 16

C_x = Dry volume concentration of X

M_x = Molecular weight of X

$$\dot{m}_x = \frac{\dot{m}_f}{(HP)\ (M_f)\ (C_{CO_2}) + C_{CO} + C_{CH_4})}\ C_x\ M_x$$

$$\dot{m}_x = \frac{11{,}540}{(52.02)\ (16)\ (.11 + .00143 + .0044)} = (119.2)\ C_x M_x$$

$$\dot{m}_{CO_2} = (119.2)\ (44)\ (.11) = 576.9\ \frac{\text{gm } CO_2}{\text{HPHr}}$$

$$\dot{m}_{HC} = (119.2)\ (16)\ (.0044) = 8.39\ \frac{\text{gm HC}}{\text{HPHr}}$$

$$\dot{m}_{CO} = (119.2)\ (28)\ (.00143) = 4.77\ \frac{\text{gm CO}}{\text{HPHr}}$$

$$\dot{m}_{NO} = (119.2)\ (46)\ (.00058) = 3.18\ \frac{\text{gm NO}}{\text{HPHr}}$$

APPENDIX D-1

Toyo Kogyo TK-039

Performance and Efficiency on Natural Gas

3000 RPM

Equiv Ratio	Vacuum in Hg	Load lbs.	HP	Fuel Gm/hr	Exhaust Temp. ^{o}F	Efficiency %
.9	4.8	66*	33	7604	1380	23.27
.9	6.2	44**	22	5975	1265	19.75
.9	10.	22***	11	4712	1286	12.52
1.0	.62	76*	38	8713	1459	23.39
1.0	7.5	51*	25.5	6196	1286	22.07
1.0	13.8	25.5***	12.75	4289	1372	15.94
1.1	.6	85*	42.5	9670	1503	23.57
1.1	7.4	57**	28.33	7604	1415	19.98
1.1	14.6	28.5***	14.25	4182	1415	18.27

* -- Wide open throttle torque

** -- 2/3 Wide open throttle torque

*** -- 1/3 Wide open throttle torque

APPENDIX D-2

Toyo Kogyo TK-039

Performance and Efficiency on Natural Gas

3600 RPM

Equiv Ratio	Vacuum in Hg.	Load lbs.	HP	Fuel Gm/hr	Exhaust Temp.°F	Efficiency %
.9	.6	69.2*	41.52	9958	1459	22.36
.9	6.5	46**	27.68	7604	1329	19.52
.9	7.4	23***	13.84	7029	1415	10.56
1.0	.62	86.7*	52.02	11540	1592	24.26
1.0	6.4	57.8**	34.68	8579	1415	21.68
1.0	13.2	28.9***	17.34	4807	1459	19.34
1.1	.65	89.5*	53.7	11700	1591	24.62
1.1	6.8	59.7**	35.80	9043	1503	21.23
1.1	12.8	29.8***	17.90	5485	1529	17.5

* -- Wide open throttle torque

** -- Wide open throttle torque (2/3)

*** -- Wide open throttle torque (1/3)

APPENDIX D-3

Toyo Kogyo TK-039

Performance and Efficiency on Natural Gas

4000 RPM

Equiv Ratio	Vacuum in Hg.	Load lbs.	HP	Fuel Gm/hr	Exhaust Temp. °F	Efficiency %
.9	.9	61*	40.67	11780	1459	18.51
.9	4.5	40.7**	27.11	8713	1415	16.65
.9	8.3	20.3***	13.55	7966	1591	9.12
1.0	.9	79.3*	52.87	12580	1591	22.54
1.0	7	52.9**	35.24	9043	1459	20.90
1.0	11	26.5***	17.62	6692	1547	14.12
1.1	.95	88*	58.67	13490	1609	23.32
1.1	6.6	58.7**	39.11	19841	1512	21.31
1.1	13.4	29.3***	19.55	6083	1591	17.23

* -- Wide open throttle torque

** -- 2/3 Wide open throttle torque

*** -- 1/3 Wide open throttle torque

APPENDIX D-4

Toyo Kogyo TK-039

Performance and Efficiency on Natural Gas

5000 RPM

Equiv Ratio	Vacuum in Hg.	Load lbs.	HP	Fuel Gm/hr	Exhaust Temp.°F	Efficiency %
.9	0	50.0*	41.7	14,300	1525	15.63
.9	5.4	33.3**	27.78	12,390	1560	12.02
.9	6.5	16.6***	13.89	11,010	1749	6.77
1.0	0	78.0*	65	15,630	1681	22.3
1.0	3.9	52.0**	43.33	12,870	1726	18.06
1.0	3.5	26.0***	21.67	7,435	1636	15.63
1.1	0	81.0*	67.5	16,240	1681	22.2
1.1	3.9	54.0**	45	11,380	1749	18.03
1.1	8.5	27.0***	22.5	8,160	1636	14.7

* -- Wide open throttle torque

** -- 2/3 Wide open throttle torque

*** -- 1/3 Wide open throttle torque

APPENDIX E

Exhaust Emissions Correlation

This Appendix is a regression analysis of data collected during experiments conducted on the Toyo Kogyo TK0839 rotary engine operating on natural gas.

The purpose of this study was to determine the relationship between exhaust emissions and 1) speed, 2) equivalence ratio, 3) power output, 4) efficiency, and 5) lean misfire. Once this relationship is determined, one may then determine what conditions would need to be traded off for minimum exhaust emissions.

The data analyzed included the following:

1. RPM--measured with an electronic tachometer and held constant at different settings by means of a vacuum operated speed control. Five different settings were used; 2100, 3000, 3600, 4000 and 5000 RPM. RPM was variable X_1 and was entered in the data matrix in 100's of RPM (e.g. 21, 30 etc).

2. Equivalence Ratio: (ER). ER is the ratio of the actual air fuel ratio to the stoichiometric air fuel ratio. Three settings were used .9 (lean), 1.0 (stoichiometric or "right" air fuel ratio) and 1.1 (rich). ER was measured by means of a Beckman Hydrocarbon analyzer(which sampled the input mixture in the intake manifold) and set by adjusting the mixture jet on the carburetor. Two dummy variables were used in the data matrix to indicate ER. These were coded as follows:

ER	X_2	X_3
.9	1	0
1.0	0	0
1.1	0	1

3. Load:--Load was measured in pounds torque on the water dynometer. At each ER at each RPM three load settings were used; full load (wide open throttle), 2/3 of full load and 1/3 of full load. Load was entered in the data matrix in pounds as X_4.

4. Efficiency (η): Efficiency was determined by calculating output horsepower and dividing by fuel input. Fuel input was measured by means of a gas flow meter. (Both horsepower and fuel input are convertible to units of heat such as BTU's). Efficiency was entered in percentage as X_5.

5. Lean misfire (LMF): Lean misfire is clearly detectable misfiring of the engine which occurs at lean mixtures and low power settings. Lean misfire was entered into the data matrix in dummy variable form. A '0' was entered if LMF was not occuring and a '1' if LMF was occuring.

6. Emissions: Hydrocarbons, carbon monoxide and oxides of nitrogen were measured. For purposes of this regression analysis a weighted emission factor was computed using the recommendations of the U. S. Environmental Protection Agency emission factor was entered as variable Y. The units are grams pollutant/horsepower hour. The mix of units (CGS & English) is consistant with current EPA regulations.

The equation used is:

Emission factor = .5 (hydrocarbons) + .009 (carbon monoxide) + .8 (nitrogen oxides).

The nomenclature utilized is as follows:

X_1 = RPM in 100's

X_2 = Dummy variable for ER

X_3 = Dummy variable for ER

X_4 = Load in pounds

X_5 = Efficiency in percent

X_6 = Dummy variable indicative of lean misfire

Y = Emission factor in Gms/Hp hour

The IM*REGRES program at the Georgia Tech Rich Computer Center was used. A total of 10 runs were made with alterations in the data used made after each run. The data matrix contained 45 columns and 7 rows.

The method of "Backward Elimination" was used to select the "best" regression equation. The T values for each variable were compared with the square root of an F value for 1 and 39 degrees of freedom for the first regression and the available degrees of freedom for subsequent cases. In this way variables were eliminated until a "best" equation was found. At each step the standard error for beta was examined. This gave an idea of the "bracket" one might expect for beta. The error sum of squares was looked at, and the correlation between variables was checked.

The original model assumed was:

$$\text{Emissions} = b_o + b_1 X_1 + b_2 X_2 + b_3 X_3 + b_4 X_4 + b_5 X_5 + b_6 X_6$$

The results of the six steps were as follows:

Step 1 -- Six Independent Variables

	0	X_1	X_4	X_5	X_6
Beta	70.625	-.124	.269	-3.449	29.870
St Err Beta	24.477	.254	.198	1.314	9.501
T	2.855	-.491	1.358	-2.626	3.144

F=27.342 (4 + 40) ESS=5626.909

To be significant T must be greater than 2.021 (95% confidence level). X_3 has lowest T but it is part of a two level dummy variable, so on the next step $X_2 + X_3$ were eliminated. At this step variables $[X_5, X_4]$ and $[X_5, X_6]$ were significantly correlated.

Step 2 -- Four Independent Variables

	0	X_1	X_4	X_5	X_6
Beta	70.625	-.124	.269	-3.449	29.870
St Err Beta	24.477	.254	.198	1.314	9.501
T	2.855	-.491	1.358	-2.626	3.144

F=27.342 (4 + 40) ESS=5626.909

To determine the contribution to the variability of $X_2 + X_3$ together the following test was performed.

$$F = \frac{\frac{RSS(\text{step 1}) - RSS(\text{step 2})}{2}}{\frac{ESS(\text{step 1})}{38}}$$

= 1.2165735 with 4 + 38 degrees of freedom.

$X_2 + X_3$ are definitely not a significant contribution to the model.

On the next run variable X_1 was eliminated since its T value was low at Step 2. It is also noted that (X_4, X_5) and (X_5, X_6) still show significant positive correlation.

Step 3 -- Three Independent Variables

	0	X_4	X_5	X_6
Beta	60.479	.210	-3.001	32.281
St Err Beta	12.973	.155	.935	8.056
T	4.662	1.350	-3.211	4.007

F = 37.062 ESS = 5660.782

At this step it was noted that the F values were getting larger and that the standard error of Beta was getting smaller. Since X_4 has a T value below 2.01 it is dropped for the next step. Also, it was noted that X_5 and X_6 are still correlated.

Step 4 -- Two Independent Variables

	0	X_5	X_6
Beta	51.346	-1.978	35.323
St Err Beta	11.177	.553	7.810
T	4.594	-3.578	4.523

F = 53.632 ESS = 5912.391

At this step all the partial T tests were significant and the residuals were low at most observations. However, X_5 and X_6 were still correlated so X_6 was eliminated and the data was run again.

Step 5 -- One Independent Variable

	0	X_5
Beta	87.937	-3.712
St Err	9.245	.480
T	9.461	-7.731

F = 59.765 ESS = 8792.081

Checking for the contribution of X_6

$$F = \frac{\frac{RSS\ (step\ 4) - RSS\ (step\ 5)}{1}}{\frac{ESS\ (step\ 4)}{42}}$$

$$= \frac{15099.612 - 12219.880}{\frac{1}{\frac{21012.026}{42}}}$$

F = 5.7561674 (1 + 42 degrees of freedom)

F > 4.08

Thus X_6 contributes significantly to the variability.

The best fit regression equation is that obtained at step 4:

$$Y = 51.346 - 1.978\ X_5 + 35.323\ X_6$$

Although X_5 and X_6 are correlated, it must be remembered that X_6 is a dummy variable representing a qualitative event (presence or absence of lean misfire).

Five more runs of various combinations of the data were made to determine if a different "starting place" would lead to a different result. It was determined that the end equation would be the same.

The practical interpretation of the results is that: anything that is done to increase the efficiency of this engine reduces emissions until a lean misfire condition is reached. One way to increase efficiency is to run the engine lean, but at a certain point (low lead) lean misfire occurs and emissions increase.

GEORGIA INSTITUTE OF TECHNOLOGY
School of Mechanical Engineering
Atlanta, Georgia

FINAL REPORT

EVALUATION AND PERFORMANCE OF NATURAL GAS ROTARY ENGINE DRIVEN HEAT PUMPS

By
Thomas Honeycheck
Sam V. Shelton
Robert Tharpe

Sponsored by
Atlanta Gas Light Company
Atlanta, Georgia

May, 1976

GEORGIA INSTITUTE OF TECHNOLOGY
School of Mechanical Engineering

FINAL REPORT

EVALUATION AND PERFORMANCE OF NATURAL GAS ROTARY ENGINE DRIVEN HEAT PUMPS

By

Thomas Honeycheck

Sam V. Shelton

Robert Tharpe

Sponsored by

Atlanta Gas Light Company
Atlanta, Georgia

May, 1976

TABLE OF CONTENTS

LIST OF TABLES

LIST OF FIGURES

Figure Page

SECTION A

INTRODUCTION

General

An unavoidable consequence of the present energy crises is the need for more efficient utilization of our natural resources. Natural gas is a very important fuel for a number of reasons. Among the fossil fuels, it is the cleanest burning, requires no refining, and is easily recovered and shipped with little or no detrimental environmental impact. These factors all contribute to the justification of investigations of more efficient utilization methods of our natural gas resources.

In the United States, space heating accounts for more than one-third of the natural gas demand, a larger percentage than any other single use. Although the present day gas furnace has a rather high efficiency compared to other heating systems, basic thermodynamics shows that it can never approach the theoretical maximum heating efficiency, of which a natural gas heat pump is capable. Thus a natural gas heat pump is the only way to dramatically improve the efficiency of natural gas heating and cooling systems.

Among the possible types of natural gas heat pumps, one of the more promising is an engine-driven reverse Rankine cycle. Unfortunately, poor engine reliability has in the

past been a major problem. Recent studies in the School of Mechanical Engineering at Georgia Tech, however, have shown that the natural gas-fueled rotary·Wankel engine is capable of providing the necessary engine reliability.

National Impact

Fuel conservation is one of the prime advantages of a natural gas heat pump. Basic thermodynamics shows that such a heat pump can theoretically approach the ideal maximum heating efficiency that nature will allow. The national impact is quite impressive. Using pragmatic marketing assumptions, the resulting savings by 1990 would be 2.8 trillion cubic feet annually. It is assumed in these calculations that the share of heating appliance market captured by the gas industry would continue to decline while the number of heat pump units was assumed to grow as in Table 1.

Table 1. Heating Market Share (Of Total Units Sold)

Year	All Gas Systems	Heat Pump Units
1970	60.8%	
1976	52.3%	3.1% (140,000)
1980	51.2%	7.7% (762,000)
1985	50.2%	21% (1,853,000)
1990	50.0%	40% (3,416,000)

It should be kept in mind that the national coal gasification effort is expected to be producing three trillion cubic feet of synthetic gas annually by 1990 (slightly more than the 2.8 trillion cubic feet which could be conserved annually by the heat pump). The capital expenditure for coal gasification, however, is expected to be about $16 billion. In addition, the annual cost of the fossil fuel required by the gasification plant would be saved.

System Concept

A cooperative project between the Atlanta Gas Light Company and the School of Mechanical Engineering at Georgia Tech was begun in May of 1973 to determine the commercial feasibility of a natural gas fueled rotary engine driven heat pump. The concept is to use a rotary engine in lieu of an electric motor to drive a conventional vapor compression heat pump which absorbs heat from the outside cold air.

Space heating is accomplished by the conventional electric heat pump means of heat rejection from the condenser, as well as the waste exhaust and waste engine cooling heat. This additional heat recovery from the engine gives the natural gas heat pump a dramatic advantage over electric systems where the waste heat is disposed of at the central power plant. The outside heat absorbed by the evaporator gives the natural gas heat pump an efficiency advantage over natural gas furnaces.

SECTION B

RESULTS

Engine Testing

The prime problem with prior engine driven heat pump systems has been engine reliability. Engine reliability testing of three different engines for a total of 6,000 hours has shown that the natural gas fueled rotary engine will give the required basic engine reliability.

The component of the rotary engine requiring the earliest replacement has been the apex seals. The wear rate on these seals was measured in the tests on natural gas and shown to be up to a factor of ten times less than on gasoline. Apex seal life times before replacement were demonstrated to be 10,000 to 30,000 hours. New metal seals in place of the earlier seals tested are now available in the engine. These new seals are expected to have a lifetime greater than the 10,000 hours shown by the carbon seals.

Engine thermal efficiency was measured as 20% on the Sachs & Fichel engine suitable for a 5 ton (cooling) heat pump and 25% on the 25 ton (cooling) heat pump Mazda engine.

After the basic engine reliability was demonstrated as discussed above, two systems were designed and constructed. These were a 5 ton (cooling) system driven by an air cooled

Sachs & Fichel 914A engine employing exhaust heat recovery and a 25 ton (cooling) system driven by a water cooled Toyo Kogyo TK0839 engine employing cooling water, oil, and exhaust heat recovery. The 5 ton system is an air-to-air type heat pump (i.e. heat is pumped from cool air to warm air) whereas the 25 ton system is a water to water type system, (i.e. heat is pumped from cool water to warm water).

At the normal temperature of 40°F evaporator and 120°F condenser, the COP's (coefficient of performance) are shown in Table 2.

Table 2

Unit	COP Cooling $\frac{Q_{cool}}{Q_{gas}}$	COP Heating $\frac{Q_{heat}}{Q_{gas}}$
5 ton	0.85	1.05
25 ton	1.05	1.60

Performance Comparison with Conventional Systems

Test results were obtained also on a residential electric heat pump and high efficiency gas furnace produced by Amana. The results are shown in Table 3 where electric resistance heat has also been included at Atlanta electric rates assuming 100% efficient conversion of electricity to space heat in the building.

The rates used for these results were as follows:

	Heating (Winter)	Cooling (Summer)
Electricity	$.02/KWHR	$.03 KWHR
Gas	$1.30/$10^6$ Btu	$1.10/$10^6$ Btu

Table 3. Comparison of Alternate Systems (Based on performance with T_L = 40°F and T_H = 120°F)

	$COPH_C$	$COPH_H$	$/10^6 Btu
Electric Resistance Furnace	---	1.00	5.86
Gas Furnace*	---	0.84	1.55
Electric Heat Pump (Cooling)	0.57	---	4.63
Electric Heat Pump (Heating)	---	0.75	2.34
Gas Heat Pump (Cooling)			
Residential	.85	---	1.29
Commercial	1.05	---	1.04
Gas Heat Pump (Heating)			
Residential	---	1.05	1.24
Commercial	---	1.60	0.81

*The gas furnace values are simply averages of the measured results, which are not restricted to T_L = 40°F and T_H = 120°F.

SECTION C

CONCLUSIONS

This report presents the results of a study of a gas furnace, an electric heat pump, and a natural gas heat pump. Since the ultimate objective is to find a system that provides year-around environmental control for a home, (i.e., both cooling and heating), the comparison is essentially between the two heat pump systems. Earlier work predicted a higher COPH for both cooling and heating for a natural gas-fueled Wankel engine-driven heat pump than for a similar system driven by an electric motor. The results of this report support that prediction.

These results should not be a startling revelation. An electric heat pump is a heat-actuated system that uses a Rankine heat engine at the generating plant to drive a refrigeration cycle through an electric motor at the dwelling. A natural gas heat pump, on the other hand, employs a heat engine to drive a refrigeration cycle right at the point of use. It seems more logical to convert a fuel to sensible heat at its point of use, rather than convert it to another form of energy at a remote generating station and then reconvert it to sensible heat. Any electric system suffers from power plant inefficiencies as well as transmission losses.

An analysis has been made by others of energy losses in natural gas and electrical transmission. The results are as follows. For short distances, approximately 10 to 20 miles, an average value of the electrical transmission efficiency, the ratio of energy out to energy in, is 95%. The losses, a 2% transmission line loss (I^2R loss) and a 3% loss in transformers, are a function of the distribution system loading, which varies greatly during the course of a year. The energy losses in natural gas transmission pipelines, however, are much smaller. The average energy requirements for transporting natural gas short distances, approximately 100 miles, is approximately 2% of the energy delivered to the pipeline inlet. The transmission efficiency is therefore 98% for this case, while it is estimated to be 95% for longer distances.

Natural gas is one of our premium fossil fuels. It is clean burning, requires no refining, and is easily recovered and shipped with little or no detrimental environmental impact. A natural gas-fueled Wankel engine-driven heat pump can provide a very efficient method of home environmental control, thus satisfying a very important energy requirement, and also, conserving our natural gas resources. In addition, this system is quite compatible with the environment.

The possible consequences of this system are rather amazing. This experimental study supports the analysis by

the American Gas Association showing that if natural gas heat pumps were available for installation beginning in 1976, the accumulative savings in natural gas would be about 12×10^{12} cubic feet by 1990 (or 3×10^{12} cubic feet annually) [1,16]. This is based on the assumption that only 40% of the raw heating unit market by 1990 will be made up of natural gas heat pumps. The quantity of gas saved would be equivalent to that projected to be produced from coal gasification at a capital expenditure of about $16 billion [1,16].

A crisis in energy is one of the most important problems that this country, and indeed the world, faces at present. Unfortunately, this problem will not vanish by itself in time. Wise utilization of our natural resources is no longer a desired goal. At this point, it is an absolute necessity, making continued research in this area extremely important.

SECTION D

RECOMMENDATIONS

From the performance data on the natural gas fueled Wankel driven heat pump obtained under this program, it is evident that the concept has: (1) the basic engine reliability required of such a system and (2) it offers operational cost during heating one-sixth that of electric resistance furnaces, approximately one-half that of a gas furnace, and one-third that of an electric heat pump.

The remaining problems are two-fold. (1) What is the capital cost of the system and (2) what is the reliabiliby of the system including accessories. It is felt these questions must be answered next in any continuing evaluation of the system. Also, since the capital cost and reliability disadvantages of the concept are more pronounced in the smaller units, attention should be focused on the larger 25 ton commercial system. The accessory reliability problems should be less than in a small residential system and the larger operating savings of the 25 ton system can more easily justify maintenance on the system accessories. At this point, the accessories, such as ignition, starter, and controls are the critical items to be considered.

Therefore, it is felt the next program to be undertaken should be a 12 month demonstration program of a daily

operating 25 ton system. This program will require considerable effort at the beginning to make sure reliable accessories are in hand, particularly the starter motor. Accessory problems can then be better solved and evaluated, seasonal operating efficiencies can be measured, and system cost better known.

CHAPTER I

INTRODUCTION

Background

An unavoidable consequence of the present energy crises is the need for more efficient utilization of our natural resources. Natural gas is a very important fuel for a number of reasons. Among the fossil fuels, it is the cleanest burning, requires no refining, and is easily recovered and shipped with little or no detrimental environmental impact. These factors all contribute to the justification of investigations of more efficient utilization methods of our natural gas resources.

In the United States, space heating accounts for more than one-third of the natural gas demand, a larger percentage than any other single use. Although the present day gas furnace has a rather high efficiency compared to other heating systems, basic thermodynamics shows that it can never approach the theoretical maximum heating efficiency, of which a natural gas heat pump is capable. Thus a natural gas heat pump might be one way to significantly improve the already high efficiency of natural gas heating and cooling.

Among the many possible types of natural gas heat pumps, one of the more promising is an engine-driven reverse

Rankine cycle. Unfortunately, poor engine reliability has been a major problem. Recent studies in the School of Mechanical Engineering at Georgia Tech, however, have shown that the natural gas-fueled rotary Wankel engine is capable of providing the necessary engine reliability [1].

Natural Gas Conservation

Fuel conservation is one of the prime advantages of a natural gas heat pump. Basic thermodynamics shows that such a heat pump can theoretically approach the ideal maximum heating efficiency that nature will allow. The national impact is quite impressive. Using pragmatic marketing assumptions, the resulting savings by 1990 would be 2.8 trillion cubic feet annually [1,2]. It is assumed in these calculations that the share of heating appliance market captured by the gas industry would continue to decline while the number of heat pump units was assumed to grow as in Table 1 [1,2].

Table 1. Heating Market Share (of Total Units Sold) [1,2]

Year	All Gas Systems	Heat Pump Units
1970	60.8%	
1976	52.3%	3.1% (140,000)
1980	51.2%	7.7% (762,000)
1985	50.2%	21% (1,853,000)
1990	50.0%	40% (3,416,000)

It should be kept in mind that the national coal gasification effort is expected to be producing three trillion cubic feet of synthetic gas annually by 1990 (slightly more than the 2.8 trillion cubic feet which could be conserved annually by the heat pump). The capital expenditure for coal gasification, however, is expected to be about $16 billion. In addition, the annual cost of the fossil fuel required by the gasification plant would be saved.

System Efficiency

In the analysis of any system an important parameter is the system efficiency, an indication of the system's merit. This term is a ratio of the desired effect relative to the input required to achieve it. In a power cycle, one is interested in the ratio of the net work output to heat input, which is termed the thermal efficiency. The concept of thermal efficiency, however, is not useful when applied to a reversed cycle (i.e. a refrigeration system or heat pump) because, in this case, the desired quantity is a transfer of heat, while the required input is some form of work or energy. Thus, an analogous term, called the coefficient of performance (COP), is usually considered. This term is of great importance in this thesis.

It would be wise at this point to consider the notation to be used throughout the following discussion.

The usual abbreviation (COP), which is used generally for coefficient of performance, can be modified by subscripts to COP_C or COP_H. The first form (COP_C) refers to a system in which the desired effect is a certain amount of heat removal (or cooling), while the latter (COP_H) refers to a system where heat addition (heating) is of prime interest. Whenever the forms COP_C and COP_H are used in this report, they refer to a cooling system in general and a heating system in general, respectively. When COP appears with no further notation, a general system efficiency is implied.

The concept of necessary input to the system suggests the need for further detail in the notation to be used. In this report, two types of COP's are defined depending on the form of input energy. In one form, the COP is defined as the cooling or heating effect relative to the net work input. The notation that will be used is COPW. Thus, $COPW_C$ and $COPW_H$ refer to the cooling and heating efficiencies based on work input to the system. The second case concerns the definition of COP as a cooling or heating effect relative to the energy content of the input fuel required to accomplish that transfer of heat. Thus, this COP is based on a heat input and the notation $COPH_C$ and $COPH_H$ will be used for the cooling and heating phases, respectively, of this type of system.

The use of the notation explained above, although perhaps somewhat different from common practice, was adopted

to avoid problems arising from the use of COP in various contexts. The primary area in which clarification is required concerns the electric heat pump system. If the cooling or heating effect is divided by the electrical input rate, which is equivalent to a work input, $COPW_C$ or $COPW_H$ is the result. To obtain $COPH_C$ or $COPH_H$ for this same system the efficiency of producing the electricity must be considered. Throughout this work a power plant efficiency of 30% was assumed. Thus, for the electrical system, $COPH_C = (0.3)X(COPW_C)$ and $COPH_H = (0.3)X(COPW_H)$. This conversion is necessary because the COP's for the gas system are based on the natural gas input rate, a heat input. In order to compare the electrical and gas systems, common parameters are required and $COPH_C$ and $COPH_H$ can be used.

Heat Pump Gas Demand

The gas heat pump uses its fuel at a rather level demand rate, another important advantage. The monthly demand for a gas furnace ($COPH_H = .7$) is compared to that for the gas heat pump ($COPH_H = 1.3$, $COPH_C = 1.0$) in Figure 1 [1]. The amazing thing to realize is that the gas heat pump in Atlanta, Georgia, for example, would heat and cool year around with less total gas than a gas furnace would require for heating only. The furnace annual load factor (average monthly demand over peak demand) is 0.38 compared to the heat pump annual load factor of 0.63. These results were derived

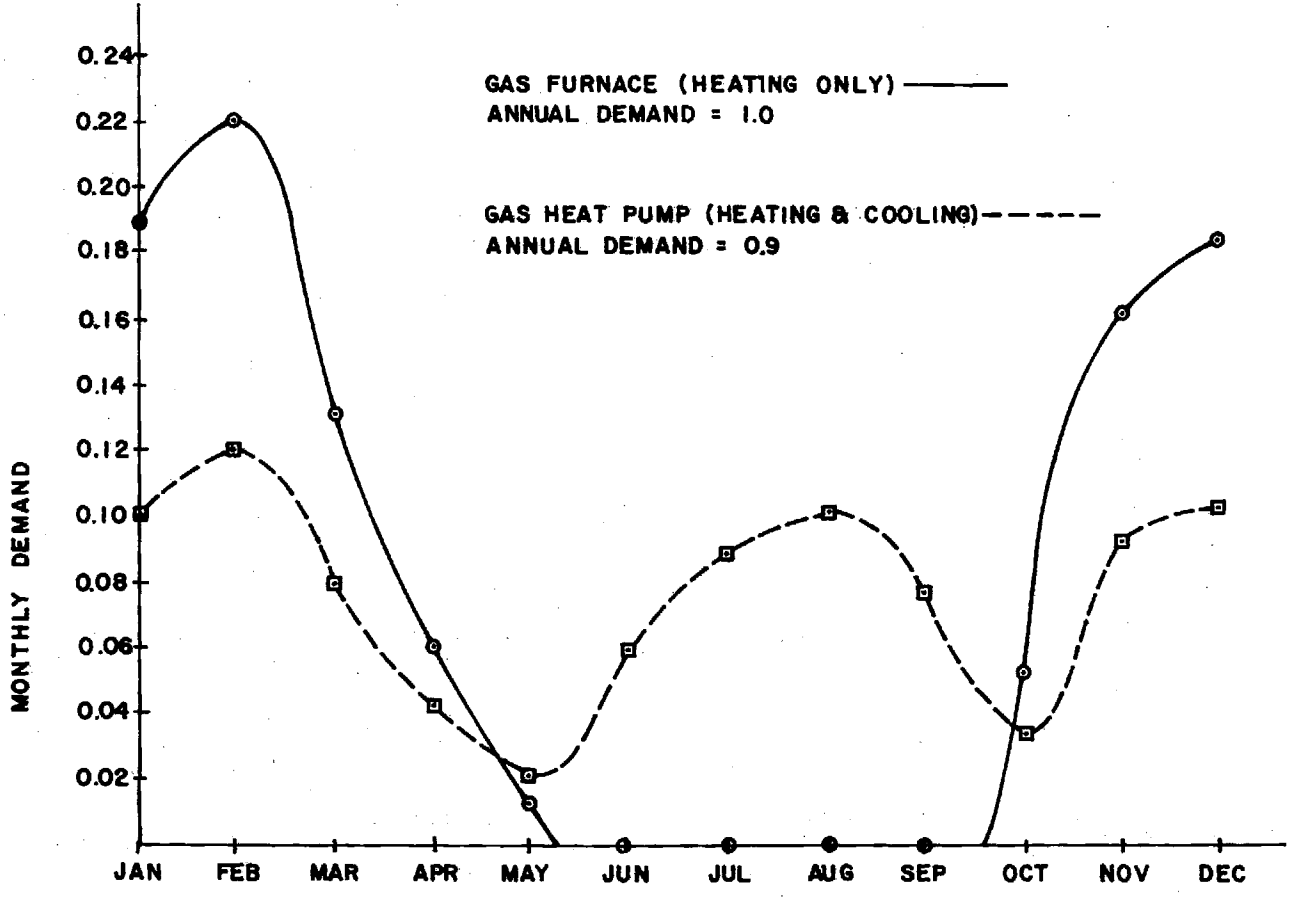

FIGURE 1.[1] MONTHLY GAS DEMAND FOR GAS FURNACE VS. GAS HEAT PUMP

for Atlanta, Georgia ten year weather conditions [1].

Air Pollution Impact

Environmental impact is an important area for consideration for any system proposed for widespread use. An electric resistance heating system with an overall system $COPH_H$ of 0.3, an electric heat pump with an overall system $COPH_H$ of 0.6, a gas furnace with a $COPH_H$ of 0.7, and a gas heat pump having a $COPH_H$ of 1.3 are compared in Tables 2 and 3 [1], assuming that the electricity for the electric systems is supplied by a 30% efficient coal-fired power plant burning 3% sulphur, bituminous coal, the type typically used in Georgia.

Table 2 compares the exhaust emissions based on the mass of pollutant emitted per 10^5 Btu of useful heat produced. Although the HC and CO emissions of the gas heat pump are higher than the other systems, a substantial reduction could possibly be achieved through the addition of a catalytic muffler on the engine. More important, however, is the gas heat pump's lower levels of NO_x and SO_x. Since the toxicity of SO_x is 125 times that of CO, two times that of HC, and 1.25 times that of NO_x, it would appear that the gas heat pump is better, healthwise, than the electric systems [1].

The total toxicity weighted emissions of each system are presented in Table 3. As can be seen, the gas heat pump emits three to five times less toxic material into the

Table 2. Emissions of Various Heating Systems (lbm pollutant)/(10^5 Btu useful) [1]

Method of Heating	Particulates	NO_x	HC	CO	SO_x	Total
Resistance	.06	.16	.0023	.0088	1.0	1.231
Electric Heat Pump	.03	.08	.0012	.0044	0.5	0.615
Gas Furnace	0	.011	.0011	.0024	0	.0246
Gaseous Heat Pump	0	.056	.32	.097	0	.44

Table 3. Toxicity Weighted Emissions of Various Heating Systems (lbm pollutant)/ (10^5 Btu useful) [1]

Method of Heating	Particulates	NO_x	HC	CO	SO_x	Total
Toxicity Weighting Factor	1.06	.8	.5	.008	1.0	
Resistance	.064	.128	.0012	.000071	1.0	1.193
Electric Heat Pump	.032	.064	.0006	.000035	0.5	0.597
Gas Furnace	0	.0087	.00055	.000019	0	.0093
Gaseous Heat Pump	0	.045	.16	.00078	0	.21

atmosphere than the electric systems. Moreover, as explained in reference 1, the gas heat pump's toxicity weighted HC emissions are over estimated and the factor of two should be much lower. The overall conclusion to be drawn is that widespread use of a gas heat pump system would result in no detrimental impact on the environment, and would offer an environmental improvement over coal source electric heating.

Heat Pump System Concept

A heat pump is a system which transfers heat from a low temperature reservoir (T_L) to a higher temperature reservoir (T_H). Energy, usually in the form of rotating shaft work to a compressor, must be supplied to accomplish this transfer (see Figure 2).

A heat pump can be used to either cool or heat a room. During the summer, the low temperature reservoir which is giving up heat (being cooled) is the room air and the high temperature reservoir which is absorbing the rejected heat is the outside atmosphere. Thus room air conditioning is achieved. The common vapor-compression cycle, used to accomplish this, is shown in Figure 3.

If a natural gas-fueled engine is used to drive the compressor, instead of an electric motor, a natural gas driven air conditioning system results.

During the winter, heating may be accomplished simply by reversing the system. The indoor coil can serve

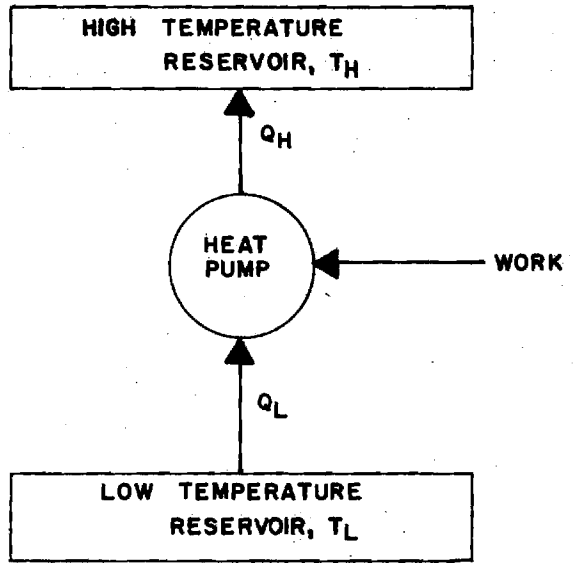

FIGURE 2.[1] THERMODYNAMIC HEAT PUMP

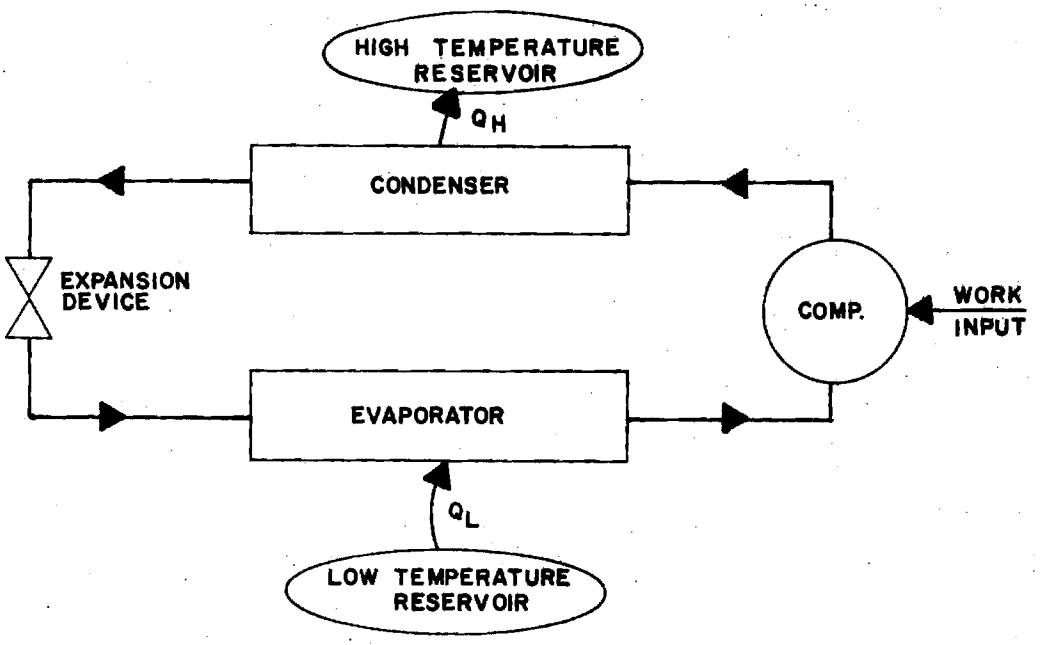

FIGURE 3.[1] VAPOR-COMPRESSION HEAT PUMP OPERATION

as the high temperature condenser to heat a room while the outside coil serves as the low temperature evaporator, absorbing heat from the atmosphere. Rather than having two systems, one for room heating and one for room cooling, a single system may be used and the condenser and evaporator functions interchanged simply by reversing the working fluid flow direction with a four-way reversing valve. If the work input to the system is provided by an electric motor, an electric heat pump results. If the work input is provided by a natural gas-fueled engine, a natural gas heat pump results.

The electric heat pump, by its basic nature, uses electricity more efficiently in space heating applications than does resistance heating. However, any electrical heating system has the disadvantage of having about two-thirds of the fossil fuel's combustion energy thrown away into rivers, lakes, or the atmosphere in the form of waste heat at the electric power plant. The power plant's remote location makes it too costly to utilize this waste heat resulting in thermal pollution as well as inefficiency.

In a natural gas heat pump, the waste heat, in this case in the form of hot exhaust gases, may be recovered to provide additional heat, as shown in Figure 4. This waste heat recovery results in a significant efficiency advantage over an electric heat pump. Thus, natural gas space heating is less costly.

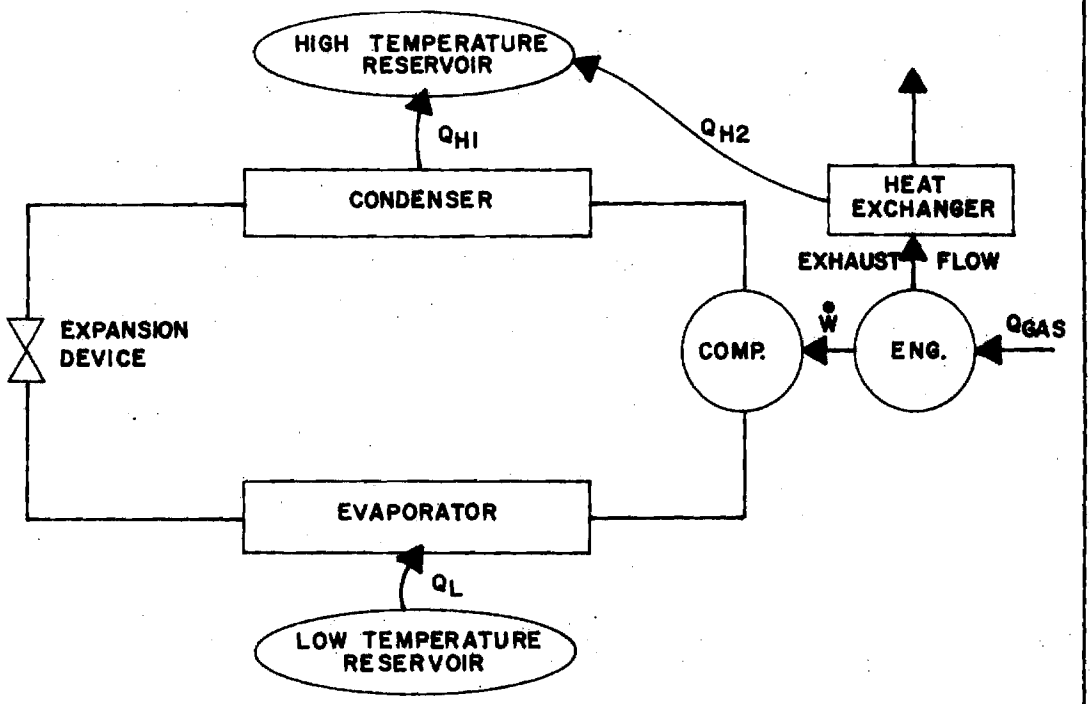

FIGURE 4.[1] NATURAL GAS HEATING BY A HEAT PUMP

Analogous to the comparison of the electric resistance furnace to the electric heat pump is the comparison of the natural gas furnace to the natural gas heat pump. The natural gas heat pump offers far more efficient utilization of natural gas than does a natural gas furnace due to the heat that the evaporator absorbs from the outside air.

This report will present for comparison the results of an experimental analysis of a natural gas furnace, an electric heat pump, and a natural gas heat pump.

CHAPTER II

HEAT PUMP PERFORMANCE ANALYSIS

Ideal Heat Pump Coefficient of Performance

The Clausius statement of the second law of thermodynamics is: "It is impossible to construct a device that operates in a cycle and produces no effect other than the transfer of heat from a cooler to a hotter body." The implication of this statement is that a system that does produce the transfer of heat from a cooler source to a hotter sink requires the input of some additional work or energy.

Basic thermodynamics show that the Carnot cycle for the working fluid of a heat engine produces the maximum work output for a given heat input. This simple cycle may be operated in the reverse direction resulting in a refrigerator or heat pump (see Figure 5). Heat is absorbed in this case from a low-temperature heat source, and a larger quantity of heat is eventually rejected to a high-temperature heat sink during the cycle. Work must be supplied from an external source to satisfy the second law. The difference between a refrigerator and a heat pump is mainly one of definition. The purpose of a refrigerator is to maintain a low-temperature source of finite size at a predetermined temperature by removing heat from it. A heat pump maintains a high-temperature

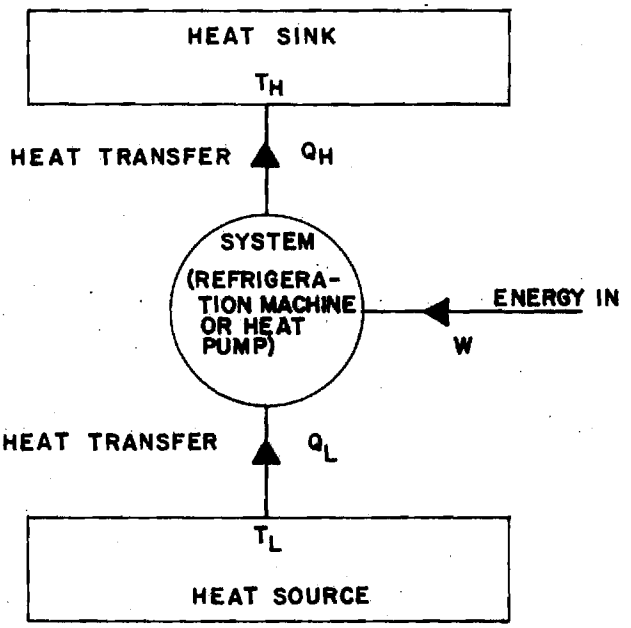

FIGURE 5. SCHEMATIC OF A CARNOT REFRIGERATOR OR HEAT PUMP

sink at a given level by supplying it with heat taken from a low temperature source.

When dealing with refrigerators and heat pumps, instead of thermal efficiency, the term usually desired is the coefficient of performance (COP). In refrigeration processes, the object is to remove the maximum quantity of heat per unit of net work input. Thus,

$$COPW_c = \frac{Q_L}{-W_{net}} = \frac{Q_{in}}{Q_{out}-Q_{in}} \tag{1}$$

The purpose of a shaft-driven heat pump is to supply the maximum quantity of heat to a high-temperature sink per unit of required net work input. Hence:

$$COPW_H = \frac{Q_H}{-W_{net}} = \frac{Q_{out}}{Q_{out}-Q_{in}} \tag{2}$$

The coefficient of performance for a Carnot, or reversible, cycle may be expressed in terms of temperatures as well as in terms of heat quantities. For heat pumps and refrigerators, heat is rejected to the high-temperature sink and heat is removed from a low-temperature source. Hence, the entropy change for a differential cycle driven by a reversible device is:

$$dS_{total} = dS_H + dS_L + dS_{device} = \frac{\delta Q_H}{T_H} - \frac{\delta Q_L}{T_L} + 0 \tag{3}$$

The maximum performance is attained when dS_{total} is zero. Thus:

$$\frac{\delta Q_H}{T_H} = \frac{\delta Q_L}{T_L} \quad \text{or} \quad \frac{Q_H}{Q_L} = \frac{T_H}{T_L} \tag{4}$$

Substituting equation (4) into equations (1) and (2) yields for a reversible work-driven system:

$$COPW_c(ideal) = \frac{Q_L}{W} = \frac{T_L}{T_H - T_L} = \frac{T_L/T_H}{1 - T_L/T_H} \tag{5}$$

$$COPW_H(ideal) = \frac{Q_H}{W} = \frac{T_H}{T_H - T_L} = \frac{1}{1 - T_L/T_H} =$$

$$\frac{T_L}{T_H - T_L} + 1.0 = COPW_c(ideal) + 1.0 \tag{6}$$

The above formulations are based on work input to the system. If one is concerned with a heat input instead, the equations are somewhat different. Consider a reversible heat engine operating between a high temperature source at T_s and a lower temperature sink at T_H, with the heat engine operating in the forward direction producing a certain amount of work (W). It can be shown that the thermal efficiency (η) of a Carnot or reversible heat engine is:

$$\eta = \frac{W}{Q_s} = 1 - \frac{T_H}{T_s} \tag{7}$$

or

$$W = Q_S \left(1 - \frac{T_H}{T_s}\right) \tag{8}$$

In these equations, Q_S represents the amount of heat input to the engine from the source at T_s. If this source represents the combustion process of an engine, for example, T_s would vary between approximately 3,000°F and ambient temperature. In this analysis, an average value of 1,000°F was assumed for T_s.

Consider a second engine operating between a source at temperature T_H and a sink at temperature T_L producing the same amount of work (W). Once again,

$$\eta = \frac{W}{Q_H} = 1 - \frac{T_L}{T_H} \tag{9}$$

or

$$W = Q_H \left(1 - \frac{T_L}{T_H}\right) \tag{10}$$

Consider now a combination of the two engines, the first a power cycle producing work (W), and the second a power cycle run in the reversed direction requiring an amount of work equivalent to (W). This combination produces a heat pump system in which the first engine provides the necessary input required by the second engine to accomplish a transfer

of heat. Equations (9) and (10) are valid for a Carnot heat pump, because all quantities are the same as for a Carnot heat engine operating between the same two temperature levels. The only difference is that the directions of heat transfer are reversed and work is required rather than produced. The work is used to "pump" heat from the heat reservoir at the cooler temperature to the reservoir at the higher temperature. Since the two work terms must be equal, equations (8) and (10) can be equated:

$$Q_S \left(1 - \frac{T_H}{T_S}\right) = W = Q_H \left(1 - \frac{T_L}{T_H}\right) \tag{11}$$

The overall system considered here can be used to provide either cooling or heating. In the cooling mode, the system is using a quantity of heat (Q_S) from the high temperature source to remove a quantity of heat (Q_L) from a low temperature reservoir, while rejecting a quantity of heat equal to (Q_H). An energy balance indicates that:

$$Q_S + Q_L = Q_H \tag{12}$$

Substituting equation (12) into equation (11) yields:

$$Q_S \left(1 - \frac{T_H}{T_S}\right) = Q_S \left(1 - \frac{T_L}{T_H}\right) + Q_L \left(1 - \frac{T_L}{T_H}\right) \tag{13}$$

or

$$\frac{Q_L}{Q_s} = \frac{T_L/T_H - T_H/T_s}{1 - T_L/T_H}$$

Thus, a COP based on heat input to the system can be defined for the cooling phase as follows:

$$COPH_C(ideal) = \frac{Q_L}{Q_s} = \frac{T_L/T_H - T_H/T_s}{1 - T_L/T_H} \qquad (14)$$

In the heating mode, the desired quantity is the heat rejected to the high temperature reservoir (Q_H). Recall:

$$Q_s \left(1 - \frac{T_H}{T_s}\right) = W = Q_H \left(1 - \frac{T_L}{T_H}\right) \qquad (11)$$

For a heat pump system with heat as the input,

$$COPH_H(ideal) = \frac{Q_H}{Q_s} = \frac{1-T_H/T_s}{1-T_L/T_H} \qquad (15)$$

The Vapor-Compression Cycle

The Carnot cycle cannot be achieved by a real working fluid. In practice, it is approached best by the vapor-compression cycle, the most important refrigeration cycle from the standpoint of commercial acceptance. The relatively high latent heats of vaporization and condensation for most fluids allow large refrigeration effects for modest rates of circulation.

The standard vapor-compression cycle is shown schematically in Figure 6, on a T-S diagram in Figure 7, and on a P-h diagram in Figure 8. The processes which comprise the standard vapor-compression cycle are:

1-2: reversible, adiabatic compression from saturated vapor to superheated vapor at the condenser pressure

2-3: heat rejection at constant pressure, desuperheating and condensation

3-4: irreversible expansion at constant enthalpy from saturated liquid to a liquid-vapor mixture at the evaporator pressure

4-1: heat addition at constant pressure in evaporation to saturated vapor.

The only difference between the heating and cooling modes is the position of the evaporator and condenser.

With the aid of a pressure-enthalpy diagram, Figure 8, the significant quantities of the cycle can be easily determined. Among these are the work of compression, the heat rejection, the refrigerating effect, and ultimately, the coefficient of performance.

The work of compression in Btu/pound of refrigerant is equal to the enthalpy change in process 1-2. From the steady-flow energy equation, with negligible changes in kinetic and potential energy, the work (W) in an adiabatic compression is simply:

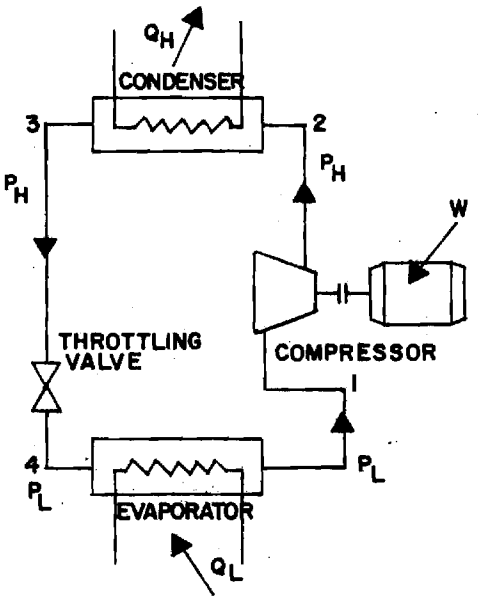

FIGURE 6. THE STANDARD VAPOR-COMPRESSION CYCLE

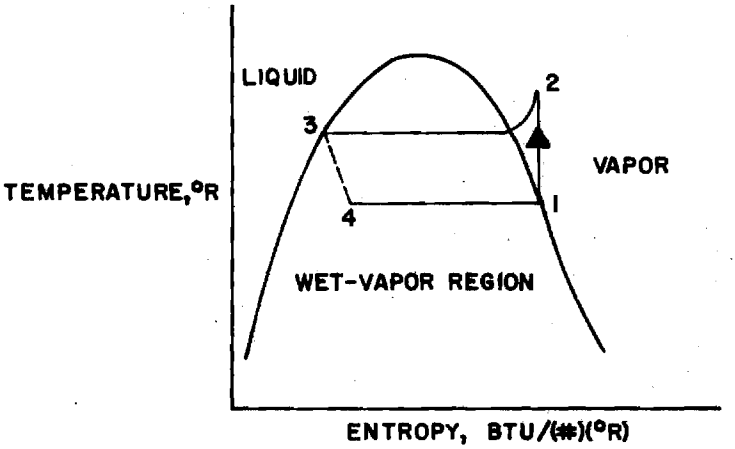

FIGURE 7. THE STANDARD VAPOR-COMPRESSION CYCLE

$$W = h_1 - h_2$$

The enthalpy difference is a negative quantity, indicating that work is done on the system. A knowledge of this quantity is important since it is the largest operating cost of the system.

The refrigerating or cooling effect in Btu/pound is the heat transferred in process 4-1, or $h_1 - h_4$. Since this process is the ultimate purpose of a cooling system, any further explanation of its importance is unnecessary.

The heat rejection in Btu/pound is the heat transferred from the refrigerant in process 2-3, which is $h_3 - h_2$. This relation also comes from the steady-flow energy equation in which the kinetic energy, potential energy, and work terms drop out. The value of $h_3 - h_2$ is negative, indicating that heat is transferred from the refrigerant. In the heating cycle this quantity is the desired effect.

The actual vapor-compression cycle suffers some inefficiencies compared with the standard cycle, as well as other changes that intentionally or unavoidably occur. Superimposing the actual cycle on the P-h diagram of the standard cycle, as in Figure 9, may be useful for comparison.

The essential differences between the actual and the standard cycle appear in the pressure drops in the evaporator and condenser, in the subcooling of the liquid leaving the condenser, and in the superheating of the vapor leaving the

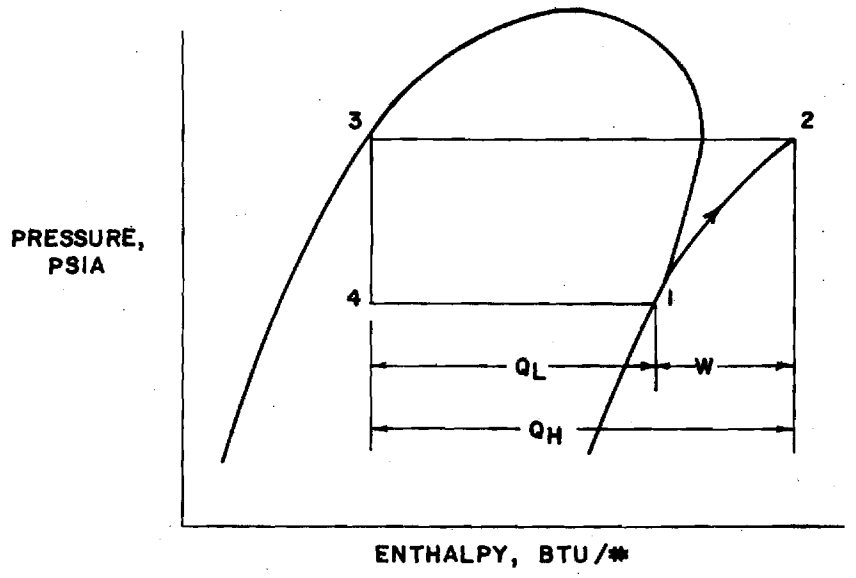

FIGURE 8. THE STANDARD VAPOR-COMPRESSION CYCLE

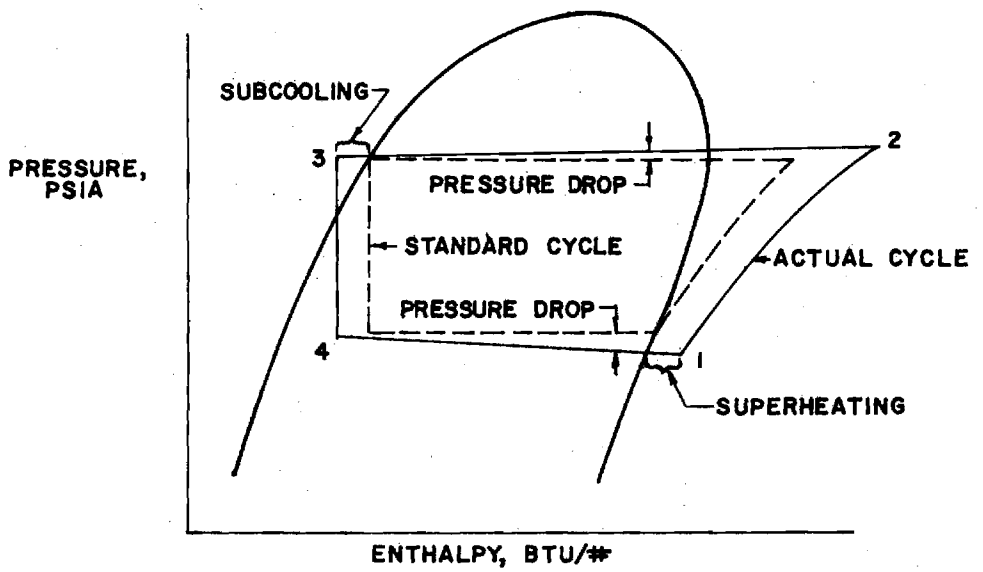

FIGURE 9.[3] ACTUAL VAPOR-COMPRESSION CYCLE COMPARED WITH THE STANDARD CYCLE

evaporator. Friction causes the pressure drops in the actual cycle, resulting in more required work in the compression process between points 1 and 2 than in the standard cycle. Subcooling of the liquid in the condenser is a normal occurrence and serves the desirable function of ensuring 100% liquid entering the expansion valve. Superheating of the vapor usually occurs in the evaporator and is recommended as a precaution against liquid droplets being carried into the compressor. Finally, the actual compression is not isentropic and inefficiencies due to friction and other losses occur [3].

Vapor-Compression Cycle Analysis

Consider, once again, the T-S diagram showing the thermodynamic path of the working fluid in the vapor-compression system (Figure 10). States 1, 2, 3, and 4 are the evaporator, compressor, condenser, and expansion valve exit conditions. State 1 is taken to be 5°F superheated and state 3 to be 5°F subcooled.

The principal disadvantage of superheating the compressor suction vapor is that the increased specific volume reduces the capacity of the compressor in terms of mass rate of circulation. Also, the top temperature of the cycle will be raised increasing the work of compression required. It is usually important, however, to avoid the admission of liquid phase fluid to the compressor, and

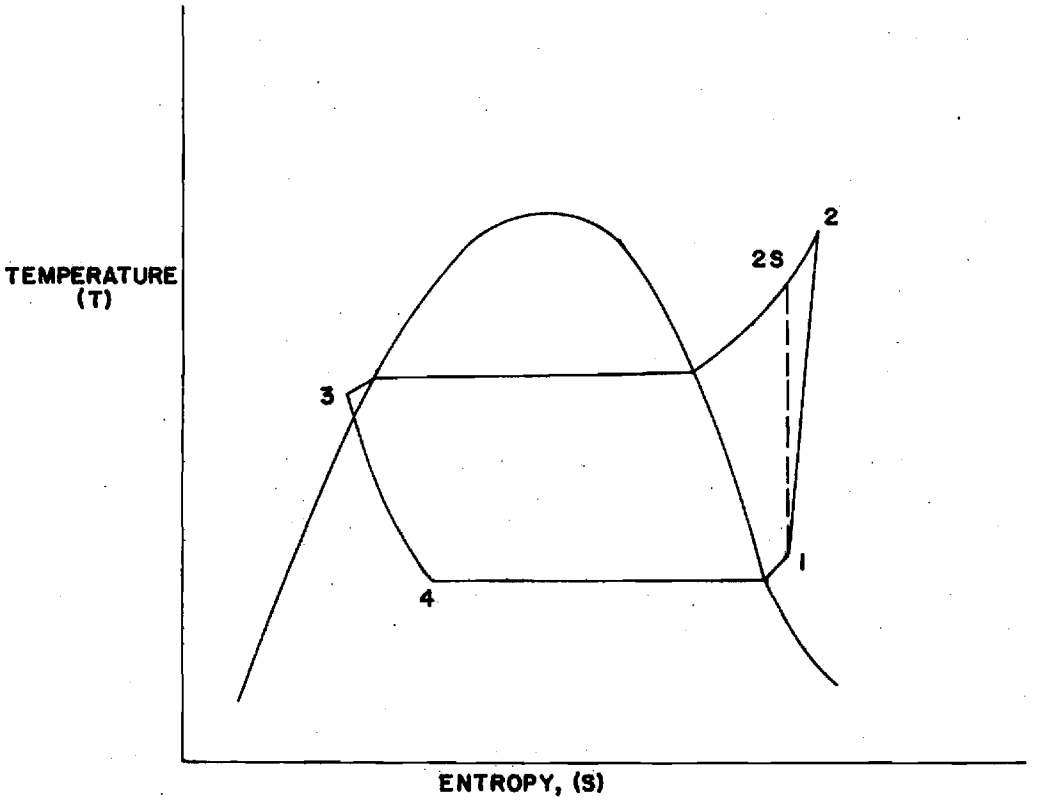

FIGURE 10.[1] WORKING FLUID T-S DIAGRAM

several degrees of superheat will ensure against this possibility.

Subcooling of the high-pressure liquid may increase the refrigerating effect. Also, if the actual system was designed to bring the fluid leaving the condenser only to the saturation line, any friction loss in the piping would result in throttling into the wet-vapor region. The resulting vapor formation and increase in specific volume would reduce the capacity of the piping, and, even more importantly, the capacity of the throttling device.

The ideal compressor work is given by:

$$\dot{W}_{ideal} = \dot{m} (h_{2s} - h_1) \tag{16}$$

where:

$\dot{m}$ = freon mass flow rate

h_{2s} = enthalpy at state 2S

h_1 = enthalpy at state 1

Inefficiencies reduce compressor performance, however, leading to a definition of compressor isentropic efficiency:

$$\eta_S = \frac{h_{2s} - h_1}{h_2 - h_1} \tag{17}$$

The actual work is:

$$\dot{W}_{act} = \dot{m} (h_2 - h_1) \tag{18}$$

Substituting equation (17) into equation (18):

$$\dot{W}_{act} = \dot{m} \left(\frac{h_{2s}-h_1}{\eta_s}\right) \tag{19}$$

The heat rejected by the condenser is given by:

$$\dot{Q}_{cond} = \dot{m} \, (h_2-h_3) \tag{20}$$

In the cooling mode, $\dot{Q}_{cond}$ is the amount of heat rejected to the atmosphere. In the heating mode, however, $\dot{Q}_{cond}$ is the desired heating effect.

The heat received by the evaporator is given by:

$$\dot{Q}_{evap} = \dot{m} \, (h_1-h_4) \tag{21}$$

$\dot{Q}_{evap}$ represents the amount of heat taken from a home, for example, in the cooling mode, while it represents the heat gained from the atmosphere in the heating mode.

The mass flow rate is given by the equation:

$$\dot{m} = \rho \, \eta_v \, \dot{V} \tag{22}$$

where:

ρ = the vapor density at the compressor inlet

η_v = the compressor volumetric efficiency

$\dot{V}$ = the compressor piston displacement per unit time

(given by the product of the compressor speed times piston displacement per revolution).

The heating mode has an additional feature for recovering heat. The exhaust gases from the engine can be drawn through a heat exchanger to provide the following waste heat recovery:

$$\dot{Q}_{rec} = F_{rec}\,\dot{Q}_{waste} = F_{rec}\,(1-\eta_{th})(\dot{W}_{comp}/\eta_{th}) \qquad (23)$$

where

F_{rec} = the fraction of waste heat recovered

η_{th} = the thermal efficiency of the engine

Therefore, the total heat available in the heating mode is:

$$\dot{Q}_{heating} = \dot{Q}_{cond} + \dot{Q}_{rec} \qquad (24)$$

The coefficient of performance (COP), the desired efficiency parameter for the gas heat pump, is the ratio of the desired heating or cooling output to the input energy of the gas. Therefore, this COP is based on the gas, or heat, input rather than the work input. For the cooling mode:

$$COPH_c = \frac{\dot{Q}_{evap}}{\dot{Q}_{gas}} \qquad (25)$$

Using:

$$\dot{Q}_{gas} = \frac{\dot{W}_{comp}}{\eta_{th}} \tag{26}$$

results in the following expression:

$$COPH_c = \frac{\dot{Q}_{evap}\ \eta_{th}}{\dot{W}_{comp}} = COPW_c\ \eta_{th} \tag{27}$$

For the heating mode:

$$COPH_H = \frac{\dot{Q}_{heating}}{\dot{Q}_{gas}} \tag{28}$$

Recalling:

$$\dot{Q}_{heating} = \dot{Q}_{cond} + \dot{Q}_{rec} \tag{29}$$

Substituting equation (23) into equation (29):

$$\dot{Q}_{heating} = \dot{Q}_{cond} + F_{rec}\ (1-\eta_{th})(\dot{W}_{comp}/\eta_{th}) \tag{30}$$

Substituting equation (30) and equation (26) into equation (28):

$$COPH_H = \frac{\dot{Q}_{cond} + F_{rec}\ (1-\eta_{th})(\dot{W}_{comp}/\eta_{th})}{\dot{W}_{comp}/\eta_{th}}$$

Simplifying:

$$COPH_H = \frac{\eta_{th}\ \dot{Q}_{cond}}{\dot{W}_{comp}} + F_{rec}\ (1-\eta_{th})$$

$$= \eta_{th}\ COPW_H + F_{rec}\ (1-\eta_{th}) \qquad (31)$$

Since the coefficient of performance of a system is a function of the temperatures under which the system operates (i.e. T_L and T_H), it would seem desirable to obtain a relationship between COP_c and COP_H and some parameter involving T_L and T_H. A logical choice are the Carnot or ideal COP's for a work-driven system. Recall:

$$COPW_c(ideal) = \left(\frac{T_L/T_H}{1-T_L/T_H}\right) \qquad (5)$$

and

$$COPW_H(ideal) = \left(\frac{1}{1-T_L/T_H}\right) \qquad (6)$$

In order to determine the desired relationships, consider the following four equations:

Electric cooling: $$COPW_c = K_1\ \left(\frac{T_L/T_H}{1-T_L/T_H}\right) \qquad (32)$$

$$\text{Gas cooling:} \quad COPH_c = K_1 \left(\frac{T_L/T_H}{1-T_L/T_H}\right) \tag{33}$$

$$\text{Electric heating:} \quad COPW_H = K_1 \left(\frac{1}{1-T_L/T_H}\right) \tag{34}$$

$$\text{Gas heating:} \quad COPH_H = K_1 \left(\frac{1}{1-T_L/T_H}\right) + K_2 \tag{35}$$

The values of K_1 and K_2 represent constants which can be determined. For the electrical system, K_1 is a function of losses such as the electric compressor inefficiency, the electric motor inefficiency, heat losses in piping, and other losses due to real fluid properties. Similarly for the gas system, K_1 is a function of system losses and component inefficiencies. It should be noted, however, that for the gas system, the maximum value that K_1 can attain is the gas engine efficiency. The constant K_2 is a function of the waste heat recovery, and does not appear in the electrical system analysis, of course, since in this case $F_{rec} = 0$.

A wide range of temperatures was chosen: for T_L = 20°F, 40°F, and 60°F, T_H was taken to be 80°F, 100°F, and 120°F. All nine combinations were considered. For these values, using Freon 22 properties, the COP's for ideal vapor-compression cycles were calculated as shown in Appendix A. In each case, an average of the nine calculated values for K_1 (and K_2) was taken as the constant in the relationship for an ideal system using a real refrigerant. Figures 11, 12, 13, and 14 present the results. Note that $COPW_H$(ideal)

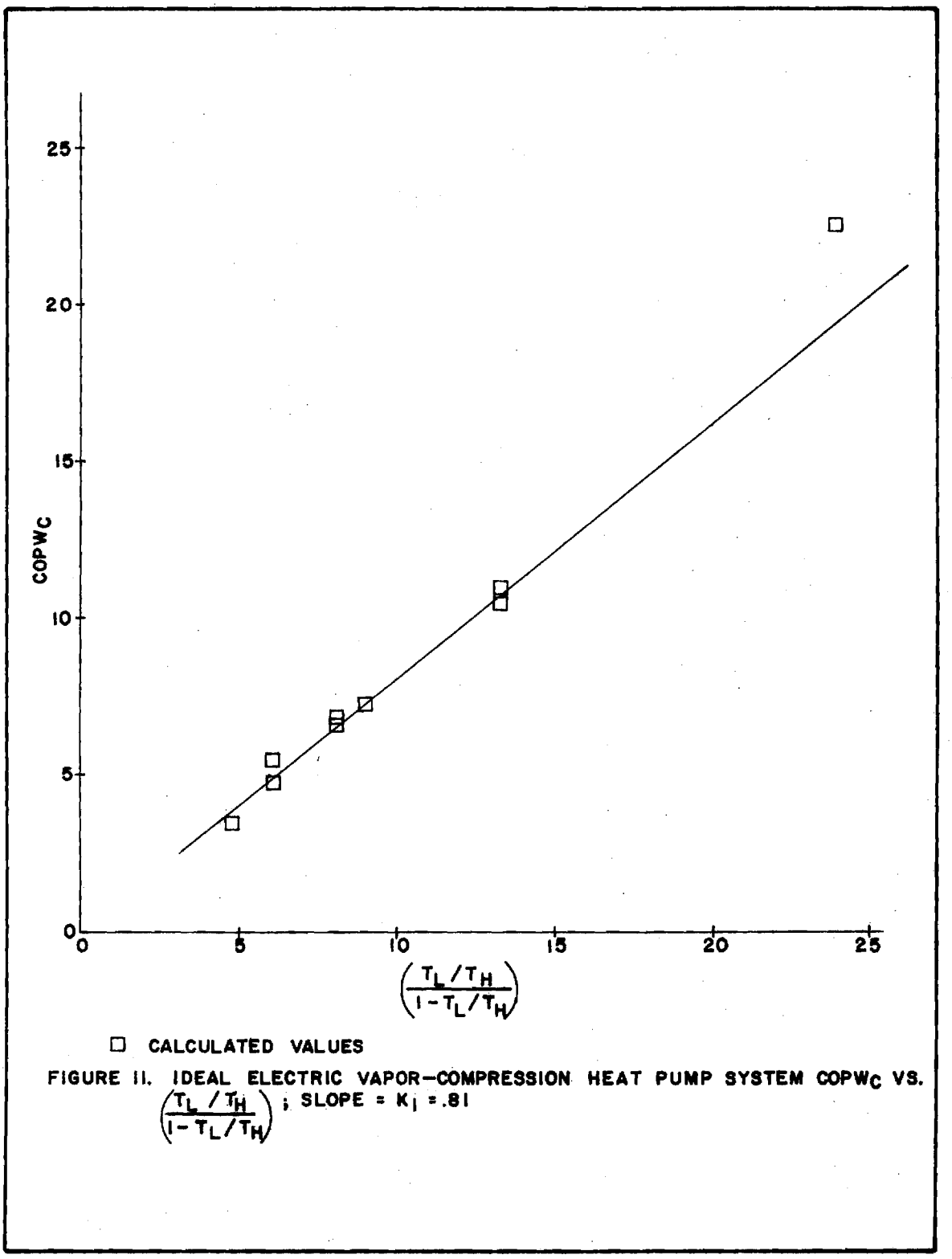

FIGURE II. IDEAL ELECTRIC VAPOR-COMPRESSION HEAT PUMP SYSTEM $COPW_C$ VS. $\left(\frac{T_L/T_H}{1-T_L/T_H}\right)$; SLOPE = K_1 = .81

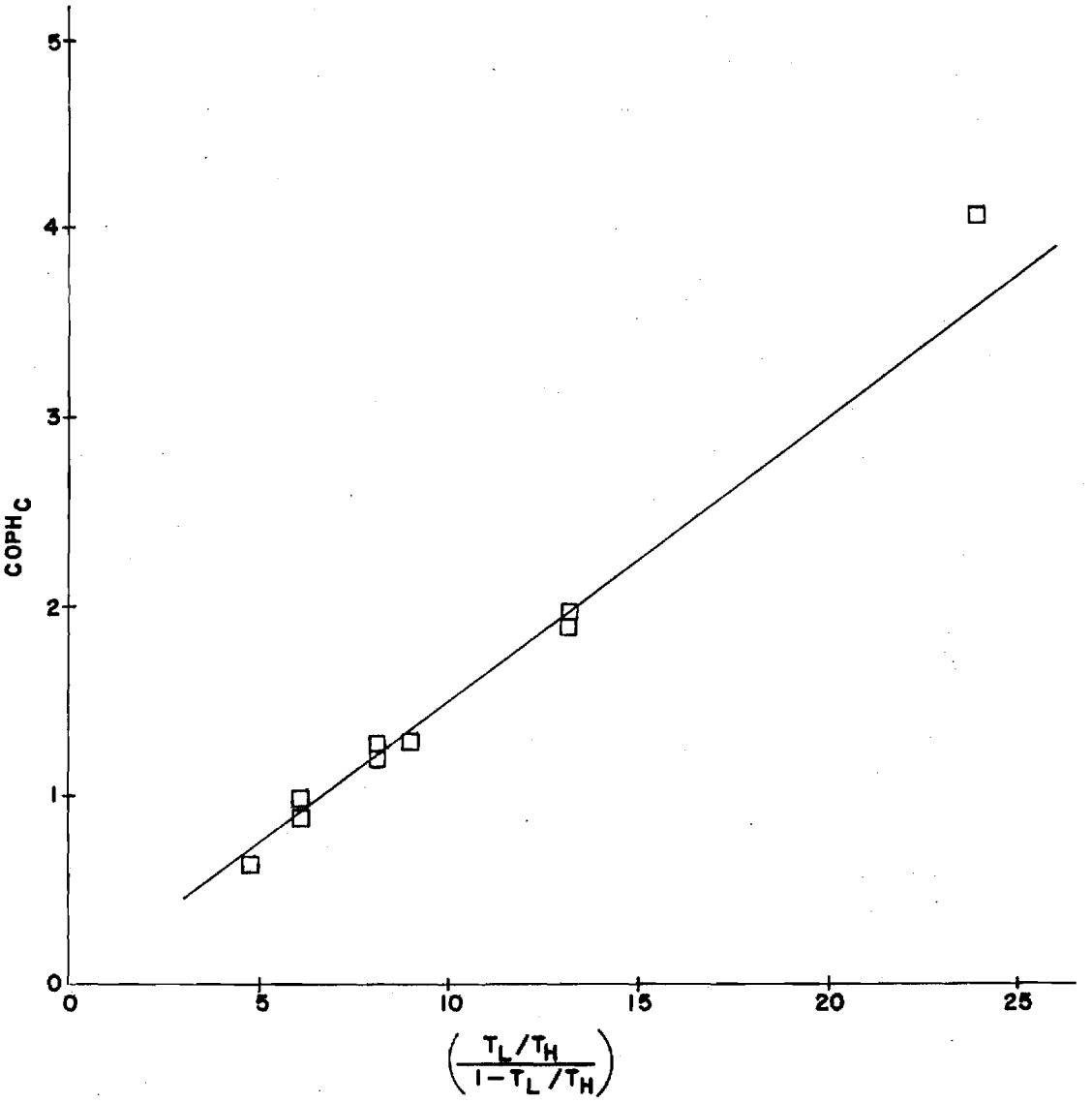

FIGURE 12. IDEAL GAS VAPOR-COMPRESSION HEAT PUMP SYSTEM COPH$_C$ VS. $\left(\frac{T_L/T_H}{1-T_L/T_H}\right)$; SLOPE = K_1 = .15

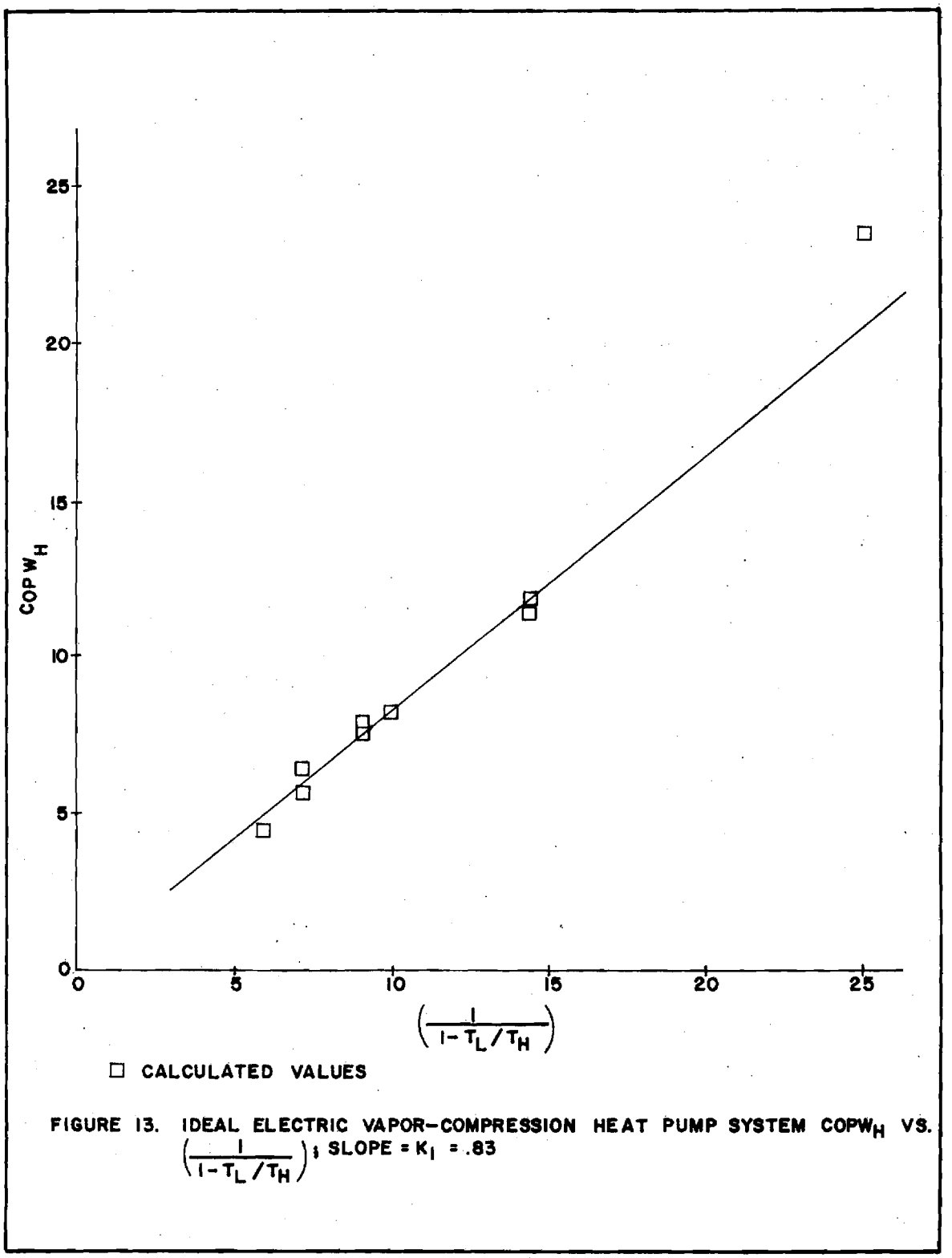

FIGURE 13. IDEAL ELECTRIC VAPOR-COMPRESSION HEAT PUMP SYSTEM $COPW_H$ VS. $\left(\frac{1}{1-T_L/T_H}\right)$; SLOPE = K_1 = .83

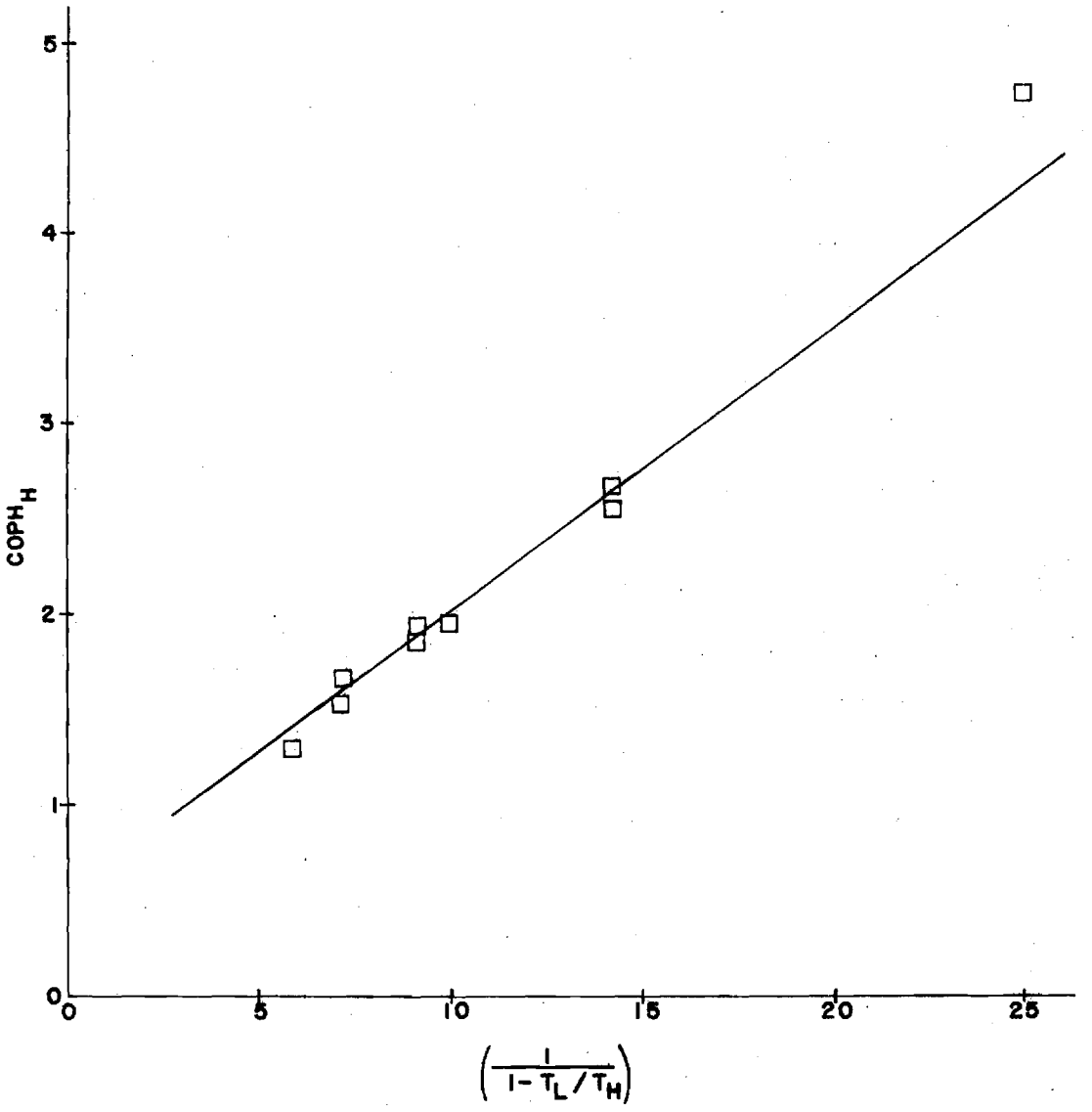

FIGURE 14. IDEAL GAS VAPOR-COMPRESSION HEAT PUMP SYSTEM WITH WASTE HEAT RECOVERY $COPH_H$ VS. $\left(\frac{1}{1-T_L/T_H}\right)$; SLOPE = K_1 = .15; K_2 = .49

approaches 1.0 as a lower limit, while $COPW_c$(ideal) approaches 0.0 as a lower limit. For the gas system, an engine efficiency of 18% with F_{rec} = .60 was assumed. Thus, in Figure 14, at $(\frac{1}{1-T_L/T_H})$ = 1.0, $COPH_H$ should equal .18 + K_2 or 0.67.

Once again, Figures 11, 12, 13, and 14 present the relationships between the ideal COPW's and the COP's for systems operating on an ideal vapor-compression cycle but using a real working fluid, Freon 22. Later in this work, similar relationships will be determined between the ideal COPW's and the COP's for the actual systems studied.

Annual Average COPH

The coefficient of performance varies with temperature which, of course, varies throughout the year. It would be desirable, therefore, to determine an annual average COP. The following allows calculation of such a value, given a certain temperature, and thus, a particular COPH.

The annual average $COPH_c$ and $COPH_H$ are given by:

$$\overline{COPH}_c = \overline{Q}_c/\overline{Q}_{gas} \tag{36}$$

$$\overline{COPH}_H = \overline{Q}_H/\overline{Q}_{gas} \tag{37}$$

where:

($\overline{\ }$) denotes annual quantities

Q_{gas} = the heating value of the natural gas used

The heating and cooling required by a residence is proportional to the temperature difference between 65°F and the outside air temperature. Therefore:

$$\dot{Q}_C = K(T_A - 65);\ T_A > 65°F \tag{38}$$

$$\dot{Q}_H = K(65 - T_A);\ T_A < 65°F \tag{39}$$

where:

T_A = the outside air temperature in °F

K = a constant, Btu/hr-°F (a typical value for K for the city of Atlanta is 1,000 Btu/hr-°F for a 1500 ft^2 home).

When T_A = 65°F, enough heat is supplied by indoor appliances to keep the indoor temperature within the comfort region. Therefore:

$$\overline{Q}_C = \int_0^{t_c} K(T-65)dt;\ T > 65 \tag{40}$$

$$\overline{Q}_H = \int_0^{t_h} K(65-T)dt;\ T < 65 \tag{41}$$

where:

t = time

t_c = the annual cooling period

t_H = the annual heating period

The annual gas demand for cooling is:

$$\overline{Q_{gas}} = \int_{o}^{t_c} \frac{K(T-65)}{COPH_c}\, dt;\ T > 65 \qquad (42)$$

Similarly for heating:

$$\overline{Q_{gas}} = \int_{o}^{t_H} \frac{K(65-T)}{COPH_H}\, dt;\ T < 65 \qquad (43)$$

Note that $COPH_c$ and $COPH_H$ in equations (42) and (43) are not constant, but vary with temperature. Making the appropriate substitutions results in the following:

$$\overline{COPH}_c = \frac{\int_{o}^{t_c} (T-65°F)dt}{\int_{o}^{t_c} \frac{(T-65°F)}{COPH_c}\, dt} \qquad (44)$$

$$\overline{COPH}_H = \frac{\int_{o}^{t_h} (65°F-T)dt}{\int_{o}^{t_h} \frac{(65°F-T)}{COPH_H}\, dt} \qquad (45)$$

These integrals can be evaluated using hourly temperature data for a given year. This data for Atlanta, Georgia, for the year 1964, is presented in reference 1 and reproduced below. The number of hours annually at 10°F temperature intervals were found for this year to be [1]:

°F	Hours/Year
0 - 9	0
10 - 19	25
20 - 29	240
30 - 39	851
40 - 49	1417
50 - 59	1433
60 - 69	1792
70 - 79	2177
80 - 89	848
90 - 99	77

Information of this type, along with $COPH_C$ and $COPH_H$, expressed as a function of outside temperature, allows evaluation of the $\overline{COPH}_C$ and $\overline{COPH}_H$ in equations (44) and (45).

CHAPTER III

GAS FURNACE STUDY

Equipment and Principle of Operation

Initially a study was made of a gas furnace type of heater manufactured by Amana Refrigeration, Inc. The heating cycle studied is accomplished by an indirect method in which a gas flame heats a circulating liquid in a Heat Transfer Module. The heated liquid (50% Ethylene Glycol and 50% distilled water) is circulated by a pump through an indoor coil. Air from the conditioned space is drawn across the indoor coil by the blower motor where it is warmed and returned to the conditioned space (see Figure 15).

The liquid heating is accomplished by using a unique, compact heat exchanger. This unit (Heat Transfer Module) consists of multiple tubes (24 passage tubes arranged so that six passes are made through the module) embedded in a nickel-plated steel ball matrix, which is oven brazed. Through this ball construction pass the products of combustion. The gas burner, located inside the steel ball matrix, consists of a stainless steel cylindrical screen with approximately 9,980 holes. The gas-air mixture burns on the outside of the screen with very minute flames.

A motor operated combustion blower is used to draw

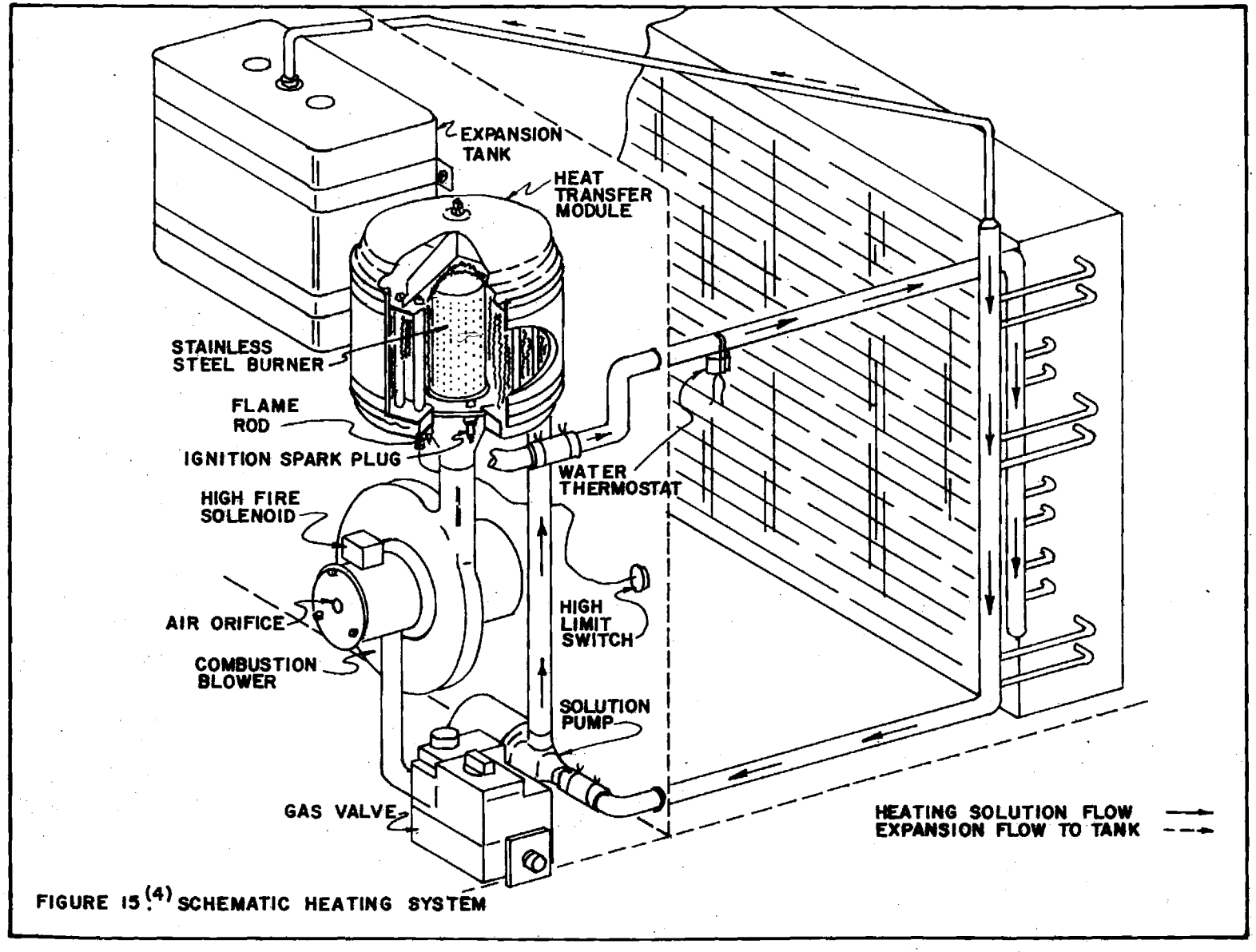

FIGURE 15.[4] SCHEMATIC HEATING SYSTEM

the gas supply from the electrically operated gas valve, at a negative pressure (below atmospheric), through a predetermined gas orifice into the mixing chamber. Primary combustion air is also drawn through a matching predetermined air orifice, to be mixed with the gas supply by the combustion blower wheel. This gas-air mixture is then discharged into the stainless steel gas burner. The mixture is ignited by the use of a specially designed spark ignitor, which is powered electrically by a direct spark ignition control. The products of combustion are power vented to the atmosphere through the flue outlet and vent cap at the side of the unit.

The heating solution, consisting of a 50% mixture of Ethylene Glycol (with corrosion inhibitor) and distilled water, is circulated by a small motor driven centrifugal pump, at a velocity of approximately 4.77 feet/second, giving turbulent flow in the heat exchanger tubes for a high rate of heat transfer. The solution circulates through the heat exchanger where it is heated and then delivered to the indoor heating coil (see Table 4). Indoor circulated air is passed over the coil by the indoor blower motor, to remove the heat and discharge it into the conditioned space. The cooled heating solution is then returned back to the water pump inlet, ready to repeat the cycle. The heating solution is circulated at approximately eight gallons/minute.

The system operates at essentially atmospheric pressure. Since the solution expands when heated and contracts when

Table 4. Indoor Heating Coil Specifications for the Gas Furnace System [5]

Face Area:	2.71 ft^2
Rows Deep:	4
Fins/in:	12
Tubes, O.D. inches:	3/8

cooled, an expansion tank is provided that is open to the atmosphere using a split rubber grommet to control the evaporation rate. This also provides a point where any air that is in the system escapes during the heating-up period. Between cycles, as the solution cools, it is siphoned out of the expansion tank back into the system.

Instrumentation

Among the parameters of importance were the water temperature before and after the heat exchanger, the water flow rate, the natural gas input, and the electrical input (see Figure 16). An iron-constantan thermocouple was attached to the surface of the water line going to the heat exchanger. Similarly, a thermocouple was attached to the return water line. The lines were then carefully insulated to reduce heat loss. The temperatures were measured on an Omega Engineering, Inc. pyrometer, designed to read directly in degrees Fahrenheit with an accuracy of ±2%. The water flow rate was measured on a standard Neptune water meter installed in the return line. The gas input was determined on a

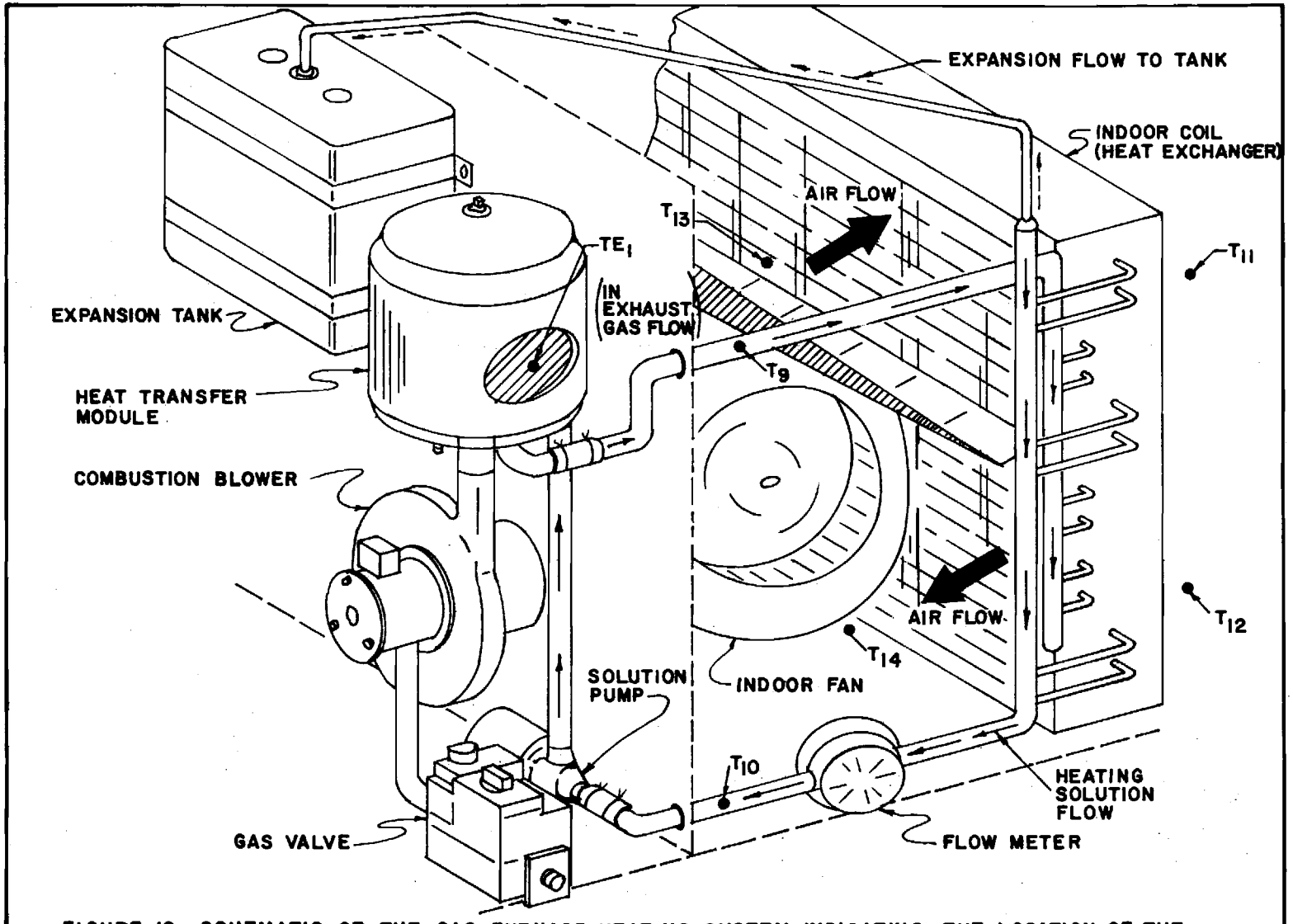

FIGURE 16. SCHEMATIC OF THE GAS FURNACE HEATING SYSTEM INDICATING THE LOCATION OF THE FLOW METER AND THERMOCOUPLES

typical residential gas meter, while a General Electric single-phase watthour meter, type 1-50-S, allowed measurement of the electrical input.

Test Results

The primary value of interest was the efficiency, defined as follows:

$$\eta = \frac{\dot{m}_w \, \Delta T_w \, C_{pw}}{\dot{Q}_{gas}} \qquad (46)$$

where:

$\dot{m}_w$ = the mass flow rate of water, #m/min

ΔT_w = the water temperature difference across the heat exchanger, °F

C_{pw} = the water specific heat, 1 Btu/(#m°F)

$\dot{Q}_{gas}$ = energy content of the gas being input, $\dot{Q}_{gas}$ = ($\dot{V}$, the volume flow rate, ft^3/min) X (the heating value of methane = 1,030 Btu/ft^3)

Four combinations were tested: a high and a low heat setting, referring to the rate of natural gas and air intake and subsequent combustion, and a high and a low fan, referring to the indoor fan speed setting. Appendix B contains a table of the data collected, and a sample η calculation. The results are presented below:

low heat low fan	low heat high fan	high heat low fan	high heat high fan
$\eta = 80.3\%$	$\eta = 84.0\%$	$\eta = 86.4\%$	$\eta = 84.8\%$

From their literature search, Calvert and Harden [6] found that the $COPH_H$ for a gas furnace can be taken to be 0.7 [1]. The term which is defined as η above is equivalent to $COPH_H$. Needless to say, the particular machine analyzed here performed better than a conventional gas furnace. This improvement is due to the efficient heat exchanger on this unit.

A gas furnace provides a very effective means of home heating. It is limited, however, to just that--heating. If summer cooling is required in addition to winter heating an additional cooling system must be provided. Herein lies one advantage of a heat pump system in which the same components can be used for both heating and cooling. Moreover, as shown in the introduction, a gas heat pump in Atlanta, Georgia, would heat and cool year around with less total gas than a gas furnace would require for heating only. The conclusion should be obvious. Although the test results for this system are included in the electric heat pump--gas heat pump comparison presented later in this work, a gas furnace alone is not the answer to total home environmental control.

CHAPTER IV

ELECTRIC HEAT PUMP STUDY

Equipment and Principle of Operation

A heat pump, electric or gas, is a system which pumps heat from a low temperature to a higher temperature, with a necessary input of energy. This energy is usually supplied in the form of rotating shaft work to a compressor. If the work input to the system is provided by an electric motor, an electric heat pump results. An Amana five-ton (cooling) Central System Air Conditioner was the unit studied in this work. System schematics are presented in Figures 17, 18, and 19.

A refrigerating or heat pump cycle is made possible by a few basic principles [7]:

(1) Heat flows from a warmer object to a cooler one. Thus something can be cooled by placing it next to something even cooler.

(2) The temperature at which a liquid boils depends upon the pressure exerted on the liquid. The boiling point of the liquid can be controlled if the pressure on it is controlled. Thus, the boiling point of a liquid can be lowered to a point below the temperature of the object to be cooled by the liquid.

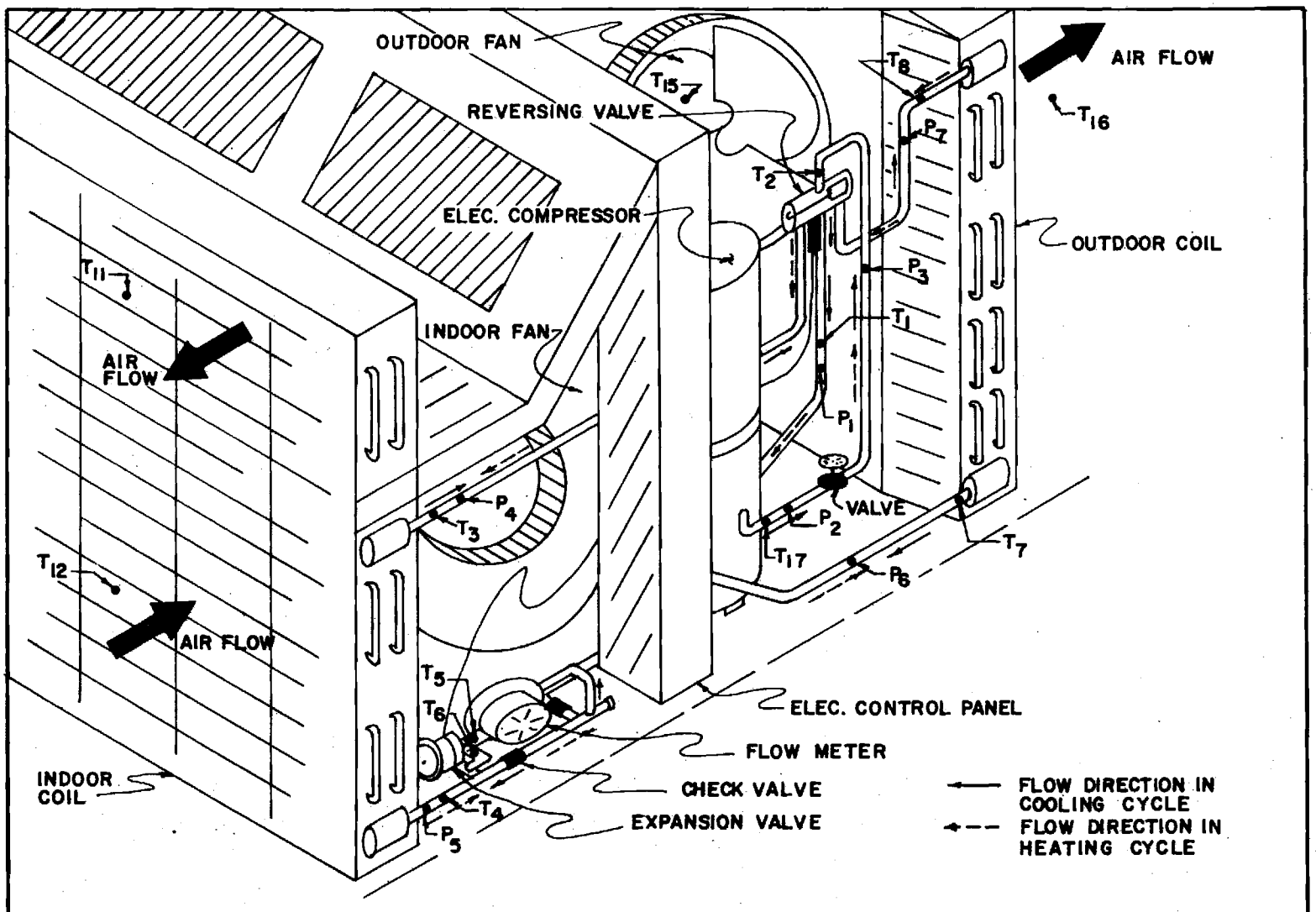

FIGURE 17. ELECTRIC HEAT PUMP SYSTEM SCHEMATIC INDICATING THE LOCATION OF MEASUREMENT POINTS

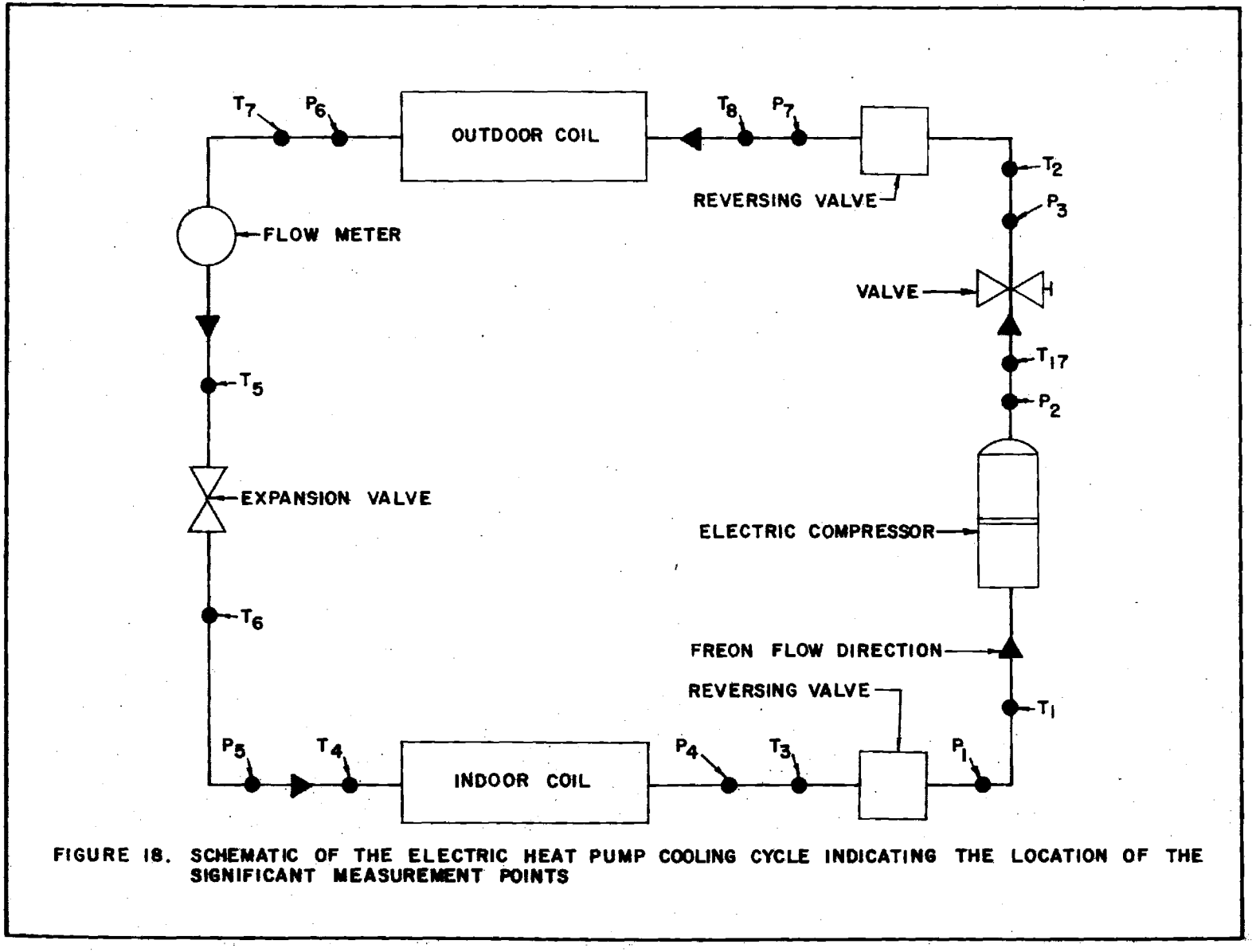

FIGURE 18. SCHEMATIC OF THE ELECTRIC HEAT PUMP COOLING CYCLE INDICATING THE LOCATION OF THE SIGNIFICANT MEASUREMENT POINTS

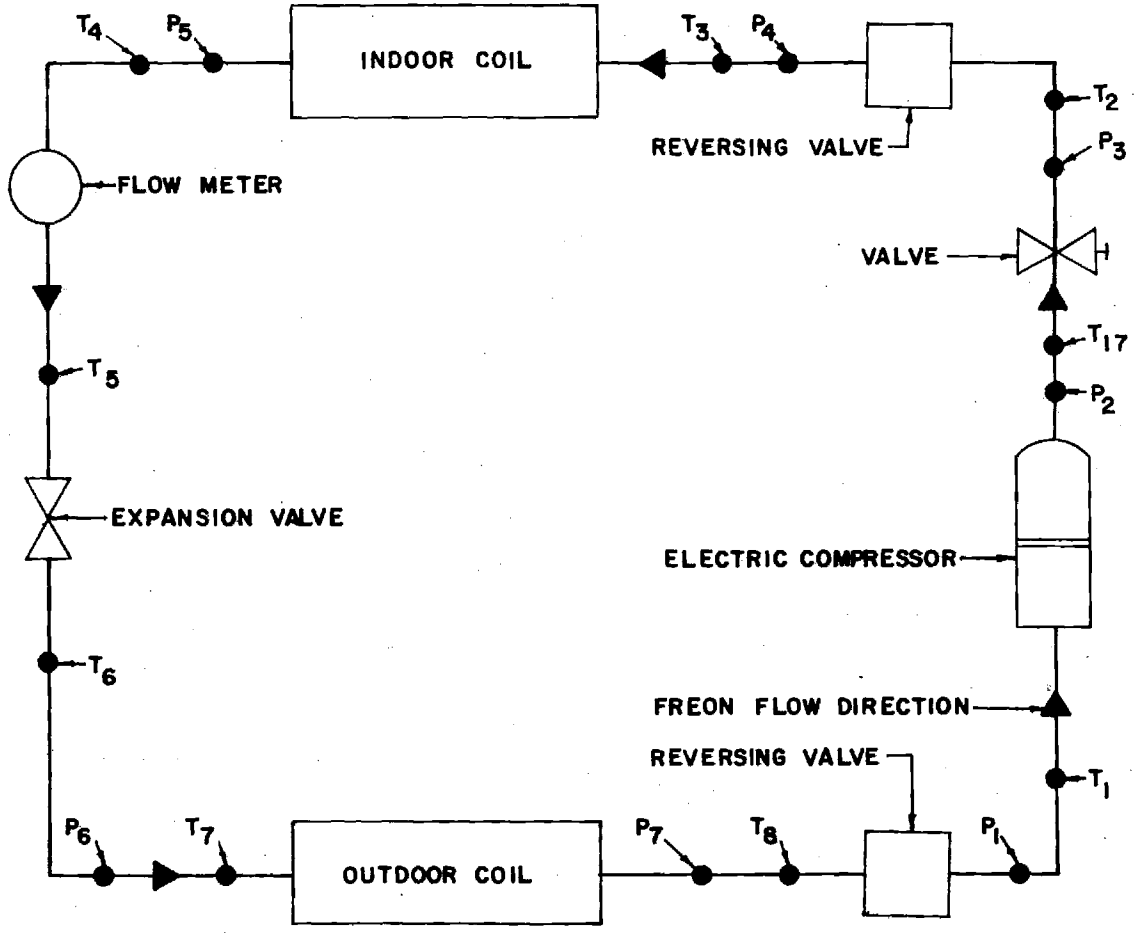

FIGURE 19. SCHEMATIC OF THE ELECTRIC HEAT PUMP HEATING CYCLE INDICATING THE LOCATION OF THE SIGNIFICANT MEASUREMENT POINTS

(3) A boiling liquid continually absorbs heat from any object placed near it. The temperature of the liquid does not rise, as the heat that is being absorbed is expended in vaporizing the liquid (latent heat of vaporization). Thus, continuous refrigeration is possible as long as there is liquid available for vaporization.

(4) Removing heat from a vapor causes the vapor to condense. Therefore, vapor can be returned to its liquid form after the cooling function has been performed by removing the heat that caused the vaporization. The vapor condensation temperature depends upon the pressure exerted on the vapor. If the pressure exerted on the vapor is high enough, the temperature of the vapor can be raised to a level where the vapor is hotter than the surrounding air. Heat will then flow from the hot vapor to the cooler surrounding air, and condensation of the vapor to a liquid will occur.

The vapor-compression cycle is one in which the working fluid alternately evaporates and condenses, with one of the intervening processes being a compression of the vapor. Refer to Figure 20.

The heart of the vapor-compression system is the compressor. Its function is two-fold. It must withdraw the fluid from the evaporator at a rate sufficient to maintain the necessary reduced pressure and temperature in the evaporator. In addition, it must compress and deliver the fluid at a temperature which is adequately above the substance

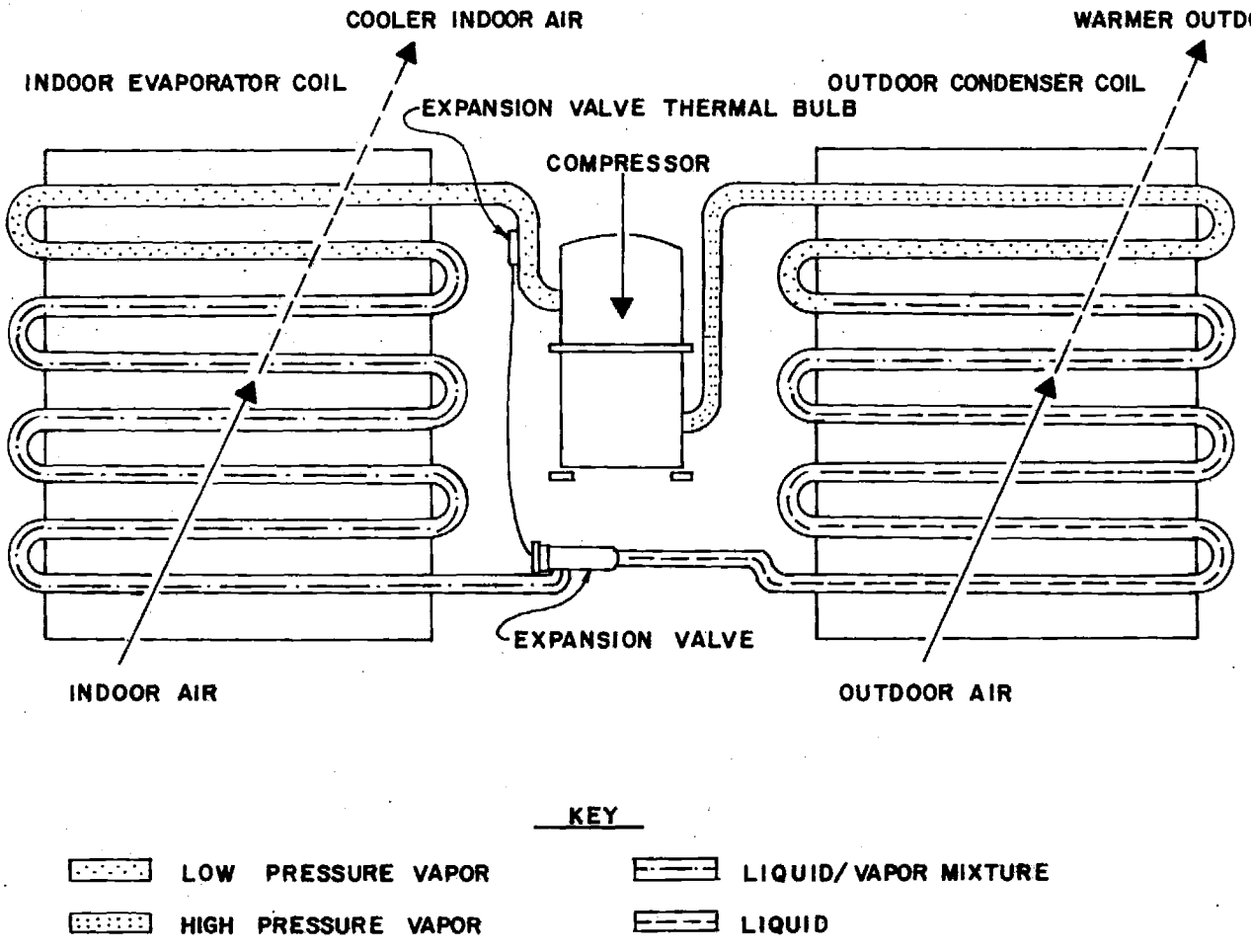

FIGURE 20. SCHEMATIC REFRIGERATION SYSTEM

to which the fluid must transfer its energy. The increase of temperature of the vapor must be accompanied by an increase of pressure.

The unit used in the electrical heat pump study was a five horsepower Tecumseh hermetic compressor (a direct-connected motor reciprocating-compressor assembly enclosed within a steel housing). Figure 21 presents some performance information supplied by the manufacturer [8].

After leaving the compressor the vapor enters the condenser in which it must first be desuperheated and then condensed, energy departing in the form of heat. The temperature during the condensation must moderately exceed that of the cooling air in order that the heat transition may proceed in the desired direction. The refrigerant pressure which must be delivered by the compressor is the saturation pressure corresponding to the condensing temperature. See Table 5 for the outdoor coil specifications (condenser in the cooling cycle).

Table 5. Outdoor Coil Specifications for the Heat Pump Systems [5]

Face Area:	7.49 ft^2
Rows Deep:	4
Fins/in:	12
Tube, O.D. inches:	3/8

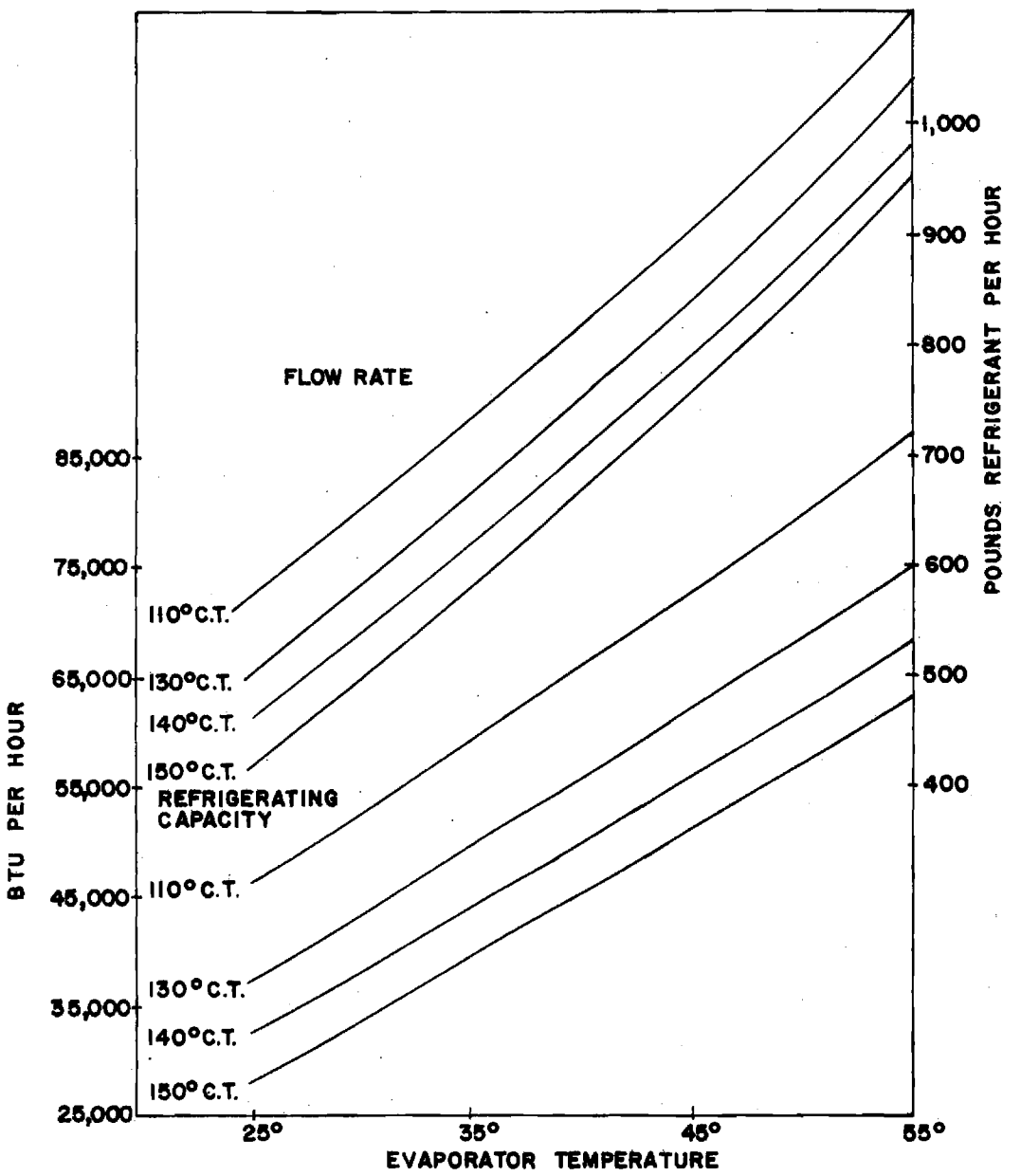

FIGURE 21B.[8] TECUMSEH COMPRESSOR PERFORMANCE CURVES (SEE TABLE 6 FOR SPECIFICATIONS)

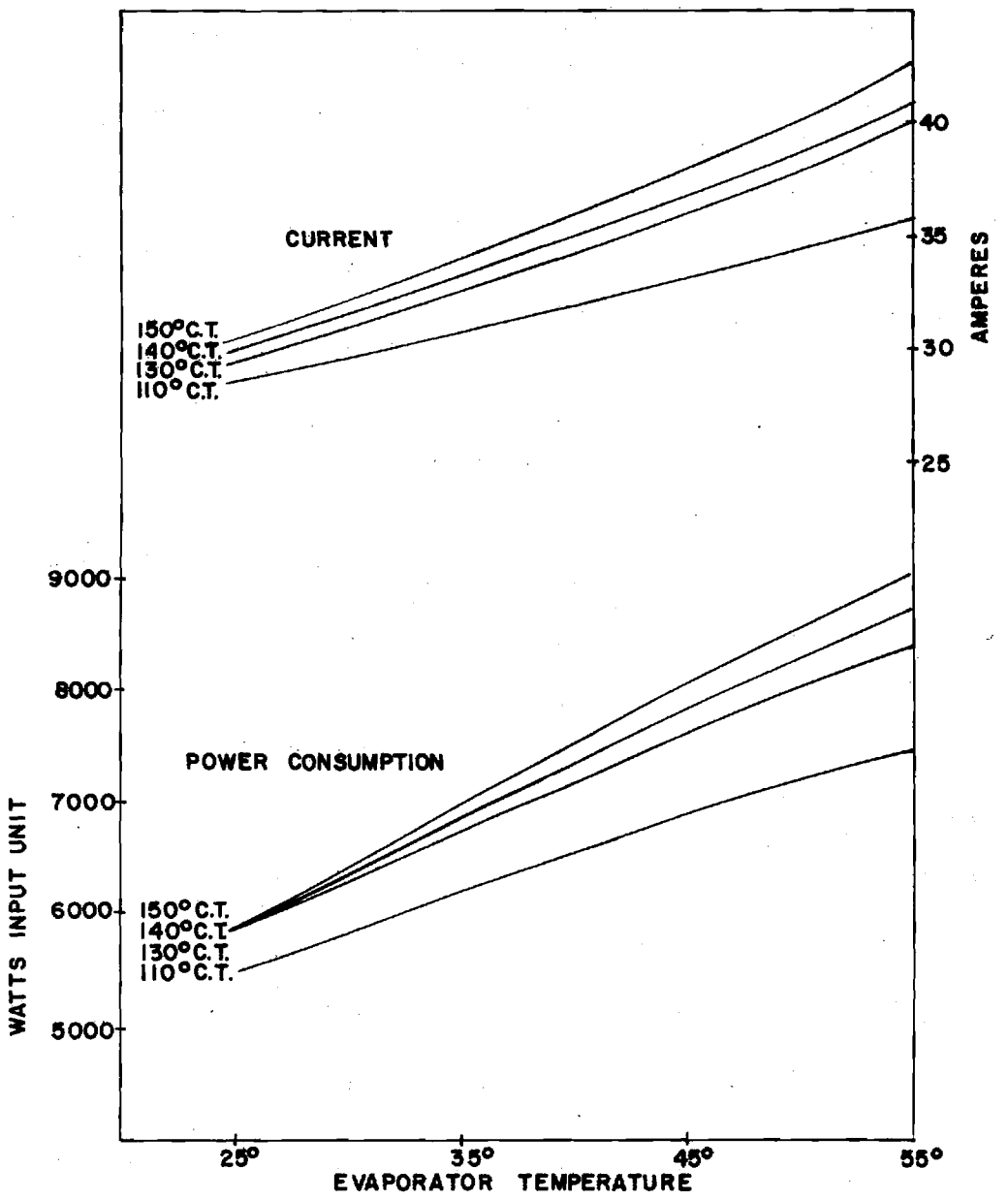

FIGURE 21A.[8] TECUMSEH COMPRESSOR PERFORMANCE CURVES (SEE TABLE 6 FOR SPECIFICATIONS)

Table 6. Specifications for the Tecumseh Compressor of Figure 21 [8]

Model:	CL5562E
Displacement:	7.24 in^3/ crankshaft revolution
Motor Type:	P.S.C.
Volts/Hz/Ph:	230/208-60-1
Tested at:	230 V.
Run Capacitor:	55 MFD
Room Ambient:	95°F
All Temperatures:	°F
Refrigerant:	R-22
Return Gas and Gas Leaving Evaporator Superheated to:	95°F
Forced Air Over the Compressor	
Liquid Subcooled 15° for all Condensing Temperatures: (C.T.)	

The working fluid next reaches the expansion valve, the purpose of which is also twofold. It must reduce the pressure of the refrigerant, and also must regulate the refrigerant flow to the evaporator. A turbine is not used because appreciable work cannot usually be recovered by the expansion of a very wet vapor through such a machine. Due to the throttling character of this process the fluid enthalpy before and after the device must be equal. A sensible portion of the liquid must vaporize and owing to the lower pressure of the vapor, its temperature must have fallen. Specifically, it must drop to the saturation temperature corresponding to the lower pressure.

A thermostatic expansion valve was installed in the unit replacing the existing capillary tube. The name "thermostatic" may be misleading because control is actuated not by the temperature in the evaporator, but by the amount of superheat of the suction gas leaving the evaporator. Designed to regulate the rate of liquid refrigerant flow into an evaporator in exact proportion to the rate of evaporation of the liquid refrigerant, the thermostatic expansion valve responds to both the temperature of the refrigerant gas leaving the evaporator, and the pressure in the evaporator.

After leaving the expansion valve the low temperature and low quality vapor mixture enters the evaporator. Here absorption of energy as heat by the working fluid from the region to be refrigerated is accomplished. Evaporation of

the refrigerant results. The degree of completeness of its evaporation depends on the rapidity of its circulation, on the temperature difference between the fluid and its environment, and on other operating conditions. The fluid temperature in the evaporator must be maintained below the temperature of the cold region to ensure heat transfer in the desired direction. The pressure maintained must be the saturation pressure corresponding to the temperature. From the evaporator, the working fluid passes into the compressor to repeat the cycle. See Table 7 for the indoor coil specifications (evaporator in the cooling cycle).

Table 7. Indoor Coil Specifications for the Heat Pump Systems [5]

Face Area:	4.75 ft^2
Rows Deep:	4
Fins/in:	13
Tube, O.D. inches:	3/8

The heating cycle uses the same components as the cooling cycle just described and the principle of operation is the same with one exception. The functions of the evaporator and condenser are interchanged. Instead of physically exchanging the two heat exchangers, it is easier to simply reverse the direction of flow of the working fluid. Since the compressor is a one-way device, the most feasible

method for changing flow direction is a reversing valve. A four-way, two-position reversing valve, operated by a three-way pilot solenoid valve, was installed in the system. See Figures 22 and 23.

The purpose of the pilot valve is to initiate the operation of the "sliding port" assembly in the main valve body, thus determining the refrigerant route through the evaporator and condenser coils, and thereby exchanging the functions of these two components to provide heating or cooling operation. A "sliding port" assembly, actuated by means of a piston arrangement, is operated by the pressure differential between the high and low sides of the refrigeration sytem. When the solenoid is energized, the right port in the pilot valve is opened, permitting the gas in the right-hand chamber of the main valve to bleed off through the capillary tube, thereby creating a pressure differential between the right and left-hand chambers. The higher pressure in the left-hand chamber causes the piston to move the "sliding port" assembly to the right producing the proper routing for the heating phase. When the solenoid is de-energized, the process is reversed. The left-hand port of the pilot valve opens, and the right port closes, allowing the pressure in the left-hand chamber to reduce. This causes the higher pressure of the right-hand chamber to move the "sliding port" to the left where it covers the opposite pair of tubes, resulting in the cooling phase.

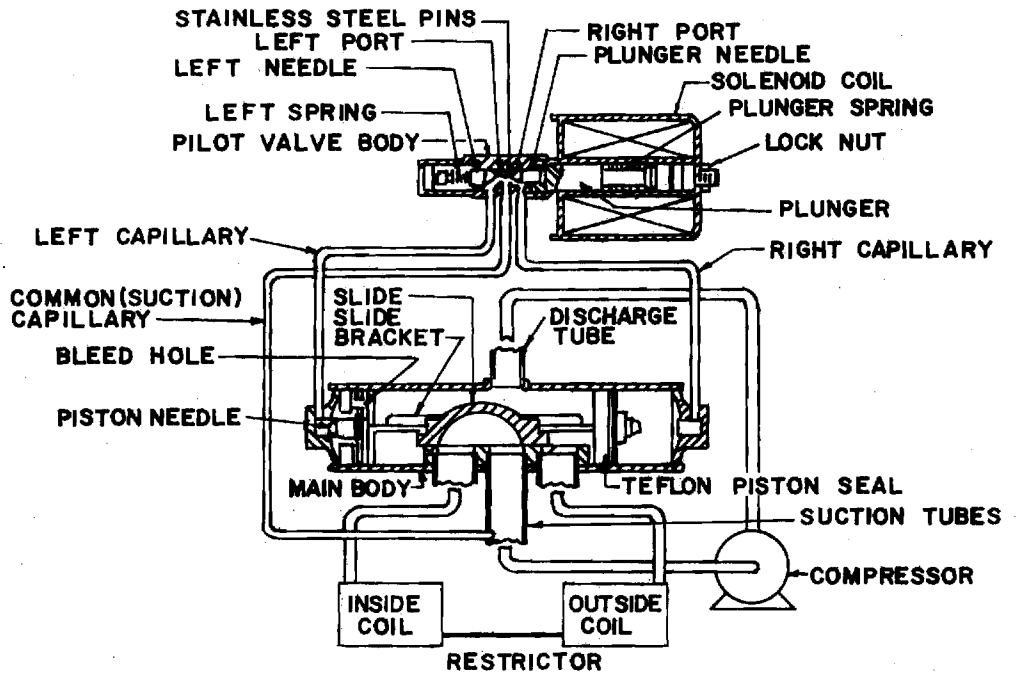

FIGURE 22.[9] SECTION VIEW OF REVERSING VALVE

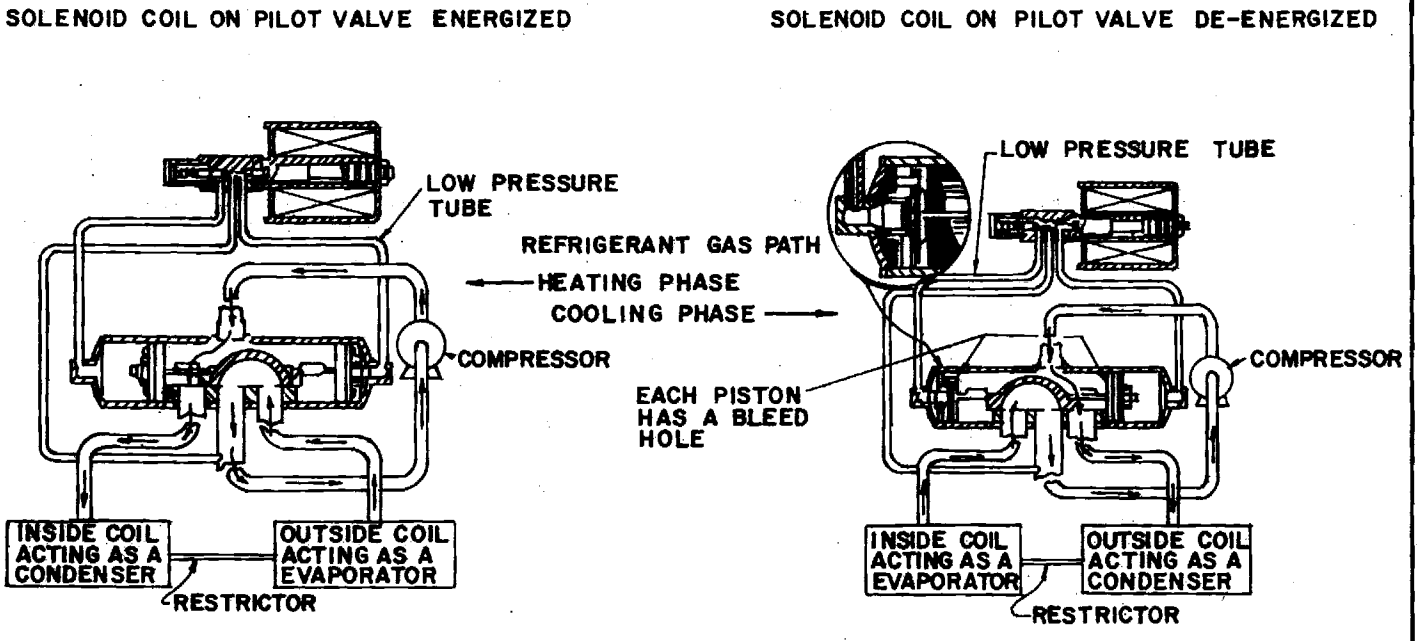

FIGURE 23.[9] REFRIGERANT GAS PATH IN REVERSING VALVE

Working Fluid

Let us consider, for a moment, the working fluid in the system under study. A refrigerant is a medium which absorbs heat by evaporating at a low temperature and gives up heat by condensing at a high temperature and pressure. An ideal refrigerant does not exist. Therefore, the particular fluid chosen for a specific application must be a compromise. It should have, however, as many of the following desirable characteristics as practicable:

(1) The latent heat of vaporization should be high. The higher this value, the greater will be the heat absorbed per pound of circulated fluid.

(2) The specific heat of the liquid should be low. The lower the specific heat of the liquid, the less heat it will pick up for a given change in temperature during either throttling or in flow through the piping and consequently the greater the refrigerating effect per pound of refrigerant.

(3) The specific volume should be low to minimize the work required per pound of refrigerant circulated.

(4) The critical temperature of the refrigerant should be higher than the condensing pressure to prevent excessive power consumption.

(5) The working fluid should have a boiling point below room temperature at atmospheric pressure and a freezing temperature well below any temperature at which the evaporator might operate.

In addition to the foregoing, it is necessary to consider items such as toxicity, flammability, explosiveness, corrosiveness, dielectric strength for a hermetically sealed system, viscosity, thermal conductivity, chemical stability, and cost. Once again, no one refrigerant has been found to meet all of these requirements.

Freon-22 or Refrigerant-22 (monochlorodifluoromethane, $CHClF_2$), a few properties of which are listed in Table 8, was used in the system analyzed in this work.

Table 8. Physical and Thermal Properties of Freon 22 [10]

Boiling Point:	-41.4°F
Freezing Point:	-256.0°F
Critical Point Temperature:	204.8°F
Critical Point Pressure:	716.0 PSIA
Specific Gravity of Liquid at Atmospheric Pressure:	1.411
Specific Heat of Liquid, Ave. 5°F to 86°F:	0.30

Freon 22 is used in a multitude of household and commercial applications. It is nontoxic and has a low power requirement per ton, and is a good low-temperature refrigerant, especially in applications utilizing reciprocating or rotary compressors. In recent years it has become the most popular refrigerant for residental air conditioning units,

because its low boiling point and high latent heat permit the use of smaller compressors and refrigerant lines, making it ideal for compact units. Freon 22 is a good refrigerant for extreme service conditions because it is stable and has unusually good thermodynamic properties, equally true whether high capacity or high temperature stability is the major consideration.

Instrumentation

The parameters of interest included cycle pressures, cycle temperatures, the freon flow rate, and the electrical input. The cycle pressures (pressures measured before and after the four main system components) were measured on two pressure gauges. One was a Solfrunt Pressure Gauge (accuracy of about ±2%). The other, a Heise gauge (accuracy of about ±1%), was used to measure pressures greater than 300 PSIG, the range of the first gauge employed. The cycle temperatures (once again, the temperatures before and after the four main system components) were measured with iron-constantan thermocouples attached to the surface of the system lines, which were then insulated. The temperatures in (°F) were read directly off an Omega Engineering Inc. pyrometer (accuracy of approximately ±2%). A Rockwell flow meter allowed measurement of the liquid freon flow rate, while a General Electric, single-phase watthour meter, type 1-50-S, was used to determine the electrical input.

A box, open on both ends, was constructed of masonite and attached to the machine over the indoor coil side. In this box was built a movable baffle, which could be fixed at various positions. When horizontal, it, in effect, had no influence on the air flow rates over the indoor coil and hence, these cycle temperatures. When vertical, however, the exhaust air was effectively trapped and recirculated back into the machine by the indoor fan intake. This, as well as positioning of the baffle at various angles between the complete horizontal and the complete vertical positions, allowed some control over the simulated indoor temperatures. Unfortunately, this technique could not be used on the outdoor coil, due to the machine configuration. Instead, the air flows, and hence the temperatures, were controlled by covering the air passageways with plastic. These modifications allowed some control over the simulated indoor and outdoor temperatures. The obtainable range of conditions, however, was not the most desirable or the most comprehensive.

The experimental data, as well as sample calculations, for both the cooling and heating modes are presented in Appendix C.

Test Results

The experimental results for the electrical cooling cycle are tabulated below where:

T_L = the low (fluid evaporating) temperature

T_H = the high (fluid condensing) temperature

Capacity (tons) = (enthalpy change across the evaporator, Btu/#m) X (the mass flow rate, #m/hr)

$$COPW_c(ideal) = \frac{T_L/T_H}{1-T_L/T_H} \quad (5)$$

$COPW_c$(actual) = (enthalpy change across the evaporator, Btu/#m) X (the mass flow rate, #m/hr) ÷ $\dot{E}$ (the electrical input rate, Btu/hr)

Table 9. Electrical Heat Pump (Cooling) Test Results

Test	T_L(°F)	T_H(°F)	Capacity (tons)	$COPW_c$(actual)	$COPW_c$(ideal)
1	45.5	136.0	4.40	1.97	5.67
2	26.0	130.0	2.48	1.38	4.56
3	12.5	122.5	2.01	1.22	4.26
4	46.5	153.0	4.44	1.78	4.88
5	26.0	149.5	2.24	1.25	4.00
6	10.5	134.0	1.85	1.13	3.76
7	19.5	139.5	1.96	1.17	4.00
8	27.5	150.5	2.13	1.12	4.00

The heating cycle electric heat pump results are presented below.

T_L = the low (fluid evaporating) temperature

T_H = the high (fluid condensing) temperature

Capacity (Btu/hr) = (enthalpy change across the condenser, Btu/#m) X (the mass flow rate, #m/hr)

$$COPW_H(ideal) = \frac{1}{1-T_L/T_H} \qquad (6)$$

$COPW_H$(actual) = (enthalpy change across the condenser, Btu/#m) X (the mass flow rate, #m/hr) ÷ $\dot{E}$ (the electrical input rate, Btu/hr)

Table 10. Electrical Heat Pump (Heating) Test Results

Test	T_L(°F)	T_H(°F)	Capacity (Btu/hr)	$COPW_H$(actual)	$COPW_H$(ideal)
1	60.5	161.5	7.66×10^4	2.25	6.25
2	57.0	154.0	8.89×10^4	2.41	6.25
3	53.0	149.0	7.88×10^4	2.14	6.25
4	42.0	138.0	5.59×10^4	1.80	6.25

A comparison of the various systems is given in Chapter VI.

CHAPTER V

NATURAL GAS HEAT PUMP STUDY

The Wankel Engine as a Stationary Prime Mover

If the required work input to a heat pump system is provided by a natural gas-fueled engine, a natural gas heat pump results. This system has advantages over both a gas furnace and an electric heat pump. The advantage of the natural gas heat pump over a gas furnace results from the "free" heat which the evaporator absorbs from the outside air. Operating the compressor with a natural gas-fueled engine allows the waste heat accompanying the engine to be recovered and also used for residential heating. A significant efficiency advantage over an electric heat pump results from this waste heat recovery. In the electric system, the waste heat is generated at the power plant, but cannot be used, resulting in thermal pollution and a lowering of efficiency.

The primary problem to be solved in order to put the natural gas heat pump idea into commercial practice concerns the prime mover. One type of engine that shows promise for high reliability in this stationary application is the Wankel rotary engine. The Wankel has certain characteristics that render it superior to a conventional piston engine

operating under similar conditions.

Operating on the Otto cycle, the Wankel engine has the same processes as a conventional reciprocating internal combustion engine. It is extremely simple in design, though, having basically only two moving parts, the rotor and the eccentric shaft (see Figure 24). The rotor revolves directly on the eccentric shaft eliminating the need for connecting rods. Also, valves and their operating mechanisms are not required since intake and exhaust gases pass through ports. Figure 25 shows an exploded view of the principle engine parts. The output torque is transmitted to the shaft through the eccentric. The internal and external gears shown are timing gears designed to maintain the phase relationship between the rotor and the eccentric shaft rotation. The smaller external gear (coaxial with the eccentric shaft) is fixed to one side of the housing [1].

Since the rotor is three-sided there are three separate cycles operating simultaneously. The processes which occur in sequence are shown in Figure 25. For each revolution of the rotor, there are three power impulses. Since the eccentric shaft rotates at three times the rotor speed, however, there is only one power pulse per rotor for each output shaft revolution [1].

The use of rotary engines in stationary applications is very attractive because of various advantages resulting from the simplicity of the Wankel design as compared to

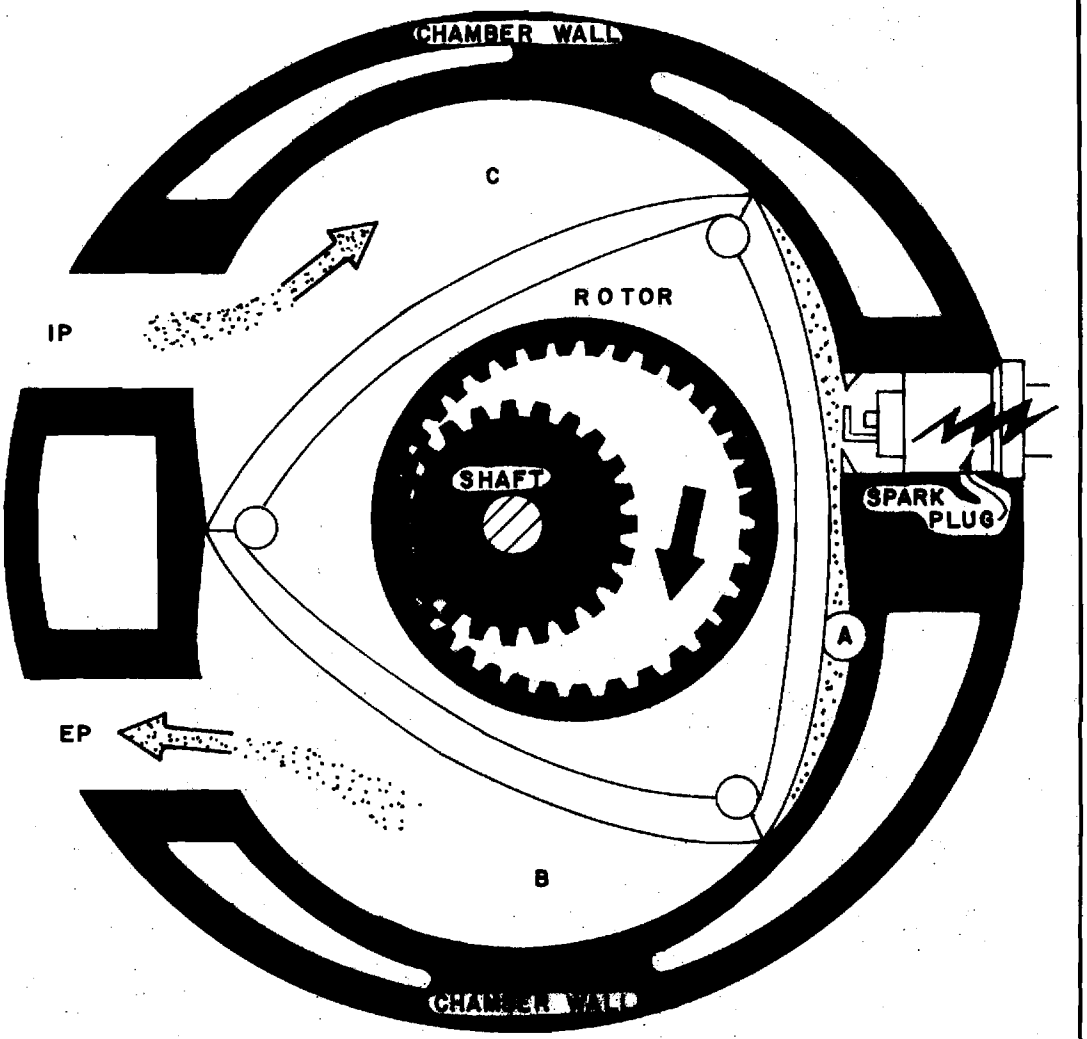

FIGURE 24.[11] ROTOR AND HOUSING OF A BASIC WANKEL ENGINE
A: COMPRESSION
B: POWER AND EXHAUST
C: INTAKE
IP = INTAKE PORT
EP = EXHAUST PORT

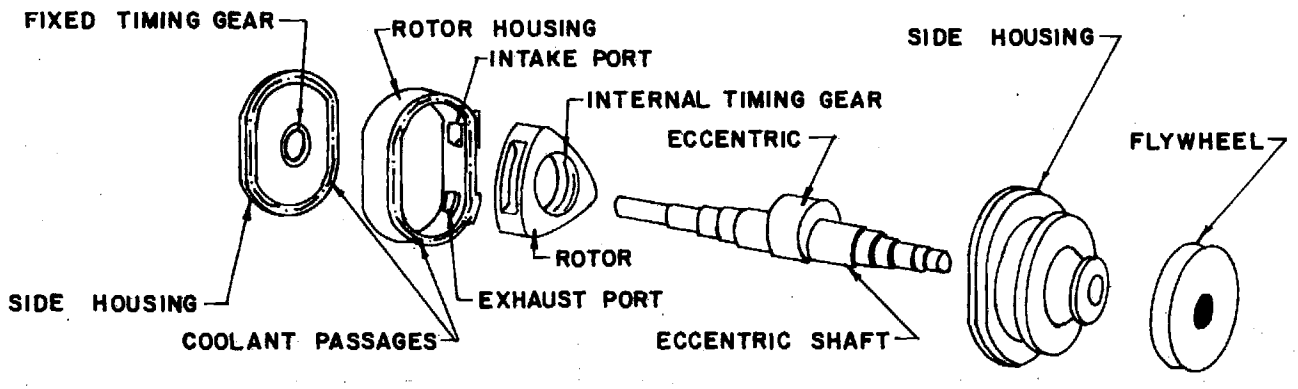

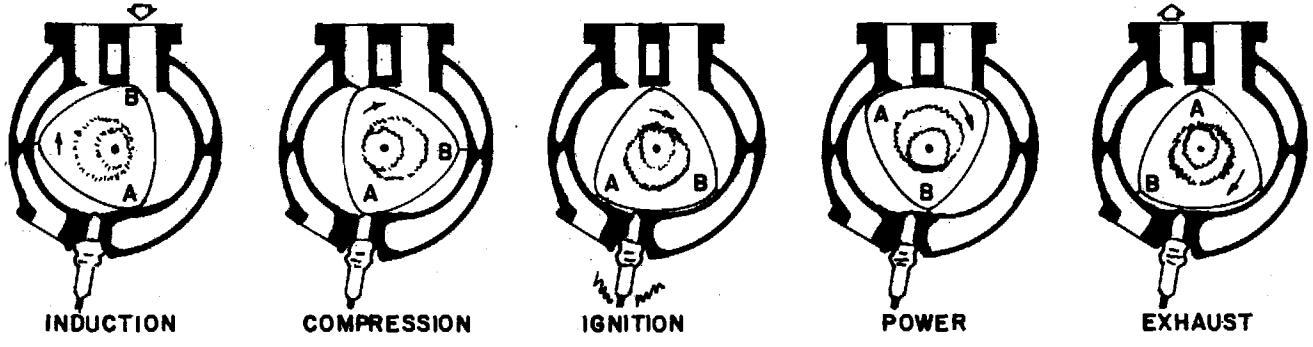

FIGURE 25.[1] BASICS OF A SINGLE ROTOR WANKEL ENGINE

conventional engines. Compared with a piston engine of comparable power output, the Wankel engine is about half the size and weight. Regardless of maximum power output, the Wankel engine has a far superior weight per horsepower ratio when compared with reciprocating engines [12]. Another major advantage is a reduction of parts, resulting in a far less complicated engine and providing greater simplicity and lower cost. Fewer moving parts also indicates less power loss due to internal friction. Finally, the small number of moving parts results in low operational costs since the required maintenance is limited, and the mechanical reliability is higher, thus extending the service life. It has been shown that the amplitude of vibration of a piston engine is over five times that of a Wankel [13]. This reduction of vibration is important in stationary long-life applications since a reduction in metal fatigue of various components results, as well as a dramatic reduction of noise levels. Finally, the Wankel engine encourages high volumetric efficiency because gas flow into and out of the combustion chamber is in a smooth sweep instead of through sharp turns or loops. In addition, compared with an intake stroke duration of 90 degrees of crankshaft rotation in a piston engine, the Wankel's suction intake occurs over 270 degrees of mainshaft rotation yielding a substantial volumetric efficiency advantage. Power output in a Wankel engine is smoother than in a piston engine because positive torque is

produced for about two-thirds of the operating cycle as opposed to one-fourth or less of a four-stroke piston engine's cycle [12].

From a wear standpoint, the most critical components of the Wankel engine are the rotor apex seals. These seals, located at the apex of each rotor where they act as gas seals, have a rather short life when the Wankel is operated with gasoline. Tests conducted at Georgia Tech, however, indicate a much longer seal life when the engine is using natural gas [1]. This increased seal life would appear to give the Wankel the long-life characteristics needed in a natural gas heat pump.

Waste heat recovery of the prime mover is another area worthy of analysis in natural gas heat pumps. If the waste heat is of a low temperature, generally in the form of 150°F to 250°F cooling air or water and 1,000°F exhaust gases, the recovery equipment required is large and the system's capital cost is consequently increased. In reciprocating I.C. engines, the waste heat is usually split such that about 60% (or more) of the waste is contained in the cooling medium and 40% (or less) is in the exhaust gases [1].

In a Wankel engine the waste heat situation is somewhat different. Due to the short exhaust passages from the combustion chamber to the exhaust manifold, little exhaust cooling can occur and temperatures in the 1500°F to 2000°F range result. The exhaust gases at these high temperatures

contain about 60% of the exhaust heat [1]. Thus, a majority of the Wankel engine's waste heat is at a high temperature making it easy to recover, resulting in smaller and less expensive heat recovery equipment.

Equipment and Instrumentation (Residential Unit)

The natural gas heat pump studied was the same electric system analyzed previously, with one major modification. The electric compressor was disconnected, and in its place, a Trane Model G, (G7H20X1), two-cylinder, reciprocating compressor driven by a Wankel engine was installed. Table 11 contains capacity data supplied by the compressor manufacturer [14].

A modification was also required on the compressor itself. Under the desired operating conditions it was determined that the required horsepower necessary to power the compressor and the capacity supplied were approximately double the values expected and desired. The problem was solved by removing one of the two pistons. The connecting rod was cut and a piston removed. The bearing and bearing cap were reattached to the crankshaft with special precautions taken to ensure against the bearing-turning or striking the compressor housing as the crankshaft rotated. Thus, problems of misbalance and improper oil lubrication were eliminated.

The engine used to power the system was a Sachs Wankel Engine Model KM914 A, single rotor, air-cooled

Table 11. Two-Cylinder Model G Compressor (3450 RPM) Performance Data [14]
Condensing Temperatures °F

Suction	110		120		130		140		150	
Temp °F	Tons	BHP	Tons	BHP	Tons	BHP	Tons	BHP	Tons	BHP
20	5.40	11.05	4.85	11.35	4.30	11.45	3.75	11.35	3.20	11.35
30	7.00	11.90	6.35	12.25	5.70	12.50	5.05	12.55	4.40	12.55
40	8.85	12.70	8.15	13.15	7.40	13.45	6.60	13.65	5.85	13.75
50	11.05	13.50	10.20	13.90	9.35	14.35	8.35	14.65	7.55	14.85

engine, a few specifications of which are given in Table 12. A Chrysler automotive solid state induction triggered (pointless) ignition system was adapted to the engine. Previous studies had been done on this engine at Georgia Tech [1]. Under the operating conditions of 3300 RPM, reference [1] predicts that the engine running on natural gas develops about eight horsepower and has a thermal efficiency of approximately 20%.

Waste heat recovery was achieved in the following manner. The Amana unit tested throughout this work was mounted approximately 36 inches above the floor on a frame built of 2-1/4 inch slotted angle material. In this part of the testing the Trane compressor and Wankel engine were placed on the floor beneath the Amana unit. See Figures 26, 27, 28, and 29 for system schematics. A stainless steel 1-1/2 inch exhaust pipe was installed between the engine exhaust and the Heat Transfer Module used in the gas furnace analysis. This module and the water pump and circulatory system were used in the exhaust heat recovery process. All unnecessary components in the gas furnace apparatus were disconnected and removed at this stage. In this testing no insulation was placed on the exhaust pipe. It was felt that the effort necessary to find, obtain, and install insulation capable of withstanding the 1,500-2,000°F temperatures was not worthwhile since the installed insulation would probably not be as effective in preventing heat loss as insulation in

Table 12. KM914 Engine Specifications [12]

Displacement:	18.5 cu. in. (303 cc)
Cooling:	Air-cooled (integral blower)
Compression ratio:	8:1
Performance (Gasoline):	20.0 horsepower at 5,000 RPM (tolerance range +5%)
Ignition timing (gasoline):	10°...12° before top dead center
Contact breaker gap:	0.014-0.018 in
Carburetor:	Tillotson diaphram carburetor HL-268A 22 mm (0.866 in) dia. or Bing butterfly valve carburetor 22 mm (0.866 in) dia.
Air filter:	Inlet mesh filter
Weight:	56 lbs., engine including starter, carburetor, and muffler
Pre-mix ratio:	40:1 fuel to oil

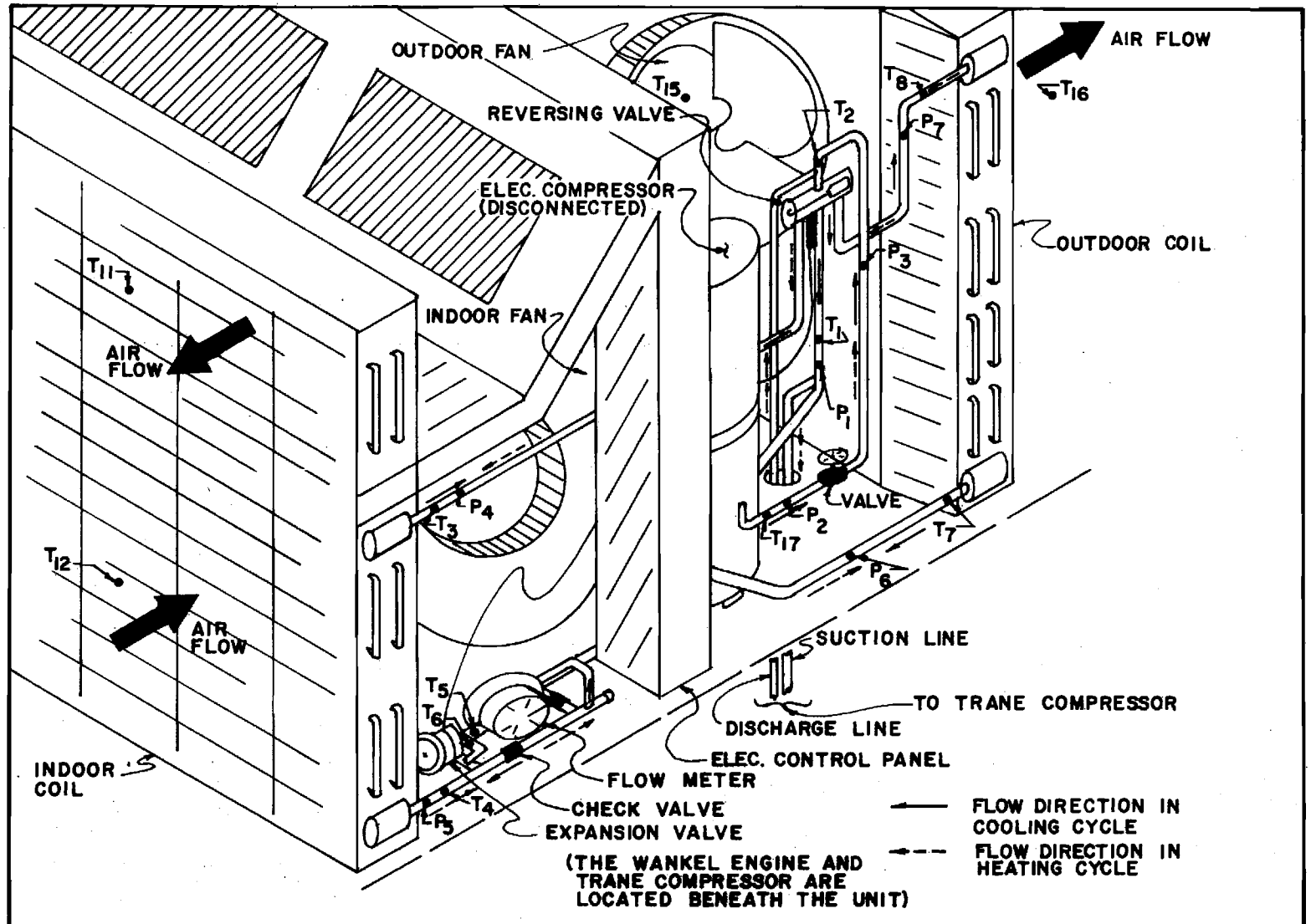

FIGURE 26. GAS HEAT PUMP SYSTEM SCHEMATIC INDICATING THE LOCATION OF MEASUREMENT POINTS

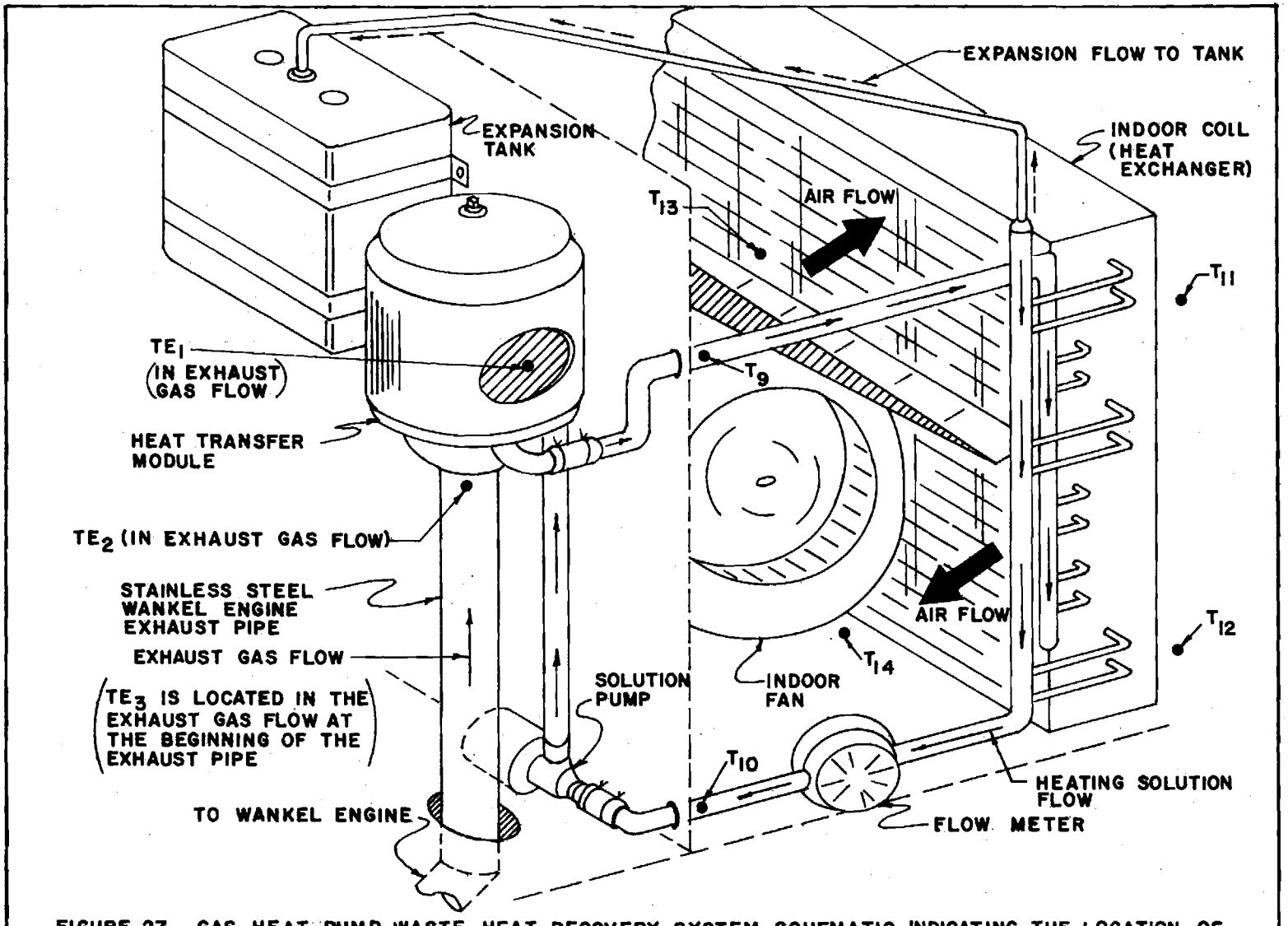

FIGURE 27. GAS HEAT PUMP WASTE HEAT RECOVERY SYSTEM SCHEMATIC INDICATING THE LOCATION OF MEASUREMENT POINTS

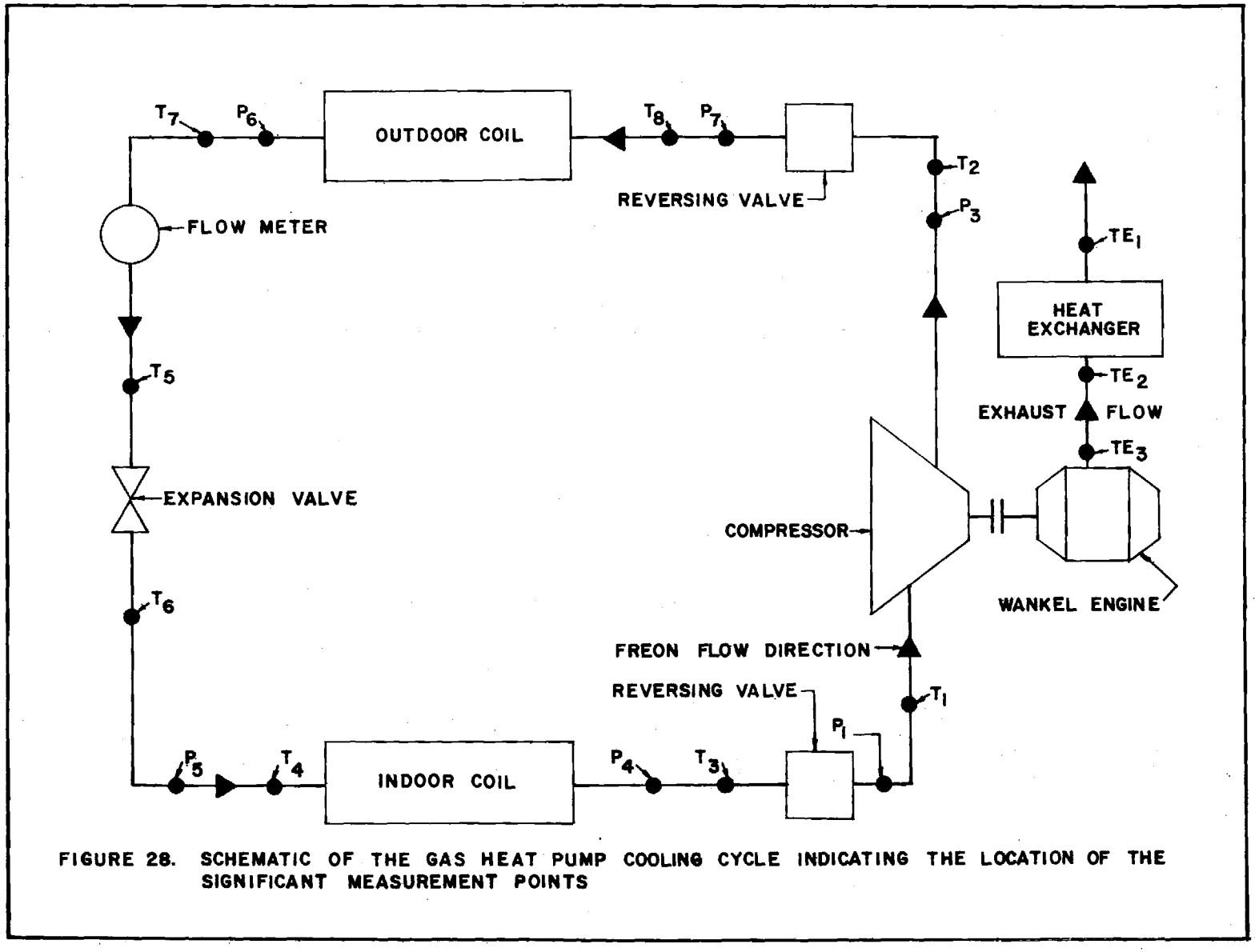

FIGURE 28. SCHEMATIC OF THE GAS HEAT PUMP COOLING CYCLE INDICATING THE LOCATION OF THE SIGNIFICANT MEASUREMENT POINTS

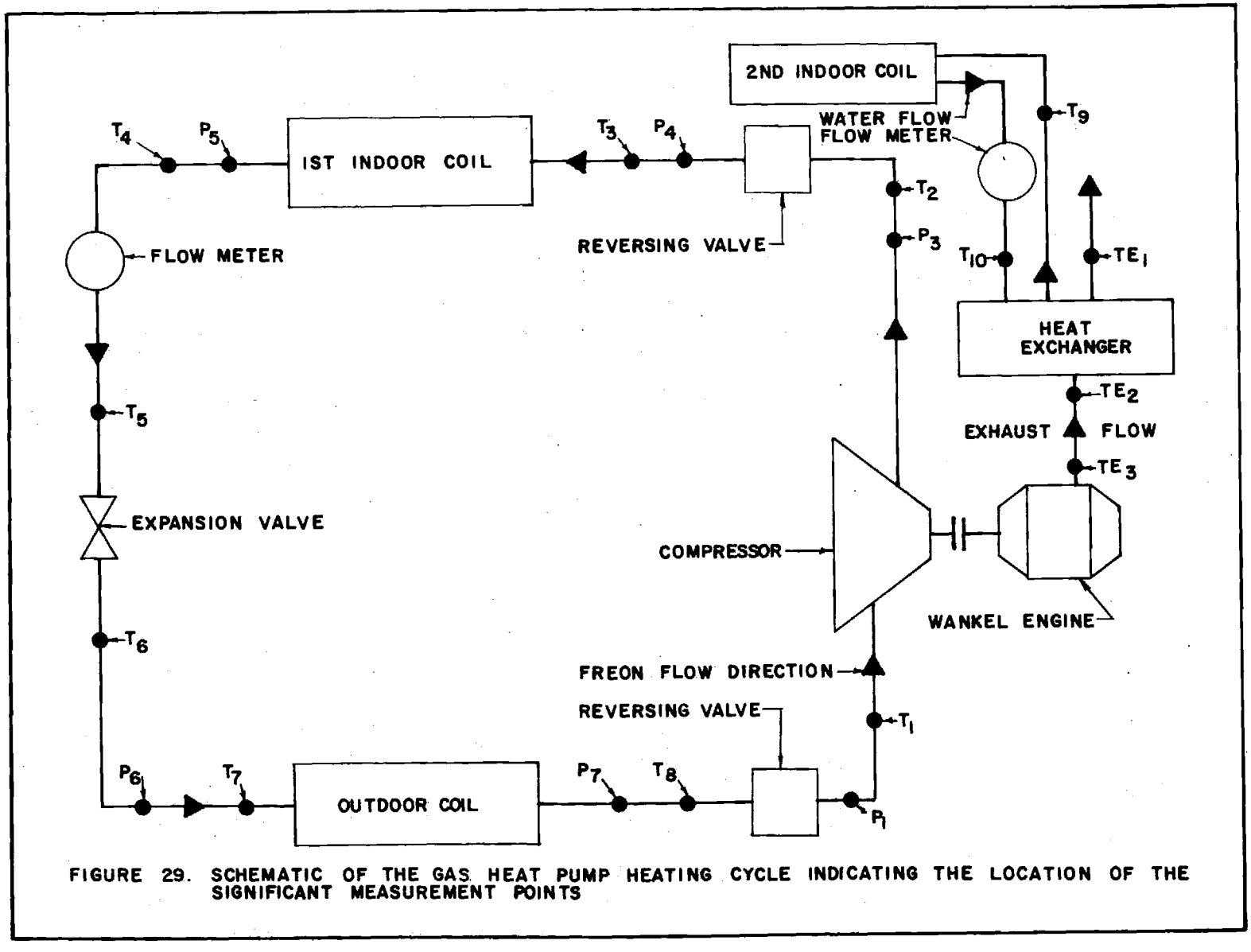

FIGURE 29. SCHEMATIC OF THE GAS HEAT PUMP HEATING CYCLE INDICATING THE LOCATION OF THE SIGNIFICANT MEASUREMENT POINTS

a commercially produced unit. Instead, three thermocouples were installed in the exhaust flow: one at the engine exhaust, a second 40 inches away, just before entry into the heat exchanger (Heat Transfer Module), and a third in the exhaust flow just after this unit, as the exhaust is about to be discharged to the atmosphere. Thus, the actual heat loss could be determined and an analysis is included predicting the possible performance if suitable insulation were installed. Insulation is recommended, of course, for any operating unit of this type.

The instrumentation of this system was similar to that previously described. The cycle temperatures and pressures, freon flow rate, and electrical input were measured with the same equipment described previously in the section on the electric heat pump. The waste heat recovery was accomplished with the water system of the natural gas furnace originally studied. Thus, the water and gas flow rates and appropriate water temperatures were obtained using the instruments described earlier in the gas furnace study. The only additional measurement made was of exhaust gas temperatures. These were made using chromel-alumel thermocouples inserted into the exhaust gas flow. The temperatures were read on an Omega type 2809 digital thermometer (accuracy = ±1%).

Equipment and Instrumentation (Commercial Unit)

The engine used to power the system is a Mazda RX-2, 2 rotor Wankel type engine identical to the engine on which the natural gas performance data was previously run (see reference 1 for performance curves). It is capable of providing 70 horsepower and operate over a speed range of up to 5000 rpm. Any pollution device which originally came with the engine was removed since it is not required with natural gas, and a natural gas mixer was adapted to the carburetor. To cool the engine oil and increase the amount of waste heat recovered, an outboard engine oil cooler built for marine applications was installed on the lower part of the engine frame and connected to the water system. Additional waste heat is recovered from a thermal reactor which is installed in the exhaust line to recover the exhaust gas heat. A two belt drive connects the engine and the compressor. A schematic of the system is shown in Figure 29a and 29b in the heating and cooling modes with the physical layout shown in Figure 29c.

The compressor is a nominal 25 ton, 25 hp, 6 cylinder Carrier unit 5F60 whose specs are in Table 12a. It was mounted to the same I-beam frame as the engine. The 10" pulley on the compressor and the 7" pulley on the engine give a drive ratio of 1.43 which enables the engine to deliver more horsepower at smaller compressor speeds. In order to facilitate starting the system, a by-pass line, with ports for

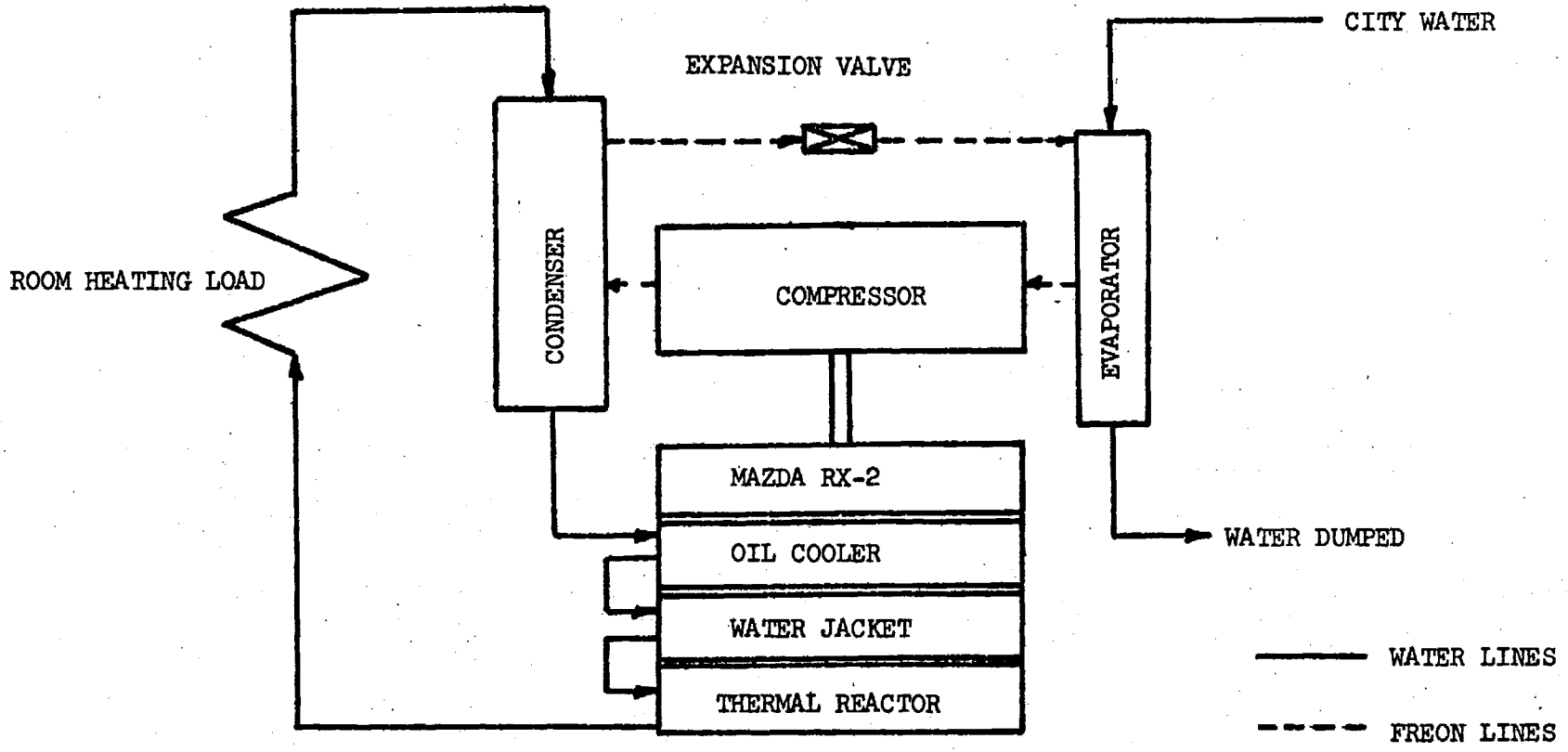

Figure 29a. HEATING OPERATION

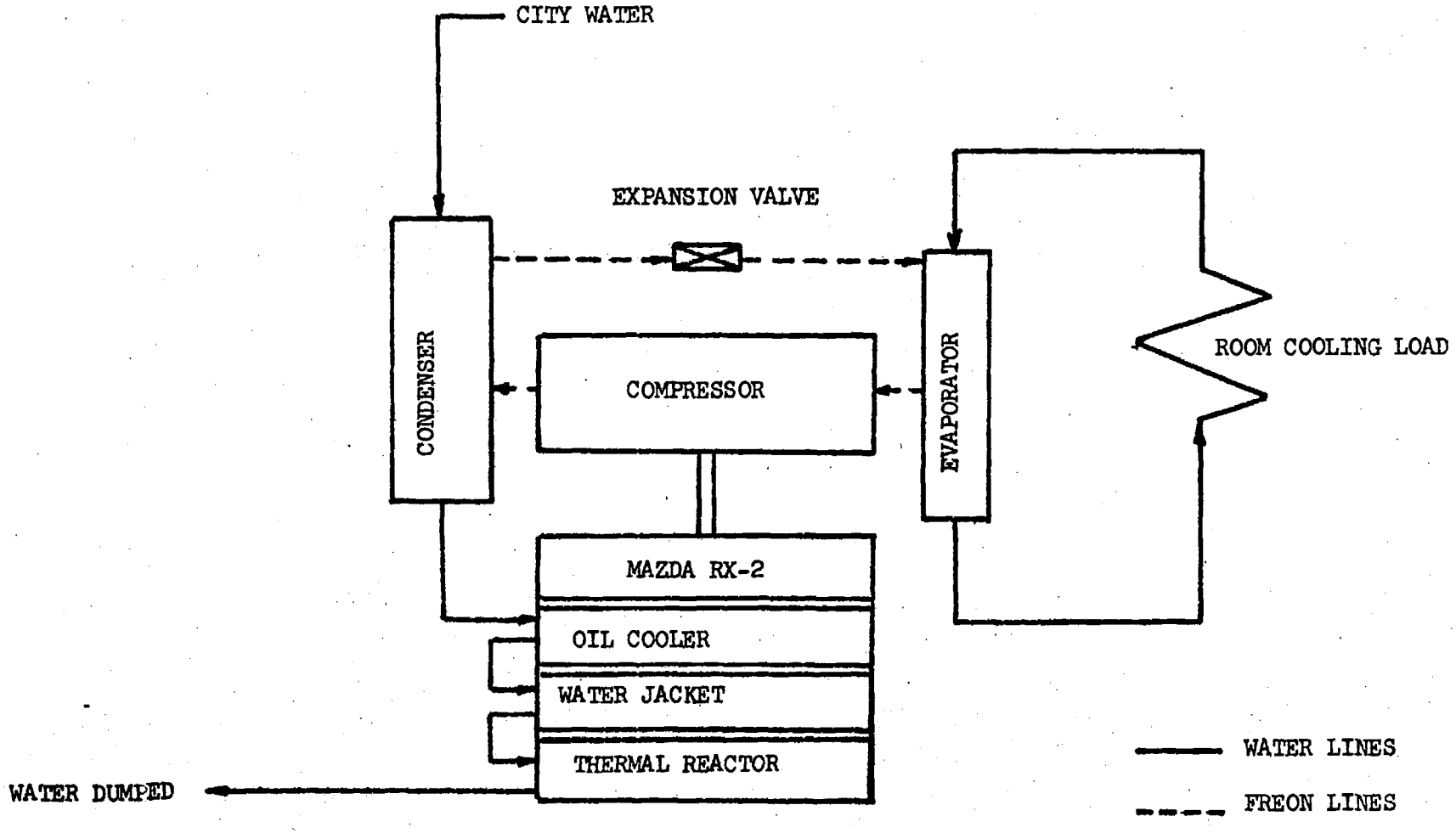

Figure 29b. COOLING OPERATION

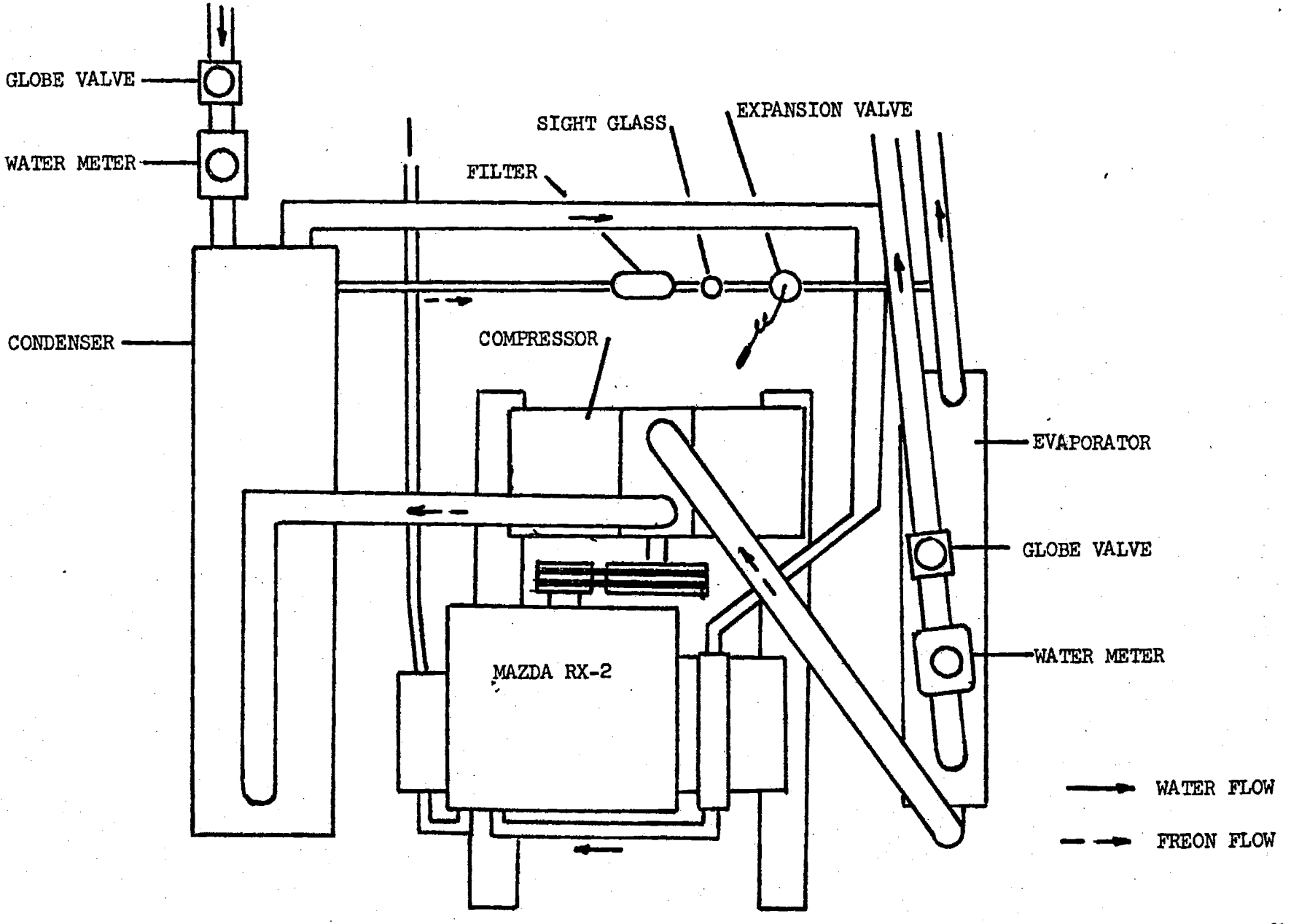

Figure 29c. ASSEMBLY

Table 12a

Carrier Model 5F60 Compressor

Physical Data

Nominal hp: 10-30

Displ. CFM @ 1750 rpm: 59.8

Cylinders: 6

Oil (pt): 13

Bone (in): 2-1/2

Stroke (in): 2

Max. rpm: 1750

Min. rpm: 400

High side max. pressure: 400 psig

Low side max. pressure: 245 psig

Connections (in)

Suction ODF: 2-1/8

Discharge ODF: 1-5/8

Ratings--R-22

SST(°F)	SDT(°F)	Cap (tons)	BHP	THR
30	100	22.5	23.9	27.5
30	120	19.1	27.2	24.7
30	135	16.5	29.5	22.3
40	100	28.2	24.7	33.3
40	120	24.2	29.1	30.1
40	135	21.1	32.0	27.3
50	100	34.8	24.8	39.8
50	120	30.2	30.5	36.1
50	135	26.6	34.1	32.9

filling and emptying the refrigerant, is installed across the condenser and evaporator lines (see Figure 29d).

The evaporator and the condenser are both nominal 25 ton units with maximum water flow rates of 65 and 50 gpm respectively. Their specs are given in Appendix F. They are mounted slightly above the ground to allow for insulation, and they are set on either side of the motor to give the operator sufficient room to work around the components. This arrangement requires slightly more Freon but makes modifications and repairs easier. In the Freon line between the evaporator and the condenser, there is a 25 ton expansion valve, a sight glass, and a filter.

The piping between all of the components is a mixture of pipe and solder joints. Whenever possible, new, clean galvanized steel pipe is used. A special gasket forming pipe dope is used on all connections to prevent leaks. Pipe was selected because of its availability, cost, and ease of assembly. The pipe size was chosen using a chart with the pressure drop in lines of different sizes for Freon 22. The 2" diameter line between the evaporator and the compressor has a pressure drop of 2.5 psi/100 ft, the 1-1/2" line between the condenser and the compressor has a higher value of 8 psi/100 ft. The liquid line has a pressure drop of 5.3 psi/100 ft. These values are within reason and are most adaptable to the components.

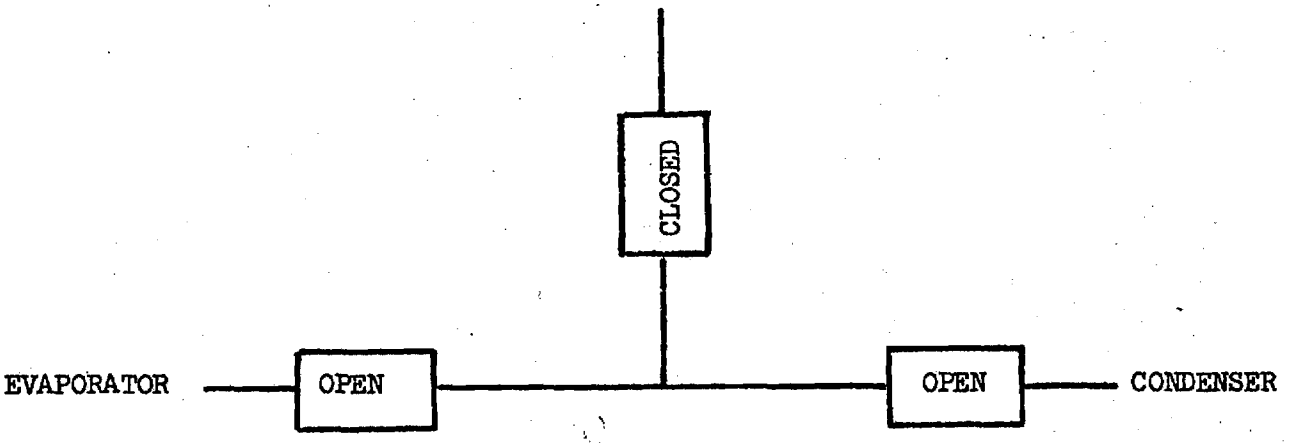

a) BY-PASS

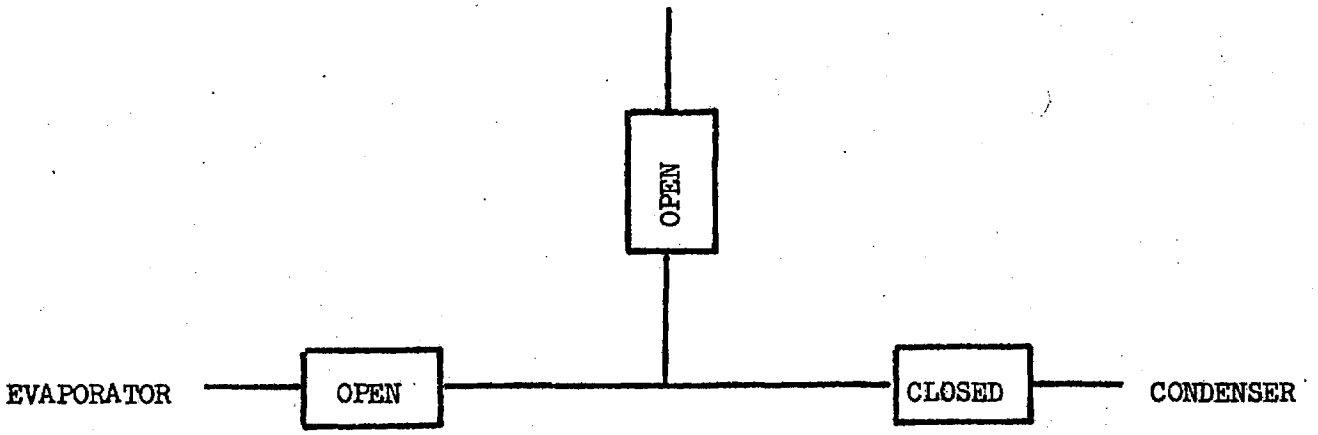

b) FILLING

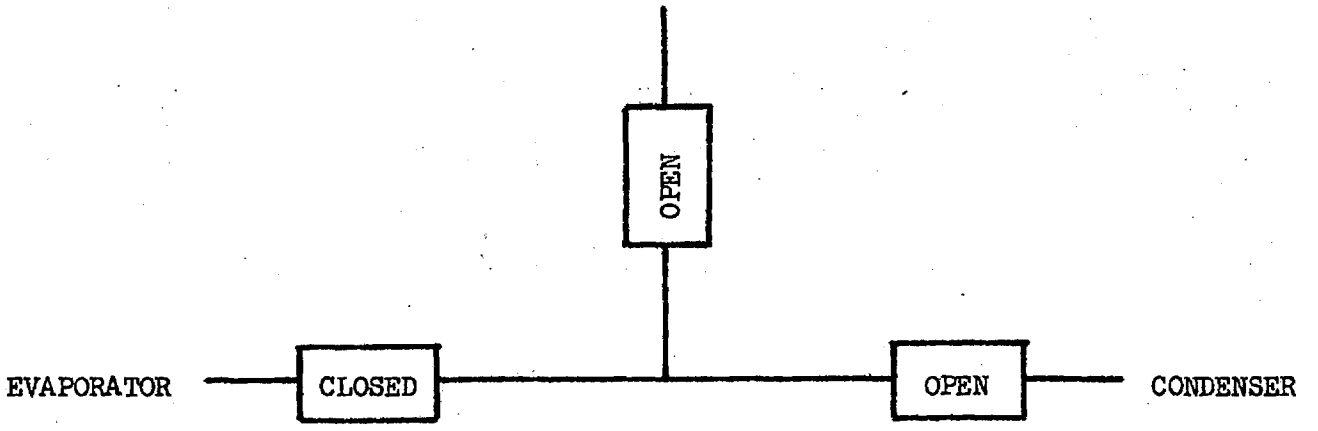

c) EMPTYING

Figure 29d. BY-PASS NETWORK

The water that flows through the evaporator and condenser is supplied in 1-1/2" pipe from a 2" main. This piping was sized to supply 50 gpm to both the condenser and evaporator with a minimum pressure drop. A globe valve is installed in each line for flow control, and a water meter is supplied for each unit for flow measurement. Each meter is rated at 50 gpm.

For experimental runs, water temperatures can be recorded after each component, i.e., the condenser, the oil cooler, the engine water jacket, the thermal reactor, and the evaporator; as well as the inlet temperatures. From these values, component performance can be computed. Pressures can also be recorded on either side of the compressor to keep track of its performance.

Performance Results (Residential Unit)

The experimental data, as well as sample calculations, for both the cooling and heating modes, is presented in Appendix D. The following results were obtained:

T_L = the low (fluid evaporating) temperature

T_H = the high (fluid condensing) temperature

Capacity (tons) = (enthalpy change across the evaporator,

Btu/#m) X (the mass flow rate, #m/hr)

$$COPH_c(ideal) = \frac{T_L/T_H - T_H/T_S}{1 - T_L/T_H} \text{ ; (assume } T_S = 1{,}000°F) \quad (14)$$

$COPH_c$(actual) = (enthalpy change across the evaporator, Btu/#m) X (the mass flow rate, #m/hr) ÷ $\dot{G}$ (the gas input rate, Btu/hr)

Table 13. Gas Heat Pump (Cooling) Test Results

Test	T_L(°F)	T_H(°F)	Capacity (tons)	$COPH_c$(actual)	$COPH_c$(ideal)
1	60.0	142.5	6.80	.674	3.21
2	61.5	141.5	11.42	1.04	3.54
3	65.0	154.25	9.73	.898	2.87

Similarly for the heating cycle:

T_L = the low (fluid evaporating) temperature

T_H = the high (fluid condensing) temperature

Capacity (Btu/hr) = (enthalpy change across the condenser, Btu/#m) X (the mass flow rate, #m/hr)

$$COPH_H(\text{ideal}) = \frac{1-T_H/T_S}{1-T_L/T_H} \; ; \; (\text{assume } T_S = 1{,}000°F) \quad (15)$$

$COPH_H$ (actual) = (enthalpy change across the condenser, Btu/#m) X (the mass flow rate, #m/hr) ÷ $\dot{G}$ (the gas input rate, Btu/hr)

Refer to Table 14 where two of the sets of values include waste heat recovery, $\dot{Q}_{rec}$.

$$\dot{Q}_{rec} = \dot{m}_w \, \Delta T_w \, C_{pw} \quad (47)$$

where:

$\dot{m}_w$ = the cooling water mass flow rate, #m/hr

ΔT_w = the water temperature change across the heat exchanger, °F

C_{pw} = water specific heat, 1 Btu/(#m°F)

At the engine exhaust the measured temperature was 1770°F. After 40 inches of uninsulated stainless steel exhaust pipe, the measured temperature was 1175°F. Finally, the exhaust passes through the Heat Transfer Module and upon exiting the temperature dropped to 170°F. (These measured values varied somewhat among the various tests, but the particular temperatures used in this calculation were chosen to give an indication of the improvement that could possibly be achieved. Thus, the maximum engine exhaust temperature measured was used.)

Table 14. Gas Heat Pump (Heating) Test Results

Test	T_L(°F)	T_H(°F)	Capacity(Btu/hr)	$COPH_H$(actual)*	$COPH_H$**	$COPH_H$***	$COPH_H$(ideal)*
1	73.0	133.0	9.42×10^4	0.83	1.11	1.29	5.90
2	81.5	137.75	8.10×10^4	0.78	1.09	1.18	6.56
3	78.25	139.5	9.26×10^4	0.87	1.18	1.37	5.90
4	67.5	148.0	8.63×10^4	0.69	0.95	1.12	4.46

*With no waste heat recovery

**With actual waste heat recovery

***With waste heat recovery assuming an insulated exhaust

If a modified $COPH_H$ is now defined as:

$$COPH_H = \frac{\dot{Q}_{cond} + \dot{Q}_{rec}}{\dot{G}} \qquad (48)$$

where:

$\dot{Q}_{cond}$ is the numerator in the previously defined equations

$\dot{G}$ is the previously defined gas input

$\dot{Q}_{rec}$ is the waste heat recovery

the values of $COPH_H$ are significantly improved. Sample calculations are included in Appendix D.

An analysis can be made to determine the benefit of insulating the exhaust, thereby recovering more of the waste heat and increasing the $COPH_H$. Defining the waste heat recovery as follows:

$$\dot{Q}_{rec} = \dot{m}_w \int_{ex} C_{pw}\, dT = \eta_{ex}\, \dot{m}_{ex} \int_{htm} C_{pex}\, dT \qquad (49)$$

where:

$\dot{Q}_{rec}$ = the waste heat recovery rate

$\dot{m}_w$ = the mass flow rate of the heat recovery water

$\int_{ex} dT$ = integration with respect to the temperature change of the heat recovery water across the heat exchanger (indoor coil)

C_{pw} = the specific heat of the heat recovery water

η_{ex} = the efficiency of heat transfer from the exhaust

gases to the heat recovery water

$\dot{m}_{ex}$ = the exhaust gas mass flow rate

$\int_{htm} dT$ = integration with respect to the temperature change of the exhaust gases across the heat transfer module

C_{pex} = the specific heat of the exhaust gases

The variation in specific heat was taken into account to provide greater accuracy.

Assuming a stoichiometric methane combustion reaction,

$$CH_4 + 2O_2 + 2(3.76)N_2 \rightarrow CO_2 + 2H_2O + 7.52N_2$$

and using Table A.7 in reference [15] for the products of combustion,

$$CO_2: \quad C_{po} = 16.2 - \frac{6.53x10^3}{T} + \frac{1.41x10^6}{T^2}$$

$$H_2O: \quad C_{po} = 19.86 - \frac{597}{\sqrt{T}} + \frac{7500}{T}$$

$$N_2: \quad C_{po} = 9.47 - \frac{3.47x10^3}{T} + \frac{1.16x10^6}{T^2}$$

a comparison between the actual heat recovery and the ideal insulated exhaust recovery that possibly could be achieved can be made.

$$\frac{\dot{Q}_{rec}(\text{insulated exhaust})}{\dot{Q}_{rec}(\text{actual})} = \frac{\eta_{ex}\ \dot{m}_{ex} \int_{630R}^{2230R} C_p\ dT}{\eta_{ex}\ \dot{m}_{ex} \int_{630R}^{1635R} C_p\ dT}$$

The enthalpy change (dh) of the mixture was calculated using:

$$dh_{mixture} = \frac{(M_{co_2}\ dh_{co_2} + M_{H_2O} dh_{H_2O} + M_{N_2} dh_{N_2})}{(M_{co_2} + M_{H_2O} + M_{N_2})} \qquad (50)$$

Sample calculations are given in Appendix D. The result is

$$\frac{\dot{Q}_{rec}(\text{insulated exhaust})}{\dot{Q}_{rec}(\text{actual})} = 1.65$$

Therefore, the $\dot{Q}_{rec}$ could be increased from 32,182.08 Btu/hr to 53,100.43 Btu/hr by exhaust pipe insulation and the $COPH_H$'s increased, as summarized once again in Table 15.

Table 15. Gas Heat Pump $COPH_H$'s

Test	(Without Waste Heat Recovery)	(With Actual Waste Heat Recovery)	(With Waste Heat Recovery Assuming an Insulated Exhaust)
1	0.83	1.11	1.29
2	0.78	1.09	1.18
3	0.87	1.18	1.37
4	0.69	0.95	1.12

A comparison of the various systems follows in Chapter VI.

Performance Results (Commerical Unit)

The performance of the nominal 25 ton commercial unit previously described was calculated for both the heating and cooling modes and the details are presented in Appendix G.

In the cooling operation, the evaporator load was set at 25 tons. The city water temperature in summer is 83.5°F. The water temperature change across the evaporator was assumed to be 12°F from an inlet temperature of 55°F. The operating points in Table 15a were found for various flows in the condenser.

In the heating operation, the evaporator load was set at 25 and 20 tons. The temperature of the city water flowing through the evaporator is 59°F for winter months. The temperature difference across the evaporator was set at 20°F to give a reasonable evaporator temperature. The inlet temperature to the condenser was set at 110° and 120°F to generate the operating points.

The results are shown in Tables 15a and 15b.

Table 15a. Cooling Operating Points

	Pt. 1	Pt. 2	Pt. 3	Pt. 4
Evaporator:				
Load-tons	25	25	25	25
Inlet temp.-°F	55	55	55	55
Outlet temp.-°F	43	43	43	43
Flow rate-gpm	50	50	50	50
Freon temp.-°F	34	34	34	34
Freon pres.-psia	75	75	75	75
Compressor:				
RPM	1800	1875	1887	1950
B.H .P.	25.8	28.3	28.9	30.6
Condenser:				
Load-Btu/min	6093	6200	6220	6300
Inlet temp.-°F	83.5	83.5	83.5	83.5
Outlet temp.-°F	93.8	98.4	102.1	108.7
Flow rate-gpm	71	50	40	30
Freon temp.-°F	103	109.5	111	120
Freon Pres.-psia	220	240	244	275
Engine:				
RPM	2574	2681	2698	2788
E.R.	1.0	1.0	1.0	1.0
Fraction of WOT	.75	.83	.92	1.0
Efficiency	23%	24%	24%	23.5%
Gas energy supplied-Btu/min	4749	5000	5107	5523
COP	1.05	1.00	0.98	0.90

Table 15b. Heating Operating Points

	Pt. 1	Pt. 2
Evaporator:		
Load-tons	25	20
Inlet temp.-°F	59	59
Outlet temp.-°F	39	39
Flow rate-gpm	30	24
Freon temp.-°F	30.4	30.4
Freon pres.-psia	70	70
Compressor:		
RPM	2475	2050
B.H.P.	46	33.5
Condenser:		
Load-Btu/min	6951	5540
Inlet temp.-°F	110	120
Outlet temp.-°F	126.7	128.3
Flow rate-gpm	50	50
Freon Temp.-°F	138	142
Freon pres.-psia	340	360
Engine:		
RPM	3539	2930
E.R.	1.0	1.0
Fraction of WOT	0.96	0.75
Efficiency	23%	23%
Gas energy supplied-Btu/min	8483	6178
Waste heat recovered	6532	4757
Final water temp.-°F	143	140.2
COP	1.59	1.65

CHAPTER VI

DISCUSSION AND CONCLUSIONS

Comparison of Results

Let us compare, at this point, the results of the various systems. Once again, relative to the electric heat pump system, an important point should be made. The COPH's desired in this study are defined as the cooling or heating output relative to the heating value of the fuel at the power plant. For an electrical system, the electrical output to the house is generally taken as 0.3 of the fuel input at the power plant, making the electrical system COPH's the product of the experimentally measured values (COPW's) and 0.3 [1].

Earlier in this work a relationship was established between the Carnot or ideal COPW's and the ideal vapor-compression cycle COP's. (See Figures 11, 12, 13, and 14.) At this stage, similar graphs, (Figures 30, 31, 32, and 33), can be formulated using the actual experimentally determined test cycles instead of ideal vapor-compression cycles. Refer to Appendix A for sample calculations and refer to the Vapor-Compression Cycle Analysis section for a brief discussion of K_1 and K_2. A comparison of the various K_1's and K_2's for the systems indicates the degree to which the actual cycles

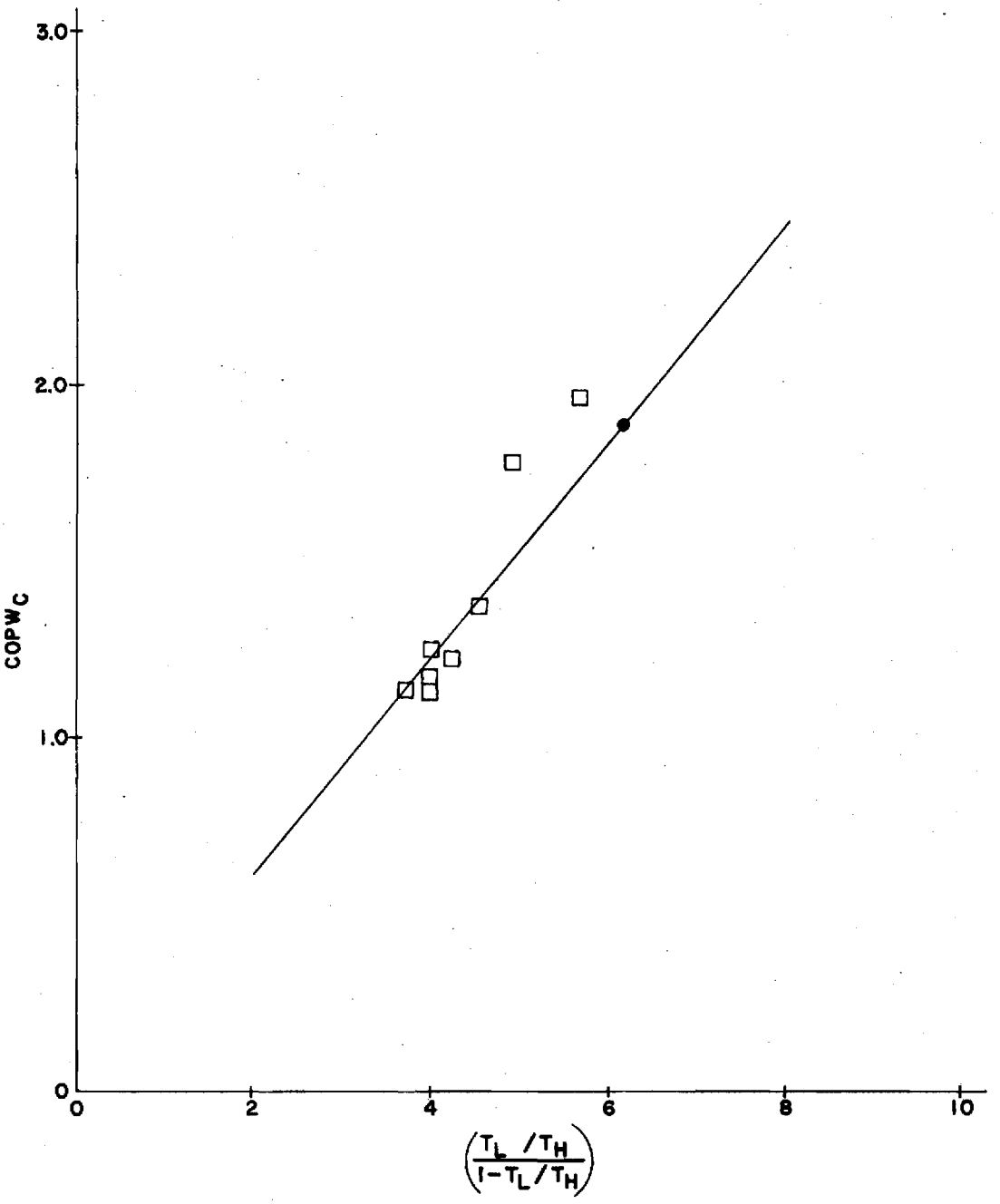

□ EXPERIMENTAL VALUES; ● T_L = 40°F & T_H = 120°F

FIGURE 30. ELECTRIC COOLING COPW$_C$ VS. $\left(\frac{T_L/T_H}{1-T_L/T_H}\right)$; SLOPE = K_1 = .31

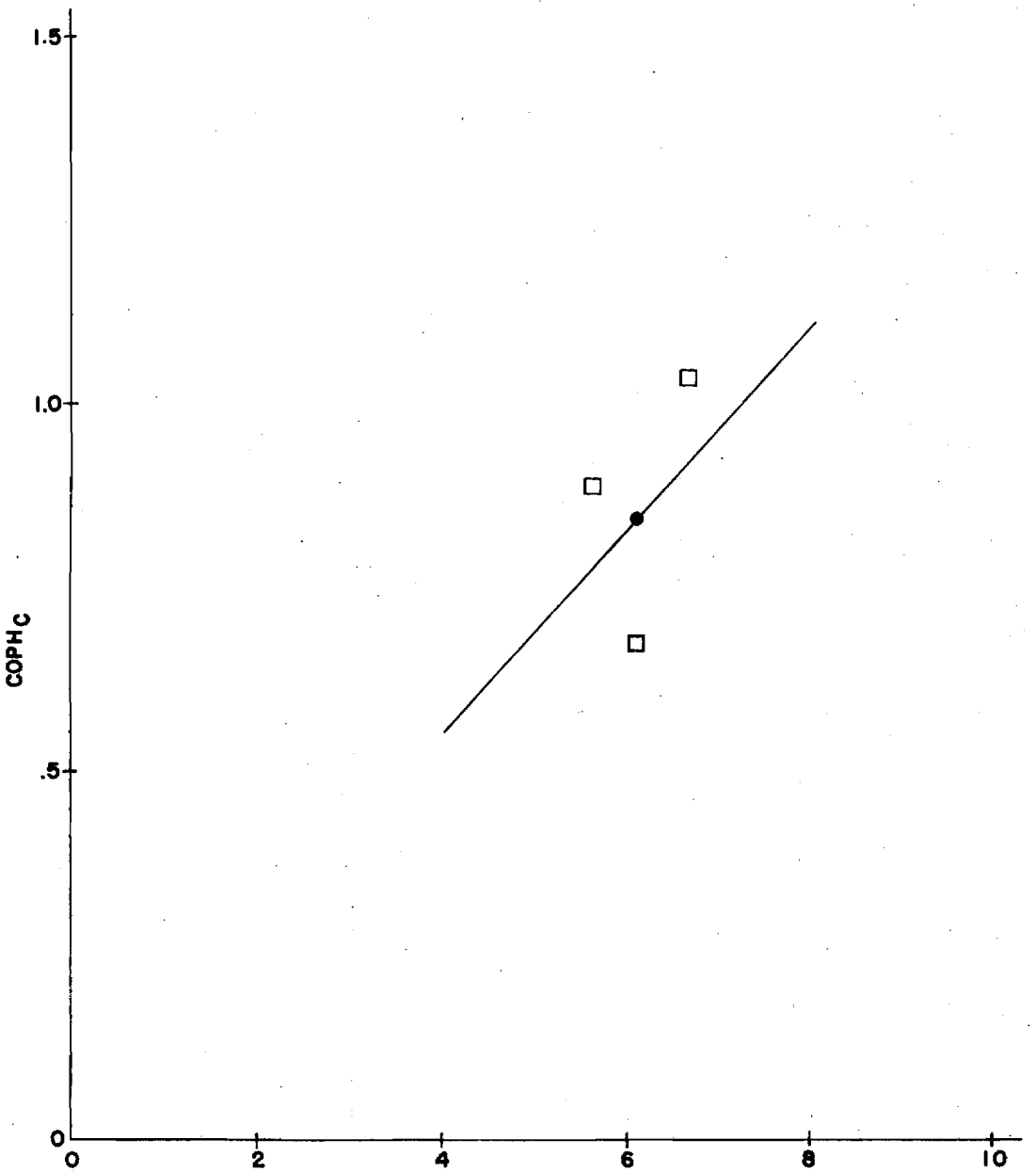

□ EXPERIMENTAL VALUES ; ● T_L = 40° F & T_H = 120° F

FIGURE 31. GAS COOLING COPH$_C$ VS. $\left(\frac{T_L/T_H}{1-T_L/T_H}\right)$; SLOPE = K_1 = .14

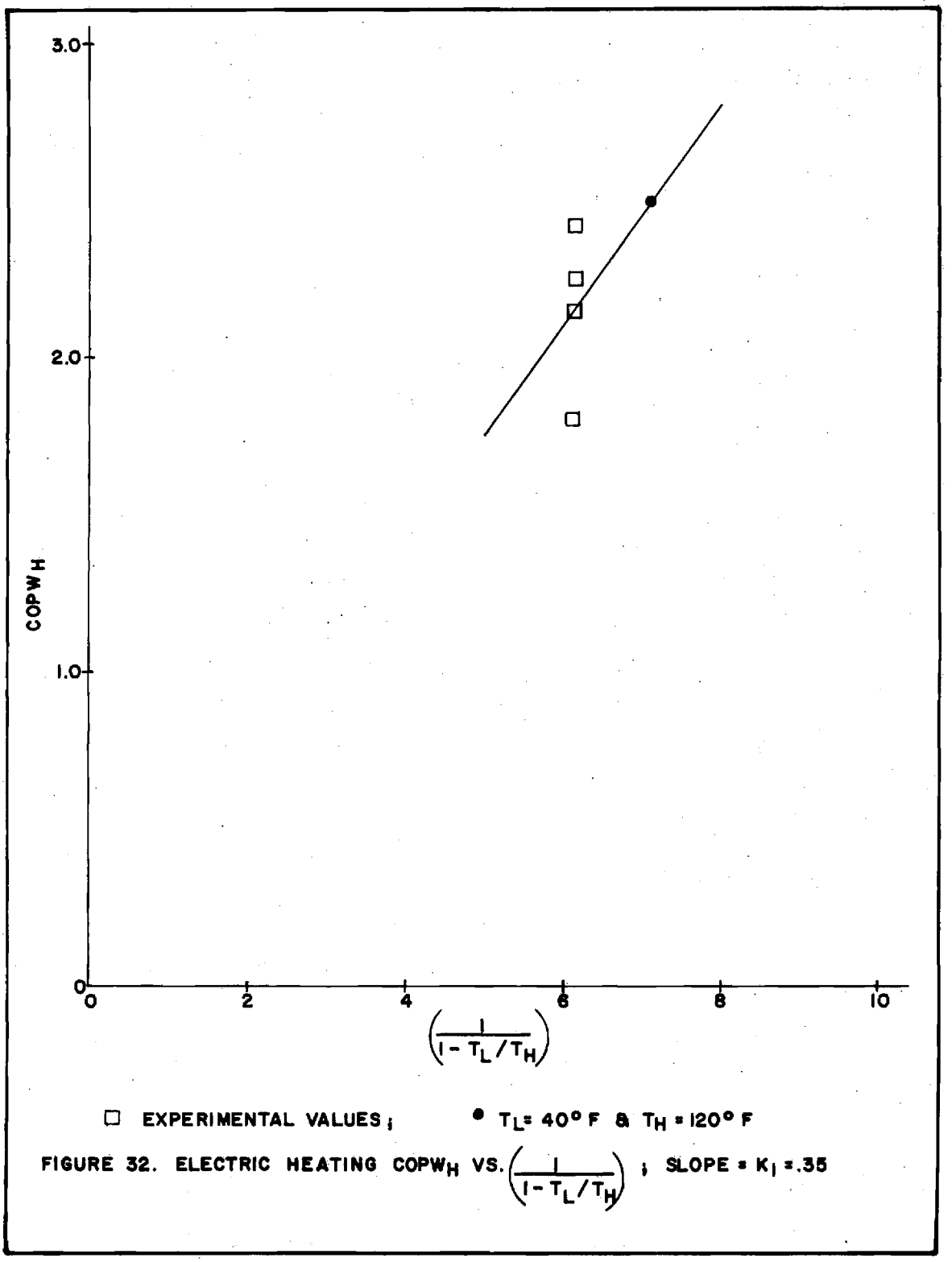

□ EXPERIMENTAL VALUES; ● T_L = 40° F & T_H = 120° F

FIGURE 32. ELECTRIC HEATING $COPW_H$ VS. $\left(\frac{1}{1-T_L/T_H}\right)$; SLOPE = K_1 = .35

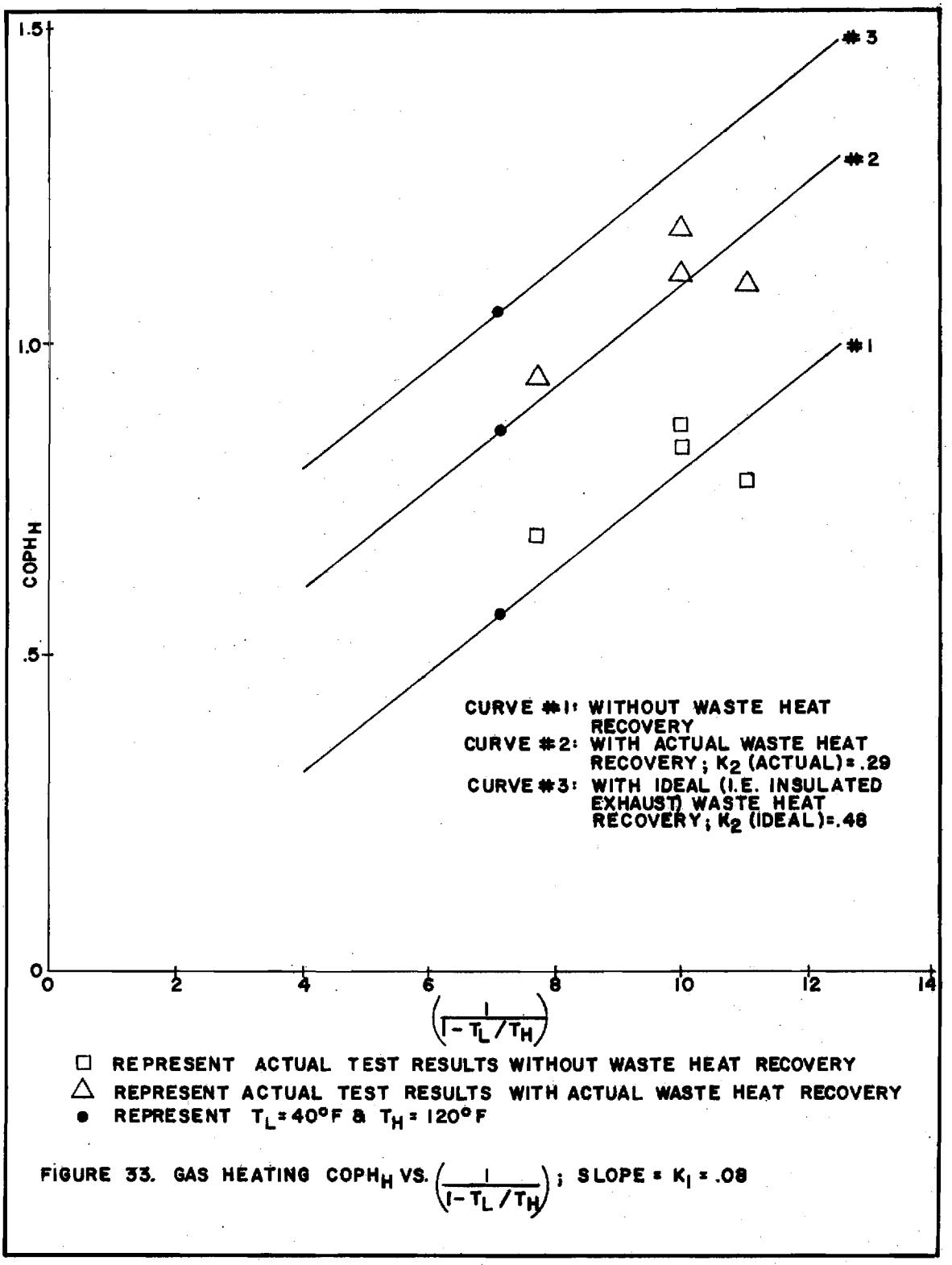

FIGURE 33. GAS HEATING $COPH_H$ VS. $\left(\frac{1}{1-T_L/T_H}\right)$; SLOPE = K_1 = .08

approach the ideal.

Once again, $(\frac{T_L/T_H}{1-T_L/T_H})$ approaches 0.0 as a lower limit while $(\frac{1}{1-T_L/T_H})$ approaches 1.0. For the electrical system, (Figure 32), at this lower limit $COPW_H$ equals 1.0. In the gas system analysis, (Figure 33), at the lower limit $COPH_H$ will equal the actual engine efficiency for the case of no waste heat recovery. If waste heat recovery is included, $COPH_H$ approaches a value equivalent to the actual engine efficiency plus the percentage of waste heat recovered.

One motivation for these graphs was to solve the problem created by the actual test result's limited range of condenser and evaporator temperatures. By developing the relationships mentioned above, much broader, and hence, much more useful results can be presented. The performance of a particular system under conditions other than those established in this experimental work can thus be estimated.

Perhaps the best method of comparing the alternate systems is to simply compare their performance at a given set of operating conditions. An analysis was performed for a representative condition of T_L = 40°F and T_H = 120°F, sample calculations of which are included in Appendix E. The results of this analysis are presented in Table 16 and Figures 34, 35, and 36.

The gas furnace data was included for completeness and somewhat limited comparison purposes. It should be recalled, however, that its performance is not dependent on

Table 16. Comparison of Alternate Systems (Based on performance with T_L = 40°F and T_H = 120°F)

System	$COPH_C$	$COPH_H$	$/10^6 Btu	Btu/$
Alternate System				
Gas Furnace*	---	0.84	1.55	6.45×10^5
Electric Heat Pump (Cooling)	0.57	---	4.63	2.16×10^5
Electric Heat Pump (Heating)	---	0.75	2.34	4.27×10^5
Residential Gas Heat Pump				
Gas Heat Pump (Cooling)	0.85	---	1.29	7.75×10^5
Gas Heat Pump (Heating) (with actual waste heat recovery)	---	0.86	1.51	6.62×10^5
Gas Heat Pump (Heating) (with waste heat recovery assuming an insulated exhaust)	---	1.05	1.24	8.06×10^5
Commercial Gas Heat Pump				
Gas Heat Pump (Cooling)	1.05	---	1.04	9.62×10^5
Gas Heat Pump (Heating)	---	1.60	0.81	12.3×10^5

*The gas furnace values are simply averages of the measured results, which are not restricted to T_L = 40°F and T_H = 120°F.

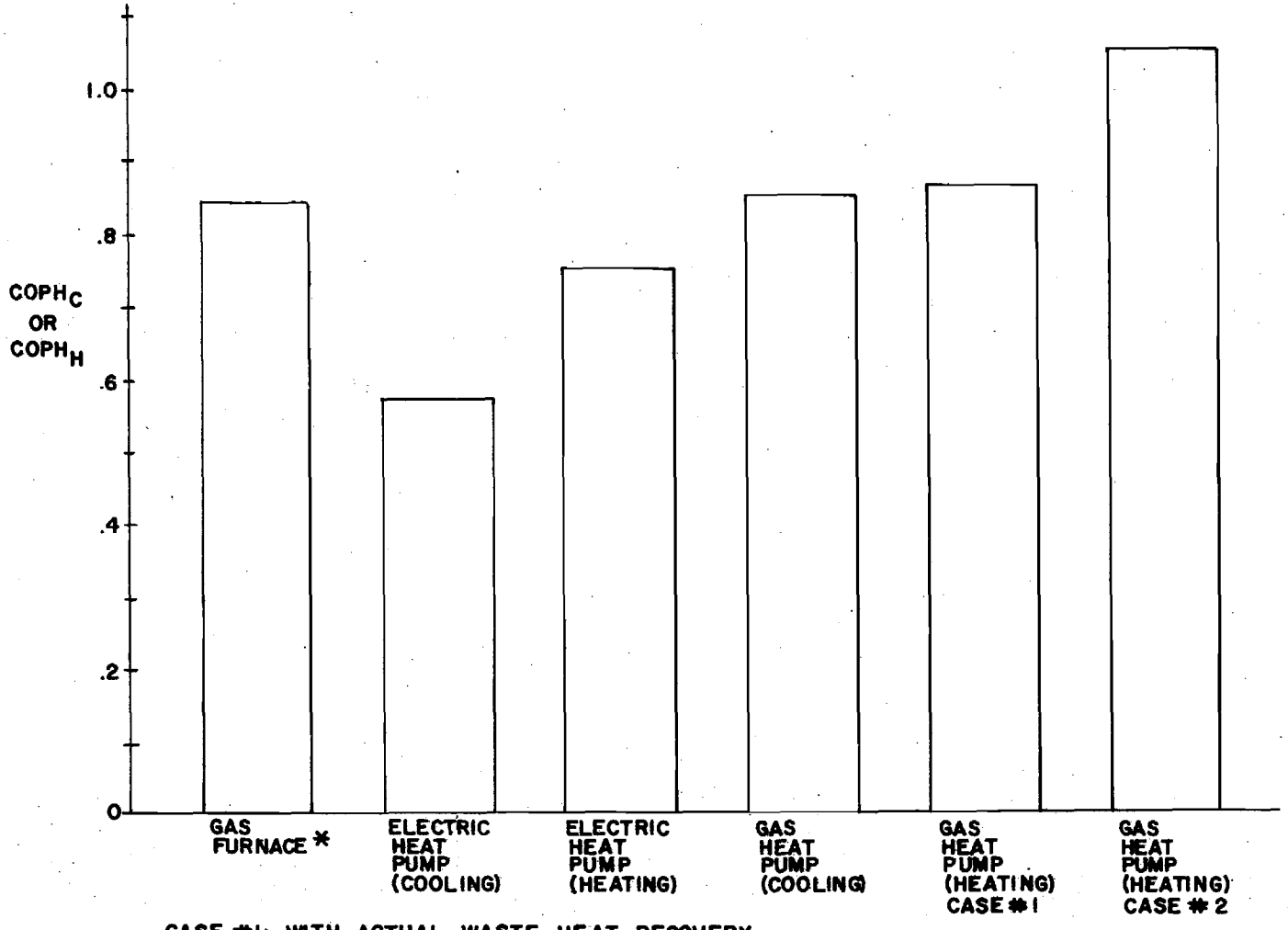

CASE #1: WITH ACTUAL WASTE HEAT RECOVERY

CASE #2: WITH WASTE HEAT RECOVERY ASSUMING AN INSULATED EXHAUST

FIGURE 34. COMPARISON OF COOLING AND HEATING COPH'S FOR ALTERNATE SYSTEMS (T_L=40°F, T_H=120°F); *SEE TABLE 16.

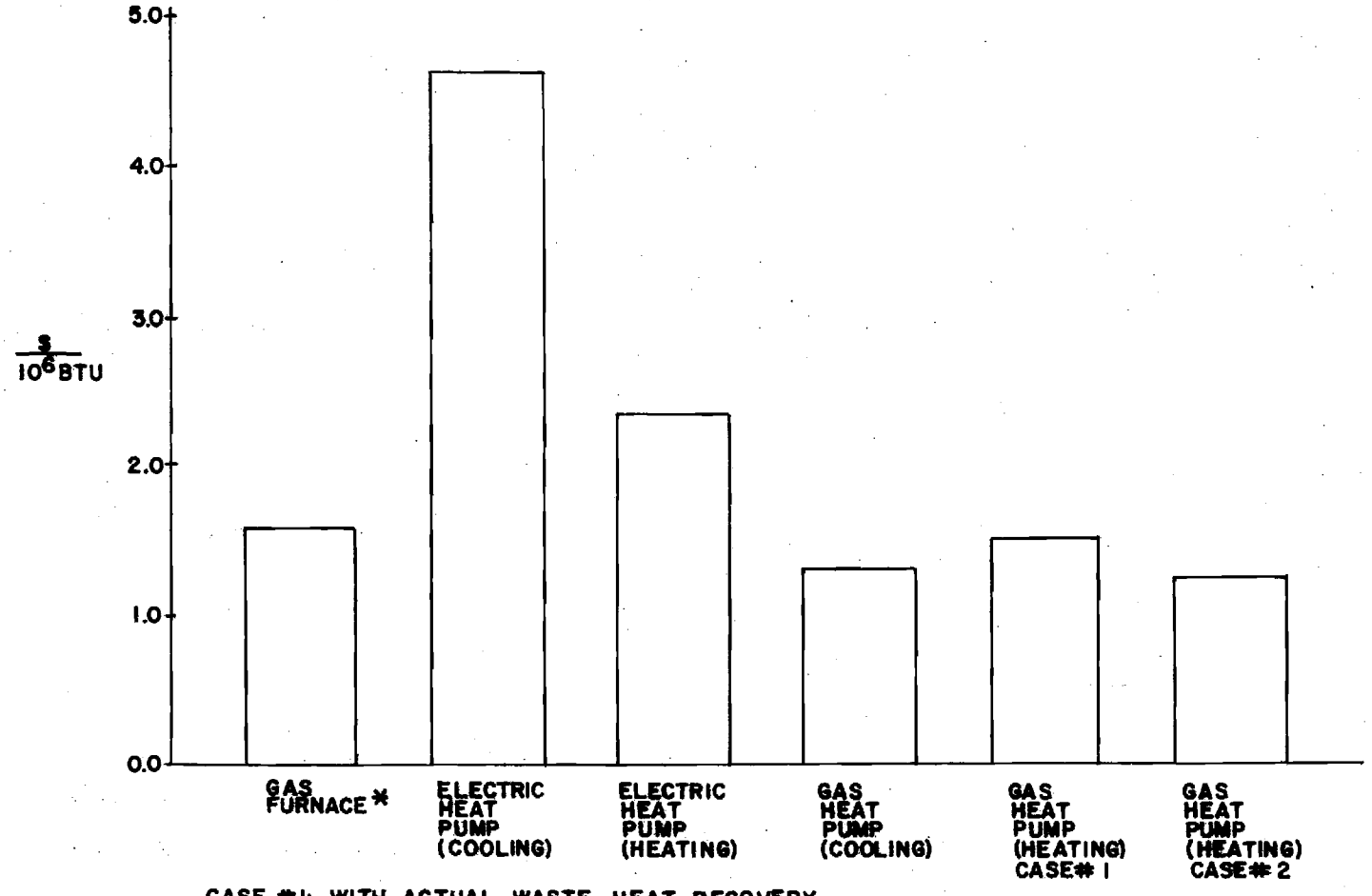

CASE #1: WITH ACTUAL WASTE HEAT RECOVERY

CASE #2: WITH WASTE HEAT RECOVERY ASSUMING AN INSULATED EXHAUST

FIGURE 35. ($/10^{6}BTU) COMPARISON OF ALTERNATE SYSTEMS (T_L = 40°F, T_H = 120°F); *SEE TABLE 16.

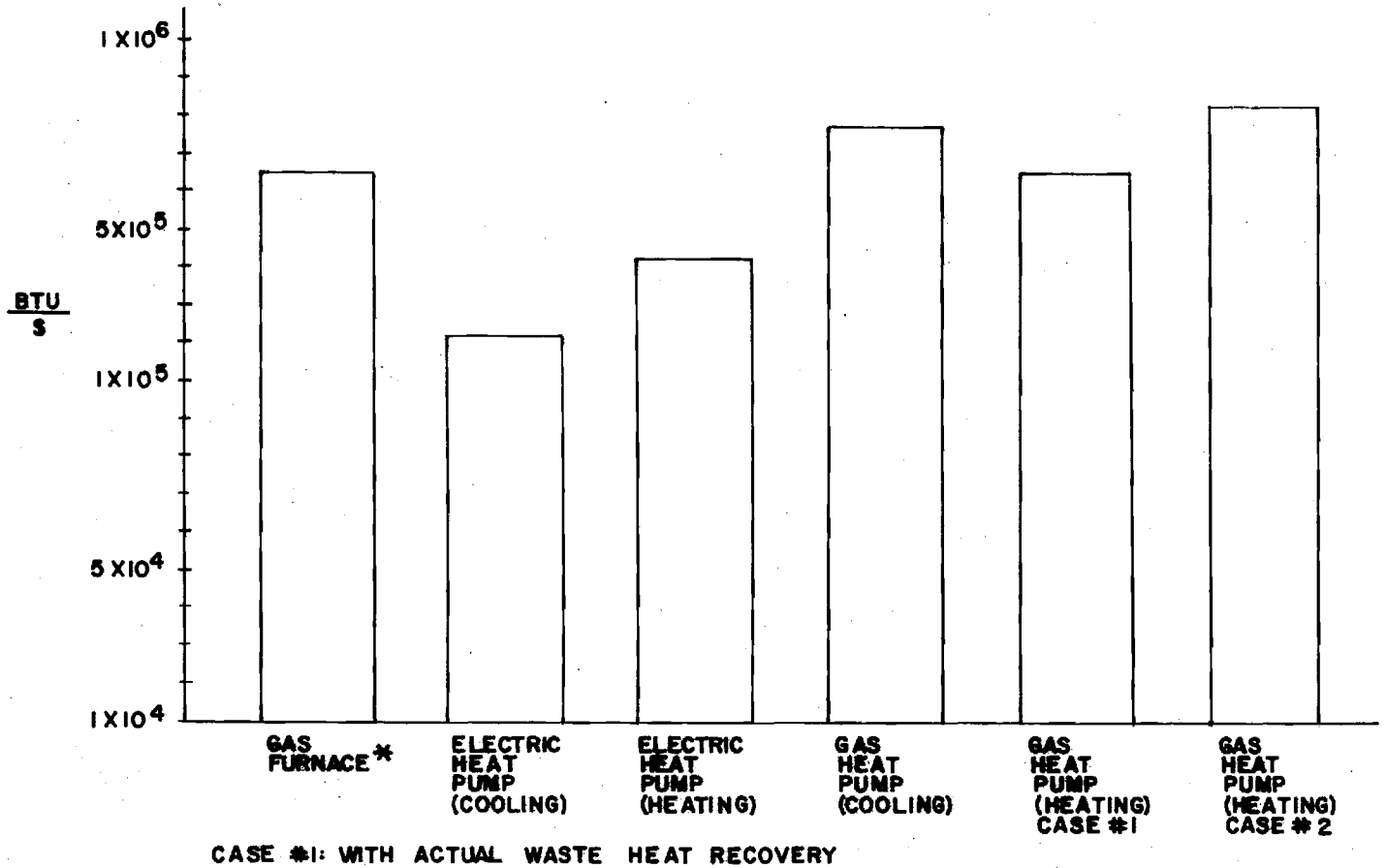

CASE #1: WITH ACTUAL WASTE HEAT RECOVERY

CASE #2: WITH WASTE HEAT RECOVERY ASSUMING AN INSULATED EXHAUST

FIGURE 36. (BTU/$) COMPARISON OF ALTERNATE SYSTEMS (T_L=40°F, T_H=120°F); *SEE TABLE 16.

T_L and T_H in the same manner as the heat pump systems. The values listed are simply the averages of its experimentally determined performance characteristics. Moreover, since it lacks a cooling mode, a true comparison between the gas furnace system and the other alternates cannot be made.

A comparison of COPH's at this particular operating condition shows the gas heat pump's COPH's to be significantly higher. In the cooling mode, the gas heat pump $COPH_C$ is about 49% greater than that of the electric heat pump. In the heating condition, the gas heat pump $COPH_H$ (with the actual waste heat recovery) is only about 2% greater than the gas furnace analyzed, but about 15% greater than the $COPH_H$ for the electric heat pump. If waste heat recovery assuming insulation is included, these values become approximately 25% greater than the gas furnace and 40% greater than the electrical system. Recall that the gas furnace analyzed here performed much better than a conventional gas furnace. Also, the electrical system values include allowance for power plant inefficiencies.

The consumer cost differential between the electric and gas systems would be even more favorable to the gas systems than these efficiency comparisons [1]. A comparison of $\$/10^6$ Btu and Btu/$ for the alternate systems would perhaps be more meaningful than COPH comparisons. These values were calculated using the parameters listed below which were confirmed by the appropriate Atlanta utilities.

Current Typical Atlanta Residential Rates

	Heating (winter)	Cooling (summer)
Electric	\$.02/KW-hr	\$.03/KW-hr
Gas	\$1.30/10^6Btu	\$1.10/10^6Btu

The cost per 10^6 Btu comparison produces some astounding results. For 10^6 Btu of cooling, using the above cost factors, the electric system cost is about 259% greater than the gas heat pump system cost. In the heating mode, the electric system cost is approximately 55% greater than that of the gas heat pump with actual waste heat recovery, and 89% greater than the gas system with waste heat recovery assuming an insulated exhaust. Similarly, the gas furnace shows a heating cost 3% greater and 21% greater than the gas heat pump with actual and insulated exhaust waste heat recovery, respectively.

To briefly summarize these comparisons, it appears that a natural gas-fueled Wankel engine-driven heat pump system could offer a dramatic reduction in energy consumption for residental heating and cooling, the two largest residential energy usages. In addition, the possible cost savings that might be realized are truly impressive.

Conclusions

This report has presented the results of a study of a gas furnace, an electric heat pump, and a natural

gas heat pump. Since the ultimate objective is to find a system that provides year-around environmental control for a home, (i.e. both cooling and heating), the comparison is essentially between the two heat pump systems. Reference [1] predicted a higher COPH for both cooling and heating for a natural gas-fueled Wankel engine-driven heat pump than for a similar system driven by an electric motor. The results of this report support that prediction.

These results should not be a startling revelation. An electric heat pump is a heat-actuated system that uses a Rankine heat engine at the generating plant to drive a refrigeration cycle through an electric motor at the dwelling [2]. A natural gas heat pump, on the other hand, employs a heat engine to drive a refrigeration cycle right at the point of use. It seems more logical to convert a fuel to sensible heat at its point of use, rather than convert it to another form of energy at a remote generating station and then reconvert it to sensible heat. Any electric system suffers from power plant inefficiencies as well as transmission losses.

An analysis was made in reference [6] of energy losses in natural gas and electrical transmission. The results are as follows. For short distances, approximately 10 to 20 miles, an average value of the electrical transmission efficiency, the ratio of energy out to energy in, is 95%. The losses, a 2% transmission line loss (I^2R loss)

and a 3% loss in transformers, are a function of the distribution system loading, which varies greatly during the course of a year. The energy losses in natural gas transmission pipelines, however, are much smaller. The average energy requirements for transporting natural gas short distances, approximately 100 miles, is approximately 2% of the energy delivered to the pipeline inlet. The transmission efficiency is therefore 98% for this case, while it is estimated to be 95% for longer distances.

Natural gas is one of our premium fossil fuels. It is clean burning, requires no refining, and is easily recovered and shipped with little or no detrimental environmental impact. A natural gas-fueled Wankel engine-driven heat pump can provide a very efficient method of home environmental control, thus satisfying a very important energy requirement, and also, conserving our natural gas resources. In addition, this system is quite compatible with the environment.

The possible consequences of this system are rather amazing. This experimental study supports the analysis by the American Gas Association showing that if natural gas heat pumps were available for installation beginning in 1976, the accumulative savings in natural gas would be about 12×10^{12} cubic feet by 1990 (or 3×10^{12} cubic feet annually) [1,16]. This is based on the assumption that only 40% of the raw heating unit market by 1990 will be made up of natural

gas heat pumps. The quantity of gas saved would be equivalent to that projected to be produced from coal gasification at a capital expenditure of about $16 billion [1,16].

A crisis in energy is one of the most important problems that this country, and indeed the world, faces at present. Unfortunately, this problem will not vanish by itself in time. Wise utilization of our natural resources is no longer a desired goal. At this point, it is an absolute necessity, making research in this area extremely important.

APPENDICES

APPENDIX A

SAMPLE CALCULATIONS FOR FIGURES 11, 12, 13, 14, 30, 31, 32, and 33

All thermodynamic properties were found in Freon 22 tables [17]. Refer to Figure 8 for the cycle considered in this analysis and the state point locations.

Assume $T_{evap} = 20°F$ and $T_{cond} = 80°F$; $\frac{T_L/T_H}{1-T_L/T_H} = 8.09$;

$\frac{1}{1-T_L/T_H} = 9.09$

$T_{evap} = 20°F = T_1 \quad \therefore h_1 = h_g = 106.383$ Btu/#m, $S_1 = S_g =$ .22379 Btu/#m°R

$T_{cond} = 80°F = T_3 \quad \therefore P_3 =$ saturation pressure at $T_3 = 158$PSIA

$h_3 = h_f = 33.109$ Btu/#m $= h_4$

Assume isentropic compression, $S_1 = S_2$

$S_2 = .22379$ Btu/#m°R and $P_2 = P_3 = 158$PSIA imply that $h_2 = 117.059$ Btu/#m

Electric Cooling: $COPW_c = \frac{\dot{Q}_{evap}}{\dot{W}} = \frac{\dot{m}(h_1-h_4)}{\dot{m}(h_2-h_1)} = \frac{(h_1-h_4)}{(h_2-h_1)}$

$$COPW_c = \frac{(106.383 - 33.109)\text{Btu/\#m}}{(117.059 - 106.383)\text{Btu/\#m}} = 6.86$$

Similarly, the other equations used are as follows:

Gas cooling: (assuming $\eta_{th} = .18$)

$$COPH_c = \frac{\eta_{th}\,\dot{Q}_{evap}}{\dot{W}} = \frac{\eta_{th}\,\dot{m}(h_1-h_4)}{\dot{m}(h_2-h_1)} = \frac{(.18)(h_1-h_4)}{(h_2-h_1)}$$

Electric heating:

$$COPW_H = \frac{\dot{Q}_{cond}}{\dot{W}} = \frac{\dot{m}(h_2-h_3)}{\dot{m}(h_2-h_1)} = \frac{(h_2-h_3)}{(h_2-h_1)}$$

Gas heating: (assuming $\eta_{th} = .18$, $F_{rec} = .60$)

$$COPH_H = \frac{\eta_{th}\,\dot{Q}_{cond}}{\dot{W}} + F_{rec}(1-\eta_{th}) = \frac{\eta_{th}\,\dot{m}(h_2-h_3)}{\dot{m}(h_2-h_1)} + F_{rec}(1-\eta_{th})$$

$$COPH_H = \frac{(.18)(h_2-h_3)}{(h_2-h_1)} + .49$$

These calculations were performed for nine sets of T_{evap} and T_{cond}.

In order to plot Figures 11, 12, 13, and 14, a relationship between the (T_L/T_H) parameter and COP was required. The following relations were formulated and solved for K_1 and K_2. The final values of K_1 and K_2 listed were, in each case, the average of the nine calculations performed.

Electric cooling: $COPW_c = K_1\left(\frac{T_L/T_H}{1-T_L/T_H}\right)$; $K_1 = .81$

Gas cooling: $COPH_c = K_1\left(\frac{T_L/T_H}{1-T_L/T_H}\right)$; $K_1 = .15$

Electric heating: $COPW_H = K_1\left(\frac{1}{1-T_L/T_H}\right)$; $K_1 = .83$

Gas heating: $COPH_H = K_1\left(\frac{1}{1-T_L/T_H}\right) + K_2$; $K_1 = .15$,

$K_2 = .49$

Similar calculations were performed to produce Figures 30, 31, 32, and 33. The only difference was the use of the actual experimentally measured cycle values instead of the ideal vapor-compression cycle values.

APPENDIX B

GAS FURNACE EXPERIMENTAL DATA

(The values tabulated below are the averages of three tests.) All temperatures are in °F.

	Low Heat Low Fan	Low Heat High Fan	High Heat Low Fan	High Heat High Fan
T9	152.3	138.3	191.3	165.0
T10	138.0	123.7	166.3	144.7
T11	123.3	108.7	149.0	126.0
T12	81.3	86.3	90.0	95.0
T13	83.0	88.0	93.3	94.7
T14	83.7	87.3	93.7	93.7
TE1	243.3	235.0	321.7	300.0
Water Flow Rate, (Gal/Min)	8.7	8.6	6.6	7.9
Gas Input, (Ft^3/Min)	1.2	1.2	1.5	1.5
Electric Input, (KW)	.37	.72	.41	.76

Sample η Calculation

For the case of low heat and low fan:

All ρ(density) values were taken from reference [18] and were considered to be the density at the average water temperature.

The heating value of the natural gas used was assumed to be 1,030 Btu/ft^3.

$$\eta = \frac{\dot{m}_w \, \Delta T_w \, C_{pw}}{\dot{Q}_{gas}} \tag{46}$$

$$\dot{m}_w = \dot{V}\rho = (8.65 \frac{gal}{min})(\frac{1 \; ft^3}{7.4805 \; gal})(\frac{61.29 \; \#m}{ft^3}) = 70.87 \frac{\#m}{min}$$

$$\Delta T_w = T_9 - T_{10} = (152.3 - 138.0)°F = 14.3°F$$

$$\dot{Q}_{gas} = \dot{V}(\text{heating value of gas}) = (\frac{1.2 \; ft^3}{min})(1{,}030 \frac{Btu}{ft^3}) =$$

$$1236.0 \frac{Btu}{min}$$

$$\eta = \frac{(70.87 \frac{\#m}{min})(14.3°F)(1 \frac{Btu}{\#m°F})}{1236.0 \frac{Btu}{min}} = .803$$

$$\eta = 80.3\%$$

APPENDIX C

ELECTRIC HEAT PUMP ANALYSIS

Electric Heat Pump Cooling Cycle Data

Eight tests were conducted. All temperatures are in °F and all pressures are in PSIG.

	Test #1	Test #2	Test #3	Test #4	Test #5	Test #6	Test #7	Test #8
T1	42	28	17	58	25	18	20	28
T2	190	180	168	216	216	186	192	216
T3	41	22	9	42	21	6	16	26
T4	50	30	16	51	31	15	23	29
T5	70	59	52	75	60	50	60	62
T6	48	26	15	52	30	16	19	29
T7	80	80	80	86	83	80	90	90
T8	192	180	165	215	216	188	189	211
T17	195	180	170	210	215	195	200	215
P1	57	40	28	62	34	28	30	40
P2	265	233	209	282	229	215	255	258
P3	252	230	205	280	226	206	250	252
P4	57	40	28	62	36	28	30	40
P5	80	58	39	85	58	40	45	55
P6	248	230	204	278	226	202	243	252
P7	252	230	205	280	228	202	250	252
Freon Flow Rate (gal/min)	1.18	0.66	0.56	1.18	0.62	0.50	0.56	0.60
Electric Input (KW)	7.85	6.32	5.76	8.79	6.32	5.76	5.89	6.65

The following thermocouples were installed to measure air temperatures at various points in and around the system: T11, T12, T13, T14, T15, and T16. Since they were installed primarily as a check and were not used in any of the calculations presented in this thesis, these values are not tabulated here.

Sample Calculations for Capacity and $COPW_C$

The calculations presented below were made for test #1. Thermodynamic properties were taken from reference [17]. Subcooled liquid properties were approximated by saturated liquid properties at that temperature. Enthalpy changes (Δh) were taken directly from a Pressure-Enthalpy Diagram (C-1) in reference [17].

$$T_7 = 80°F, \quad \text{thus} \quad V_f = .013492 \ ft^3/\#m$$

$$\dot{V}\left(\frac{ft^3}{hr}\right) = \left(1.18 \frac{gal}{min}\right)\left(60 \frac{min}{hr}\right)\left(\frac{1 \ ft^3}{7.4805 \ gal}\right) = 9.5 \frac{ft^3}{hr}$$

$$\dot{m}\left(\frac{\#m}{hr}\right) = \frac{\dot{V}}{V_f} = \frac{9.5 \ ft^3/hr}{.013492 \ ft^3/\#m} = 704.12 \frac{\#m}{hr}$$

$$\text{Capacity } \left(\frac{Btu}{hr}\right) = \dot{Q}_{evap} = \dot{m}(h_1 - h_4)$$

$$\text{Capacity} = \left(704.12 \frac{\#m}{hr}\right)(109-34)\frac{Btu}{\#m} = \left(5.28 \times 10^4 \frac{Btu}{hr}\right)\left(\frac{hr \ ton}{12{,}000 \ Btu}\right)$$

$$= (4.40 \text{ tons})$$

$$\dot{E}\left(\frac{Btu}{hr}\right) = (7.85\ kw)\left(\frac{56.89\ Btu}{min\ kw}\right)\left(\frac{60\ min}{hr}\right) = 2.68x10^4\ \frac{Btu}{hr}$$

$$COPW_c = \frac{\dot{Q}_{evap}}{\dot{E}} = \frac{5.28x10^4\ Btu/hr}{2.68x10^4\ Btu/hr} = (1.97)$$

Electric Heat Pump Heating Cycle Data

Four tests were conducted. All temperatures are in °F and all pressures are in PSIG.

	Test #1	Test #2	Test #3	Test #4
T1	74	73	56	50
T2	204	220	215	206
T3	201	214	208	201
T4	122	102	98	102
T5	116	97	90	90
T6	82	74	65	64
T7	74	69	58	48
T8	71	66	48	36
T17	220	244	238	226
P1	123	115	72	60
P2	345	370	342	314
P3	338	368	335	311
P4	337	366	333	310
P5	320	357	323	300
P6	129	121	96	81
P7	123	115	86	64
Freon Flow Rate, (gal/min)	1.62	1.58	1.40	1.03
Electric Input, (KW)	9.97	10.80	10.80	9.09

The following thermocouples were installed to measure air temperatures at various points in and around the system: T11, T12, T13, T14, T15, and T16. Since they were installed primarily as a check and were not used in any of the calculations presented in this thesis, these values are not tabulated here.

Sample Calculations for Capacity and $COPW_H$

The calculations presented below were made for test #1. Thermodynamic properties were taken from reference [17]. Subcooled liquid properties were approximated by saturated liquid properties at that temperature. Enthalpy changes (Δh) were taken directly from a Pressure-Enthalpy Diagram (C-1) in reference [17].

$$T_4 = 122°F, \quad \text{thus} \quad v_f = .014768 \ ft^3/\#m$$

$$\dot{V}\left(\frac{ft^3}{hr}\right) = \left(1.62 \ \frac{gal}{min}\right)\left(\frac{60 \ min}{hr}\right)\left(\frac{1 \ ft^3}{7.4805 \ gal}\right) = 13.0 \ \frac{ft^3}{hr}$$

$$\dot{m}\left(\frac{\#m}{hr}\right) = \frac{\dot{V}}{v_f} = \frac{13.0 \ ft^3/hr}{.014768 \ ft^3/\#m} = 880.96 \ \frac{\#m}{hr}$$

$$\text{Capacity } \left(\frac{Btu}{hr}\right) = \dot{Q}_{cond} = \dot{m}(h_2 - h_3)$$

$$\text{Capacity} = \left(880.96 \ \frac{\#m}{hr}\right)(132-45) \ \frac{Btu}{\#m} = \left(7.66 \times 10^4 \ \frac{Btu}{hr}\right)$$

$$\dot{E} = (9.97 \text{ kw})\left(\frac{56.89 \text{ Btu}}{\text{min kw}}\right)\left(\frac{60 \text{ min}}{\text{hr}}\right) = 2.68\text{x}10^{4} \frac{\text{Btu}}{\text{hr}}$$

$$COPW_{H} = \frac{\dot{Q}_{cond}}{\dot{E}} = \frac{7.66\text{x}10^{4} \text{ Btu/hr}}{3.40\text{x}10^{4} \text{ Btu/hr}} = (2.25)$$

APPENDIX D

GAS HEAT PUMP ANALYSIS

Gas Heat Pump Cooling Cycle Data

Three tests were conducted. All temperatures are in °F and all pressures are in PSIG.

	Test #1	Test #2	Test #3
T1	90	85	85
T2	192	186	190
T3	68	76	74
T4	41	52	56
T5	82	88	110
T6	47	54	62
T7	94	100	118
T8	187	183	187
TE1	172	170	165
TE2	1170	1175	1172
TE3	1758	1770	1760
P1	66	82	83
P3	211	235	297
P4	66	80	86
P5	71	86	93
P6	197	210	265
P7	208	231	292
Freon Flow Rate, (gal/min)	1.75	3.11	2.96
Natural Gas Flow Rate, (ft^3/min)	1.95	2.13	2.11
Electric Input, (KW)	1.85	1.85	1.85

The following thermocouples were installed to measure air temperatures at various points in and around the system: T11, T12, T13, T14, T15, and T16. Since they were installed primarily as a check and were not used in any of the calculations presented in this thesis, these values are not tabulated here. The exhaust temperatures were recorded, but the waste heat recovery calculation was not included in this case, of course, since the desired effect is cooling.

Sample Calculations for Capacity and $COPH_c$

The calculations presented below were made for test #1. Thermodynamic properties were taken from reference [17]. Subcooled liquid properties were approximated by saturated liquid properties at that temperature. Enthalpy changes (Δh) were taken directly from a Pressure-Enthalpy Diagram (C-1) in reference [17].

$$T_7 = 94°F, \quad \text{thus} \quad v_f = .013864 \ ft^3/\#m$$

$$\dot{V}\left(\frac{ft^3}{hr}\right) = \left(1.75 \frac{gal}{min}\right)\left(\frac{60 \ min}{hr}\right)\left(\frac{1 \ ft^3}{7.4805 \ gal}\right) = 14.05 \frac{ft^3}{hr}$$

$$\dot{m}\left(\frac{\#m}{hr}\right) = \frac{\dot{V}}{v_f} = \frac{14.05 \ ft^3/hr}{.013864 \ ft^3/\#m} = 1{,}013.50 \frac{\#m}{hr}$$

$$\text{Capacity } \left(\frac{Btu}{hr}\right) = \dot{Q}_{evap} = \dot{m}(h_1 - h_4)$$

$$\text{Capacity} = (1{,}013.50\ \tfrac{\#m}{hr})(116.5-36)\tfrac{Btu}{\#m} = (8.16\text{x}10^4\ \tfrac{Btu}{hr})$$

$$(\frac{hr\ ton}{12{,}000\ Btu}) = 6.80\ tons$$

$$\dot{G}(\tfrac{Btu}{hr}) = \dot{V}(\tfrac{ft^3}{hr})(\text{heating value of natural gas, Btu/ft}^3)$$

Assume the heating value of methane to be 1,030 Btu/ft^3.

$$\dot{G} = (1.95\ \tfrac{ft^3}{min})(\tfrac{60\ min}{hr})(1{,}030\ \tfrac{Btu}{ft^3}) = 1.21\text{x}10^5\ \tfrac{Btu}{hr}$$

$$COPH_c = \frac{\dot{Q}_{evap}}{\dot{G}} = \frac{8.16\text{x}10^4\ Btu/hr}{1.21\text{x}10^5\ Btu/hr} = (.674)$$

Gas Heat Pump Heating Cycle Data

Four tests were conducted. All temperatures are in °F and all pressures are in PSIG.

	Test #1	Test #2	Test #3	Test #4
T1	104	106	102	92
T2	219	219	222	211
T3	183	190	186	186
T4	92	92	93	112
T5	88	86	85	104
T6	52	51	52	68
T7	68	65	66	58
T8	90	88	85	76
T9	114	113	115	124
T10	106	106	108	118
TE1	175	165	172	182
TE2	1190	1160	1175	1156
TE3	1680	1705	1705	1657
P1	103	93	94	85
P3	210	198	211	260
P4	206	196	206	255
P5	195	186	197	241
P6	115	110	113	98
P7	107	99	104	90
Water Flow Rate, (gal/min)	8.11	8.11	8.11	8.11
Freon Flow Rate, (gal/min)	1.62	1.40	1.58	1.71
Natural Gas Flow Rate, (ft^3/min)	1.85	1.68	1.71	2.03
Electric Input, (KW)	1.85	1.85	1.85	1.85

The following thermocouples were installed to measure air temperatures at various points in and around the system: T11, T12, T13, T14, T15, and T16. Since they were installed primarily as a check and were not used in any of the calculations presented in this thesis, these values are not tabulated

here.

Sample Calculations for Capacity and $COPH_H$

The calculations presented below were made for test #1. Thermodynamic properties were taken from reference [17]. Subcooled liquid properties were approximated by saturated liquid properties at that temperature. Enthalpy changes (Δh) were taken from a Pressure-Enthalpy Diagram (C-1) in reference [17].

$$T_4 = 92°F, \quad \text{thus} \quad v_f = .013809 \ ft^3/\#m$$

$$\dot{V}\left(\frac{ft^3}{hr}\right) = \left(1.62 \frac{gal}{min}\right)\left(\frac{60 \ min}{hr}\right)\left(\frac{1 \ ft^3}{7.4805 \ gal}\right) = 13.0 \frac{ft^3}{hr}$$

$$\dot{m}\left(\frac{\#m}{hr}\right) = \frac{\dot{V}}{v_f} = \frac{13.0 \ ft^3/hr}{.013809 \ ft^3/\#m} = 942.14 \frac{\#m}{hr}$$

$$\text{Capacity } \left(\frac{Btu}{hr}\right) = \dot{Q}_{cond} = \dot{m}(h_2 - h_3)$$

$$\text{Capacity} = \left(942.14 \frac{\#m}{hr}\right)(136-36) \frac{Btu}{\#m} = 9.42 \times 10^4 \frac{Btu}{hr}$$

$$\dot{G}\left(\frac{Btu}{hr}\right) = \dot{V}\left(\frac{ft^3}{hr}\right)\left(\text{heating value of natural gas, } \frac{Btu}{ft^3}\right)$$

Assume the heating value of methane to be $1{,}030 \frac{Btu}{ft^3}$.

$$\dot{G} = (1.85 \frac{ft^3}{min})(\frac{60 \text{ min}}{hr})(1,030 \frac{Btu}{ft^3}) = 1.14x10^5 \frac{Btu}{hr}$$

$$COPH_H = \frac{\dot{Q}_{cond}}{\dot{G}} = \frac{9.42x10^4 \text{ Btu/hr}}{1.14x10^5 \text{ Btu/hr}} = .83 \quad \text{without waste heat recovery}$$

Sample Calculation of Waste Heat Recovery

Sample calculation of actual waste heat recovery:

$$\dot{Q}_{rec} = \dot{m}_w \Delta T_w C_{pw} \tag{47}$$

$$T_9 = 114°F, \quad T_{10} = 106°F, \quad \Delta T_w = T_9 - T_{10} = 8°F$$

The average temperature = 110°F which implies, from reference [18], that $\rho_w = 61.86$ #m/ft^3.

$$\dot{m} = \rho\dot{V} = (61.86 \frac{\#m}{ft^3})(65.03 \frac{ft^3}{hr}) = 4,022.76 \frac{\#m}{hr}$$

$$\dot{Q}_{rec} = (4,022.76 \frac{\#m}{hr})(8°F)(\frac{1 \text{ Btu}}{\#m \ °F}) = 32,182.08 \frac{Btu}{hr}$$

$$\dot{Q}_{rec} = 32,182.08 \frac{Btu}{hr}$$

For gas heat pump heating cycle test #1:

$$COPH_H = \frac{\dot{Q}_{cond} + \dot{Q}_{rec}(actual)}{\dot{G}} = \frac{(9.42x10^4 + 32,182.08)Btu/hr}{1.14x10^5\ Btu/hr}$$

$$= 1.11$$

$COPH_H = 1.11$ with the actually measured waste heat recovery

Sample Calculation of Possible Waste Heat Recovery

The following calculation is based on the premise that the Wankel engine exhaust pipe can be insulated such that the heat loss will be minimized. The actual heat recovery is based on a temperature difference of (1175°F-170°F = 1005°F). Since the temperature of the exhaust gases at the combustion chamber outlet was measured to be as high as 1770°F, the following calculation gives an indication of the performance improvement possible with appropriate exhaust pipe insulation. The temperature difference considered is (1770°F-170°F = 1600°F). Assuming a stoichiometric methane combustion reaction,

$$CH_4 + 2O_2 + 2(3.76)N_2 \rightarrow CO_2 + 2H_2O + 7.52N_2$$

and using Table A.7 in reference [15] for the products of combustion,

$$CO_2: \quad C_{po}\left(\frac{Btu}{\#mole°R}\right) = 16.2 - \frac{6.53x10^3}{T} + \frac{1.41x10^6}{T^2}$$

$$H_2O: \quad C_{po}\left(\frac{Btu}{\#mole°R}\right) = 19.86 - \frac{597}{\sqrt{T}} + \frac{7500}{T}$$

$$N_2: \quad C_{po}\left(\frac{Btu}{\#mole°R}\right) = 9.47 - \frac{3.47x10^3}{T} + \frac{1.16x10^6}{T^2}$$

a comparison between the actual heat recovery and the heat recovery that ideally could be achieved with an insulated exhaust can be performed.

$$CO_2: \quad dh = \int_{T=630°R}^{T=2230°R} Cp\, dT = (1.93x10^4 \frac{Btu}{\#mole})(\frac{44\#mole}{\#m}) = 8.49x10^5 \frac{Btu}{\#m}$$

$$CO_2: \quad dh = \int_{T=630°R}^{T=1635°R} Cp\, dT = (1.14x10^4 \frac{Btu}{\#mole})(\frac{44\#mole}{\#m}) = 5.02x10^5 \frac{Btu}{\#m}$$

$$H_2O: \quad dh = \int_{T=630°R}^{T=2230°R} Cp\, dT = (1.49x10^4 \frac{Btu}{\#mole})(\frac{18\#mole}{\#m}) = 2.68x10^5 \frac{Btu}{\#m}$$

$$H_2O: \quad dh = \int_{T=630°R}^{T=1635°R} Cp\, dT = (8.90x10^3 \frac{Btu}{\#mole})(\frac{18\#mole}{\#m}) = 1.60x10^5 \frac{Btu}{\#m}$$

$$N_2: \quad dh = \int_{T=630°R}^{T=2230°R} Cp\, dT = (1.21x10^4 \frac{Btu}{\#mole})(\frac{28\#mole}{\#m}) = 3.39x10^5 \frac{Btu}{\#m}$$

$$N_2: \quad dh = \int_{T=630°R}^{T=1635°R} Cp\ dT = (7.39x10^3\ \frac{Btu}{\#mole})(\frac{28\#mole}{\#m}) = 2.07x10^5\ \frac{Btu}{\#m}$$

The enthalpy change of the mixture was calculated as follows:

$$dh_{mixture} = \frac{\sum_{i=1}^{3} dh_i\ M_i}{M_{mixture}} \qquad (50)$$

where:

M = mass

i refers to the ith component

$$(8.49x10^{5}\frac{Btu}{\#m})(1\ mole\ CO_2)(\frac{44\#m}{mole}) + (2.68x10^{5}\frac{Btu}{\#m})$$

$$(2\ moles\ H_2O)(\frac{18\#m}{mole}) + (3.39x10^{5}\frac{Btu}{\#m})(7.52molesN_2)$$

$$dh_{\substack{mixture \\ (2230°R)}} = \frac{(\frac{28\#m}{mole})}{(1moleCO_2)(\frac{44\#m}{mole}) + (2molesH_2O)(\frac{18\#m}{mole}) + (7.52molesN_2)(\frac{28\#m}{mole})}$$

$$dh_{\substack{mixture \\ (2230°R)}} = 4.07x10^5\ \frac{Btu}{\#m}$$

$$dh_{\substack{\text{mixture}\\(1635°R)}} = \frac{(5.02\times10^{5}\frac{Btu}{\#m})(1\ \text{mole}\ CO_2)(\frac{44\#m}{\text{mole}}) + (1.60\times10^{5}\frac{Btu}{\#m})(2\text{moles}H_2O)(\frac{18\#m}{\text{mole}}) + (2.07\times10^{5}\frac{Btu}{\#m})(7.52\text{moles}N_2)(\frac{28\#m}{\text{mole}})}{(1\text{mole}CO_2)(\frac{44\#m}{\text{mole}}) + (2\text{moles}H_2O)(\frac{18\#m}{\text{mole}}) + (7.52\text{moles}N_2)(\frac{28\#m}{\text{mole}})}$$

$$dh_{\substack{\text{mixture}\\(1635°R)}} = 2.46\times10^{5}\ \frac{Btu}{\#m}$$

$$\frac{\dot{Q}_{rec}(\text{insulated exhaust})}{\dot{Q}_{rec}(\text{actual})} = \frac{\eta_{ex}\dot{m}_{ex}\int_{T=630°R}^{T=2230°R} Cp\ dT}{\eta_{ex}\dot{m}_{ex}\int_{T=630°R}^{T=1635°R} Cp\ dT} = \frac{dh_{\text{mixture}(2230°R)}}{dh_{\text{mixture}(1635°R)}} = 1.65$$

$$\dot{Q}_{rec}(\text{insulated exhaust}) = 1.65\ \dot{Q}_{rec}(\text{actual})$$

$$\dot{Q}_{rec}(\text{actual}) = 32{,}182.08\ \text{Btu/hr}$$

$$\dot{Q}_{rec}(\text{insulated exhaust}) = 53{,}100.43\ \text{Btu/hr}$$

For gas heat pump heating cycle test #1:

$$COPH_H = \frac{\dot{Q}_{cond} + \dot{Q}_{rec}(\text{insulated exhaust})}{\dot{G}}$$

$$= \frac{(9.42\times10^{4} + 53{,}100.43)\text{Btu/hr}}{1.14\times10^{5}\ \text{Btu/hr}} = 1.29$$

$COPH_H = 1.29$ with the ideal insulated exhaust waste heat recovery

APPENDIX E

SAMPLE CALCULATIONS FOR FIGURES 35 AND 36

Electric cooling: From Figure 30 at $T_L = 40°F = 500°R$ and $T_H = 120°F = 580°R$ or $\frac{T_L/T_H}{1-T_L/T_H} = 6.14$, $COPW_c = 1.90$
using a cost factor of \$.03/KW-hr,

$$(\frac{1}{1.90})(\frac{\$.03}{kw\text{-}hr})(\frac{kw\text{-}hr}{3413.40Btu})(\frac{10^6}{10^6}) = (\frac{4.63}{10^6 Btu})$$

or taking the reciprocal:

$$\frac{10^6 Btu}{\$4.63} = (\frac{2.16x10^5 Btu}{\$})$$

Gas heating (without waste heat recovery): From Figure 33 at $T_L = 40°F = 500°R$ and $T_H = 120°F = 580°R$ or $\frac{1}{1-T_L/T_H} = 7.14$, $COPH_H = .57$
using a cost factor of $\$1.30/10^6$ Btu,

$$(\frac{1}{.57})(\frac{\$1.30}{10^6 Btu}) = (\frac{\$2.28}{10^6 Btu})$$

or taking the reciprocal:

$$\frac{10^6 Btu}{\$2.28} = (\frac{4.39x10^5 Btu}{\$})$$

APPENDIX F

COMMERCIAL UNIT CONDENSER AND EVAPORATOR SPECIFICATIONS

STANDARD

SHELL and TUBE CC

SHELL AND TUBE CLEANABLE CONDENSERS

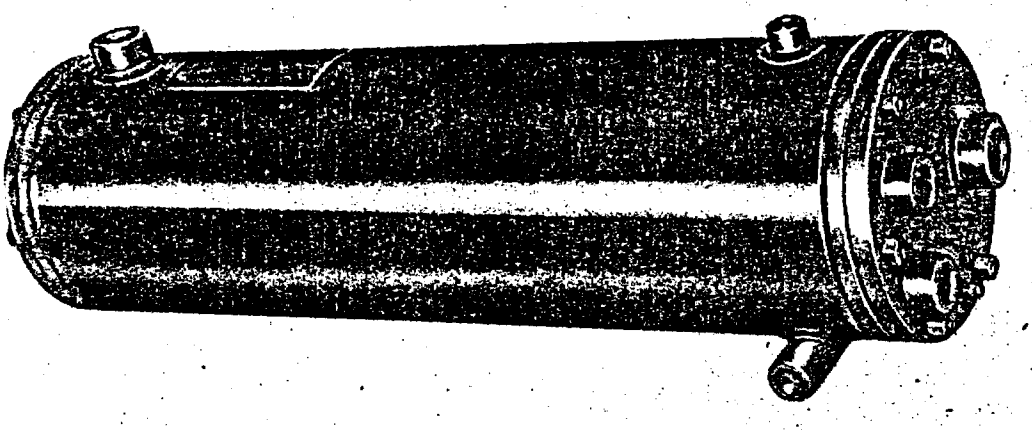

SPECIFICATIONS

Model No.	Nom'l HP	Dimensions Inches D	L	A	F. P. T. Inches P	Q	S	W	T	Pumpdown R 12 Lbs.	R 502 Lbs.	R 22 Lbs.	Water Pressure Drop psi 1-1/2 GPM	3 GPM	Gaskets Water & Return	Fig.	Ship Wt. Lbs.
SST-1000	10	8-5/8	48-1/2	3-1/4	1-1/4	3/4*	1/2	1	1-1/4	62	58	55	6.0	3.2	4408	13	160
SST-1500	15	8-5/8	55-3/4	3-1/4	1-1/2	1*†	1/2	1-1/4	1-1/2	66	62	60	10	5.5	4408	13	180
SST-1555	15	10-3/4	54	4-1/4	1-5/8S	1*†	1/2	1-1/4	1-1/2	112	106	100	7	4.2	6608	13	230
SST-2005	20	10-3/4	63	4-1/4	2-1/8S	1*†	1/2	1-1/2	2	115	109	103	5.5	3.3	6608	13	270
SST-2026	20	12-3/4	63	4-1/4	2-1/8S	1*†	1/2	1-1/2	2	158	149	142	5.5	3.3	6608	13	337
SST-2505	25	10-3/4	66	4-1/4	2-1/8S	1-1/4*†	1/2	1-1/2	2	118	111	106	6.2	3.7	6608	13	305
SST-2527	25	12-3/4	66	4-1/4	2-1/8S	1-1/4*†	1/2	1-1/2	2	162	153	146	6.2	3.7	6608	13	381
SST-3005	30	10-3/4	70-1/4	4-1/4	2-3/8S	1-1/4*†	1/2	1-1/2	2	121	114	109	8.5	5.1	6608	13	350
SST-3028	30	12-3/4	70-1/4	4-1/4	2-3/8S	1-1/4*†	1/2	1-1/2	2	166	157	150	8.5	5.1	6608	13	438

*Bottom Tangential Fitting.

† MPT

** Liquid outlet is shown on left side facing water plate. If right side outlet is required specify with order.

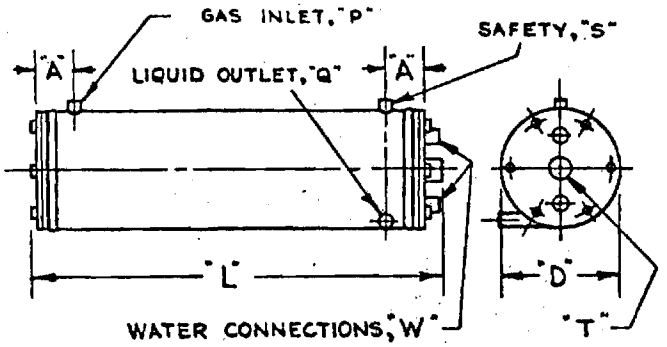

FIG. 13

SURFACE AND WATER FLOW DATA

Model	Total Cond. Surface Sq. Ft.	Maximum Water Flow GPM City	Tower
SST 1000	56.5	20.0	40.0
SST 1500	80.5	25.0	50.0
SST 1555	83.9	30.0	60.0
SST 2005, 2026	120	42.0	84.0
SST 2505, 2527	146	50.0	100.0
SST 3005, 3028	169	50.0	100.0

MAXIMUM WATER FLOW RATES

Standard Water Cooled Condensers

The water flows tabulated below are for seven feet per secon water velocity through the tubes, which is the maximur velocity suggested to avoid the possibility of impingemer corrosion and consequent tube failures.

DENSERS 10 to 30 HP

CONDENSER PERFORMANCE

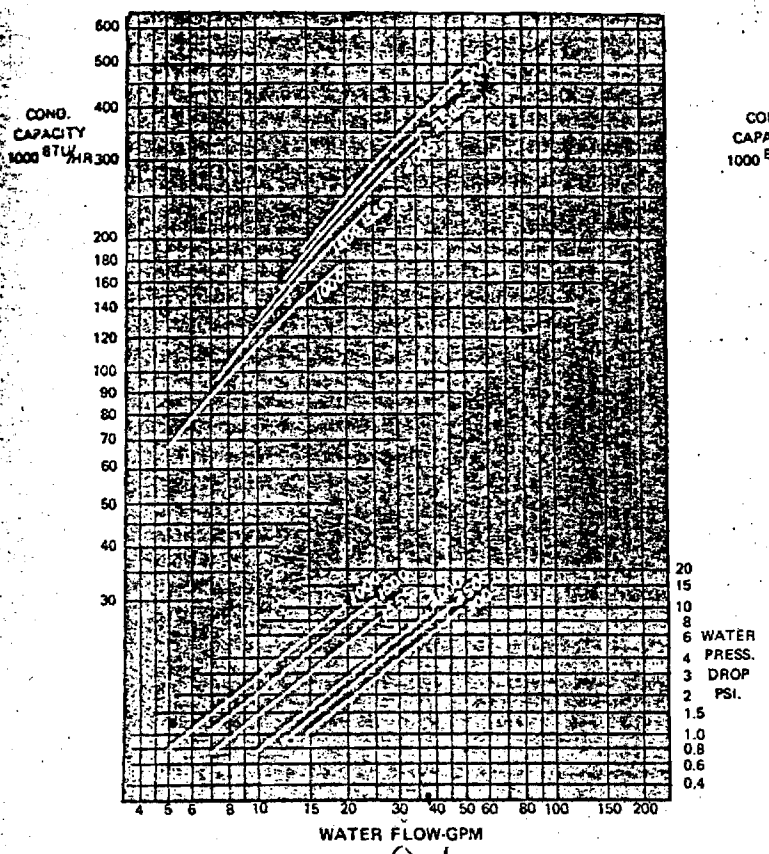

CONDENSER PERFORMANCE

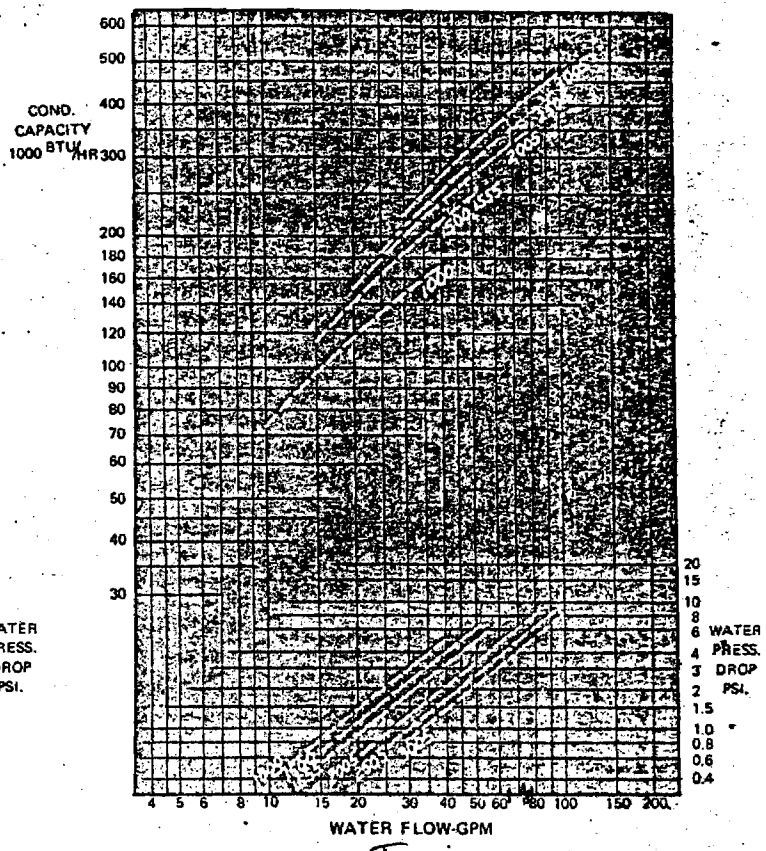

GASKET INSTALLATION INSTRUCTIONS

PREPARATION

The tube sheet, gasket faces, and studs must be wiped clear of all loose particles. If the threads have been damaged, they should be re-run with a 1/2 - 20 die, or a thread-cleaning nut. One or two drops of oil should be put on each stud.

MOUNTING

1. Slip gasket over studs, with gasket ridge(s) or notch(es) aligned with the corresponding punch marks on the tube sheet. The side of the gasket with the sealing ridge goes against the tube sheet, the smooth side always faces out. Never force a gasket over the studs on any other position; water flow and hence condensing performance will be impaired or completely blocked.

2. Slip the outer plate over the studs, with the alignment marks on the edge of the plate corresponding to the gasket ridge(s) or notch(es).

3. Tap the plate with a mallet or block of wood to seat the gasket and plate in position.

4. Turn the nuts down snug with the fingers.

TIGHTENING

1. With a torque wrench:
Tighten nuts in rotation, approximately one-third turn at a time, to a torque between 30 and 35 lb-ft. (If an impact-type tool is used, extreme care is required to avoid over-tightening the nuts. Note the drawings below.)

2. By hand:
Tighten nuts in rotation, 1/4 turn at a time. Note the drawings below. A total of 3/4 to 1 turn will be required with a new gasket; a total of 1/2 to 3/4 turn when replacing a used gasket.

NOTE:
Watch the side of the gasket when tightening the nuts.
A slight bulge only is more than ample to seal over 70 psi water pressure.
Even at this point, the nuts will not, and should not, feel tight.

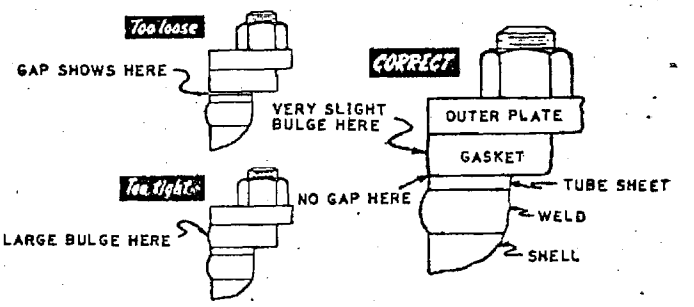

'CH' INNER-FIN WATER CHILLERS

Single Circuit Models

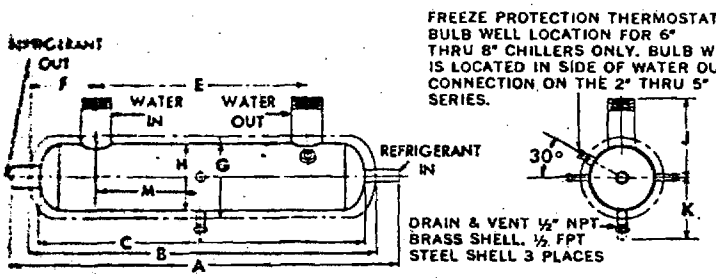

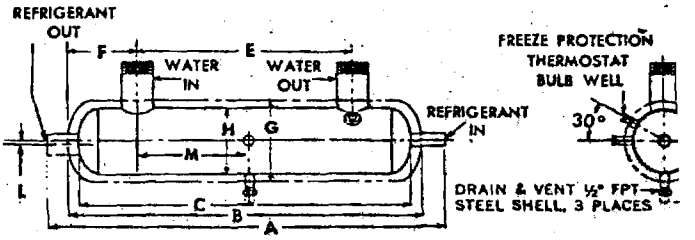

Nominal 1.5 thru 50 Ton Models

Nominal 60 thru 115 Ton Mod

NOM.* TONS	MODEL	A	B	C	E	F	G STD. INSULATION	G HEAVY INSULATION	H	J	K	L	M	W-IN W-OUT O.D.S. (NPT)	R-IN O.D. (I.D.)	R-OUT O.D. (I.D.)	VOL. OF SPACE IN SHELL GALS.	MIN. LBS. REFRIG. CHG.	TOTAL INS., WGTS. WITH WATER LBS.	S W I
1.5	CH224	35⅜	31⅜	29⅛	23⅛	4⅛	4½	5⅜	2⅜	7⅛	4	—	11⅜	⅞	⅜	1⅛	.20	1.0	40	
2	CH324	34⅜	30½	29⅛	22⅜	3⅞	5⅛	6⅞	3	6⅞	4 15/16	—	11⅜	1⅛	⅝	1¼	.30	1.0	48	
4	CH336	46⅜	42½	41⅛	34⅜	3⅞	5⅛	6⅞	3	6⅞	4 15/16	—	17⅜	1⅛	⅝	1¼	.44	1.4	63	
5	CH348	58⅜	54½	53⅛	46⅜	3⅞	5⅛	6⅞	3	6⅞	4 15/16	—	23⅜	1⅛	⅝	1⅛	.60	1.9	79	1
3.5	CH424	34⅜	31¼	29⅞	22⅛	4½	6¼	8	4⅛	7⅝	3½	—	11⅛	1⅜	⅞	1⅜	.55	1.8	76	
7.5	CH436	46⅜	43¼	41⅞	34⅛	4½	6¼	8	4⅛	7⅝	3½	—	17⅛	1⅜	⅞	1⅜	.82	2.7	98	1
10	CH448	58⅜	55¼	53⅞	46⅛	4½	6¼	8	4⅛	7⅝	3½	—	23⅛	1⅜	⅞	1⅜	1.10	3.7	130	1
11	CH536	48⅛	43⅜	42⅛	33⅜	4⅞	7½	9	5⅜	8¾	4⅛	—	16⅞	1⅜	⅞	2⅛	1.44	4.5	149	1
15	CH548	60⅛	55⅜	54⅛	45⅜	4⅞	7½	9	5⅜	8¾	4⅛	—	22⅞	1⅜	⅞	2⅛	1.93	6.0	182	1
24	CH560	72⅛	67⅜	66⅛	57⅜	4⅞	7½	9	5⅜	8¾	4⅛	—	28⅞	1⅜	⅞	2⅛	2.42	7.5	228	2
20	CH636	48⅞	44¼	42⅞	33⅛	5½	8⅝	10⅜	6½	7½	4¾	—	16⅝	(2)	(1⅛)	(2⅛)	2.00	6.7	204	2
25	CH648	60⅞	56¼	54⅞	45⅛	5½	8⅝	10⅜	6½	7½	4¾	—	22⅝	(2)	(1⅛)	(2⅛)	2.73	9.0	254	2
35	CH660	72⅞	68¼	66⅞	57⅛	5½	8⅝	10⅜	6½	7½	4¾	—	28⅜	(2)	(1⅛)	(2⅛)	3.42	11.2	318	3
47	CH760	74⅛	69¼	68⅜	56⅛	8⅝	9⅞	12⅜	7¾	9⅞	5⅜	—	28⅛	(3)	(1⅛)	(2⅝)	5.00	15.6	426	3
50	CH860	75⅝	70¾	69⅛	53½	8⅝	11⅛	14	8⅞	10½	5⅞	—	26¾	(3)	(1⅛)	(2⅝)	6.25	40.0	545	6
60	CH1048	65½	61¼	59¼	41½	9⅞	12⅜	14⅜	10	11½	6½	2⅛	20¾	(4)	(1⅜)	(3⅛)	7.5	45.0	564	5
75	CH1060	77½	73¼	71¼	53½	9⅞	12⅜	14⅜	10	11½	6½	2⅛	26¾	(4)	(1⅜)	(3⅛)	9.4	56.3	706	6
90	CH1160	77½	73½	71½	53½	10	14	15¼	11⅛	12⅛	7	2⅛	26¾	(4)	(1⅜)	(3⅛)	11.1	67.5	830	8
100	CH1254	73½	68⅝	66⅝	47½	10½	14⅝	16⅜	12¼	12¾	7⅜	2⅛	23¾	(4)	(1⅜)	(4⅛)	12.0	74.0	850	9
110	CH1260	79½	74⅜	72⅝	53½	10½	14⅝	16⅜	12¼	12¾	7⅜	2⅛	26¾	(4)	(1⅜)	(4⅛)	13.3	82.5	954	9
115	CH1360	79½	76⅜	74⅜	53½	11⅜	16⅜	18⅜	13⅜	13⅜	8⅛	3¼	26¾	(4)	(1⅜)	(4⅛)	17.6	104.0	1140	12

* Based on: Water in 55°F; Water out 45°F; Refrigerant 35°F.

NOTE: Chillers are designed for simple thermal valve refrigerant feed. Valves should be of the externally equalized type and be set for 5° superheat and suction-liquid heat interchangers must be used to attain maximum capacity. See Form No. 8050 or 8051 for selection of proper heat interchangers.

INSULATION: Markedly superior Urethane* "foam-in-place" insulation enclosed in 20 gauge galvanized sheet metal jacket. Finish is attractive blue lacquer.

Standard insulation is ample for commercial temperature applications. Heavy insulation is available for low temperature applications.

*For comparative purposes, "k" factors are listed below for popular insulating materials.

Urethane	.13
Expanded Polystyrene	.25
Rockcork	.35 (avg.)

In addition to having a low "k" factor, Urethane by virtue of it's closed cell construction, is an excellent vapor barrier with high structural strength.

Design Pressures: Standard construction is suitable for R-12, R-22, or R-502 Systems.

ORDERING INSTRUCTIONS

Specify quantity and complete model number. *Example:*

CH 6	36	A	I	T
Shell Diameter 6½" OD 6" NOM.	Nominal Tube Length 36"	Baffle Spacing A (See rating tables for proper selection)	Add I to Model No. as shown if insulation is desired. Add II to Model if Heavy Insulation is desired.	Add T for To Connection, Bottom, RS f Right Side, o LS for Left with respect R-in end.

Chillers CH636 and larger are constructed of ASME approved materials and will be furnished with code stamp and national board number.

Chillers CH560 and smaller are covered by Underwriters' Laboratory Approval and Listing.

INNER-FIN WATER CHILLERS

RATINGS 'CH' MODELS

RANGE 6°F (WATER IN—WATER OUT)

Tons Rating Shown For R-12 or R-22

W Out — R Out	5°F	6°	7°	8°	9°	10°	11°	12°	13°	14°	15°	MAX. G.P.M.
MODEL	TONS	TONS	TONS	TONS	TONS	TONS	TONS	TONS	TONS	TONS	TONS	
CH224A			.8	1.0	1.2	1.4	1.7	1.9	2.2	2.6	2.9	12
CH324A					1.7	2.0	2.3	2.5	2.9	3.3	3.7	16
CH324B						1.7	1.9	2.1	2.4	2.7	3.1	24
CH336A		1.7	2.1	2.5	3.1	3.8						16
CH336B			1.9	2.3	2.7	3.2	3.9	4.7	5.6			24
CH348A	2.0	2.5	3.0	3.6								16
CH348B	1.7	2.2	2.6	3.2	3.8	4.5	5.4					24
CH424A				3.0	3.4	3.9	4.4	5.0	5.6	6.4	7.2	33
CH424B						3.4	3.8	4.2	4.7	5.3	5.9	44
CH436A	3.0	3.5	4.1	4.9	5.8	6.8	8.2					33
CH436B	2.9	3.2	3.9	4.6	5.4	6.4	7.5	8.8	10.4			44
CH448A	4.1	5.0	6.0	7.2	8.8							33
CH448B	3.5	4.5	5.6	6.8	8.2	10.0						44
CH536A	4.5	5.4	6.3	7.3	8.5	10.0	11.6	13.5	15.8			58
CH536B	4.1	5.0	5.8	6.8	7.9	9.1	10.5	12.2	14.0	16.3	18.7	90
CH548A	6.5	7.9	9.5	11.4	13.5							58
CH548B	5.9	7.2	8.6	10.2	12.0	14.1	16.0	20.0				90
CH560B	9.5	11.5	13.7	16.5	20.0							90
CH636A		8.6	10.6	13.2	15.5							70
CH636B		7.5	9.3	11.5	14.0	17.3	21.0					106
CH648A	10.4	12.5	15.3									70
CH648B	9.5	11.5	13.7	16.5	20.0	(24.5)						106
CH660B	12.7	16.0	20.0	24.4								106
CH660C	11.8	15.0	18.3	21.9	26.0	32.2						141
CH760A	18.5	22.7	27.9	34.0								126
CH760B	17.6	21.7	26.2	31.5	27.0	42.6						168
CH860AB	19.5	24.3	30.0	36.0	42.8	50.0	57.7					236
CH860B	18.5	23.2	28.5	34.2	40.5	47.5	54.6	61.8	69.2			283
CH1048A	22.5	28.0	34.0	40.3	47.8	55.2	63.0					216
CH1048B	19.5	24.3	30.0	36.0	42.8	50.0	57.7	65.5	73.2	81.0		324
CH1060A	29.0	35.7	43.2	52.0								216
CH1060B	25.6	31.7	39.0	47.0	55.8	65.3	75.2					324
CH1160A	35.1	44.6	54.6									238
CH1160B	31.8	40.1	49.5	59.6	70.3	81.8						358
CH1160C	29.6	37.6	45.2	53.5	63.0	73.3	79.7	86.2				475
CH1254A	38.6	49.0	60.1									264
CH1254B	34.9	44.1	54.5	65.6	77.3	89.9	102.5					396
CH1260B	41.8	52.9	65.4	78.7	92.7							396
CH1260C	36.4	46.2	55.6	65.8	77.5	90.2	98.0	106.0				526
CH1360C		55.4	66.7	79.0	93.2	108.0	117.5	127.3				656

RANGE 8°F (WATER IN—WATER OUT)

Tons Rating Shown For R-12 or R-22

W Out — R Out	5°F	6°	7°	8°	9°	10°	11°	12°	13°	14°	15°	MAX. G.P.M.
MODEL	TONS	TONS	TONS	TONS	TONS	TONS	TONS	TONS	TONS	TONS	TONS	
CH224A			.9	1.1	1.3	1.5	1.8	2.0	2.3	2.7	3.0	12
CH324A					1.7	2.0	2.2	2.5	2.9	3.3	3.7	16
CH324B						1.7	1.9	2.2	2.4	2.8	3.1	24
CH336A	1.7	2.0	2.4	2.7	3.2	3.7	4.3	5.1				16
CH336B		1.6	1.9	2.3	2.6	3.1	3.6	4.2	4.9	5.6	6.6	24
CH348A	2.2	2.7	3.2	3.7	4.3	5.0						16
CH348B	2.0	2.5	2.9	3.3	3.9	4.5	5.2	6.1	7.0			24
CH424A						3.7	4.1	4.7	5.2	5.9	6.7	33
CH424B						3.4	3.8	4.3	4.9	5.5	6.2	44
CH436A		3.4	4.1	4.8	5.9	7.0	8.4	10.0				33
CH436B		3.2	3.8	4.6	5.5	6.5	7.8	9.3	11.2	13.2		44
CH448A	4.1	5.0	6.0	7.2	8.6	10.4						33
CH448B	4.0	4.9	5.8	6.9	8.2	9.8	11.6	14.0				44
CH536A		5.8	6.8	8.1	9.5	11.4	13.4	16.0	18.5			58
CH536B		5.3	6.2	7.2	8.5	9.7	11.5	13.3	15.5	18.0	21.0	90
CH548A	6.9	8.3	9.8	11.5	13.5	15.8	18.5					58
CH548B	6.1	7.5	8.9	10.5	12.5	14.5	17.0	20.0	23.3			90
CH560B	8.0	11.0	14.0	17.5	21.5	27.0						90
CH636A	6.9	8.8	11.0	13.2	16.2	20.0	23.4					70
CH636B		7.5	9.2	11.5	14.0	17.0	21.0	26.0	32.0	35.4		106
CH648A	9.0	12.0	15.5	19.5								70
CH648B	8.0	11.0	14.0	17.5	21.5	27.0	33.5					106
CH660B	14.2	15.5	20.0	25.2	32.0							106
CH660C	13.0	14.5	17.5	22.0	26.0	32.0	39.0	47.0				141
CH760A	19.7	24.3	29.2	35.0	41.2	47.5						126
CH760B	19.0	24.0	27.5	33.0	38.5	44.0	50.0	56.0				168
CH860AB	20.5	25.5	31.0	37.0	44.0	51.0	58.5	66.0	74.0			236
CH860B	19.4	24.4	29.4	35.2	41.8	48.5	55.5	62.6	70.4	78.5		283
CH1048A	24.0	29.0	35.5	41.5	49.0	56.5	64.0					216
CH1048B	20.5	25.5	31.0	37.0	44.0	51.0	58.5	66.0	74.0	82.0	90.0	324
CH1060A	30.5	37.0	45.0	53.5	63.5							216
CH1060B	27.5	33.5	40.0	48.5	57.0	66.4	76.0	86.0	95.5	106.0		324
CH1160A	37.5	47.0	57.5	68.0	79.0							238
CH1160B	33.5	42.5	52.0	61.5	72.0	83.5	95.0	106.0	118.4			358
CH1160C	31.1	39.9	47.8	55.3	64.8	75.1	85.7	95.7	106.5	118.4		475
CH1254A	41.2	51.7	63.2	74.8	86.9							264
CH1254B	36.8	46.7	57.2	67.6	79.2	91.8	104.5	116.6	129.8	143.0		396
CH1260B	44.1	55.9	68.6	81.0	95.0	110.1	125.0					396
CH1260C	38.2	49.1	58.8	68.0	79.7	92.4	105.4	117.7	131.0	145.6		526
CH1360C		58.8	70.6	81.6	95.7	110.0	126.5	141.2	157.0	175.0		656

INNER-FIN WATER CHILLERS
RATINGS 'CH' MODELS

RANGE 10°F (WATER IN—WATER OUT)

Tons Rating Shown For R-12 or R-22

W Out — R Out	5°F	6°	7°	8°	9°	10°	11°	12°	13°	14°	15°	MAX. G.P.M.
MODEL	TONS	TONS	TONS	TONS	TONS	TONS	TONS	TONS	TONS	TONS	TONS	
CH224A			1.0	1.2	1.4	1.6	1.9	2.1	2.4	2.8	3.1	12
CH324A				1.7	1.9	2.1	2.3	2.6	2.9	3.3	3.7	16
CH324B					1.6	1.8	2.0	2.2	2.5	2.7	3.0	24
CH336A		2.3	2.6	3.1	3.5	4.0	4.6	5.2	6.0			16
CH336B		2.0	2.3	2.6	3.0	3.4	3.9	4.4	5.1	5.8	6.5	24
CH348A	2.6	3.0	3.5	4.0	4.6	5.2	5.9					16
CH348B	2.3	2.7	3.1	3.6	4.1	4.8	5.3	6.1	7.0	7.9	8.9	24
CH424A					3.2	3.6	4.2	4.8	5.5	6.3	7.2	33
CH424B							3.5	4.0	4.7	5.3	6.1	44
CH436A	3.3	3.9	4.6	5.4	6.1	7.5	8.7	10.2	11.0			33
CH436B		3.5	4.1	4.8	5.5	6.6	7.8	9.1	10.7	12.6	15.0	44
CH448A	4.4	5.3	6.2	7.4	8.7	10.3	12.0	14.4				33
CH448B	3.8	4.6	5.4	6.4	7.6	9.0	10.7	13.0	15.5			44
CH536A	5.6	6.6	7.7	9.0	10.5	12.0	14.0	16.5	19.0	22.0		58
CH536B	5.1	6.0	6.9	7.9	9.0	10.5	11.8	13.5	15.5	17.6	20.0	90
CH548A	7.8	9.0	10.5	12.4	14.5	16.6	19.0	22.3				58
CH548B	7.0	8.0	9.4	11.0	12.6	14.5	17.0	19.5	23.0	25.5	28.0	90
CH560B	11.0	13.0	15.5	18.0	21.0	24.5	28.5	33.0				90
CH636A	8.2	9.8	11.5	13.9	16.4	20.0	23.0	27.2	32.5			70
CH636B	7.0	8.0	9.5	11.4	13.5	16.0	19.0	22.5	26.5	31.5	37.2	106
CH648A	12.6	14.5	16.5	19.5	22.7	26.5						70
CH648B	11.0	13.0	15.5	18.0	21.0	24.5	33.0					106
CH660B	18.5	21.0	23.5	26.7	30.0	35.0	35.0	38.5	43.4			106
CH660C	16.6	19.0	21.5	24.0	28.0	31.5	36.0	40.0	45.5			141
CH760A	20.7	25.2	30.2	36.0	42.2	48.5	55.0					126
CH760B	20.0	24.0	28.5	34.0	39.5	45.0	51.0	57.0	63.0	69.5		168
CH860AB	21.5	26.5	32.0	38.0	45.0	52.0	59.0	66.5	74.0	82.0	90.0	236
CH860B		25.2	30.4	36.1	42.8	49.4	56.0	63.2	70.2	78.0	85.5	283
CH1048A	25.0	30.5	37.0	43.5	50.5	58.0	66.0	74.0	82.0	90.0		216
CH1048B	21.5	26.5	32.0	38.0	45.0	52.0	59.0	66.5	74.0	82.0	90.0	324
CH1060A	32.0	39.0	47.5	56.0	65.0	74.5	84.5					216
CH1060B	29.0	35.0	42.0	50.0	58.5	67.0	76.5	86.0	96.0	106.0	116.0	324
CH1160A	40.0	49.5	59.0	69.5	81.0	93.0						238
CH1160B	35.0	44.0	53.5	63.0	73.5	84.5	96.0	107.0	119.0	130.0	142.0	358
CH1160C		40.5	49.2	58.0	67.5	77.7	88.2	98.4	109.5	119.2	130.0	475
CH1254A	44.0	54.4	64.9	76.4	89.1	102.3	114.0					264
CH1254B	38.5	48.4	58.8	69.3	80.8	92.9	105.6	117.7	130.9	143.0	156.2	396
CH1260B	46.2	58.0	70.5	83.2	96.9	111.4	126.7	139.9				396
CH1260C		49.8	60.5	71.3	83.0	95.6	108.5	121.0	134.7	146.6	160.6	526
CH1360C		59.8	72.6	85.6	99.6	114.7	130.2	145.2	161.6	175.9	192.7	656

RANGE 12°F (WATER IN—WATER OUT)

Tons Rating Shown For R-12 or R-22

W Out — R Out	5°F	6°	7°	8°	9°	10°	11°	12°	13°	14°	15°	MAX. G.P.M.
MODEL	TONS	TONS	TONS	TONS	TONS	TONS	TONS	TONS	TONS	TONS	TONS	
CH224A			1.1	1.3	1.5	1.7	2.0	2.2	2.6	3.0	3.4	12
CH324A					1.7	1.9	2.2	2.5	2.8	3.2	3.7	16
CH324B							1.7	1.9	2.2	2.5	2.8	24
CH336A	1.9	2.3	2.7	3.1	3.5	4.0	4.5	5.2	6.0	6.8	7.8	16
CH336B	1.7	2.1	2.4	2.7	3.0	3.6	3.9	4.5	5.1	5.8	6.5	24
CH348A	2.8	3.2	3.6	4.1	4.6	5.3	6.0	6.8				16
CH348B	2.4	2.8	3.2	3.6	4.1	4.6	5.2	5.9	6.7	7.6		24
CH424A					3.4	3.9	4.4	4.9	5.6	6.3	7.1	33
CH424B						3.4	3.8	4.4	4.9	5.5	6.3	44
CH436A	4.1	4.8	5.5	6.2	7.1	8.0	9.2	10.5	12.0	13.4	15.0	33
CH436B	3.7	4.4	5.0	5.7	6.4	7.3	8.2	9.4	10.5	12.0	13.5	44
CH448A	5.8	6.7	7.7	8.6	9.7	10.8	12.1	13.5	15.3	17.0		33
CH448B	5.2	6.1	7.0	7.9	8.8	10.0	11.2	12.5	14.1	15.9		44
CH536A	5.6	6.7	7.8	9.0	10.5	12.3	14.2	16.5	19.0	22.0	25.1	58
CH536B	5.2	6.0	6.9	8.0	9.1	10.5	12.0	14.0	16.0	18.5	21.2	90
CH548A	8.5	10.0	11.5	13.0	15.0	17.0	19.5	22.0	25.0	28.8		58
CH548B	8.0	9.2	10.4	11.7	13.3	15.0	17.2	19.5	22.0	25.0		90
CH560B	14.1	16.2	18.3	20.5	23.0	26.0	29.0	33.0	37.0	41.1		90
CH636A	8.9	10.5	12.2	14.3	16.8	19.7	23.1	27.0	32.0			70
CH636B	6.8	8.0	9.5	11.2	13.4	15.6	18.5	22.0	26.0	30.8	36.0	106
CH648A	15.3	17.5	19.8	22.1	25.0	28.4	32.0	36.0				70
CH648B	14.1	16.2	18.3	20.5	23.0	26.0	29.0	33.0				106
CH660B	20.0	22.5	25.1	28.2	31.8	31.8	35.5	39.8	44.2	50.0		106
CH660C	18.1	19.5	22.0	24.8	28.0	31.9	36.0	41.0	46.0	52.0	58.5	141
CH760A	21.2	26.3	31.5	39.1	43.0	49.6	56.4	63.0				126
CH760B	20.5	25.5	30.0	35.3	41.0	46.7	52.7	59.0	65.0	71.5	78.0	168
CH860AB	22.0	27.2	33.0	39.0	45.0	52.5	59.8	67.0	74.5	82.0	89.5	238
CH860B			31.3	37.0	42.8	50.0	56.8	63.6	70.7	78.0	85.0	283
CH1048A	26.7	32.0	38.0	44.5	52.0	59.5	67.5	75.2	83.0	91.5	99.0	216
CH1048B	22.0	27.2	33.0	39.0	45.7	52.5	59.8	67.0	74.5	82.0	89.5	324
CH1060A	33.0	41.0	49.0	57.5	67.0	76.5	86.5	96.5	106.0			216
CH1060B	30.0	37.0	44.0	51.5	59.8	68.5	77.5	86.5	96.0	106.0	115.0	
CH1160A	43.0	52.0	62.0	72.5	84.5	96.0	108.0	120.0				238
CH1160B	37.0	46.0	55.5	65.0	75.0	86.0	97.0	108.0	120.0	132.0	144.0	358
CH1160C		42.3	51.0	59.7	68.9	79.0	89.1	99.1	110.2	121.0	132.2	475
CH1254A	47.3	57.2	68.2	79.7	92.9	105.6	118.8	132.0	145.2			264
CH1254B	40.7	50.6	61.0	71.5	82.5	94.6	106.7	118.8	132.0	145.2	158.4	396
CH1260B	47.5	60.7	73.1	85.8	99.0	113.5	128.0	142.6	157.3	172.1	183.1	396
CH1260C		52.0	62.7	73.4	84.7	97.2	109.6	121.9	135.5	148.8	162.6	526
CH1360C		62.4	75.2	88.1	101.6	116.6	131.5	146.3	162.6	178.6	195.1	656

INNER-FIN WATER CHILLERS
RATINGS 'CH' MODELS

RANGE 20°F
(WATER IN—WATER OUT)

W Out — R Out	5°F	6°	7°	8°	9°	10°	11°	12°	13°	14°	15°	MAX.
MODEL	TONS	TONS	TONS	TONS	TONS	TONS	TONS	TONS	TONS	TONS	TONS	GPM
CH224A			1.1	1.3	1.5	1.7	2.0	2.2	2.6	3.0	3.4	12
CH324A				1.8	1.9	2.2	2.4	2.7	3.1	3.5	3.9	16
CH324B				1.7	1.8	2.0	2.2	2.4	2.7	3.0	3.3	24
CH336A	2.0	2.4	2.8	3.3	3.8	4.4	5.0	5.6	6.2	6.9	7.6	16
CH336B	1.9	2.2	2.6	3.0	3.4	3.9	4.3	4.8	5.3	5.8	6.3	24
CH348A	2.8	3.3	3.9	4.5	5.1	5.8	6.3	7.1	7.9			16
CH348B	2.5	3.0	3.5	3.9	4.4	4.8	5.5	6.3	6.9			24
CH424A			3.3	3.5	3.8	4.1	4.5	5.0	5.6	6.3	7.1	33
CH424B			3.0	3.2	3.5	3.9	4.3	4.7	5.2	5.7	7.1	44
CH436A	4.1	4.8	5.6	6.4	7.2	8.4	9.6	10.7	12.0	13.2	14.4	33
CH436B	3.7	4.3	4.9	5.7	6.5	7.5	8.6	9.7	10.9	12.1	13.3	44
CH448A	5.2	6.2	7.3	8.5	9.9	11.1	12.4	13.8	15.2	16.6	18.0	33
CH448B	4.7	5.7	6.8	7.9	9.0	10.3	11.6	12.8	14.2	15.7	16.9	44
CH536A		7.5	9.2	10.8	12.5	13.5	15.6	17.4	19.8	21.8	24.0	58
CH536B			5.8	7.5	9.0	10.8	12.5	14.6	16.5	18.6	20.5	90
CH548A	9.5	11.0	12.6	14.2	16.0	18.0	20.0	21.8	24.0	26.0	28.2	58
CH548B	8.6	9.8	11.2	12.7	14.3	16.1	18.0	20.0	22.0	24.1	26.3	90
CH560B	11.7	14.2	17.0	19.9	22.7	25.8	29.0	32.7	35.5	39.4	44.5	90
CH636A	9.6	11.7	14.3	17.2	20.2	23.4	26.6	29.8	33.4	36.5	39.2	70
CH636B	8.5	10.0	11.7	13.8	16.1	18.3	21.5	24.4	27.3	30.4	33.5	106
CH648A	14.0	17.0	20.0	23.1	26.3	29.6	33.0	36.2	39.8	43.3		70
CH648B	11.7	14.2	17.0	19.9	22.7	25.8	29.0	32.7	35.5	38.9		106
CH660B	22.0	23.1	25.0	28.5	33.0	39.3	47.6	54.0				106
CH660C	19.2	21.3	22.7	25.0	28.5	33.3	39.7	47.8	56.0	64.2	72.5	141
CH760A		30.3	35.2	40.5	46.4	52.5	58.8	65.2	69.9	78.6		126
CH760B	24.5	28.7	33.1	38.3	44.0	49.8	55.8	62.0	68.3	74.8	81.2	168
CH860AB			37.0	42.8	48.8	55.2	61.7	68.4	75.5	82.5	89.0	236
CH860B					46.4	52.4	58.5	65.0	71.6	78.4	84.5	283
CH1048A	32.2	37.2	43.0	49.3	56.2	63.5	70.8	78.2	86.0	94.0	102.0	216
CH1048B	28.5	32.0	37.0	42.8	48.8	55.2	61.7	68.4	75.5	82.5	89.0	324
CH1060A	42.0	48.0	55.2	63.3	71.7	80.5	90.0	99.3	109.0	119.0	129.5	216
CH1060B		43.6	49.3	57.0	63.4	71.5	80.0	89.0	98.0	108.0	118.0	324
CH1160A	51.0	60.5	71.0	82.0	93.0	105.0	117.0	129.0	141.0			238
CH1160B	47.0	54.0	62.8	72.0	82.0	92.5	103.0	114.0	125.0	136.0		358
CH1160C					75.4	85.0	94.5	104.6	114.7	125.8	136.7	475
CH1254A	56.1	66.5	78.1	90.2	102.3	115.5	128.7	141.9				264
CH1254B	51.7	59.4	69.0	79.2	90.2	101.7	113.3	125.4	137.5	149.6		396
CH1260B	61.4	70.5	82.1	94.1	107.2	119.6	134.3	148.3	162.6	177.5	192.7	396
CH1260C					92.7	104.6	116.2	128.6	141.1	154.7	168.1	526
CH1360C					111.2	125.5	139.4	154.3	168.3	185.6	201.7	656

Tons Rating Shown For R-12 or R-22

RATINGS 'DCH'-DUAL CIRCUIT CHILLERS

RANGE 6°F
(WATER IN—WATER OUT)

W Out — R Out	5°F	6°	7°	8°	9°	10°	11°	12°	13°	14°	15°	MAX.
MODEL	TONS	TONS	TONS	TONS	TONS	TONS	TONS	TONS	TONS	TONS	TONS	GPM
DCH636A		7.6	9.3	11.6	13.6	16.3						70
DCH636B		6.6	8.2	10.0	12.3	15.2	18.5	21.2	24.4			106
DCH648A	9.1	11.0	13.4	16.1								70
DCH648B	8.3	10.1	14.5	17.6	21.6	25.0						106
DCH748A	11.4	14.4	18.0	22.0	27.2							126
DCH748B	10.6	13.5	16.5	19.7	23.4	29.0	35.1	40.4				168
DCH760A	17.3	21.2	26.0	31.8								126
DCH760B	16.4	20.1	24.7	30.2	35.2							190
DCH860B	17.3	22.5	26.7	32.1	33.0	44.5	51.2	57.9	64.9			282
DCH1048A	20.3	25.2	30.6	36.2	43.0	49.6	56.7					216
DCH1048B	17.6	21.9	27.0	32.4	38.5	45.0	51.9	59.0	65.8	72.9		324
DCH1060B	24.1	29.7	36.7	44.2	52.5	61.5	70.7					324
DCH1160A	33.2	42.1	51.6									238
DCH1160B	30.0	38.0	46.9	56.4	66.5	77.4						358
DCH1160C	28.0	35.5	42.7	50.6	59.5	69.2						475
DCH1260B	39.8	50.4	62.2	75.0	88.2	102.5						396
DCH1260C	36.9	46.8	57.8	69.8	82.0	95.2	110.5					526
DCH1360B	43.0	57.1	71.2	85.4	99.7	114.6						495
DCH1360C	42.1	53.4	65.9	79.6	93.5	108.5	126.0					656

Tons Rating Shown For R-12 or R-22

APPENDIX G

SAMPLE CALCULATION PROCEDURE AND GRAPHS FOR COMMERCIAL UNIT PERFORMANCE

Sample Calculation for Heating

Assume:

$$Q_{evap} = 20 \text{ tons}$$

$$\dot{M}_{cond} = 50 \text{ GPM}$$

$$[T_{evap}]_{in} = T_{city\ water} = 59°F$$

$$[T_{cond}]_{in} = 120°F$$

$$\Delta T_{evap} = 20°F$$

$$\dot{M}_{evap} = \frac{20 \text{ (tons)}(200 \frac{\text{Btu}}{\text{min ton}})}{(1.0 \frac{\text{Btu}}{\text{lb°F}})(20°F)} = 200 \frac{\text{lb}}{\text{min}}$$

$$= \frac{200 \frac{\text{lb}}{\text{min}}}{8.34 \frac{\text{lb}}{\text{gal}}} = 24 \text{ GPM}$$

From evaporator charts, at $\Delta T = 20°F$ and

$$Q_{evap} = 25 \text{ tons}$$

$$T_{evap} - [T_{evap}]_{out} = 8.6°$$

$$T_{evap} = [59-20] - 8.6° = 30.4°$$

Assume RPM_{comp} = 2100 rpm

To find the capacity at 2100 multiply the capacity at 1750 from the charts by 1 + [(2100-1750).00056]. Redraw the curve and pick off the T_{cond} at 20 tons. Know the temps. Find B.H.P. at 1750 and multiply it by 1 + [(2100-1750).00067]. To get B.H.P. = 35.8

$$Q_{cond} = W + Q_{evap}$$

$$= \frac{35.8(2545)}{60} + 20\ (200) = 55.8\ \frac{Btu}{Min}$$

For an $\dot{M}_c$ = 50 GPM, the condenser chart

$$Q_c = 290000, \quad T_{in} = 85°, \quad T_{cond} = 105$$

$$Q_c = (FUA)(\overline{\Delta T_m})$$

$$\overline{\Delta T_m} = \frac{T_{out} - T_{in}}{\ln\left(\frac{T_{cond} - T_{in}}{T_{cond} - T_{out}}\right)}$$

Solving for

$$T_{out} = T_{in} + \frac{Q}{\dot{m}\ c_p}$$

and then solving for (FUA)

$$(FUA) = 21642$$

$$\overline{\Delta T}_{m_1} = \frac{5518\ (60)}{21642} = 15.3$$

$$T_{out} = \frac{5518}{50\ (8.34)} + T_{in} = T_{in} + 8.3$$

$$= 128.3$$

$$\overline{\Delta T}_{m_2} = \frac{8.3}{m\ (\frac{26}{17.7})} = 21.5$$

$$\overline{\Delta T}_{m_1} \neq \overline{\Delta T}_{m_2}$$

Assume new rpm and try again once $\overline{\Delta T}_{m_1} = \overline{\Delta T}_{m_2}$, then find what throttle setting delivers the h.p. and $(rpm)_{eng}$

$$(RPM)_{eng} = 1.43\ (rpm)_{comp}$$

Then find η_t

Divide $\frac{H.P.}{\eta_t}$ = heat supplied = H.S.

.8 (H.S. - H.P.) = heat recovered

Final water temp = $(T_{cond})_{out} + \frac{H.R.}{50\ (8.34)}$

$$COP_{heat} = \frac{H.R. + Q_{cond}}{H.S.}$$

Use same technique for find cooling operating points.

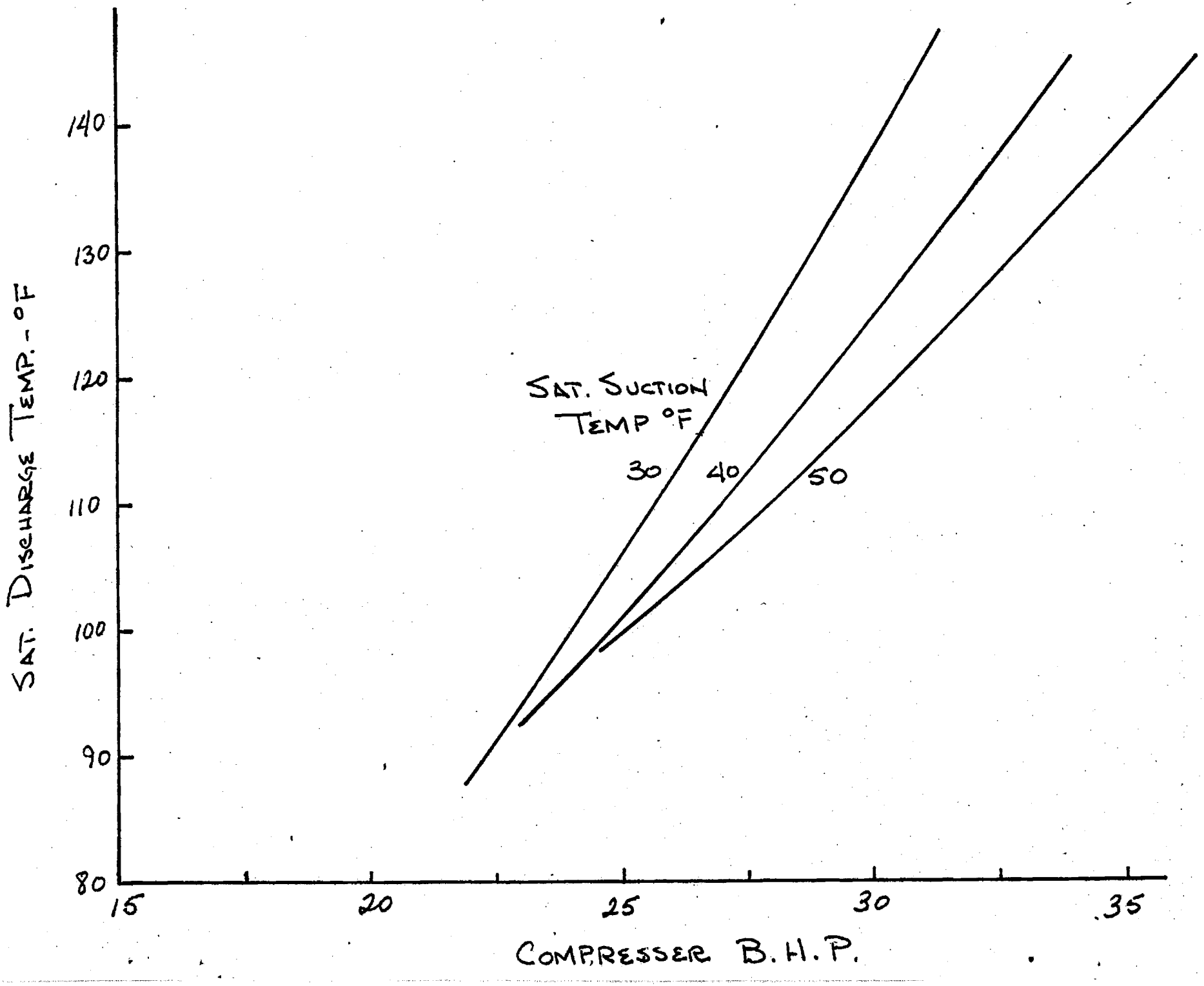
SAT. DISCHARGE TEMP. - °F
140
130
120
110
100
90
80
SAT. SUCTION TEMP °F
30
40
50
15
20
25
30
35
COMPRESSER B.H.P.

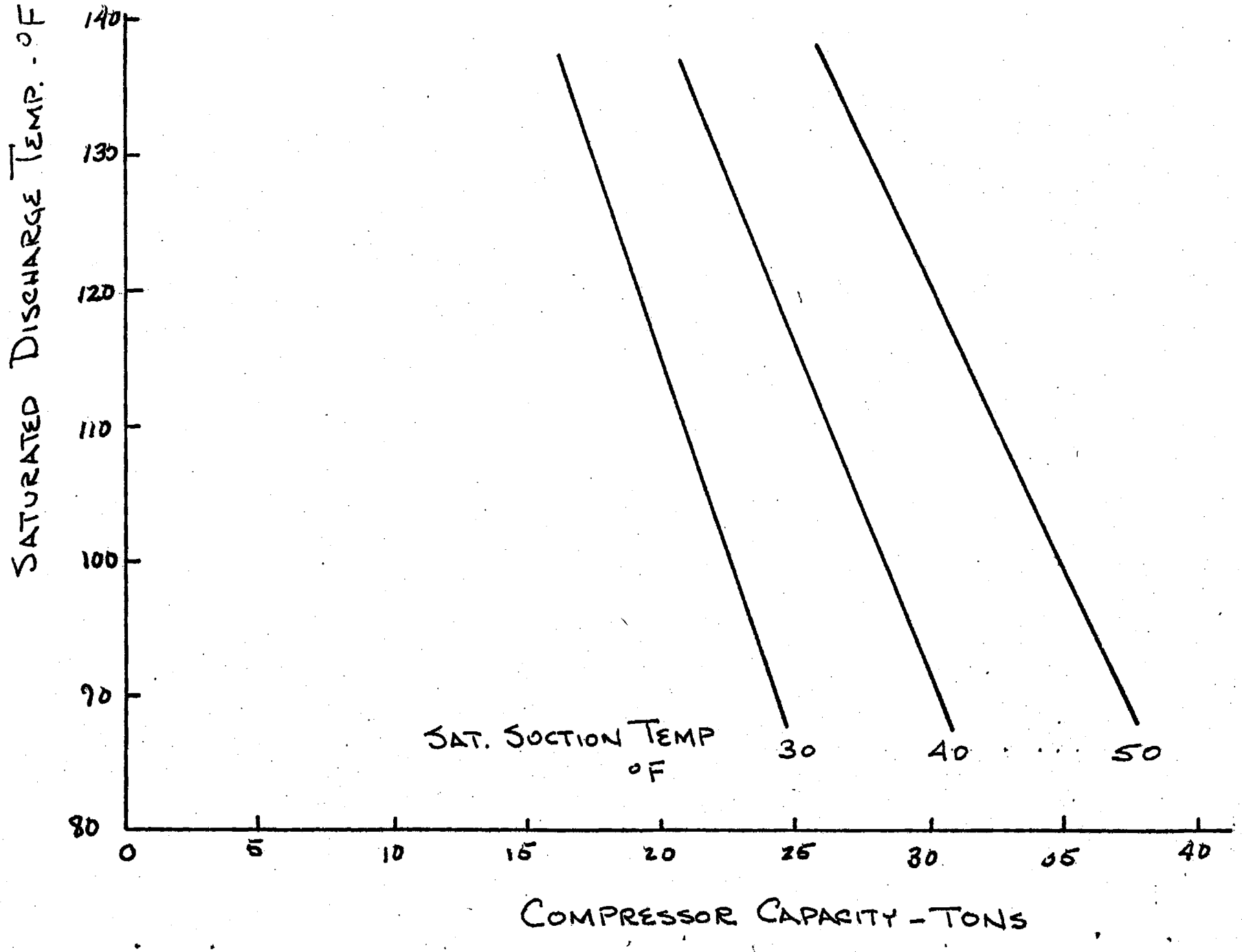
SATURATED DISCHARGE TEMP. - °F
140
130
120
110
100
90
80
0
5
10
15
20
25
30
35
40
COMPRESSOR CAPACITY - TONS
SAT. SOCTION TEMP °F
30
40
50

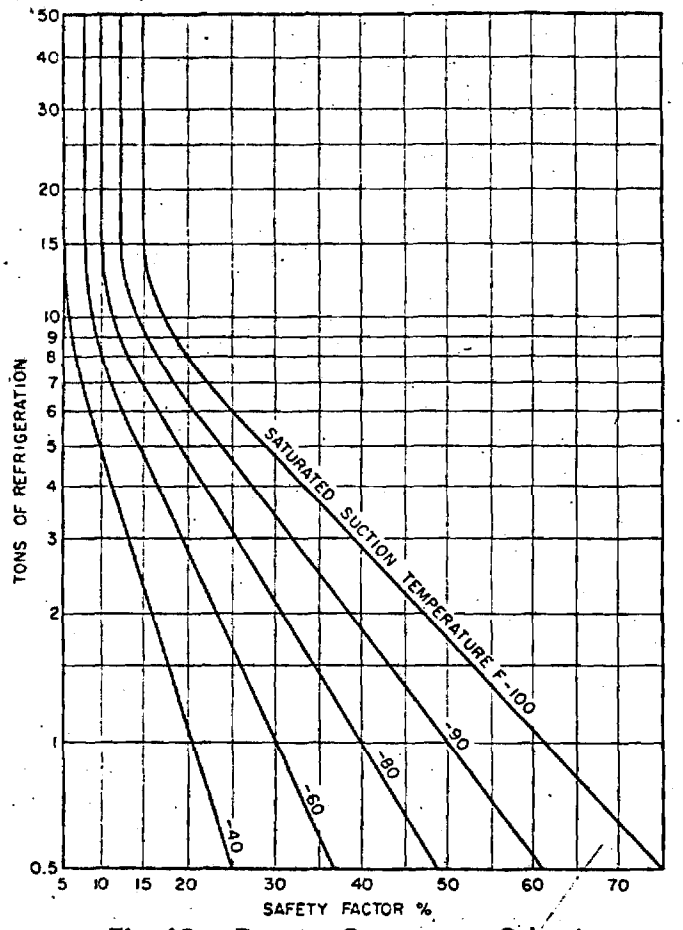

Fig. 12 — Booster Compressor Selection Safety Factors

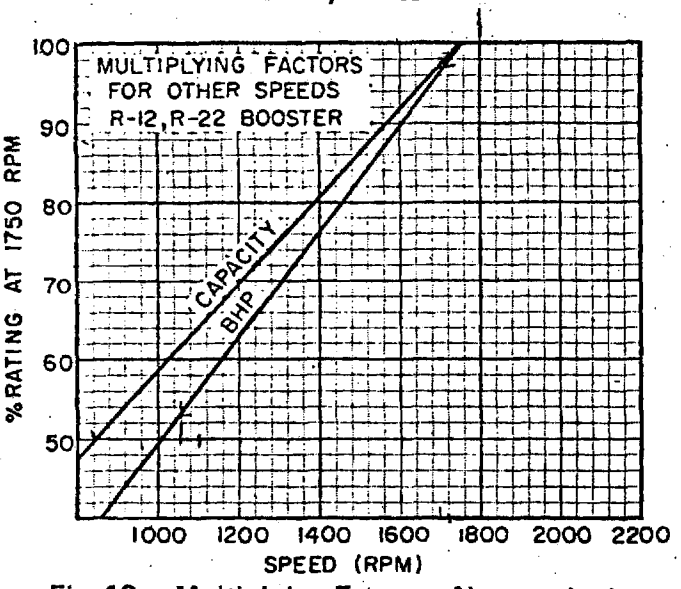

Fig. 13 — Multiplying Factors - Nonstandard Speeds

above the saturation temperature corresponding to the intermediate pressure.

Oil Separators and Lubrication — In Freon cascade-type systems, where evaporators and suction lines are properly designed for oil return to the compressor, oil separators are not usually used.

In direct stage systems, however, oil may tend to accumulate in one of the stages and thus result in lack of lubrication in the other machine. By the use of oil transfer lines, equalization of the oil level between crankcases can be achieved by manual operation at periodic intervals. Automatic control of proper oil return to both compressors is effected by the use of a high stage discharge line oil separator, returning oil to the high stage machine, and a high side float, connected to the high stage machine crankcase, which continually drains excess oil from this crankcase down to the next lower stage compressor (Fig. 11).

For booster application, the factory oil charge should be drained and replaced with a suitable viscosity oil for the low temperature application.

Control Pressurestat for Booster Application — The standard dual pressure switch furnished with the 5F,H compressor cannot be used for booster application. Replace it with an appropriate low temperature dual pressurestat that can operate at the values shown in Table 17. Any commercial pressure switch is acceptable; for example, an Allen-Bradley Bulletin 836, type L33 for R-12 or type 1 for R-22.

Table 17 — Control Pressurestats for Low Stage Application

CHARACTERISTICS		REFRIGERANT 12	REFRIGERANT 22
Switch Action	- High	Open on press. rise	Open on press. rise
	- Low	Open on press. fall	Open on press. fall
Range	- High	20" Vac to 65 psig	30" Vac to 110 psig
	- Low	30" Vac to 20 psig	30" Vac to 25 psig
Differential	- High	8 to 30 psi adjust.	12 to 30 psi adjust.
	- Low	5 to 15 psi adjust.	9 to 30 psi adjust.
Max Pressure	- High	200 psig	300 psig
	- Low	120 psig	300 psig

Discharge Valve Springs — When 5H compressors are used for booster applications where the discharge pressure is below 10 psig, the standard discharge valve springs furnished with the machine should be replaced with an equal number of lighter weight springs, part number 5H41-1801.

No change in discharge valve springs is recommended for the 5F compressors.

Water-Cooled Heads — The standard 5F,H compressors are not equipped with water-cooled heads but they are available on special order. Water cooling of the heads is not generally necessary in R-12 and R-22 booster applications. For these applications with R-22 involving high compression ratios, 5 or above, 5F,H booster compressors should be equipped with water-cooled heads.

Motor Selection Data — In staged refrigeration systems, the high stage compressor starts first and runs until the low stage pressure has been reduced to a predetermined level before the low stage machine starts. With direct staged arrangements, the high stage machine draws gas from the evaporator thru the low stage machine bypass during this initial period. The size of the selected motor must be related to the maximum condition at which the booster compressor can operate.

BIBLIOGRAPHY

1. A Study of Natural Gas Rotary Engine Driven Heat Pumps, First Annual Report, Georgia Institute of Technology, S. V. Shelton (principal investigator), July, 1974.

2. Kennedy, D., "The Potential of the Heat Activated Heat Pump," American Gas Association Monthly, April, 1973.

3. Stoecker, W. F., Refrigeration and Air Conditioning, McGraw-Hill Book Co., 1958.

4. Amana Electric Gas Package Unit, Service Instructions, Amana Refrigeration, Inc., Amana, Iowa.

5. Installation, Operation, and Maintenance Instructions for Electric-Gas Package Unit Cooling and Heating, Part No. A46815-4, Amana Refrigeration, Inc., Amana, Iowa.

6. Calvert, F. O., Harden, D. G., "A Comparative Study of Residential Energy Usage," Proceedings of the Inter-society Energy Conversion Engineering Conference, Paper 739103 (1973) p. 410-415.

7. Schweitzer, Gerald, Ebeling, A., Basic Air Conditioning, Volume 1, Hayden Book Co., Inc., New York, 1971.

8. Linzmaier, J., Personal Correspondence, Tecumseh Products Company, Atlanta, Georgia, 30340, April, 1975.

9. Ranco Reversing Valves, Bulletin 1919-1, Ranco, Inc., 601 West Fifth Avenue, Columbus 1, Ohio.

10. Granet, Irving, Thermodynamics and Heat Power, Reston Publishing Co., Inc., Reston, Virginia, 1974.

11. Perry, H. Allen, "On the Way: A Completely Different Auto Engine," The American Legion Magazine, March, 1972, p. 18-23, 42-45.

12. Norbye, Jan P., The Wankel Engine, Chilton Book Co., Philadelphia, Pennsylvania, 1971.

13. Keller, Helmut, "Small Wankel Engines," Society of Automotive Engineers, Paper No. 680572, 1968.

14. Trane Model G Compressors, Catalog DS-COM3, The Trane Company, La Crosse, Wisconsin, 54601, 1970.

15. Van Wylen, Gordon J., Thermodynamics, John Wiley & Sons, Inc., 1959.

16. The Wall Street Journal, August 7, 1974, page 8.

17. Thermodynamic Properties of Freon 22 Refrigerant, Booklet T-22, E. I. DuPont de Nemours & Co., Inc., Wilmington, Delaware 19898, 1964.

18. Streeter, Victor L., Fluid Mechanics, McGraw-Hill Book Company, 1958.